The effects of Sulf1 on canonical and non-canonical Wnt signalling in *Xenopus*

Simon Wilfred Fellgett

Thesis submitted for the degree of Doctor of Philosophy

The University of York
Department of Biology

September 2013

Abstract

Heparan sulphate proteoglycans are large macromolecules expressed on the cell surface. They are an important part of the extracellular matrix and regulate multiple cell signalling pathways. Sulf1 is an extracellular sulfatase that specifically removes 6-O linked sulphate groups from heparan sulphate chains. The activity of Sulf1 alters the ability of heparan sulphate chains to regulate FGF, BMP, hedgehog and Wnt signalling pathways. The original work that identified Sulf1 (Dhoot et al., 2001), demonstrated that Sulf1 enhanced the ability of Wnt1 to activate canonical Wnt signalling. This thesis uses *Xenopus* to investigate the effects of Sulf1 on canonical and non-canonical Wnt signalling in the early embryo. Sulf1 has ligand specific effects on different Wnt ligands, inhibiting the ability of Wnt8a, but not Wnt3a, to activate canonical Wnt signalling. In addition Sulf1 potentiates the ability of Wnt4 to activate non-canonical Wnt signalling and Wnt11b to activate both canonical and non-canonical Wnt signalling. Confocal analysis of animal caps expressing fluorescently tagged Wnt ligands shows that Sulf1 can enhance the range of diffusion of both Wnt8a and Wnt11b. The ability of Sulf1 to regulate Wnt ligand diffusion may explain some of the differential effects of Sulf1 on Wnt signalling. The results described in this thesis are discussed in terms of Sulf1 regulating Wnt morphogen gradients during development. The differential effects of Sulf1 on canonical and non-canonical Wnt signalling described here requires more than the existing 'catch and present' model (Ai et al., 2003). A new model is presented here.

Table of contents

List of Figures

List of Tables

Acknowledgments

I would like to thank my supervisor Betsy Pownall for her tireless support during my PhD. Her knowledge and enthusiasm for science has shown me that a life in science, although hard work, would be a fantastic career for anyone. In addition, the support that Harv Issacs has provided over the four years has helped me to become a more rounded researcher. His interest in football has spared the rest of the lab from my ramblings! I would like to thank the rest of the members of the frog laboratory past and present. Thanks also go to Nick Bland, for all of his help at the start of my PhD and for not throttling me. He taught me to not always assume that someone else is right over me and to always be suspicious of my data, that and Sunderland fans. I would like to thank Fiona, for her help with RNA synthesis and for making sure that everything in the lab was equally allocated. Laura for the countless questions she has helped me with during my research and Hannah for reminding me that you start out in science because it is fun and exciting! Finally, a massive thank you has to go to Simon Ramsbottom as well for his help with practically everything from *insitu's* to bikes, including the development of the confocal animal cap assay.

Outside of the lab, I would like to thank the Tom's and Eleanor from Louise Jones's lab, for all the time spent laughing (and crying) about science and the world. Especially Tom Brabbs for coping with being my house mate for 15 months. Thanks to Phil and Dan for using up lab reagents, stealing my pipettes, but generally being great guys to work with. I'd like to say thanks to all of my PhD friends who started with me and have suffered in parallel on their respected projects, especially Rich and Steve! Also I have to thank Jo, for being a friendly face to chat to on many occasions and for providing a place for me to live during my final year. In addition, I would also like to thank all of the guys I have played football with over my time in York, you've helped keep me sane during my PhD. Special thanks to Dan, Joe and Adrian, for many a fun night drinking and for showing me that there are at least three people in the department less handsome than me.

I could not have survived the PhD without all the help and support I have had from Di and Richard. Di (also known as my work mum), has convinced me that all lab technicians are brilliant with one notable exception! Di has a tireless attitude to helping people in the lab, regardless of what time it is, or how ridiculous the request is. In addition her knowledge of techniques is second to none, pity she likes cricket, but no one is perfect. I also could not have got this far without Richard. To say that I have been a difficult child would be an understatement, but he has always been prepared to patiently provide help and advice on pretty much anything. Both his breadth and depth of knowledge baffles me, but it is something to aim for in my future career. Thank you to both of you.

Finally I have to thank my family for getting me this far. My mum and dad for supporting me in whatever I have chosen to do in life, you are both an inspiration. In addition thanks to my mum for actually reading my thesis (may not happen again). Thanks also go to my brother and sister for always providing me with an escape from PhD, even if it was just worrying about them and to my grandad Wilf for always providing me with a loving escape from my troubles during my research. Your house has been a sanctuary on many a tough day! The biggest thanks of all though must go to my beautiful partner Jess. You have put up with me through thick and thin, regardless of how little I can be around, or where my mind is. The thought of coming home to see you always brightens my day and it is safe to say I could not have done half of this without you.

The final lines of this though are best filled by a quote from my supervisor after reading the first draft of a summary paragraph in my general discussion.

'*Repetitive, not based on any literature and just wrong*'

Positive criticism and support right until the end!

Thanks everyone.

Author's declaration

I declare that this is an original piece of work, conducted under the supervision of M.E.Pownall at The University of York. None of the work presented in this thesis has been previously published or submitted for a qualification either at The University of York or at any other institution. Some parts of this work have however been presented in posters at the 13th/14th International *Xenopus* conference (2010/2012) and the North of England Cell Biology Conference (2010). In addition some of the work was presented in a talk at the UK *Xenopus* meeting (2013). All the data presented here is my own work.

Signed ----------

Simon Fellgett

1.0 Introduction

1.1.0 Determination of cell fate by morphogens

During development a limited number of signalling molecules are required to pattern the whole of the embryo. One way of achieving this is by signalling molecules inducing different effects based on the concentration of the signal interpreted by receiving cells. Morphogens are signalling molecules that are secreted from a localised source and diffuse away, establishing a concentration gradient. Cells exposed to this gradient are able to adopt qualitatively different cell fates in a concentration specific manner. This ensures that even if a subset of cells is removed from the organism, the overall pattern of cell fates is maintained. The 'French flag model' has been used to describe how cells adopt different fates based on the concentration of signal received. In this model, cells close to the source of the signal adopt fate 1 (red), cells further away adopt fate 2 (white) and cells at the edge of the gradient adopt fate 3 (blue). The 'French flag model' depends on thresholds, with red being induced as a high threshold target gene close to the source. In contrast blue serves as the default state when the concentration of signalling molecule is below the required threshold. As the model depends on thresholds, having more or less cells will not affect the overall pattern of the flag, reviewed by (Gurdon and Bourillot, 2001; Neumann and Cohen, 1997; Wolpert, 1969).

To be classified as a morphogen a signalling molecule must have several properties. The signalling molecule must be released from a source and form a long range concentration gradient. In addition, in the French flag model, cells within this gradient must be able to respond to this signal with two or more qualitatively different responses. Cells should interpret the morphogen directly rather than a secondary secreted factor from a neighbouring cell. The wingless (Wg) protein illustrates the principles of morphogen gradients in *Drosophila*. Wg is expressed along the dorsal/ventral boundary of the wing disc (Cadigan et al., 1998; Zecca et al., 1996). Wg is secreted apically and diffuses away from the dorsal/ventral boundary forming an extracellular concentration gradient (Gallet et al., 2008; Strigini and Cohen, 2000). This leads to the graded activation of gene expression with cells close to the dorsal/ventral boundary expressing the high threshold Wg target gene *senseless* (Nolo et al., 2000;

Phillips and Whittle, 1993). Cells further away from the boundary express the low threshold Wg target gene *distaless* (Neumann and Cohen, 1997; Zecca et al., 1996).

Cells have developed complex mechanisms in order to regulate both the formation of morphogen gradients and the perception of positional information. These mechanisms range from regulating morphogen secretion and internalisation, to the ability of morphogens to associate with the cell surface and bind to specific receptors. The extracellular matrix (ECM) is intimately involved in the regulation of morphogen gradients. Heparan sulphate proteoglycans are components of the ECM, which have important roles in morphogen gradient formation during development (Yan and Lin, 2009). This thesis will focus on the role of the endosulfatase Sulf1 in remodelling HSPGs on the surface of cells and how this affects Wnt signalling and Wnt ligand diffusion in the early embryo and tissue explants.

1.2.0 Identification the Wg pathway in *Drosophila*

Genetic analysis of the *Drosophila* embryo has been important in defining the Wg signalling pathway. Wg was identified in *Drosophila* as the first member of the Wg/Wnt family of glycoproteins. The *Wg* gene was identified in an ethyl methanesulfonate (EMS) screen for mutant *Drosophila* (Sharma, 1973). The mutation caused a loss of wings and also disrupted haltere development, hence being termed wingless. The initial *Wg* mutant was not fully penetrant and hence homozygous viable, however a homozygous embryonic lethal Wg mutation was identified soon after (Babu, 1977; Sharma and Chopra, 1976). Following this Wg was shown to have a role in segment polarity in the *Drosophila* embryo. The cuticle of developing *Drosophila* embryos is subdivided into 14 segments that contribute to the formation of the head, thorax and abdomen of the adult fly. Wg patterns cells in both the anterior and posterior half of the segment repressing denticle formation in the posterior halve of the segment. *Wg* mutation leads to a loss of posterior pattern in each of the segments, with this replaced by a mirror image of the anterior pattern. This leads to a loss of both naked cuticle and segment boundaries resulting in lethality

Table 1.1; Canonical Wg/Wnt signalling components.

Drosophila	**Vertebrate**	**Protein type**	**Reference**
Wingless (Wg)	Wnt	Secreted glycoproteins	(Sharma, 1973); (Nusse and Varmus, 1982); (Rijsewijk et al., 1987)
Drosophila Frizzled2 (DFz2)	Frizzled	Seven pass transmembrane proteins	(Bhanot et al., 1996); (Niehrs, 2012)
Arrow	Low density lipoprotein5/6 (LRP5/6)	Single pass transmembrane protein	(Wehrli et al., 2000); (Brown et al., 1998); (Hey et al., 1998)
Dishevelled (Dsh)	Dishevelled (Dvl)	Cytoplasmic proteins	(Perrimon and Mahowald, 1987); (Wallingford and Habas, 2005)
Casein Kinase1α (CK1α)	Casein Kinase1α (CK1α)	Serine/threonine kinase	(Yanagawa et al., 2002); (Zhang et al., 2006)
Double time (Dbt)	Casein Kinase1ε (CK1ε)	Serine/threonine kinase	(Zilian et al., 1999); (Peters et al., 1999)
Gilgamesh	Casein Kinase1γ (CK1γ)	Serine/threonine kinase	(Zhang et al., 2006); (Davidson et al., 2005)
Zeste-white3/Shaggy (ZW3)	Glycogen synthase kinase-3β (GSK-3β)	Serine/threonine kinase	(Bourouis et al., 1990); (Siegfried et al., 1992)
Axin	Axin	Cytoplasmic scaffolding protein	(Hamada et al., 1999a); (Willert et al., 1999)
Adenomatous polyposis coli (APC)	Adenomatous polyposis coli (APC)	Cytoplasmic protein	(Munemitsu et al., 1995); (Rubinfeld et al., 1996)
Armadillo	β-catenin	Protein has structural roles in the cell and functions during Wnt/Wg signalling	(Wieschaus et al., 1984); (McCrea et al., 1991); (Seto and Bellen, 2004)
Legless	B-Cell CLL/Lymphoma9 **(**Bcl9)	Cytoplasmic/nuclear protein	(Kramps et al., 2002)
Pygopus	Pygopus	Nuclear PHD finger domain containing proteins	(Belenkaya et al., 2002); (Kramps et al., 2002)
Groucho	Gro-related gene (Grg) family members	Transcriptional repressor proteins	(Cavallo et al., 1998); (Roose et al., 1998)
Pangolin/Lymphoid enhancing factor/T cell factor (Pan/Lef/Tcf)	Lymphoid enhancing factor/T cell factor (Lef/Tcf)	HMG domain transcription factors	(Behrens et al., 1996); (Brunner et al., 1997); (Molenaar et al., 1996)

(Nüsslein-Volhard and Wieschaus, 1980). A table detailing the components of the Wg signalling pathway and their vertebrate homologues is shown (Table 1).

1.2.1 The Wg signalling pathway

The loss of naked cuticle in Wg mutants has been used to determine other components in the Wg signalling cascade. These include the receptors frizzled (Fz) and arrow, components of the destruction complex and the effector armadillo. Sequence analysis revealed that Wg encoded a cysteine rich secreted glycoprotein (Rijsewijk et al., 1987). The Wg protein is secreted into the ECM of the developing *Drosophila* segments and is able to diffuse away from cells expressing it, being taken up by neighbouring cells (González et al., 1991; van den Heuvel et al., 1989). The importance of Wg secretion was highlighted by the discovery of the D*rosophila* segment polarity gene *porcupine*. *Porcupine* encodes a member of the O-acyltransferase family of proteins, which transfer organic acids onto proteins, reviewed by (Hofmann, 2000). Mutations in *porcupine* result in a loss of naked cuticle and a decrease in the protein levels of the downstream Wg target armadillo (Perrimon et al., 1989; Riggleman et al., 1990). On further investigation it was shown that mutations in *porcupine* inhibit the secretion of Wg leading to its accumulation in the cytoplasm (van den Heuvel et al., 1993).

Activation of Wg signalling in neighbouring cells requires the presence of Wg receptors. *Drosophila* Frizzled 2 (DFz2) is required for the formation of naked cuticle in *Drosophila* embryos and Wg has been shown to bind DFz2 on the surface of *Drosophila* S2 cells (Bhanot et al., 1996). The frizzled family of proteins possess seven transmembrane spanning domains, which show topological similarity, but not sequence similarity to the G protein coupled receptor (GPCr) superfamily (Vinson et al., 1989). In addition to DFz2, Wg signalling also requires the protein arrow. *Arrow* encodes a single pass transmembrane protein related to the low density lipoprotein (LDL) receptor family. Mutations in *arrow* result in a loss of naked cuticle in the developing *Drosophila* and this cannot be rescued by over-expressing Wg (Wehrli et al., 2000).

Activation of Wg signalling inside the cell depends on the cytoplasmic stability of the protein armadillo. Mutations in *armadillo* phenocopy *Wg* mutations, leading to loss of naked cuticle in *Drosophila* embryos (Peifer et al., 1991; Wieschaus et al., 1984). In the absence of Wg the cytoplasmic levels of armadillo are kept low by the actions of the destruction complex. The first member of the complex to be identified was zeste-white 3 (ZW3, also known as shaggy). *ZW3/shaggy* encodes a serine/threonine (ser/thr) kinase that is the homologue of vertebrate glycogen synthase kinase-3β (GSK-3β) (Bourouis et al., 1990; Siegfried et al., 1992). Loss of *ZW3* expression results in an increase in the cytoplasmic levels of armadillo and a loss of denticle formation in *Drosophila* embryos (Peifer et al., 1994a; Perrimon and Smouse, 1989). ZW3 is a negative regulator of armadillo positioned upstream of it in the Wg signalling pathway.

In addition to ZW3, axin, E-APC and CK1α are also part of the destruction complex. Axin acts as a molecular scaffold for the destruction complex as it is able to bind ZW3, E-APC and armadillo (Morin et al., 1997; Willert et al., 1999). LOF mutations in axin or knockdown of *axin* leads to the formation of an entirely naked cuticle in *Drosophila* embryos (Hamada et al., 1999a; Willert et al., 1999). E-APC is a *Drosophila* homologue of the vertebrate tumor suppressor gene *adenomatous polyposis coli (APC)*. In addition to binding axin, E-APC has been shown to interact with the armadillo repeat domain of armadillo. The SW480 colon cancer cell line has a high level of stable β-catenin due to a mutation in APC (Morin et al., 1997). Over-expression of E-APC in SW480 cells inhibits β-catenin (the vertebrate homologue of armadillo) stabilisation (Hamada et al., 1999b; McCrea et al., 1991). CK1α is a member of the casein kinase 1 (CK1) family of ser/thr kinases that phosphorylate a wide variety of substrates in eukaryotes, reviewed in (Knippschild et al., 2005). In *Drosophila* CK1α phosphorylates armadillo in order to keep the cytoplasmic levels of armadillo low. Knockdown of *CK1α* leads to the ectopic stabilisation of armadillo in *Drosophila* embryos and S2 cells (Yanagawa et al., 2002).

CK1α acts as a priming kinase, phosphorylating β-catenin and priming it for phosphorylation by ZW3 (Yanagawa et al., 2002). Armadillo is present as a phosphoprotein in *Drosophila* embryos and LOF mutations in *Wg* lead to an increase in the levels of phospho-armadillo (Peifer et al., 1994b). The *ArmS10*

mutant is a gain of function (GOF) armadillo mutant that lacks three out of the four predicted phosphorylation sites for ZW3/GSK3-β (Pai et al., 1997; Peifer et al., 1994b). The ArmS10 mutant is resistant to degradation by the destruction complex and induces the formation of naked cuticle in the absence of Wg (Pai et al., 1997). In the absence of Wg, CK1α and ZW3 phosphorylates armadillo to keep the cytoplasmic levels of the protein low.

Activation of the Wg pathway leads to the accumulation of armadillo in the cytoplasm and nucleus of cells in the developing *Drosophila* segments (Orsulic and Peifer, 1996). The activation of Wg signalling requires the segment polarity gene *dishevelled* (*Dsh*). LOF mutations in *Dsh* lead to a loss of naked cuticle indicating a role in the Wg signalling cascade (Perrimon and Mahowald, 1987). Dsh is downstream of arrow as over-expression of *Dsh* rescues naked cuticle in *arrow* LOF mutants. However *Dsh, ZW3* double LOF mutants display a naked cuticle phenotype placing Dsh upstream of ZW3 and the destruction complex (Peifer et al., 1994a). Wg induces the phosphorylation of Dsh in cell culture and over-expression of Dsh stabilises armadillo independent of Wg (Yanagawa et al., 1995). Dsh is required downstream of Wg to stabilise armadillo and activate Wg signalling

The Drosophila homologues of CK1ε/γ are also important in Wg signalling. Double time (Dbt) and gilgamesh are the *Drosophila* homologues of vertebrate CK1ε and CK1γ respectively. LOF mutation in either gene inhibits the expression of *senseless* in the *Drosophila* wing disc. Over-expression of gilgamesh and to a lesser extent Dbt, results in the phosphorylation of the cytoplasmic domain of arrow in cell culture (Zhang et al., 2006). CK1ε/γ are required for Wg signalling *in vivo.*

Activation of Wg signalling leads to the stabilisation of armadillo in the cytoplasm allowing it to translocate into the nucleus. Legless and pygopus are required for the nuclear translocation of armadillo. *Legless* is the *Drosophila* homologue of the human gene *Bcl9* and LOF mutations in *legless* result in a loss of naked cuticle in *Drosophila*. In addition LOF mutations in *legless* reversed the naked cuticle phenotype caused by *ArmS10* in *Drosophila* (Kramps et al., 2002). *Pygopus* encodes a nuclear PHD finger domain

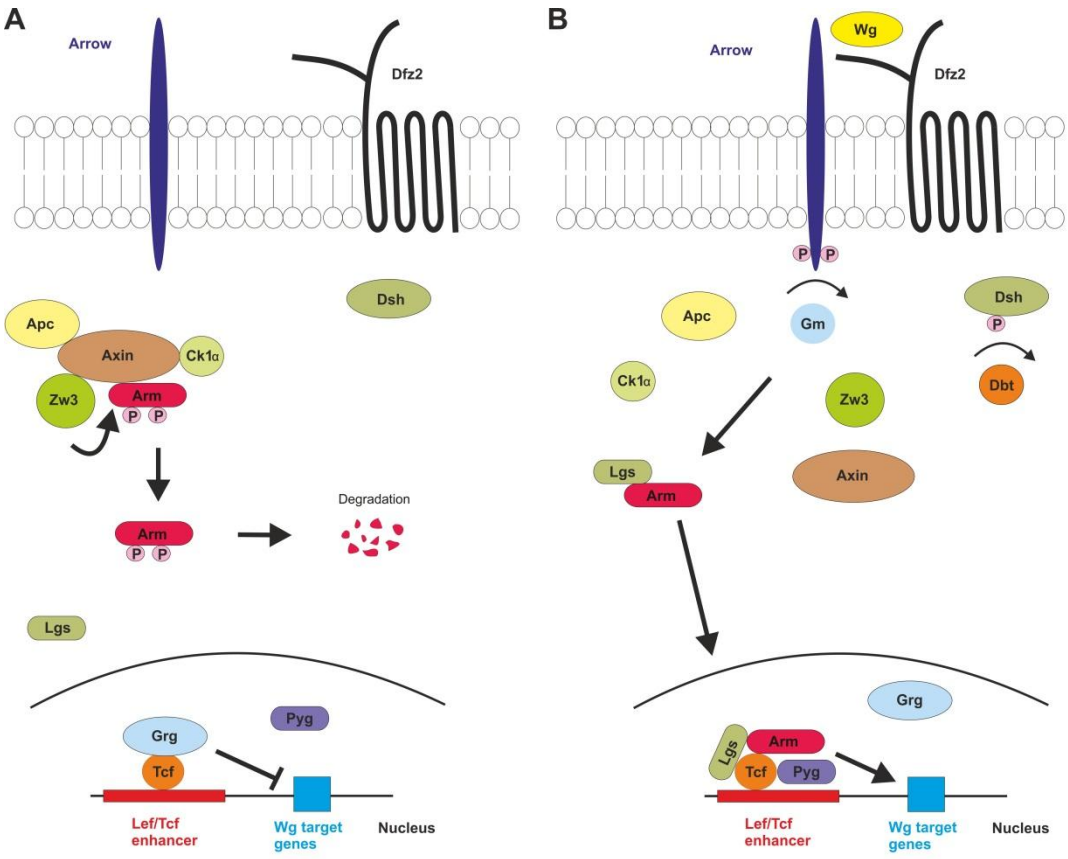

Figure 1.1; Wg signalling in *Drosophila.*
[A] In the absence of Wg armadillo is bound by the destruction complex leading to its phosphorylation and degradation. Groucho binds to Tcf in the nucleus and represses the transcription of Wg dependent genes. [B] In the presence of Wg arrow and Dsh are phosphorylated by members of the CK1 family. This then leads to the dissociation of the destruction complex and stabilisation of armadillo in the cytoplasm. Armadillo interacts with legless and pygopus to translocate into the nucleus where it displaces groucho, forming a transcriptional activation complex. Wingless (Wg), *Drosophila* frizzled 2 (DFz2), dishevelled (Dsh), adenomatous polyposis coli (Apc), zeste white 3 (ZW3), casein kinase 1 (CK1), armadillo (Arm), legless (Lgs), pygopus (Pyg), groucho (Grg), T cell factor (Tcf), lymphoid enhancing factor (Lef), gilgamesh (GM), double time (Dbt), phosphate (P), adapted from (Kikuchi et al., 2009).

containing protein required for Wg signalling. LOF *pygopus* mutants show a loss of naked cuticle as well as loss of *senseless* and *distaless* expression in the wing disc (Belenkaya et al., 2002; Kramps et al., 2002; Thompson et al., 2002). Pygopus is found mainly in the nucleus, whereas legless is able to shuttle between the cytoplasm and nucleus. Legless and pygopus are important for the nuclear localisation of armadillo in response to Wg signalling (Townsley et al., 2004).

Pygopus contains a transactivation domain and is able to drive Gal4 gene expression when fused to the Gal4 DNA binding domain in cell culture

(Belenkaya et al., 2002). Activation of Wg gene expression requires the interaction of armadillo with members of the Lymphoid enhancing factor/T cell factor (Lef/Tcf) family of DNA binding proteins. Members of the Lef/Tcf family bind DNA via the HMG domain, allowing the recruitment of transcriptional activation/repressor complexes, reviewed in (Clevers and van de Wetering, 1997). Vertebrate Tcf1 binds to members of the Grg family of proteins, which are homologues of *Drosophila* groucho, a known transcriptional repressor (Fisher and Caudy, 1998; Roose et al., 1998). When the nuclear levels of armadillo are low, groucho binds *Drosophila* Tcf forming a transcriptional repressor complex (Cavallo et al., 1998). In the presence of armadillo, groucho is displaced from Tcf allowing the binding of armadillo. This allows the formation of a transcriptional activation complex consisting of legless, pygopus, Lef/Tcf and armadillo activating Wg gene transcription (Belenkaya et al., 2002; Brunner et al., 1997; Ishitani et al., 2003; Kramps et al., 2002; van de Wetering et al., 1997). A model of the Wg signalling pathway in shown in Figure 1.1.

1.2.2 The *Drosophila* planar cell polarity pathway

The outer cuticle of the adult *Drosophila* contains a stereotypical arrangement of sensory bristles/cellular hairs on the wing, abdomen, thorax and ommatidia of the eye. Mutations that affect the orientation of these bristles are known as 'polarity' mutants and are components of the planar cell polarity (PCP) signalling cascade, reviewed in (Adler, 2002; Gray et al., 2011). A table detailing the core components of the PCP pathway is shown (Table 2). The *Fz* locus was originally identified as a PCP mutant that did not affect gross development of *Drosophila*. In the wildtype *Drosophila* wing the bristle cells are all orientated distally, in line with the major axes of the wing. Homozygous mutations in *Fz* led to disorientation of bristle cells in the wing disc. Bristle cell polarity was not completely randomised in these mutants, instead regions existed in the wing where normal polarity was maintained (Adler et al., 1987; Gubb and García-Bellido, 1982).

The stereotypical arrangement of bristles in *Drosophila* has been used as a system to identify other components of the PCP pathway. Fz localises to the distal/apical compartments of polarised epithelial cells in the wing disc. LOF

Table 1.2; Core components of the PCP pathway.

Drosophila	***Vertebrate***	**Protein type**	**Reference**
Frizzled (Fz)	Frizzled (Fz)	Seven pass transmembrane protein	(Gubb and García-Bellido, 1982; Niehrs, 2012)
Vangogh/Strabismus (Stbm)	Vangogh like (Vangl)	Four pass transmembrane protein	(Jessen and Solnica-Krezel, 2004; Jessen et al., 2002; Taylor et al., 1998; Wolff and Rubin, 1998)
Flamingo/Starry night	Celsr	Seven pass transmembrane protein	(Boutin et al., 2012; Chae et al., 1999; Usui et al., 1999)
Dishevelled (Dsh)	Dishevelled (Dvl)	Cytoplasmic protein	(Theisen et al., 1994; Wallingford and Habas, 2005)
Prickle	Prickle	Cytoplasmic protein containing LIM domains	(Gubb and García-Bellido, 1982; Gubb et al., 1999)
Diego	Inversin	Cytoplasmic ankyrin repeat protein	(Feiguin et al., 2001; Lienkamp et al., 2012)

mutation in *Dsh* leads to the disorientation of bristles in the legs, thorax and eyes of *Drosophila* (Theisen et al., 1994). Over-expression of Dsh also caused defects in cell polarity in the developing wing disc and a specific subdomain of Dsh, the DEP domain, was required for this phenotype (Axelrod, 2001). Dsh is downstream of Fz in establishing cell polarity, as LOF mutations in *Dsh* rescued wing PCP defects caused by the over-expression of Fz (Krasnow et al., 1995).

Van gogh/strabismus (Stbm) encodes a four pass transmembrane protein that localises to the proximal domain of polarised cells along with the cytoplasmic protein prickle. *Stbm* mutant *Drosophila* show polarity defects in the wings and eyes of adult flies (Taylor et al., 1998; Wolff and Rubin, 1998). The PCP phenotype caused by LOF mutations in *Stbm* was suppressed by LOF mutations in *prickle. Prickle* encodes a LIM domain protein that acts cell autonomously to regulate PCP. LOF mutations in *prickle* cause polarity defects in the *Drosophila* eye, wing and legs (Gubb and García-Bellido, 1982; Gubb et al., 1999). Stbm and prickle localise to the proximal boundary of polarised epithelial cells in the wing disc, with Fz and Dsh accumulating distally. LOF mutations in *Fz* or *Dsh* result in a loss of the asymmetric localisation of prickle. LOF mutations in *prickle* or *Stbm* cause a loss of the asymmetric localisation of Fz (Axelrod, 2001; Strutt, 2001; Tree et al., 2002). Prickle can bind Dsh and

over-expression of prickle inhibited the ability of Fz to induce the translocation of Dsh to the cell membrane in U2OS cells (Tree et al., 2002). Stbm and prickle and Fz and Dsh form separate complexes on proximal and distal membranes respectively, repressing the activity of each other, thus maintaining cell polarity.

Flamingo and diego are two other proteins involved in establishing PCP. Flamingo encodes a seven transmembrane domain member of the cadherin superfamily. LOF mutations in *flamingo* result in cell polarity defects in the ommatidia and wing discs (Usui et al., 1999). *Diego* encodes an ankyrin repeat protein that functions as a scaffolding protein inside the cell. LOF mutations in *diego* result in polarity defects in the ommatidia and wing discs that resemble those of *flamingo* mutants. Flamingo and diego localise to both proximal and distal membranes in polarised epithelial cells. LOF mutations in *flamingo* lead to a loss of membrane localised diego and vice versa (Feiguin et al., 2001; Usui et al., 1999). LOF mutations in *flamingo* resulted in a loss of Fz and Dsh accumulation on the distal cell membranes of wing disc cells (Axelrod, 2001; Strutt, 2001). In addition LOF mutations in *Dsh* caused a reduction in the levels of flamingo associating with the cell membrane (Usui et al., 1999). The planar cell polarity genes depend on each other for their correct localisation inside the cell. Loss of one gene results in the miss-localisation of others resulting in PCP defects. A diagram of the *Drosophila* PCP pathway can be seen (Figure 1.2).

1.3.0 The vertebrate Wnts

To date 19 members of the Wg/Wnt family of secreted glycoproteins have been identified in vertebrates, reviewed by (Nusse and Varmus, 2012). Wg signalling is important for patterning *Drosophila* embryos and initial investigations into the function of the Wnt proteins provided similar evidence in vertebrates. The *Xenopus* embryo possesses a highly efficient system for the translation of mRNA into protein. Microinjection of capped mRNA provides a stable transcript that is efficiently translated into protein by the embryo, reviewed in (Soreq and Huez, 1985). Over-expression of mRNA encoding *Wnt1* in the animal hemisphere of *Xenopus* embryos lead to the bifurcation of the neural tube. Histological sectioning of embryos over-expressing Wnt1 revealed the presence of a secondary neural tube and somites (McMahon and Moon, 1989). The

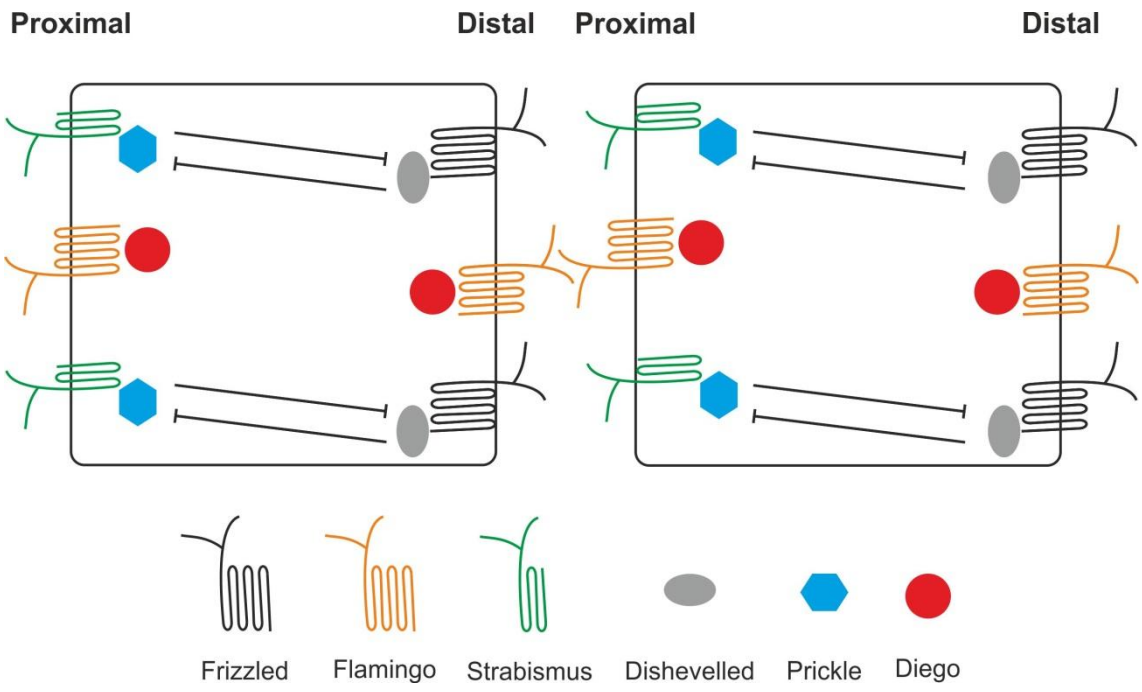

Figure 1.2; The Drosophila planar cell polarity pathway.
The *Drosophila* planar cell polarity pathway ensures that bristle/hair cells that form during *Drosophila* development have the correct orientation. Strabismus and prickle localise to the proximal membrane while frizzled and dishevelled are found distally. Flamingo and its partner diego localise to both proximal and distal membranes. Cross inhibitory interactions between strabismus-prickle and Frizzled-dishevelled maintain cell polarity.

findings of this experiment were akin to those of Spemann and Mangold in the 1920's. Transplantation of tissue from the dorsal marginal zone (DMZ) of one embryo to the ventral marginal zone (VMZ) of a second embryo resulted in the induction of secondary neural and muscular structures. The secondary structures consisted of cells from the host embryo, not those from the transplanted DMZ. The transplanted DMZ was able to organise the cells in the host embryo to form a second neural tube and hence became known as the organiser. Wnt1 was acting like an organiser to pattern the formation of a secondary axis.

Wnt ligands can be broadly divided into two separate categories based on their activities in *Xenopus*. Canonical Wnt ligands are able to induce axis duplication and rescue axis formation in UV ventralized embryos. In contrast non-canonical Wnt ligands are unable to either duplicate, or rescue axis formation in *Xenopus*, but instead cause a shortening of the embryonic axis (Du et al., 1995). A table displaying the signalling activities of various Wnt ligands can be seen (Table 3).

Table 1.3; Wnt ligand signalling activities			
Wnt ligand	**Classification**	**Activity in *Xenopus***	**Reference**
Wg	Canonical	Axis duplication and rescue of UV ventralized embryos	(Chakrabarti et al., 1992)
Wnt1	Canonical	Axis duplication	(McMahon and Moon, 1989)
Wnt3a	Canonical	Axis duplication	(Wolda et al., 1993)
Wnt4	Non-canonical	Axial shortening and inhibition of activin induced convergent extension	(Du et al., 1995)
Wnt5a	Non-canonical	Axial shortening and inhibition of activin induced convergent extension	(Moon et al., 1993)
Wnt8a	Canonical	Axis duplication and rescue of UV ventralized embryos	(Moon et al., 1993; Sokol et al., 1991)
Wnt11b	Non-canonical	Axial shortening and inhibition of activin induced convergent extension	(Du et al., 1995; Ku and Melton, 1993)

1.3.1 Wnt/Wg synthesis and secretion

The secretion of Wnt/Wg depends on the action of the enzyme porcupine and the chaperone evenness interrupted (Evi). Porcupine protein localises to the endoplasmic reticulum (Kadowaki et al., 1996) and is required for Wg secretion (van den Heuvel et al., 1993). Wnt/Wg is hydrophobically modified and these modifications are required for its secretion/activity. Porcupine catalyses the addition of palmitoleic acid to serine 209 on Wnt3a. Mutation of serine 209 on Wnt3a to alanine (Wnt3aS209A) inhibits Wnt3a secretion, and Wnt3aS209A mutants are unable to activate canonical Wnt signalling in *Xenopus* (Takada et al., 2006). Wnt3a is also postranslationally modified by the addition of palmitate to cysteine 77 (Willert et al., 2003). Mutation of cysteine 77 to alanine inhibits the ability of Wnt3a to stabilise β-catenin in *Mouse* L cells (Willert et al., 2003). In *Drosophila,* palmitate modification at cysteine 93 and palmitoleic acid modification at serine 239 are required for Wg secretion/activity (Franch-Marro et al., 2008a). Wnt/Wg is hydrophobically modified by the action of porcupine and this is required for Wnt/Wg secretion/signalling.

Evi, also known as Wntless/Sprinter (Bänziger et al., 2006; Goodman et al., 2006) was identified in an RNAi screen for genes involved in Wg signalling

(Bartscherer et al., 2006). Evi encodes a multipass transmembrane protein that acts as a chaperone to traffic Wg from the golgi to the cell surface (Bänziger et al., 2006; Bartscherer et al., 2006). LOF mutations in *Evi* blocks Wg secretion and leads to a loss of naked cuticle in *Drosophila* larva and a loss of *senseless* expression in the developing wing disc (Bartscherer et al., 2006). Evi requires the action of the retromer complex in order to facilitate Wnt/Wg secretion. Of the five retromer subunits identified in *Yeast;* Vps26, Vps29 and Vps35 are highly conserved in mammals. The retromer is required for the recycling of components targeted to the endosome to the trans golgi network, reviewed by (Attar and Cullen, 2010). After trafficking Wnt to the plasma membrane, Evi is internalised and targeted to the early endosomes. From here the retromer complex then recycles it back to the golgi to prevent its degradation in multi vesicular bodies (Belenkaya et al., 2008; Franch-Marro et al., 2008b). LOF mutations in *Vps35* lead to the intracellular accumulation of Wg in the wing disc and a decrease in the expression of *senseless* (Belenkaya et al., 2008; Franch-Marro et al., 2008b).

The retromer is important for the secretion Wnt ligands in vertebrates as well. Knockdown of *Vps35* in L cells inhibits the secretion of Wnt3a and Wnt5a (Belenkaya et al., 2008). *Evi* has a dynamic expression pattern during *Xenopus* development (Kim et al., 2009). Microinjection of a morpholino targeting *Evi* causes a reduction in the size of the eyes and inhibits the formation of the pronephros in *Xenopus*. In addition knockdown of *Vps35* causes defects in blastopore/neural tube closure and leads to a reduction in the size of the eyes in *Xenopus.* The retromer is required to recycle Evi from the early endosomes to the golgi, where it can then act as a chaperone to transport Wnt/Wg to the cell surface.

1.3.2 The canonical Wnt receptors

There is a high degree of conservation between components of the Wg signalling pathway in *Drosophila* and the canonical Wnt pathway in vertebrates. Wnt ligands bind to members of the Fz family of receptors to activate Wnt signalling. There are 10 members of the Fz family in vertebrates, which all have 7 transmembrane spanning domains, reviewed in (Niehrs, 2012). Fz receptors

bind Wnt ligands via N terminal cysteine rich domains (CRDs) (Bhanot et al., 1996; Hsieh et al., 1999b). Fz receptors are vital for the development of the vertebrate embryo. Over-expression of Fz8 in the VMZ of a four cell stage embryo induces axis duplication. Over-expression of a dominant negative (DN*) fragment of Fz8 containing the CRD causes axial defects in *Xenopus* embryos (Deardorff et al., 1998). LOF mutations in *Fz5* in mouse are embryonic lethal, with mice dying due to defects in yolk sac angiogenesis (Ishikawa et al., 2001).

Activation of the canonical Wnt pathway also requires LRP5/6, which are homologues of the *Drosophila* gene *arrow* (Wehrli et al., 2000). Mice with LOF mutations in *LRP6* display severe developmental abnormalities dying at birth. The abnormalities are remarkably similar to the *swaying (Wnt1)* and *vestigial tail (Wnt3a)* LOF mutants (Pinson et al., 2000). In *Xenopus* over-expression of LRP6 in the VMZ of four cell embryos induces axis duplication. Activation of canonical Wnt signalling requires the cytoplasmic domain of LRP6. LRP6ΔC is a C terminal deletion mutant, which is missing the majority of its cytoplasmic domain. Over-expression of LRP6ΔC inhibits the ability of Wnt2, Wnt3a and Wnt8a to activate canonical Wnt gene expression in animal cap tissue. The N terminal region of LRP6 binds to Wnt1 and this region of LRP6 forms a complex with the CRD of Fz8 in a Wnt1 dependent manner (Tamai et al., 2000). One conclusion from this is that LRP5/6 and Fz form a complex in the presence of Wnt to activate canonical Wnt signalling. Analysis of the X-ray crystal structure of Wnt8a bound to the CRD of Fz8 has revealed a patch of approximately 10 amino acids at the opposite end of Wnt8a to the Fz8 CRD binding region. LRP6 may bind to this region of Wnt8a to form a Wnt signalling complex with Fz8 *in vivo* (Janda et al., 2012).

Inhibiting the formation of Wnt-Fz-LRP5/6 complexes disrupts canonical Wnt signalling. Dickkopf1 (Dkk1) is a member of a family of secreted proteins expressed in the organiser domain of *Xenopus* embryos (Glinka et al., 1998). Microinjection of mRNA encoding *Dkk1* into both ventral blastomeres of a four cell embryo supressed the ability of Wnt8a, but not Dvl to induce axis duplication (Glinka et al., 1998). Dkk1 binds with high affinity to LRP5/6 disrupting the ability of LRP5/6 to bind Wnt1 and the Fz8CRD. Loss of

formation of Wnt1-Fz8CRD-LRP5/6 complexes inhibits the ability of Wnt1 to activate canonical Wnt signalling (Semenov et al., 2001).

1.3.3 The canonical Wnt signalling pathway

In the absence of Wnt

In the absence of Wnt, the cytoplasmic levels of β-catenin are kept low by the actions of the destruction complex. As in *Drosophila* this complex consists of axin1, APC, CK1α and GSK-3β. Axin1 provides a molecular scaffold for the destruction complex. Axin1 is the least abundant component of the destruction complex and is the limiting factor in β-catenin degradation (Lee et al., 2003). Axin1 contains an N terminal RGS domain (regulator of G protein synthesis), central GSK-3β and β-catenin binding domains and a C terminal DIX (Dvl and axin) domain (Hart et al., 1998; Ikeda et al., 1998; Itoh et al., 1998). Over-expression of axin1 in the DMZ of *Xenopus* embryos inhibits the formation of the embryonic axis and this requires the RGS and GSK-3β binding domains (Fagotto et al., 1999; Itoh et al., 1998). GSK-3β recruitment to the destruction complex, enhances the ability of GSK-3β to phosphorylate axin1, APC and β-catenin (Hart et al., 1998; Ikeda et al., 1998; Jho et al., 1999). Phosphorylation of axin1 enhances its stability and ability to bind β-catenin. GSK-3β induced phosphorylation of axin1 enhances the ability of axin to inhibit canonical Wnt signalling in cell culture (Jho et al., 1999; Yamamoto et al., 1999).

APC binds to β-catenin via the central domain of the protein and to the RGS domain of axin (Munemitsu et al., 1995; Rubinfeld et al., 2001). Similar to axin1, APC is phosphorylated by GSK-3β and this enhances the binding of APC to β-catenin (Rubinfeld et al., 1996). In addition to functioning in the destruction complex, APC also has a role in the nuclear export of armadillo. In the SW480 cell line APC is mutated and found in both the cytoplasm and the nucleus, a distribution mirrored by β-catenin. The C terminal region of APC contains a nuclear export signal and over-expression of a mutant version of APC lacking the nuclear export signal is unable to inhibit Wnt signalling in the SW480 cells (Rosin-Arbesfeld et al., 2000). APC functions in the destruction complex and may have a role in the nuclear export of β-catenin.

The phosphorylation of β-catenin by GSK-3β and CK1α primes β-catenin for ubiquitination and destruction in the proteasome. Phosphorylated β-catenin is bound by β-Trcp an Fbox/WD40 repeat protein. β-Trcp then recruits other components of the ubiquitination machinery (Liu et al., 1999a). Treatment of cells with an inhibitor of proteolysis leads to the accumulation of ubiquitin bound β-catenin and this requires its phosphorylation by GSK-3β (Aberle et al., 1997; Orford et al., 1997). In addition, a phosphorylation resistant form of β-catenin accumulates in cells without ubiquitin binding (Aberle et al., 1997). β-Trcp binds to GSK-3β phosphorylated β-catenin inside the cell. This primes β-catenin for ubiquitination and degradation in the proteasome keeping the cytoplasmic levels of β-catenin low.

In the presence of Wnt

The signalosome has been proposed as a model for how the presence of Wnt ligands activates canonical Wnt signalling. The model depends on the aggregation of Fz and LRP6 receptors, and the formation of Dvl-axin polymers at the plasma membrane (Bilic et al., 2007). Dvl contains three highly conserved domains for interactions with different signalling proteins. The DIX domain lies at the N terminal of Dvl and can interact with DIX domains on axin and other Dvl proteins. At the centre of Dvl there is a PDZ domain (post synaptic density, *Drosophila* disc large and zonula occludens-1), which interacts with multiple signalling proteins. At the C terminus of Dvl is the DEP domain (Dishevelled, Egl-10 and Pleckstrin), which has roles in non-canonical Wnt signalling, reviewed by (Wallingford and Habas, 2005). The DIX domains of axin and Dvl allow the two proteins to polymerise and form dynamic assemblies. In addition, deletion of the DIX domain of Dvl inhibits its ability to polymerise and activate canonical Wnt signalling (Schwarz-Romond et al., 2007a). Dvl forms highly dynamic puncta in the cytoplasm of cells which can rapidly grow in size by collision and fusion events and these puncta are able to recruit axin (Schwarz-Romond et al., 2005, 2007b).

In the signalosome, model the binding of Wnt to Fz and LRP6 induces the formation of Fz-LRP6 aggregates. This requires Dvl, which is thought to form a molecular scaffold along with axin on the inside of the plasma membrane. This

scaffold is then thought to recruit other proteins such as GSK-3β and CK1ε and/or CK1γ to the plasma membrane (Bilic et al., 2007). GSK-3β and CK1γ have both been shown to phosphorylate LRP6 (Davidson et al., 2005; Zeng et al., 2005) and CK1ε binds to axin along with Dvl and is required for Dvl to activate canonical Wnt signalling (Kishida et al., 2001; Peters et al., 1999).

Once assembled, the phospho-LRP6 aggregates overlap with caveolin both on the cell membrane and inside the cell. It is thought that the Fz-LRP6-Dvl-Axin-GSK-3β macromolecular complexes are then internalised in a caveolin dependent manner. This would provide a mechanism to spatially separate components of the destruction complex such as axin, from β-catenin in the cytoplasm. In the absence of the destruction complex, β-catenin would then accumulate in the cytoplasm (Bilic et al., 2007). Another protein that may be important in the disruption of the destruction complex is the GSK-3β inhibitor Frat (Yost et al., 1998). Frat is able to bind to a complex containing Dvl, axin and GSK-3β and reduce the ability of this complex to bind β-catenin (Li et al., 1999). Disruption of the destruction complex allows β-catenin to accumulate in the cytoplasm and then translocate to the nucleus. Once inside the nucleus β-catenin forms a complex with Lef/Tcf DNA binding proteins, which allows the activation of gene transcription (Behrens et al., 1996; Brannon et al., 1997; Huber et al., 1996; Molenaar et al., 1996). A diagram of the canonical Wnt pathway can be seen (Figure 1.3).

1.4.0 Establishing the organiser domain

Canonical Wnt signalling is required for the establishment of the dorsal axis, which depends on the presence of maternally deposited dorsal determinants in the oocyte, reviewed in (De Robertis and Kuroda, 2004). Following fertilisation, the embryo undergoes microtubule dependent cortical rotation that establishes the dorsal/ventral polarity of the embryo. If cortical rotation is blocked by irradiation with UV or nocodazole treatment, which both disrupt microtubules, the embryo becomes ventralized and the axis fails to form (Elinson, 1985; Elinson and Rowning, 1988; Malacinski et al., 1977; Vincent et al., 1986). Cortical rotation leads to the dorsal accumulation of nuclear β-catenin

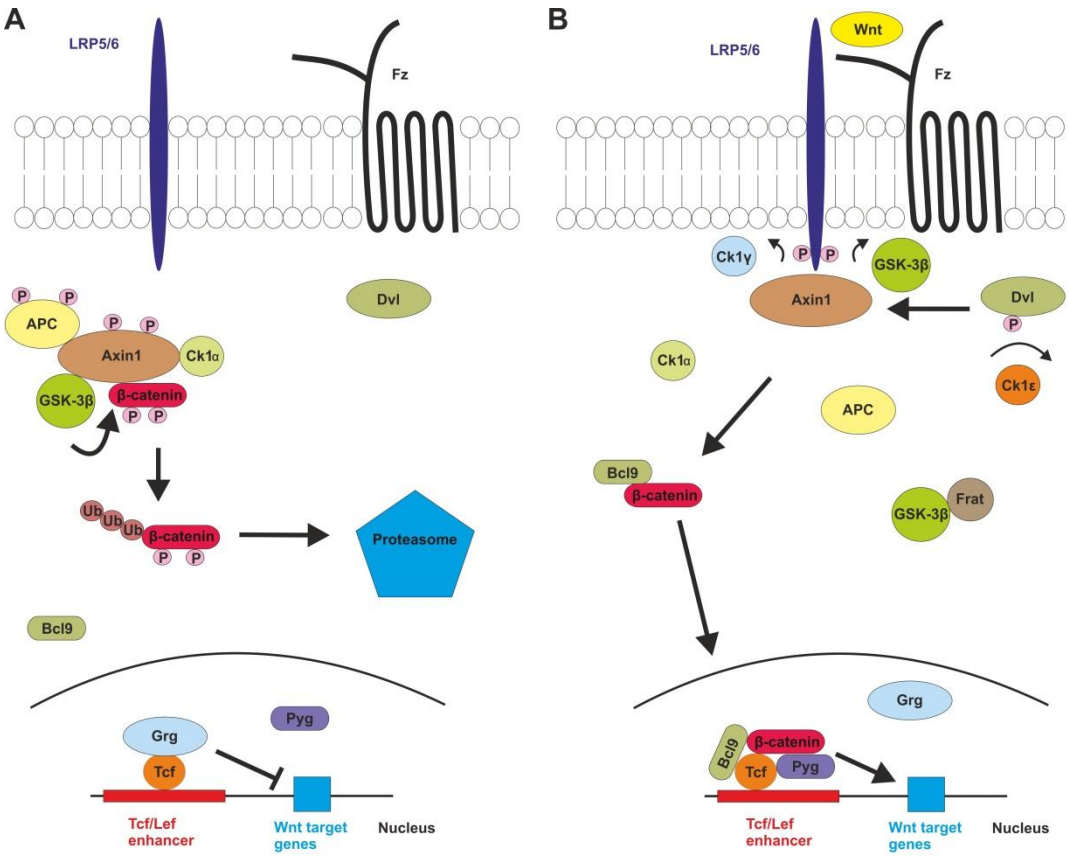

Figure 1.3; The canonical Wnt signalling pathway.
[A] In the absence of Wnt, β-catenin is bound by the destruction complex leading to its phosphorylation. This primes β-catenin for ubiquitination and destruction in the proteasome. Members of the Grg family bind Tcf in the nucleus and represses the transcription of Wnt dependent genes. [B] In the presence of Wnt LRP5/6 and Dvl are phosphorylated by members of the CK1 family and GSK-3β. Axin1 and APC become dephosphorylated and Axin1 binds to the cytoplasmic domain of LRP5/6. GSK-3β is bound and inhibited by the protein Frat. This leads to the dissociation of the destruction complex and stabilisation of β-catenin in the cytoplasm. β-catenin interacts with Bcl9 and pygopus to translocate into the nucleus where it displaces members of the Grg family from Tcf forming a transcriptional activation complex. Frizzled (Fz), low density lipoprotein receptor 5/6 (LRP5/6) dishevelled (Dvl), glycogen synthase kinase-3β (GSK-3β) adenomatous polyposis coli (APC), casein kinase 1 (CK1), pygopus (Pyg), T cell factor (Tcf), lymphoid enhancing factor (Lef), phosphate (P), figure adapted from (Kikuchi et al., 2009).

(Schneider et al., 1996; Schohl and Fagotto, 2002). β-catenin was originally identified as a structural protein that binds to E-cadherin at the plasma membrane (Nagafuchi and Takeichi, 1988; Orsulic et al., 1999; Ozawa et al., 1989). Over-expression of E-cadherin or maternal depletion of β-catenin inhibits axis formation in *Xenopus* embryos (Heasman et al., 1994). A diagram showing the formation of the organise can be seen (Figure 1.4).

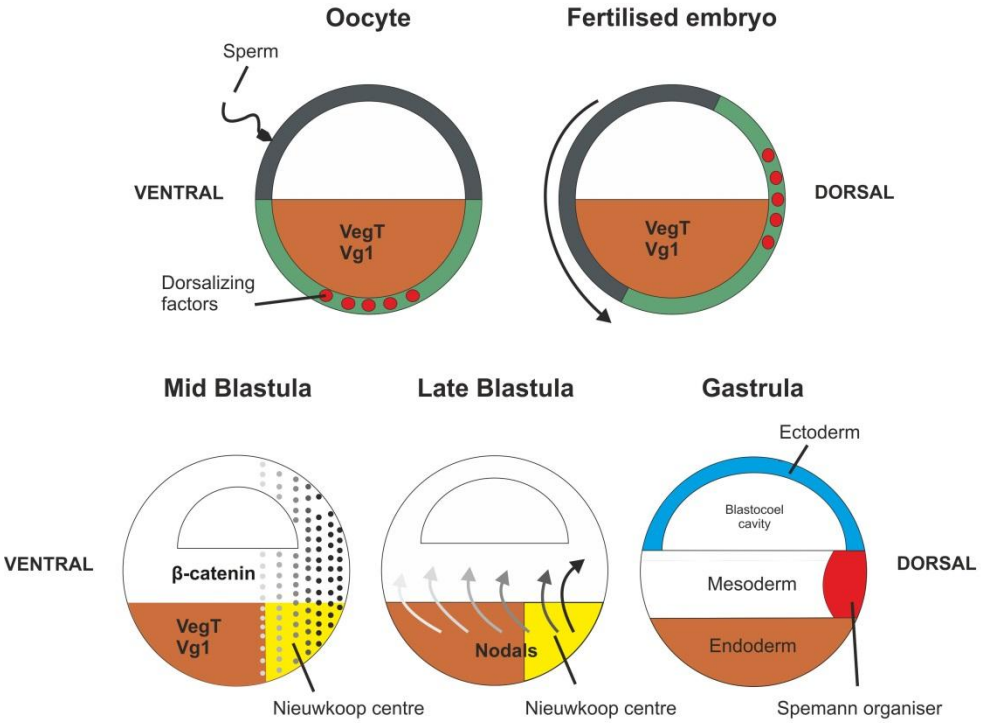

Figure 1.4; Early development of the *Xenopus* embryo.
The sperm entry point marks the future ventral side of the oocyte. Sperm entry activates cortical rotation in which the outer cortex of the embryo rotates relative to the internal cytoplasm. This results in the localisation of dorsalizing factors opposite the sperm entry point. The maternal mRNAs VegT and Vg1 are asymmetrically localised to the vegetal pole of the *Xenopus* oocyte/embryo. The overlap of nuclear β-catenin, VegT and Vg1 in the doso-vegetal embryo results in the formation of the Nieuwkoop centre that, after the mid blastula transition, synthesises and secretes nodal-related signals. Nodal-related signals induce the formation of the mesoderm with the highest levels of nodal signal, together with nuclear β-catenin; inducing the Spemann organiser (organiser) in the dorsal mesoderm. Figure adapted from (De Robertis and Kuroda, 2004).

1.4.1 Cell behaviour during gastrulation

Gastrulation involves a complex set of cell rearrangements that establish the vertebrate body plan of the embryo. Several types of cell behaviour underpin gastrulation, which include epiboly, emboli, convergence and extension. The onset of gastrulation is marked by the formation of bottle cells in the dorso-vegetal region of the embryo. Bottle cells undergo constriction at the apical membrane while elongating along the anterior/posterior axis. The effect of this is to form a wedge between the vegetal endoderm and mesoderm of the embryo, leading to the formation of the blastopore groove (Keller, 1981; Shih and Keller, 1994).

Cellular epiboly begins before the start of gastrulation. The driving force behind this is radial intercalation. Deep cells of the DMZ extend protrusions into the cells above them, the cells then interdigitate causing a reduction in thickness, but increase in width. At the same time, cells in the superficial layer flatten and divide to increase the area of the superficial layer (Keller, 1980). The force of epiboly is driven by the deep cells and this in turn drives the start of emboli at the blastopore lip (Keller, 1981).

The anterior mesoderm begins to migrate as loosely packed cells that attach to the deep cells of the ectoderm by cellular protrusions (Keller and Schoenwolf, 1977). Cells of the posterior mesoderm migrate on mass rather than as loosely packed individual cells. On involution, these cells undergo medial/lateral convergent extension. Cells lengthen and then converge along the medial/lateral axis in order to extend along the anterior/posterior axis. Convergent extension is the driving force behind gastrulation and failure of the marginal zone to involute before convergent extension begins results in the formation of exogastrula (Keller and Danilchik, 1988; Keller et al., 1985). Convergent extension during gastrulation drives the blastopore lip across the yolk plug causing the blastopore to close. As this proceeds, mesoderm from increasingly ventral regions involutes into the embryo. Eventually convergent extension drives the closure of the blastopore, marking the end of gastrulation (Keller and Danilchik, 1988). At this stage the mesoderm and endoderm have relocated inside the embryo and the anterior/posterior axis of the embryo has been established.

1.4.2 Regulating vertebrate gastrulation

Fibroblast growth factor (FGF), bone morphogenetic protein (BMP) and Wnt signalling are all involved in regulating vertebrate gastrulation (Solnica-Krezel, 2005). Activation of the FGF signalling pathway involves the dimerization of two ligand bound FGFrs, which are stabilised by heparan sulphate protegoglycans. The intracellular domains of the FGFr dimers then cross phosphorylate each other, transmitting the signal intracellularly and activating downstream signalling pathways, reviewed in (Dorey and Amaya, 2010). *Xenopus* embryos microinjected with mRNA encoding *DN* FGFr1* fail to gastrulate. Injected

embryos progress normally through early development, but by neurula stages show defects in the posterior axis, such as a lack of somites and a failure of the blastopore to close (Amaya et al., 1991; Isaacs et al., 1994). FGF signalling has also been shown to direct cell migration during vertebrate gastrulation. During *Chick* gastrulation cells from the epiblast migrate inside the embryo through the primitive streak, reviewed by (Solnica-Krezel, 2005). FGF4a was shown to act as a chemo attractant and FGF8b a chemo replant to cells from the middle of the primitive streak (Yang et al., 2002). FGF signalling has roles in directing cell migration and regulating convergent extension during vertebrate gastrulation.

BMPs belong to the transforming growth factor β (TGF-β) family of signalling molecules that includes nodals and activins. BMP ligands bind to type I and type II BMP receptors, inducing the formation of receptor dimers that activate downstream signalling, reviewed in (Miyazono et al., 2010). During *Zebrafish* gastrulation the mesoderm can be broadly divided into regions undergoing high levels of convergent extension and regions that neither converge nor extend (Myers et al., 2002; Sepich et al., 2000). High levels of BMP signalling are correlated with cells displaying no convergent extension behaviour (Nguyen et al., 1998; Nikaido et al., 1997). Over or under activation of BMP signalling alters the animal-vegetal length of the mesendoderm in *Zebrafish* (Hammerschmidt et al., 1996; Hild et al., 1999; Myers et al., 2002) BMP signalling regulates convergent extension during *Zebrafish* gastrulation.

1.5.0 The role of non-canonical Wnt signalling during gastrulation

Non-canonical Wnt signalling plays an important role in regulating vertebrate gastrulation. Over-expression of Wnt5a or Wnt11b causes a reduction in the length of the anterior/posterior axis of *Xenopus* embryos (Du et al., 1995; Moon et al., 1993). The *Zebrafish* mutants *pipetail (Ptl)* and *silberblick (Sbl)* have LOF mutations in *Wnt5a* and *Wnt11b* respectively. Both mutants display medial/lateral convergent extension defects during gastrulation and a shortening of the anterior/posterior axis (Hammerschmidt et al., 1996; Heisenberg et al., 2000; Kilian et al., 2003). In *Mouse,* LOF mutations in *Wnt5a*

disrupt the formation of the primitive streak and cause a severe reduction in the length of the anterior/posterior axis (Yamaguchi et al., 1999). Wnt5 and Wnt11 are required for medial/lateral convergent extension during gastrulation. Over-expression or LOF of *Wnt5*/*Wnt11* results in shortening of the anterior/posterior axis of the embryo.

Gastrulation is a complex process and activin treated animal caps provide a simplified model to analyse cell behaviour. By mid blastula stage the blastocoel cavity has formed and it is simple to dissect tissue from the ectoderm to culture in saline solution. Explants that are cultured alone in saline solution round up to form spherical balls of tissue. However treatment of freshly isolated animal caps with the TGF-β/Nodal like factor activin induces the formation of dorsal mesoderm (Smith, 1987). At Nieuwkoop and Faber stage 10, Nieuwkoop and Faber, (1994), activin treated animal caps undergo medial/lateral convergent extension, mimicking the movements of the dorsal mesoderm *in vivo* (Asashima, 1990). A similar culture model can be obtained by isolating tissue explants from the DMZ. Explants are taken from the embryo at early gastrula stages (NF 10-10.5) and then cultured in saline solution. Similar to activin treated animal caps, DMZ explants undergo medial/lateral convergent extension at the same time as sibling embryos (Wilson and Keller, 1991). Both of these models have been used to investigate the effects of signalling proteins on medial/lateral convergent extension *in vitro.*

1.5.1 The PCP pathway regulates cell behaviour during gastrulation

Homologues of the *Drosophila* PCP pathway are important for regulating gastrulation in vertebrates. Fz7 is expressed in the dorsal region of gastrula stage *Xenopus* embryos and over-expression of Fz7 inhibits blastopore closure and causes a severe shortening of the anterior/posterior axis (Djiane et al., 2000). The Wnt co-receptor Ror2 also functions in PCP signalling. *Mouse* knockout models of *Ror2* show randomisation of auditory hair cell polarity in the organ of corti (Yamamoto et al., 2008b). Over-expression of Ror2 inhibits convergent extension in *Xenopus* embryos. Ror2 synergises with both Wnt11b

and Fz7 to inhibit convergent extension during *Xenopus* gastrulation (Hikasa et al., 2002).

RhoA, Rac and Cdc42 belong to the Rho family of small GTPases. Rho GTPases cycle between active GTP bound and inactive GDP bound states. Guanine nucleotide exchange factors (GEFs) promote the binding of GTP to the Rho GTPases activating the proteins. GTPase activating proteins (GAPs) promote the natural GTPase activity of Rho family proteins, which hydrolyses GTP returning the GTPases to an inactive state. Members of the RhoA, Rac and Cdc42 subfamilies of have all been shown to play roles in regulating the cytoskeleton, reviewed by (Heasman and Ridley, 2008). The *Drosophila* homologues of RhoA and Rac have roles in PCP signalling. Over-expression of Dsh in the *Drosophila* wing disc disrupts the planar polarisation of bristles (Axelrod, 2001; Theisen et al., 1994). *LOF* mutations in *RhoA* or *Rac*, but not cdc42, supressed PCP phenotypes caused by Dsh over-expression (Boutros et al., 1998). One conclusion from this is that RhoA and Rac function downstream of Dsh in the *Drosophila* PCP pathway.

Dvl, RhoA and Rac are all members of the PCP pathway in vertebrates. Over-expression of Dvl or Xdd1 inhibited the ability of Keller explants to undergo medial/lateral convergent extension (Wallingford et al., 2000). Over-expression of wildtype RhoA rescues gastrulation defects caused by DN* versions of Dvl in *Xenopus* (Kim and Han, 2005). Activation of RhoA requires the formin homology protein dishevelled associated activator of morphogenesis (Daam1) and the weak activating GEF (wGEF). Daam1 binds to the PDZ and DEP domains of Dvl and acts as a molecular scaffold to bind wGEF and RhoA. Over-expression of wGEF in *Xenopus* embryos causes gastrulation defects (Tanegashima et al., 2008) and knockdown of *wGEF* or *Daam1* inhibits activin induced convergent extension in animal caps (Habas et al., 2001; Tanegashima et al., 2008). Jun N terminal kinase (JNK) and Rho associated kinase (Rock) lie downstream of Rac and RhoA. Transfection of HEK293T cells with DN*Rac, but not DN*Rho inhibited Wnt1 induced phosphorylation of the JNK target c-Jun (Habas et al., 2003). In *Xenopus* c-Jun phosphorylation in response to Wnt11b or Dvl was supressed by microinjecting mRNA encoding *DN*RhoA* (Kim and Han, 2005). Rock is downstream of RhoA and both over-expression or

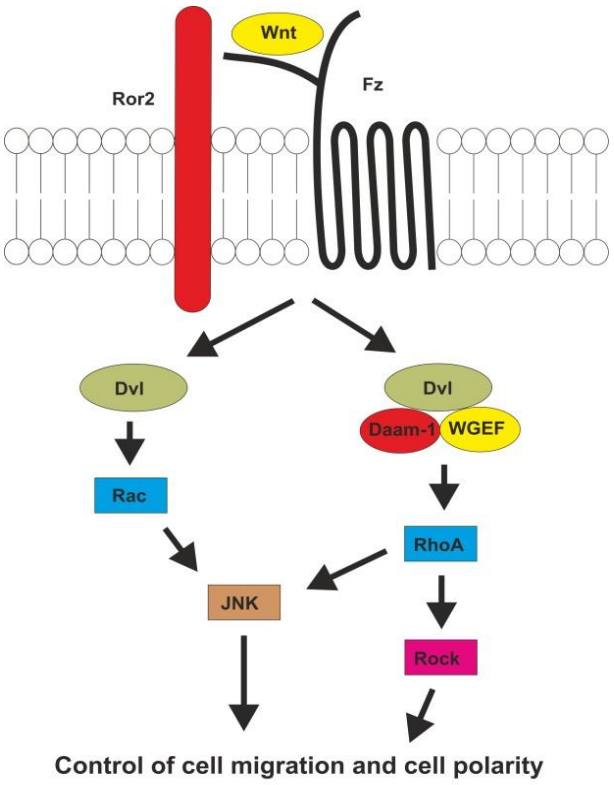

Figure 1.5; The vertebrate PCP pathway.
Diagram of the vertebrate PCP pathway. In the presence of Wnt, Fz and Ror2 form a complex. This leads to the downstream activation of Dvl and the small GTPases Rac and RhoA. Rac and RhoA in turn activate JNK and Rock, which have downstream roles in regulating cell polarity and cell migration. Fz (Frizzled), Dvl (vertebrate Dvl), wGEF (weak activating GEF), Daam1 (dishevelled associated activator of morphogenesis) JNK (Jun N terminal kinase), Rock (Rho associated kinase), figure adapted from (Kikuchi et al., 2009).

knockdown of *Rock* inhibits convergent extension in DMZ explants (Kim and Han, 2005). A diagram depicting the vertebrate PCP pathway is shown (Figure 1.5).

1.5.2 The Wnt/calcium pathway

The Wnt/calcium pathway is another branch of non-canonical Wnt signalling in vertebrates. Microinjection of mRNA encoding *Wnt5a* or *Fz2* increases both the frequency and amplitude of calcium fluxes in *Zebrafish* embryos (Slusarski et al., 1997a, 1997b). Wnt5a and Fz2 synergise to enhance calcium flux when over-expressed together in *Zebrafish,* however Wnt8a and Fz2 do not (Slusarski et al., 1997b). Heterotrimeric G proteins are important for activating the Wnt calcium pathway. Fz2 induced calcium fluxes were inhibited by microinjecting mRNA encoding the A protomer of pertussis toxin (Slusarski et al., 1997b). Wnt can activate intracellular calcium signalling via heterotrimeric G proteins in vertebrates.

The Wnt/calcium pathway has roles in regulating cell fate, migration and polarity during development. Calcium waves are observed in DMZ explants undergoing convergent extension and inhibiting intracellular calcium release blocks these

movements (Wallingford et al., 2001). In addition calcium spikes have been observed in DMZ cells prior to them undergoing medial/lateral polarisation (Shindo et al., 2010). Dvl lies downstream of Wnt and Fz in the Wnt/calcium pathway. Over-expression of a DvlΔDIX mutant in *Zebrafish* also induces calcium flux and this is insensitive to pertussis toxin (Sheldahl et al., 2003). The Dvl induced calcium influx leads to the activation of protein kinase C (PKC) and calcium/calmodulin kinase II (CamKII). Microinjection of *Xenopus* embryos with mRNA encoding *Wnt5a, Wnt11b* or *Fz2* lead to an increase in CamKII activity (Kuhl et al., 2000). CamKII has roles in regulating convergent extension and the dorsal/ventral polarity of *Xenopus* embryos. Endogenous CamKII activity is higher on the ventral side of the early *Xenopus* embryo than on the dorsal side. Over-expression of a constitutively active version of CamKII on the dorsal side of the *Xenopus* embryo ventralized the embryo inhibiting axis formation. In addition, over or under activation of CamKII signalling inhibits convergent extension movements in Keller explants (Kuhl et al., 2001). CamKII has roles in regulating dorsal ventral polarity and convergent extension in *Xenopus*.

PKC has roles in regulating tissue separation and cell polarity during gastrulation. PKCα is localised primarily in the cytoplasm when microinjected into *Xenopus* animal caps. Over-expression of DvlΔDix induces the translocation of PKCα to the plasma membrane (Sheldahl et al., 2003) PKCα is important for regulating cell-cell adhesion in *Xenopus* embryos. Knockdown of *Fz7* in DMZ results in a loss of segregation behaviour between DMZ and animal cap explants. Interestingly segregation can be rescued by over-expressing PKCα in DMZ explants (Winklbauer et al., 2001).

Cdc42 and PKCδ are both important for regulating convergent extension in *Xenopus*. Microinjection of mRNA encoding Cdc42, or a morpholino targeting *Cdc42* results in a shortening of the anterior/posterior axis of *Xenopus* embryos. Interestingly, DN*Cdc42 was able to rescue the inhibition of activin induced convergent extension in animal caps, caused by Wnt5a or PKCα (Choi and Han, 2002). PKCδ is important in regulating medial/lateral convergent extension during gastrulation. Microinjection of morpholinos targeting *PKCδ* into both dorsal and ventral blastomeres caused truncation of the anterior/posterior axis of *Xenopus* embryos and inhibited blastopore closure. In

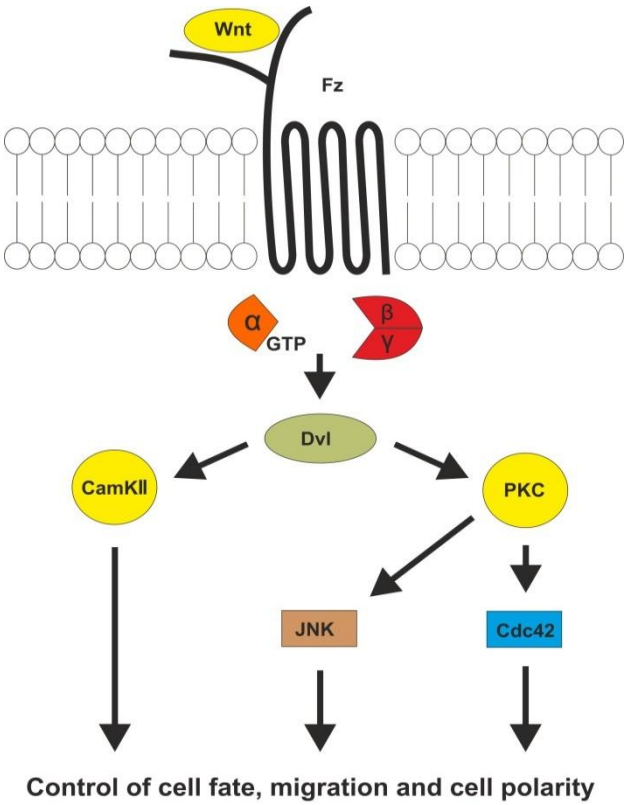

Figure 1.6; The Wnt/calcium pathway Diagram of the Wnt calcium pathway. In the presence of Wnt, Dvl is activated by heterotrimeric G proteins. This leads to an influx of calcium and the activation of CamKII and PKC. CamKII has roles in regulating dorsal/ventral cell fate and convergent extension. PKC activates JNK and Cdc42 downstream, which affects cell adhesion, polarity and medial/lateral convergent extension. Fz (frizzled), α,β, γ (α,β,γ subunits of a heterotrimeric G protein), Dvl (vertebrate dishevelled), CamKII (calcium/calmodulin kinase II), PKC (protein kinase C), JNK (jun N terminal kinase) figure adapted from (Kikuchi et al., 2009)

addition knockdown of *PKCδ* inhibited both medial/lateral elongation and convergent extension in DMZ explants. PKCδ also has a role in activating JNK downstream in the Wnt/calcium pathway (Kinoshita et al., 2003). A diagram of the Wnt/calcium pathway can be seen (Figure 1.6).

1.6.0 Cross regulation of the canonical and non-canonical Wnt signalling pathways

Cross talk occurs between the canonical and non-canonical Wnt signalling pathways. Over-expression of Wnt8a on the ventral side of the embryo induces the formation of a secondary axis (Christian et al., 1991; Sokol et al., 1991). Microinjection of mRNA encoding *Wnt5a, Wnt11b* or a constitutively active version of *CamK*II together with *Wnt8a* inhibits the ability of *Wnt8a* to induce axis duplication in *Xenopus* (Kuhl et al., 2000; Torres et al., 1996). However Wnt5a is unable to supress axis duplication caused by over-expressing DN* GSK-3β. One conclusion from this, is that Wnt5a and Wnt11b inhibit canonical Wnt signalling upstream of β-catenin. In addition over-expression of mRNA encoding *Lef1* or *Xnr3,* blocks the inhibitory effects of constitutively active CamKII on DMZ convergent extension (Kuhl et al., 2001).

Several mechanisms have been proposed to explain the cross inhibitory effects of the canonical and non-canonical Wnt signalling pathways. Maye et al., (2004) proposed receptor competition, as a method for non-canonical inhibition of canonical Wnt signalling. Wnt11 selectively inhibited the ability of Wnt1, but not Wnt7a to activate canonical Wnt signalling in NIH3T3 cells. As *Wnt11* was not co-transfected with *Wnt1* or *Wnt7a* it is unlikely to form oligomers with either Wnt. This favours a model in which Wnt11 selectively competes with Wnt1 to bind Fz (Maye et al., 2004). Wnt5a inhibits the ability of Wnt3a to bind the Fz2CRD in HeLaS3 cells (Sato et al., 2009). Non-canonical Wnt ligands can actively compete with canonical Wnt ligands to bind to Fz.

Dvl functions in both the canonical and non-canonical Wnt signalling cascades. Work in *Drosophila* has suggested that Dvl may be a limiting factor in the activation of different Wnt signalling pathways. Wu et al., (2004) demonstrated that there is a limited pool of Dsh in *Drosophila* that can be sequestered at the apical face of cells inhibiting Wg signalling. In vertebrates activation of non-canonical Wnt signalling by Wnt11b results in the translocation of Dvl from the cytoplasm to the cell membrane (Yamanaka and Nishida, 2007). Re-direction of Dvl to the plasma membrane in response to non-canonical signalling may prevent Dvl functioning in the canonical Wnt pathway.

Wnt5a is able to inhibit canonical Wnt signalling via Siah1 and NEMO-like kinase (NLK) dependent pathways. Siah1 contains a RING finger domain which is known to interact with ubiquitin conjugating enzymes (Budhidarmo et al., 2012; Hu et al., 1997). Wnt5a is able to target a GSK-3β resistant form of β-catenin for degradation via Siah1 (Topol et al., 2003). In addition Wnt5a is able to induce the phosphorylation of Tcf/Lef factors via NLK and this requires CamKII (Ishitani et al., 2003). Phosphorylation of Tcf4 had been shown to inhibit the ability of Tcf4-β-catenin complexes, but not Tcf4, to bind DNA (Ishitani et al., 1999). Cross regulation of the canonical and non-canonical Wnt signalling pathways occurs at multiple levels.

1.6.1 Activating the canonical and non-canonical Wnt signalling cascades

At present it is unclear how Wnt ligands specifically activate canonical and non-canonical Wnt signalling pathways. A sequence alignment of three canonical and three non-canonical Wnts can be seen (Figure 1.7). The hydrophobic leader sequence and 22 conserved cysteine residues are characteristics of the Wnt family of signalling molecules (Christian et al., 1991; Ku and Melton, 1993; Moon et al., 1993; Rijsewijk et al., 1987). Work by Du et al., (1995) demonstrated that it was the C terminal 140 amino acids that are required for Wnt8a to activate canonical Wnt signalling. No consistent differences in the C terminal portions of Wnt1, 3a and 8a compared to Wn4, 5a and 11b could be identified that would easily explain the differential abilities of the ligands to activate canonical and non-canonical Wnt signalling (Figure 1.7). Wnt ligands are highly insoluble and consequently little is known about the 3d structure of the signalling molecules (Miller, 2002). Recently the X-ray structure of Wnt8a was discovered by crystallising it bound to the CRD of Fz8 (Janda et al., 2012). Determining the X-ray crystal structure of other Wnt ligands may shed light on how Wnt ligands activate different signalling pathways.

Wnt ligands possess some intrinsic specificity for binding particular Fz receptors. Wnt8-AP binds DFz2, Fz4,5,7 and 8, but not Fz3 or 6 when transfected in Cos cells (Hsieh et al., 1999a). The presence of specific Wnt receptors is important for activating canonical/non-canonical Wnt signalling pathways. Microinjection of mRNA encoding *Fz5*, together with *Wnt5a* results in axis duplication in *Xenopus* (He et al., 1997). In addition *Wnt5a* is able to activate canonical Wnt signalling when transfected together with *Fz4* and *LRP6* in HEK293 cells (Mikels and Nusse, 2006). The presence of specific Wnt receptors helps dictate which Wnt signalling pathway is activated.

Collagen triple helix repeat containing protein1 (cthrc1) localises to the ECM of cells (Pyagay et al., 2005). Cthrc1 interacts with Vangl2 to regulate PCP signalling in *Mouse.* Cthrc1$^{+/-}$; Vangl2$^{+/-}$ heterozygous mice display normal hair cell polarity in the organ of corti. In contrast Cthrc1$^{-/-}$; Vangl2$^{+/-}$ mice show a

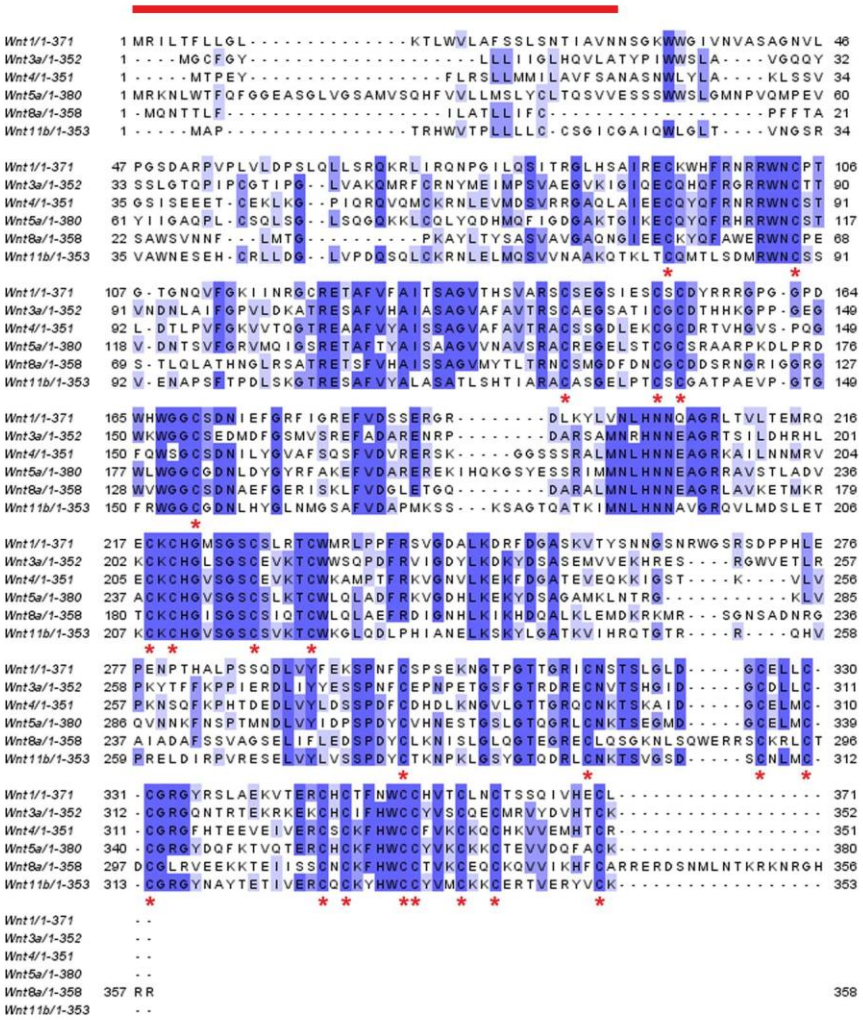

Figure 1.7; Sequence alignment of six vertebrate Wnts.
Sequence alignment of six vertebrate Wnts using 'Muscle' with default settings. Red bar indicates the hydrophobic leader sequence of the Wnts required for their secretion. Asterisks mark conserved cysteine residues characteristic of the Wnt proteins.

loss of hair cell polarity in the organ of corti. Cthrc1 enhances the ability of Wnt3a and Wnt5a to activate Rac, but inhibits the ability of Wnt3a to activate Topflash in HEK293T cells (Yamamoto et al., 2008b). Topflash is a canonical Wnt reporter that contains Tcf/Lef binding sites upstream of thymidine kinase promoter that drives the expression of luciferase (Molenaar et al., 1996). Cthcr1 favours the formation of Wnt-Fz-Ror2 receptor complexes, which activate non-canonical Wnt signalling.

Par1 and diversin have roles in regulating the activation of canonical and non-canonical Wnt signalling. Three isoforms of Par1 have been identified in vertebrates. Par1A and Par1BX are required for the activation of canonical Wnt

signalling (Ossipova et al., 2005). In contrast, Par1BY was shown to regulate convergent extension during *Xenopus* gastrulation and the translocation of Dvl-GFP to the plasma membrane in response to Fz8 (Kusakabe and Nishida, 2004; Ossipova et al., 2005). Diversin is an ankyrin repeat protein related to diego. Diversin interacts with multiple components of the Wnt signalling pathway including axin, CK1ε and Dvl (Moeller et al., 2006; Schwarz-Romond et al., 2002). Diversin inhibits the ability of Dvl to stabilise β-catenin in HEK293 cells (Schwarz-Romond et al., 2002). In contrast diversin enhanced the ability of Dvl to activate JNK signalling in these cells (Moeller et al., 2006; Schwarz-Romond et al., 2002). Par1 and diversin are able to regulate both canonical and non-canonical Wnt signalling.

Wnt ligands do possess some intrinsic specificity for activating canonical/non-canonical Wnt signalling pathways. However the presence of specific receptors, ECM proteins and proteins inside the cell helps dictate which Wnt pathway is activated.

1.6.2 Intracellular trafficking of Wnt receptor complexes

Internalisation of ligand-receptor complexes are important for cell signalling (Gagliardi et al., 2008). The binding of Wnt induces the formation of Fz-LRP5/6 or Fz-Ror2 receptor complexes and different complexes influence which Wnt signalling pathway is activated. It is possible that the different Wnt signalling complexes may be internalised by different endocytic routes. Lipid rafts are detergent resistant microdomains with a specific lipid and protein composition, reviewed by (Bethani et al., 2010). Inside lipid rafts, microdomains such as caveolae and flotillin provide specific routes of internalisation into the cell. Outside lipid raft domains, clathrin dependent internalisation is the major route of entry into the cell, reviewed by (Hanzal-Bayer and Hancock, 2007; Yanez-Mo et al., 2009).

Work in cell culture has indicated that activation of canonical Wnt signalling requires caveolin dependent endocytosis. Treatment of cells with Wnt3a results in the internalisation of Fz5 and LRP6 that colocalise with caveolin positive vesicles in HeLaS3 cells. Knockdown of *caveolin* but not *clathrin* inhibits β-

catenin stabilisation in HeLaS3 cells (Yamamoto et al., 2006). Other research has shown that activated (phosphorylated) LRP6 and constitutively active versions of LRP6 colocalise with caveolin in HeLa cells (Bilic et al., 2007; Yamamoto et al., 2008a). Interestingly, Dkk1 has been shown to redistribute activated LRP6 from detergent insoluble to detergent soluble membrane fractions in HEK293T cells. In addition, *clathrin* knockdown reduced the ability of DKK1 to inhibit Wnt3a induced β-catenin stabilisation in HeLa cells (Yamamoto et al., 2008a). The data suggests that the route of Wnt receptor internalisation may influence its ability to activate Wnt signalling.

Clathrin dependent endocytosis is important for the activation of non-canonical Wnt signalling. The phosphorylation and activation of Rac in response to Wnt5a can be prevented by knocking down *clathrin* in HelaS3 cells (Sato et al., 2009). β-arrestins bind to active GPCrs and recruit clathrin and the clathrin adaptor AP-2 to induce receptor internalisation, reviewed by (Le Roy and Wrana, 2005). In cell culture, the internalisation of Fz4 in response to Wnt5a requires β-arrestin2 and in *Xenopus* DMZ explants knockdown of β-*arrestin2* prevents the colocalisation of Dvl with AP-2(Chen et al., 2003; Kim et al., 2008). Over-expression of β-arrestin2 in *Xenopus* embryos inhibits gastrulation in whole embryos. In addition over-expression of β-arrestin2 results in the activation of RhoA in a Dvl, Daam1 dependent manner (Kim and Han, 2007). The data suggests that clathrin dependent endocytosis is important for Wnt PCP signalling, whereas caveolin dependent internalisation is important for canonical Wnt signalling.

1.7.0 Heparan sulphate proteoglycans

Wg forms a long range morphogen gradient in order to pattern the *Drosophila* wing disc (Strigini and Cohen, 2000). LOF mutations in genes involved in heparan sulphate proteoglycan (HSPG) formation cause a reduction in the levels of Wg protein present in the wing disc (Bornemann et al., 2004; Haerry et al., 1997; Takei et al., 2004). In addition LOF mutations in HSPG formation inhibits the expression of both high and low threshold Wg target genes (Han et al., 2004). One conclusion from this is that HSPGs are required for Wg diffusion and signalling *in vivo*.

HSPGs consist of repeated chains of disaccharides bound to a protein core. HSPGs show a high degree of evolutional conservation with members of this family found in vertebrates and invertebrates alike (Cano-Gauci et al., 1999; Nakato et al., 1995; Ohkawara et al., 2003; Rogalski et al., 1993; Topczewski et al., 2001). There are several different classes of HSPG, which include syndecans, glypicans and perlecans. HSPGs are able to bind to a wide variety of extracellular proteins which include collagen, fibronectin, integrins and a plethora of cell signalling ligands and receptors. Because of this mutations affecting HSPG biosynthesis/function produce a wide array of developmental defects and diseases, reviewed by (Bernfield et al., 1999; Sarrazin et al., 2011).

1.7.1 Membrane bound HSPGs

Syndecans

There are four members of the syndecan family in vertebrates, which insert into the membrane via a transmembrane domain (Sarrazin et al., 2011; Saunders et al., 1989). Syndecans bare predominantly heparan sulphate (HS) chains, but they also attach chondroitin and dermatan sulphate chains (Lee et al., 2004; Rapraeger et al., 1985). Members of the syndecan family possess up to five glycosaminoglycan (GAG) chains. Syndecans 1 and 3 attach GAG chains at both the N and C termini of the extracellular domain (Carey et al., 1992; Gould et al., 1992; Saunders et al., 1989). In contrast Syndecans 2 and 4 only attach GAG chains at the N terminus of the extracellular domain (David et al., 1992; Kojima et al., 1992; Marynen et al., 1989). Mutations in the syndecan family cause a wide variety of disorders including defects in memory, angiogenesis and muscular dystrophy, reviewed by (Sarrazin et al., 2011).

Glypicans

Glypicans are structurally related to syndecans, but attach to the plasma membrane via a glycophosphatidylinositol (GPI) anchor (David et al., 1990). There are six members of the glypican family in vertebrates, glypican1-6 and they all possess 2-3 GAG attachment sites near the C terminus of the extracellular domain, reviewed by (Hacker et al., 2005). Two different glypicans

have been identified in *Drosophila*. *Division abnormally delayed (dally)* encodes the *Drosophila* ortholog of vertebrate glypican3 and 5 (Filmus et al., 2008). *Dally like protein (dlp)* encodes the *Drosophila* ortholog of glypican4 and 6 (Filmus et al., 2008; Khare and Baumgartner, 2000).

Dally and Dlp both attach to the cell membrane via GPI anchors, however Dlp can be shed from the surface of the *Drosophila* wing disc by the actions of notum. *Notum* encodes a secreted α/β-hydroxylase that antagonises Wg signalling. GOF mutations in *notum* cause a loss of wing formation in *Drosophila* (Giráldez et al., 2002). Notum cleaves dlp, but not dally, allowing dlp to be released from the cell surface (Giráldez et al., 2002; Kreuger et al., 2004). *Knypek* encodes a *Zebrafish* ortholog of glypican4/6. LOF mutations in *knypec* inhibit medial/lateral convergent extension during gastrulation (Topczewski et al., 2001). In humans mutations in glypican3 cause the X linked Simpson-Golabi-Behmel syndrome (Pilia et al., 1996).

Perlecans

Perlecans were originally isolated from Engelbreth-Holm-Swarm sarcoma in mice. In normal mouse tissue perlecans are found associated with the basement membrane of cells (Hassell et al., 1980). The core protein of perlecan can be subdivided into five domains numbered I-V from the N to C terminals (Dolan et al., 1997). Perlecans associate with the basement membrane by binding to components of the ECM. Perlecans are able to bind heparin, fibronectin, fibulin and the nidogen-laminin complex by the IV and V domains (Brown et al., 1997; Hopf et al., 1999; Mongiat et al., 2003). The *Drosophila* gene *terribly reduced optic lobes* (trol) encodes the *Drosophila* homologue of vertebrate perlecan. LOF mutations in *trol* cause fuzzy eye phenotypes in adult *Drosophila* indicating a role for trol in PCP signalling (Datta and Kankel, 1992; Theisen et al., 1994). In mice LOF mutations in the perlecan coding gene *Hspg2* causes exencephally and skeletal abnormalities (Arikawa-Hirasawa et al., 1999). A diagram of syndecan, glypican and perlecan structure can be seen (Figure 1.8)

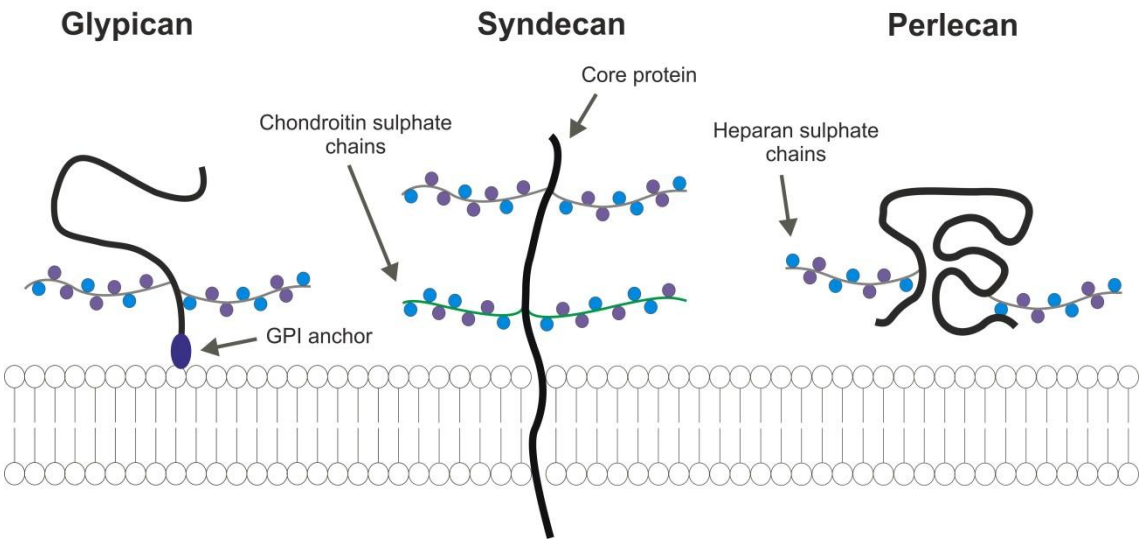

Figure 1.8; Heparan sulphate proteoglycans
Diagram showing three types of HSPG; glypicans attach to the membrane via a glycophosphatidylinositol anchor, syndecans have a transmembrane domain and perlecans associate with components of the extracellular matrix. All three types of HSPG carry HS chains with syndecans also being able to carry chondroitin and dermatan sulphate chains. Figure adapted from (Kikuchi et al., 2009).

1.7.2 HSPG synthesis

Chain initiation

HS chain synthesis is initiated in the endoplasmic reticulum (ER). GAG chain formation begins after the protein core has been translated with the formation of a tetrasaccharide linker. The linker consists of Xylose, Galactose and Glucuronic acid (GlcA) and is linked to serine residues that are N-terminal to Glycine in the protein core (Esko and Selleck, 2002; Hacker et al., 2005; Roden and Smith, 1966). Formation of the linker requires the enzymes xylosyltransferase (XT), galactosyltransferases I and II (GalTI and II) and glucuronosyltransferase I (GlcATI) (Almeida et al., 1999; Bai et al., 2001; Baker et al., 1972; Kearns et al., 1993a, 1993b; Kitagawa et al., 1998; Lindahl and Roden, 1965; Okajima et al., 1999; Wei et al., 1999). The tetrasaccharide linker is common to heparan, chondroitin and dermatan sulphate, reviewed by (Esko and Selleck, 2002).

Chain polymerisation

HS biosynthesis continues with the addition of repeated units of N-acetylglucosamine (GlcNAc) and GlcA that are catalysed by members of the exostosin family of genes (EXT) (Zak et al., 2002). Polymerisation is initiated by the addition of GlcNAc to the final residue in the linker (GlcA), which is catalysed by the EXT-like gene (EXTL) 2 (Kitagawa et al., 1999). EXTL3 is also capable of initiating polymerisation and is the vertebrate homologue of the *Drosophila* gene *brother of tout velu (botv)* (Han et al., 2004; Kim et al., 2001). HS chain polymerisation requires two members of the EXT family; EXT1 and 2. EXT1 and 2 are the vertebrate homologues of the *Drosophila* genes *tout velu (ttv)* and *sister of tout velu (sotv)* respectively (Bellaiche et al., 1998; Bornemann et al., 2004; Han et al., 2004). The genes encode enzymes that catalyse the addition of both GlcNAc and GlcA to growing HS chains. EXT1 and 2 function together in a complex that catalyses the formation of HS chains (Lind et al., 1998; McCormick et al., 2000; McCormick et al., 1998; Senay et al., 2000).

HS biosynthesis is dependent on the availability of GAG substrates. The *Drosophila* segment polarity gene *fringe connection* encodes a UDP-Xylose, UDP-GlcNAc, UDP-GlcA transporter. LOF mutations in *fringe connection* block HS synthesis in *Drosophila* (Selva et al., 2001). UDP-glucose dehydrogenase catalyses the decarboxylation of UDP-glucose to create UDP-GlcA, reviewed by (Esko and Selleck, 2002). The *Drosophila* segment polarity gene *sugarless* encodes the *Drosophila* homologue of UDP-glucose dehydrogenase (Binari et al., 1997; Häcker et al., 1997; Haerry et al., 1997; Hempel et al., 1994). LOF mutations in the *sugarless* inhibit HS chain formation in *Drosophila* (Haerry et al., 1997).

Chain modifications

Once the HS polymer has formed, the chain undergoes a series of modifications. Initially the acetyl group attached to the nitrogen residue of GlcNAc is removed and replaced by a sulphate group to create GlcNS. This N-deacetylation/N-sulphation (NDST) is carried out by members of the NDST family of enzymes. There are four members of the NDST family in vertebrates

(Aikawa and Esko, 1999; Aikawa et al., 2001; Brandan and Hirschberg, 1988; Kusche-Gullberg et al., 1998; Pettersson et al., 1991). The action of NSDT family members requires the presence of the sulphate donor 3'-phosphoadenosine 5'-phosphosulfate (PAPS) (Robbins and Lipmann, 1956). The *Drosophila* segment polarity gene *sulfateless* encodes the *Drosophila* homologue of vertebrate NDST1. LOF mutations in *sulfateless* block HSPG synthesis in *Drosophila* (Lin and Perrimon, 1999).

Following the N-deacetylation/N-sulphation of GlcNAc to GlcNS, GlcA is converted to iduronic acid (IdoA) by heparosan-N-sulfate d-glucuronosyl5-epimerase (C5-epimerase). *C5-epimearse* encodes a type II membrane protein that catalyses the conversion of GlcA to IdoA (Crawford et al., 2001; Li et al., 2001). N sulphated disaccharides are the substrate for C5 epimerise and epimerisation occurs on GlcA residues linked to GlcNS by C1 (Jacobsson et al., 1984). Following epimerisation, 2-O-sulfotransferase (2-OST) catalyses the addition of a sulphate group to C2 of IdoA (Bäckström et al., 1979; Jacobsson et al., 1984). 2-OST is capable of 2-O-sulphating both GlcA and IdoA although IdoA is the favoured substrate when both are present (Rong et al., 2000, 2001).

There are three isoforms of 6-O-sulfotransferase (6-OST) in vertebrates 6-OST1, 2 and 3. 6-OST encode type II transmembrane proteins that catalyse the addition of sulphate to the C6 residue of GlcNS on both GlcNS-IdoA and GlcNS-GlcA disaccharides (Jemth et al., 2003). Seven forms of 3-O-sulfotransferase (3-OST) have been identified in vertebrates and different forms of 3-OST show different substrate specificities (Liu et al., 1999b; Zhang et al., 2001). A diagram illustrating the HS biosynthetic pathway can be seen (Figure 1.9).

1.7.3 HSPGs regulate a variety of developmental signalling pathways

Ttv, botv and *sotv* are all homologues of vertebrate genes required for HS chain polymerisation. LOF mutations in *Ttv, botv* and *sotv* cause multiple defects during *Drosophila* development, which can be attributed to defective hedgehog (hh), Wg, FGF and decapentaplegic (Dpp) signalling

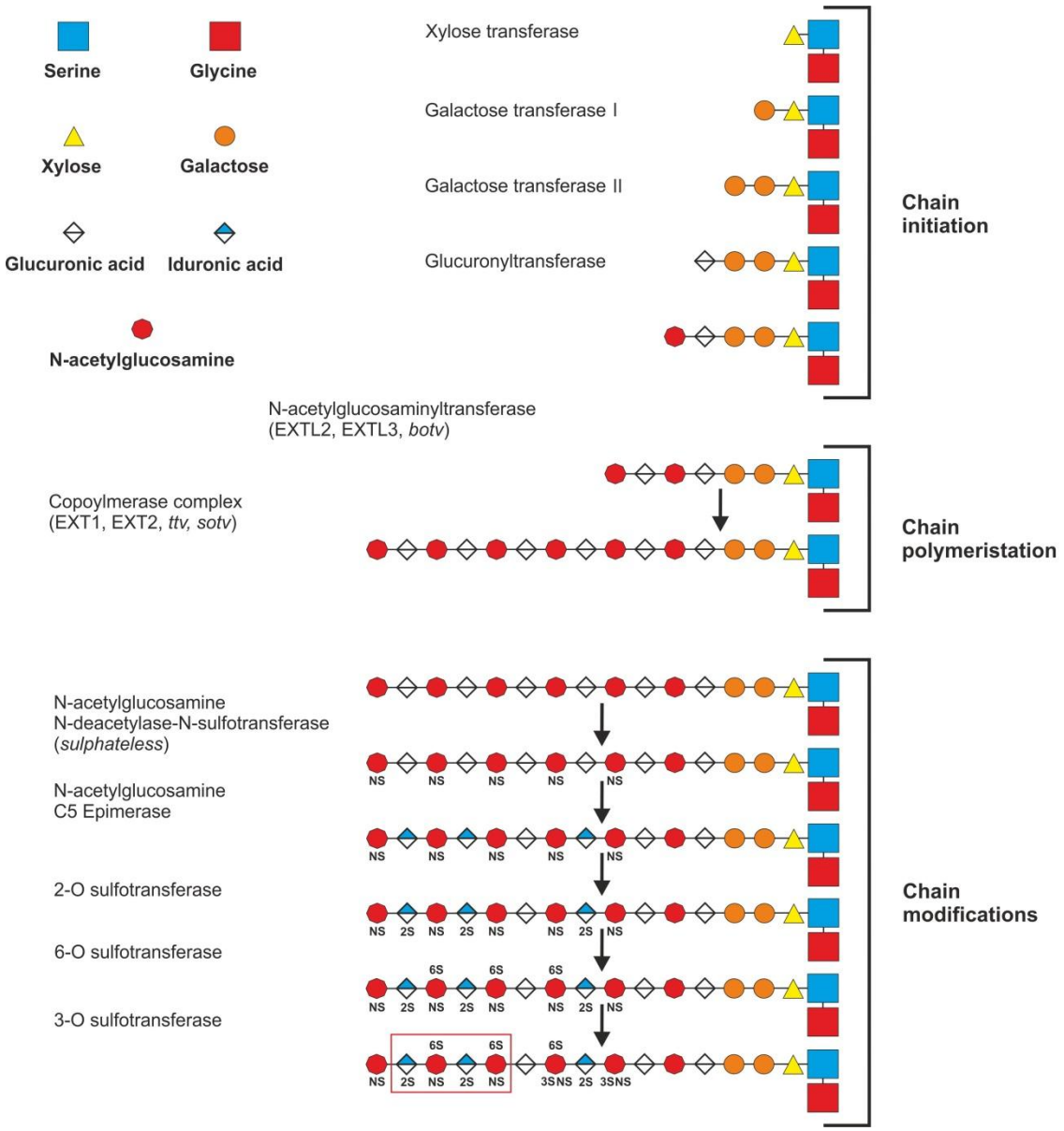

Figure 1.9; The heparan sulphate biosynthetic pathway.
Heparan sulphate (HS) biosynthesis begins with the formation of the linker region in the endoplasmic reticulum/ golgi apparatus. Once the linker has formed the chain then undergoes polymerisation with the alternate addition of alternative N-acetylglucosamine (GlcNAc), glucuronic acid (GlcA) residues. Following polymerisation the GlcNAc residues undergo N-deacetylation/N-sulphation to generate GlcNS. GlcA residues present in GlcNS-GlcA disaccharides are then converted to iduronic acid (IdoA) by epimerisation. The addition of O-linked sulphates then occurs by the action of 2/3/6-O-sulfotransferase to generate mature HS. The red box on the bottom HS chain indicates the preferred substrate for the enzyme Sulf1. Figure adapted from (Esko and Selleck, 2002).

(Bellaiche et al., 1998; Bornemann et al., 2004; Han et al., 2004; Takei et al., 2004; The et al., 1999). Dpp is the *Drosophila* homologue of BMP2/4 in vertebrates, reviewed by (Raftery and Sutherland, 1999). In addition LOF mutations in *sugarless* inhibits Wg and FGF signalling in *Drosophila* (Binari et al., 1997; Häcker et al., 1997; Haerry et al., 1997; Lin et al., 1999). Homozygus

LOF mutations in *ttv, botv, sotv* and *sugarless* are all lethal (Bellaiche et al., 1998; Häcker et al., 1997; Han et al., 2004).

Homozygous knockout mutations for *EXT1* in *Mouse* are embryonic lethal. Knockout *Mouse* embryos were consistently smaller than wildtype embryos and showed delayed formation of extra-embryonic tissue. In addition, the mesoderm failed to form in *EXT1* knockout embryos as assayed by the expression of the mesodermal marker *brachyury* (Lin et al., 2000; Smith et al., 1991). In Humans, LOF mutations in *EXT1* and *EXT2* cause the autosomal dominant disease hereditary multiple exostoses (Ahn et al., 1995; Stickens et al., 1996). The disease is characterised by the thickening/deformation of growing bones and the formation of multiple exostoses around areas of active growth (Hennekam, 1991; Solomon, 1964). HSPGs are required for the development of vertebrates and invertebrates. LOF mutations in HSPG biosynthesis, which are not lethal result in disease.

1.7.4 HSPGs require sulphate modifications to activate cell signalling

LOF mutations in *sulfateless* cause a loss of naked cuticle in *Drosophila* larvae and inhibit *distaless* expression in the wing disc (Lin and Perrimon, 1999). In addition work by Baeg et al., (2001) demonstrated that sulfateless is required for the stability of extracellular Wg in the wing disc. The *Drosophila* genes *heartless* and *breathless* encode the homologues of vertebrate *FGFr2* and *FGFr1* respectively. LOF mutations in *heartless* disrupt the migration and organisation of the *Drosophila* mesoderm during gastrulation and LOF mutations in *breathless* disrupts tracheal cell migration (Beiman et al., 1996; Gisselbrecht et al., 1996; Klämbt et al., 1992). LOF mutations in *sulfateless* inhibit both mesodermal migration and tracheal formation in *Drosophila* (Lin et al., 1999). Phosphorylated (active) MAPK is detected during mesoderm and tracheal migration and *heartless, breathless* or *sulfateless* mutant *Drosophila* show reduced MAPK activity (Lin et al., 1999). Sulphated HS is required for Wg and FGF signalling during *Drosophila* development.

Sulphated HS is also important during *Mouse* development. *NDST1* knockout mice die perinatally appearing cyanotic. Analysis of lung function in knockout mice revealed that the lungs failed to inflate after birth. Cross sections through the lungs revealed that *NDST1* knockout mice had a reduced alveolar surface area and less secreted surfactant in the lungs (Fan et al., 2000; Ringvall et al., 2000). Targeted disruption of the *Mouse 2-OST* gene also causes lethality. *2-OST* knockout mice are either stillborn or die within 24 hours of birth, with bilateral renal agenesis (Bullock et al., 1998). HS sulphation is important for development in mice and loss of HS sulphation results in lethality.

The *Drosophila* homologue of 6-OST has roles in regulating FGF and Wg signalling. *Drosophila 6-OST* is expressed in the developing trachea in a similar pattern to FGFr1 (Kamimura et al., 2001; Klämbt et al., 1992). LOF mutations of *6-OST* causes a loss active MAPK signalling in the trachea, disrupting both tracheal migration and branching (Kamimura et al., 2001). Members of the 6-OST family are important during vertebrate development. The majority of 6-OST1 knockout mice die during embryogenesis. Those that survive to birth are smaller than wildtype littermates and die perinatally. Analysis of the placentas of KO mice revealed a 50% reduction in the number of foetal micro vessels in the placenta compared to wildtype mice (Habuchi et al., 2007). 6-OST1 and 6-OST2 are both important for limb growth in the developing *Chick* embryo. In addition RNAi mediated knockdown of *6-OST1/2* in the mesoderm lead to abnormal limb bud development and truncation of electroporated limbs (Kobayashi et al., 2010).

HSPGs act directly as co-receptors for FGF signalling. Analysis of the crystal structure of FGF ligand-receptor complexes revealed that two molecules of HSPG are important to stabilise the FGF ligand-receptor dimers, in order to activate FGF signalling (Pellegrini et al., 2000; Schlessinger et al., 2000). HS binds to bFGF via the 2-O sulphate group *in-vitro* (Maccarana et al., 1993). Chlorate is a chemical inhibitor of protein sulphation (Baeuerle and Huttner, 1986). Treatment of 3T3 cells with chlorate inhibits the ability of bFGF to activate mitogenesis (Guimond et al., 1993). Native heparin is able to potentiate the binding of bFGF to the extracellular domain of FGFr1 *in-vitro.* Importantly, neither 2-O or 6-O desulphated heparin are able to potentiate

bFGF-FGFr1 interactions (Rusnati et al., 1994). Selective removal of the 6-O sulphate group of heparin inhibited the ability of bFGF to bind FGFr1, but not to heparin (Wang et al., 2004). The 2 and 6-O sulphate groups of HS are required for HS to function as a co-receptor during FGF signalling.

1.8.0 Post synthetic modification of HSPGs by the extracellular sulfatases Sulf1 and 2

The ability of HS to regulate signalling during development is dependent on specific sulphate groups. One prediction from this is that enzymes that are capable of altering HS sulphation will also impact on cell signalling. The enzymes Sulf1 and 2 modify HSPGs post-synthetically to regulate HS sulphation and cell signalling during development.

Sulf1

Sulf1 was originally identified in a screen for sonic hedgehog (Shh) responsive genes during somite formation. Sulf1 shows a high degree of homology to the lysosomal exo-sulfatase glucosamine-6-sulphatase (Dhoot et al., 2001). Glucoasmine-6-sulfatase cleaves 6-O linked sulphates from the non-reducing side of glucosamine (Kresse et al., 1980; Robertson et al., 1992). The catalytic domains of Sulf1 and glucosamine-6-sulfatase both possess a highly conserved cysteine residue required for sulfatase function (Dhoot et al., 2001). This conserved cysteine is post translationally modified to formylglycine (Schmidt et al., 1995; Selmer et al., 1996). Mutation of the formylglycine generating enzyme Sumf1 leads to the autosomal recessive disorder multiple sulfatase deficiency, reviewed by (Diez-Roux and Ballabio, 2005).

Unlike glucosamine-6-sulfatase, Sulf1 is an endo-sulfatase, which removes the 6-O sulphate group from intact heparin chains (Morimoto-Tomita et al., 2002). The domain structure of HS is not uniform and can broadly be divided into regions of high sulphation and regions of high acetylation (Maccarana et al., 1996). Sulf1 is highly specific and catalyses the removal of 6-O sulphate groups from trisulphated GlcNS6S-IdoA2S disaccharides in high sulphate

regions of HS (Frese et al., 2009; Lamanna et al., 2008; Morimoto-Tomita et al., 2002; Viviano et al., 2004).

In addition to a conserved catalytic domain, Sulf1 contains an N terminal secretion peptide, central hydrophilic domain and highly conserved C terminal domain (Dhoot et al., 2001). Sulf1 is secreted onto the surface of cells, but is not released into the surrounding media. However deletion of the hydrophilic domain of Sulf1 facilitates its release from the surface of CHO cells (Dhoot et al., 2001). In addition, deletion of the hydrophilic domain leads to the loss of Sulf1 from the surface of HEK293 cells and inhibits the ability of Sulf1 to remove 6-O sulphate groups from HS *in vitro* (Frese et al., 2009). The cell surface localisation of Sulf1 is not dependent on it binding HS as Sulf1 is found localised to the cell membrane of pgsA745 cells (Dhoot et al., 2001). pgsA745 cells lack xylotransferase activity and cannot synthesis HS chains (Esko et al., 1985). A diagram of the structure of Sulf1 and its substrate can be seen (Figure 1.10).

Sulf 2

Sulf2 is highly homologous to Sulf1 along the length of its sequence. The two sequences are particularly well conserved in the catalytic domain and at the N and C termini of the hydrophilic domains (Ai et al., 2006). The high level of homology in the catalytic domain includes the essential cysteine residue required for formylglycine modification (Morimoto-Tomita et al., 2002). Similar to Sulf1, the hydrophilic domain is required for the cell surface localisation and catalytic activity of Sulf2 (Ai et al., 2006). Sulf2 displays an identical substrate specificity to Sulf1 targeting the 6-O sulphate groups of IdoA2S-GlcNS6S disaccharides in HS and showing no activity against chondroitin sulphate (Ai et al., 2006; Morimoto-Tomita et al., 2002). GAG chains that have been treated with Sulf1 cannot be further desulphated by the action of Sulf2 and vice versa (Ai et al., 2006). Sulf2 is highly homologous to Sulf1 and has the same activity on HS chains.

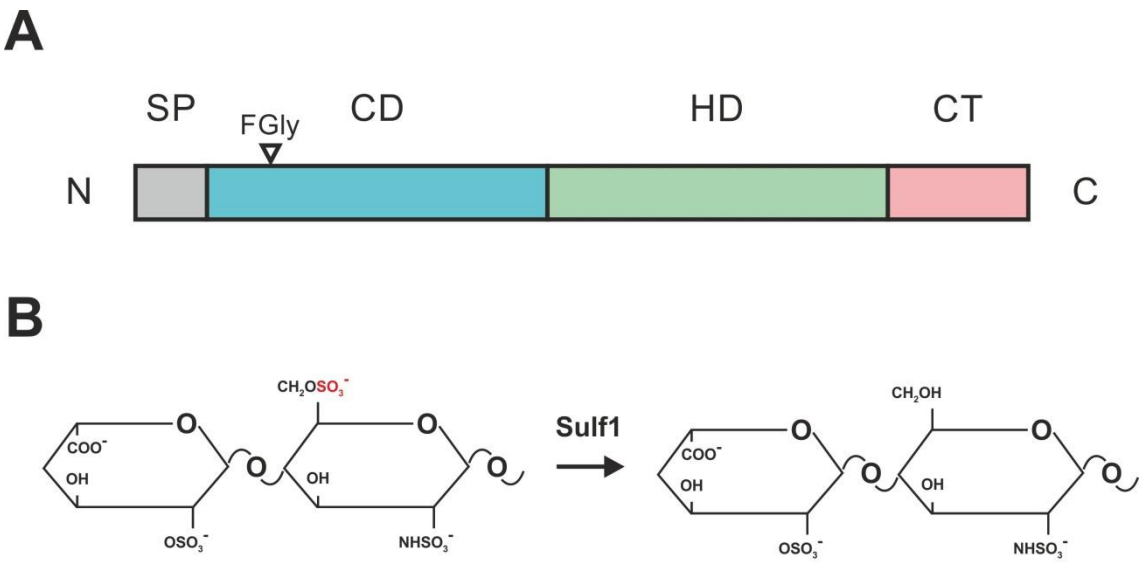

Figure 1.10; The domain structure and target substrate of Sulf1
Sulf1 can be divided into four separate domains. An N terminal signal peptide sequence, catalytic domain, hydrophilic domain and C terminal domain. The open arrowhead marks the site of the formylglycine modification. (B) Sulf1 catalyses the removal of the 6-O sulphate from GlcNS6S-IdoA2S disaccharides. The target sulphate group is marked in red. SP (signal peptide), FGly (formylglycine), CD (catalytic domain), HD (hydrophilic domain) and CT (C terminal domain). Figure adapted from (Esko and Selleck, 2002; Frese et al., 2009)

1.8.1 Sulf1 has a regulatory function during development

Sulf1 displays a high level of evolutionary conservation with homologues found in *Human, Mouse, Quail, Zebrafish, Xenopus, Drosophila* and *Sea Urchin* (Dhoot et al., 2001; Freeman et al., 2008; Fujita et al., 2009; Gorsi et al., 2010; Kleinschmit et al., 2010; Morimoto-Tomita et al., 2002). Knockout studies have shown that Sulf1/2 have redundant roles during *Mouse* development. *Sulf1* or *Sulf2* knockout mice are viable, fertile and do not possess any gross abnormalities (Holst et al., 2007). *Sulf1*/2 double knockout pups die perinatally and show a reduction in both size and weight. Analysis of the major organs showed that although all organs were present the kidneys of double knockout mice were significantly smaller than those of *Sulf1*/2 heterozygous mice (Holst et al., 2007). *Sulf1* and *2* are expressed in an overlapping pattern during skeletal development in mice. *Sulf1*/*2* double knockout mice display a shortening and broadening of the sternum, shortening of the radial bones and fusion of tail vertebrae (Ratzka et al., 2008). The non-essential role for Sulf1

during *Mouse* development suggests that Sulf1 is involved in the fine tuning of different signalling pathways.

In *Drosophila* LOF *Sulf1* mutant flies are viable and fertile. LOF *mutations* in *Sulf1* results in ectopic chemo/mechanosensory bristles at the wing boundary and an increase in the size of the L2-L3 inter vein region. Analysis of Wg/Hh target genes reveals subtle defects in the expression of these genes in *Sulf1* LOF mutants (Kleinschmit et al., 2010; Wojcinski et al., 2011). In *Zebrafish* microinjection of morpholinos targeting *Sulf1* lead to a disruption of somite structure. Somites become rounder in injected fish and show a decrease in width. In addition *Sulf1* knockdown fish show defects in the migration of the lateral line primordia (Meyers et al., 2013). *Sulf1* is expressed in the paraxial mesoderm, somites, pronephros, floor plate and neural crest during *Xenopus* development. Knockdown of *Sulf1* in *Xenopus* leads to the truncation of the anterior/posterior axis with a specific reduction in head structures including the cement gland and eyes (Freeman et al., 2008). Sulf1 is expressed in a wide variety of tissues during development and is involved in the fine tuning of cell signalling pathways.

1.8.2 Sulf1 modulates multiple cell signalling pathways

FGF signalling

The 6-O sulphate group of HS is required for the formation of FGF ligand-receptor complexes (Rusnati et al., 1994) and bFGF activity in cell culture (Guimond et al., 1993). One prediction from this is that Sulf1 will inhibit FGF signalling by catalysing the removal of the 6-O sulphate group from HS chains. Microinjection of mRNA encoding *Sulf1* inhibits FGF2, Wang et al., (2004), and FGF4, Freeman et al., (2008); Wang et al., (2004), induced activation of di-phospho ERK (dpERK). DpERK is a downstream component of the activated FGF signalling cascade, reviewed by (Dorey and Amaya, 2010). Work by Frese et al., (2009); Lamanna et al., (2008) demonstrated that MEF cells isolated from *Sulf1* and *Sulf2* double knockout mice respond more strongly to FGF2 treatment than wildtype MEFs. In *Xenopus* embryos, microinjection of morpholinos targeting *Sulf1* cause an increase in the endogenous levels of dpERK. This can

be rescued by co-injecting mRNA encoding *Sulf1* (Freeman et al., 2008). *In vitro* treatment of heparin with Sulf1 inhibited the ability of FGF2 to bind FGFr1, but not to heparin (Wang et al., 2004). Sulf1 inhibits the ability of FGF ligands to bind FGF receptors and activate signalling *in vivo*.

BMP signalling

Sulf1 regulates BMP signalling in cell culture and during embryonic development. Noggin is a secreted protein that binds to BMP ligands inhibiting BMP signalling (Zimmerman et al., 1996). Sulf1 induces the release of noggin from CHO cells and this results in an increase in BMP4 induced Phopho-smad1/5/8 in these cells (Viviano et al., 2004). Phospho-smad1/5/8 are downstream components of the activated BMP signalling pathway, reviewed by (Miyazono et al., 2010). In contrast, work in *Xenopus* and *Zebrafish* suggests an inhibitory role for Sulf1 in BMP signalling. Freeman et al., (2008) showed that microinjection of mRNA encoding *Sulf1,* inhibits the ability of BMP4 to induce phospho-smad1 (p-smad1). In addition microinjection of morpholinos targeting Sulf1 caused an increase in the levels of p-Smad1 in whole embryos. At the ligand-receptor level, over-expression of Sulf1 inhibited the ability of BMP4 to interact with the BMPr Alk3 (Freeman et al., 2008). In *Zebrafish,* morpholino mediated knockdown of *Sulf1* leads to an increase in the levels of p-smad5/8 in embryos and disrupts the migration of the lateral line primordia (Meyers et al., 2013). Sulf1 has different effects on the activation of BMP signalling between cell culture and *Xenopus/Zebrafish*.

Wnt signalling

Sulf1 was initially shown to enhance the ability of the canonical Wnt ligand Wnt1 to activate canonical Wnt signalling. Transfection of one population of C2C12 cells with *Wnt1* and a separate population with *Topflash* leads to the activation of Topflash when the two populations are cultured together. Transfection of Sulf1 together with Topflash, enhanced the ability of Wnt1 to activate canonical Wnt signalling (Ai et al., 2003; Dhoot et al., 2001). Treatment of glypican1 with Sulf1 inhibits the ability of glypican1 to co-immunoprecipitate Wnt8a. In addition transfection of HEK293T cells already expressing *Wnt8a,* with *Sulf1,* inhibited the ability of Wnt8a to bind to the surface of the cells (Ai et al., 2003). Together

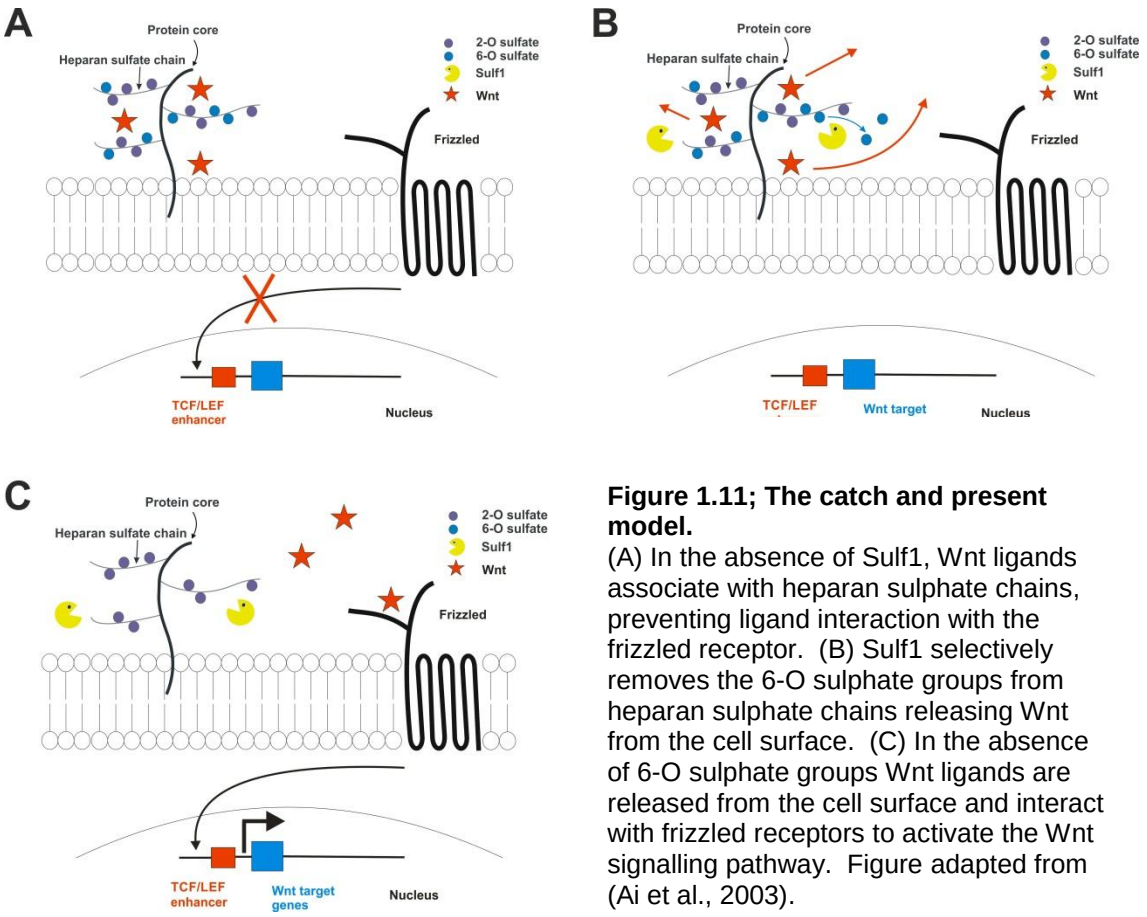

Figure 1.11; The catch and present model.
(A) In the absence of Sulf1, Wnt ligands associate with heparan sulphate chains, preventing ligand interaction with the frizzled receptor. (B) Sulf1 selectively removes the 6-O sulphate groups from heparan sulphate chains releasing Wnt from the cell surface. (C) In the absence of 6-O sulphate groups Wnt ligands are released from the cell surface and interact with frizzled receptors to activate the Wnt signalling pathway. Figure adapted from (Ai et al., 2003).

this data showed that Sulf1 reduced the binding of Wnt to HSPGs and enhanced the activation of canonical Wnt signalling. A 'catch and present' model was developed to describe the effects of Sulf1 on canonical Wnt signalling (Figure 1.11). In the absence of Sulf1, Wnt ligands are localised to the surface of cells by binding to HS chains (Figure1.11A). In the presence of Sulf1, Wnt ligands are released from the surface of cells and are able to activate canonical Wnt signalling (Figure1.11B-C) (Ai et al., 2003).

The catch and present model is supported by findings from (Tang and Rosen, 2009). Sulf1 and Sulf2 enhanced the ability of Wnt1 and Wnt3a to activate Topflash in HEK293 cells. Targeted knockout of *Sulf1* and *Sulf2* in *Mouse* myoblasts inhibits the ability of Wnt3a to stabilise β-catenin (Tran et al., 2012). In addition RNAi mediated knockdown of *Sulf2* inhibited the expression of the canonical Wnt target gene axin2 (Jho et al., 2002) in *Mouse* odontoblast like cells (Hayano et al., 2012). Treatment of HS with Sulf1 reduced the binding affinity of Wnt10a *in vitro* (Hayano et al., 2012). Sulf1 enhances the ability of Wnt ligands to activate the canonical Wnt signalling pathway in cell culture.

Data generated using the *Drosophila* homologue of Sulf1 cannot be explained by the catch and present model. LOF mutations or RNAi mediated knockdown of *Sulf1* in *Drosophila* enhances both the levels of extracellular Wg and the activation of the Wg signalling pathway (Kleinschmit et al., 2010; You et al., 2011). In contrast, over-expression of Sulf1 reduced the levels of extracellular Wg and inhibited Wg signalling in *Drosophila* (Kleinschmit et al., 2010; You et al., 2011). This is opposite to what would have been predicted by the catch and present model.

In *Xenopus,* microinjection of mRNA encoding *Xenopus tropicalis Wnt11b2* (*XtWnt11b2*) or *Sulf1* into one ventral blastomere does not induce axis duplication. However microinjection of *XtWnt11b2* together with *Sulf1* causes the induction of a secondary axis. In addition, over-expression of XtWnt11b2 together with Sulf1 results in the ectopic induction of *chordin* and *Xenopus nodal related (Xnr) 3* expression in gastrula stage embryos (Freeman et al., 2008). *Chordin* and *Xnr3* are organiser specific genes, which are ectopically induced in response to canonical Wnt signalling (see chapter 3 for a discussion of these). Sulf1 is altering the signalling ability of the non-canonical Wnt ligand XtWntllb2 to activate canonical Wnt signalling. In addition, Sulf1 enhances the ability of Wnt11b to co-immunoprecipitate the canonical Wnt co-receptor LRP6 (Freeman et al., 2008). The data presented here are not in keeping with the predictions made from the catch and present model. The role of Sulf1 in regulating canonical Wnt signalling in the embryo is likely to be more complex.

1.9.0 Aims of this study

The temporal and spatial regulation of Wnt signalling is vital for normal development. The canonical Wnt signalling pathway has roles in regulating gene expression and cell fate decisions. The non-canonical Wnt pathway has roles in regulating cell migration and polarity as well as restricting the activity of the canonical Wnt pathway. Sulf1 has been shown to regulate Wnt/Wg signalling in *Human* and *Mouse* cell lines and in *Xenopus* and *Drosophila* embryos. However the findings reported in these studies do not provide a common role for Sulf1 in regulating Wnt/Wg signalling. In addition, with the exception of some work done by (Tran et al., 2012) a role for Sulf1 in regulating non-canonical Wnt signalling has not been described.

The aims of this thesis are to determine:

- The effects of Sulf1 on the abilities of Wnt3a, Wnt8a and Wnt11b to activate canonical Wnt signalling

- The effects of Sulf1 on the abilities of Wnt4, Wnt8a and Wnt11b to activate non-canonical Wnt signalling

A mechanism for the effects of Sulf1 on Wnt8a and Wnt11b signalling in *Xenopus.*

2.0 Materials and Methods

2.1 Materials and solutions

2.1.1 Summary of materials

Acetic anhydride (Sigma)

Acrylamide mix (BioRad)

Activin (Sigma)

Anti-Digoxigenin-AP, Fab fragments (Roche)

Agar Technical (Oxoid)

Agarose (Melford)

Agarose (Ultra Pure AgaroseTM 1000: Invitrogen)

Ammonium acetate (Ambion)

Ammonium persulfate (APS: Fisher Scientific)

Ampicillin (Sigma)

BM® chemiluminescent substrate kit (Roche)

BMTM Purple (Roche)

Bicarbonate (VWR International)

Boehringer Mannheim blocking reagent (BMB: Roche)

Bovine serum albumin (BSA, fraction 5: Sigma)

Bromophenol blue (Sigma)

Calcium nitrate (Ca(NO3)2: Sigma)

Calf alkaline intestinal phosphatase (Promega)

Centrifuge tube 50ml (CELLSTAR®)

CHAPS (sigma)

Chloroform (Sigma)

L-Cysteine (Sigma)

L-Cysteine hydrochloride monohydrate (Sigma)

Digoxygenin nucleotide triphosphate labelling mix 10X (DIG NTP mix: Roche)

Disodium phosphate (Na2HPO4: Sigma)

Dithiothreitol (DTT: Sigma)

DNA ladder 1Kb (Promega)

DNA loading buffer (Invitrogen)

dNTPs (Invitrogen)

Dual luciferase® reporter assay system kit (Promega)

Ethanol (Fisher Scientific)

Ethidium bromide (Sigma)

Ethylenediaminetetraacetic acid (EDTA: Sigma)

Ethylene glycol tetraacetic acid (EGTA: Fisher Scientific)

Ficoll 400 (Sigma)

First strand cDNA synthesis kit (Invitrogen)

Foetal calf serum (Sigma)

Formamide (Ambion)

Gentamycin (Melford)

Glacial acetic acid (Fisher Scientific)

Glass cover slips, No.1.5 (Scientific Laboratory Supplies)

Glass pull needles (Narishige)

Glycine (Fisher Scientific)

Glycerol (Fisher Scientific)

Heparin 100µg/ml (Sigma)

Human Chronic Gonadotropin (HCG: Chorulon: Intervet)

HyperfilmTM ECL® (Amersham)

Isopropanol (Fisher Scientific)

Leibovitz L15 media with L-glutamine (L15: Fisher Scientific)

Lamb serum (Fisher)

Lithium chloride (LiCl: Sigma)

Maleic acid (Sigma)

Magnesium phosphate (MgSO4: Fisher)

Magnesium chloride (Mg2Cl: Sigma)

Methanol (Fisher Scientific)

Methylated GTP cap analogue (Ambion)

Micromulti plate Terasaki 10ul (Terasaki plate: Sarstedt)

Molecular grade water (Fisher)

4-Morpholinepropanesulfonic acid (MOPs: Sigma)

Nail Varnish (Maybelline forever strong: Boots)

Non-fat milk powder (Milk: Sainsburys)

PagerulerTM prestained protein ladder (Fermentas)

PCR master mix (Promega)

PDVF membrane (Millipore)

Petri dish (55mm: VWR International)

Petri dish (90mm: Sterilin)

Pfu turbo DNA polymerase (Promega)

pGem T easy kit (Promega)

Phenol-chloroform (Sigma)

Phosphosafe® homogenising buffer (Sigma)

12x75 Polystyrene graduated tubes (Star labs)

Polyvinylpyrrolidone (PVP-40: Sigma)

Potassium chloride (KCl: Fisher Scientific)

Potassium diphosphate (KH_2PO_4: Sigma)

Proteinase K (Roche)

Phusion® high fidelity DNA polymerase (Biolabs)

PVC insulation tape (Sigma)

QIAprep® Spin Miniprep kitTM (Qiagen)

QIAquick Gel Extraction Kit (Qiagen)

Restriction enzymes buffers (Promega and Roche)

RNAsin plus (Promega)

RQ1 RNAse-Free DNAse (RQ1 DNAse: Sigma)

SP6 MEGAscriptTM kit (Ambion)

Sodium acetate (NaOAc: Sigma)

Sodium chloride (NaCl: Fisher Scientific)

Sodium dodecyl sulphate (SDS: Melford)

SSC buffer 20X (Sigma)

Subcloning EfficiencyTM DH5αTM competent cells (Invitrogen)

Superfrost slides (Thermo Fisher Scientific)

SYBR® Safe (Invitrogen)

T3 MEGAscriptTM kit (Ambion)

T4 DNA ligase (Promega)

Taq polymerase (Invitrogen)

Taq polymerase master mix (Promega)

Tetramethylethylenediamine (TEMED: Sigma)

Transcription buffer 5X (Sigma)

Triethoanolamine (Sigma)

Tri reagent (Sigma)

Tris base (Invitrogen)

Tryptone (Oxoid)

Tween® 20 (Sigma)

Yeast (Oxoid)

Yeast sodium salt ribonucleic acid (Yeast RNA: ICN Biomedicals)

2.1.2 Summary of solutions

Alkaline phosphatase buffer (AP buffer)

- 100mM Tris base
- 50mM MgCl2
- 100mM NaCl
- 0.1% Tween
- pH 9.5

Cysteine *Xenopus laeivs*

- Normal amphibian medium (NAM)/10 + 2.5% L-cysteine hydrochlorate monohydrate (pH7.8)

Cysteine *Xenopus tropicalis*

- Modified Ringer's saline/9 (MRS/9) + 3% L-cysteine (pH7.8)

Denhart's Solution

- 0.02% BSA
- 0.02% PVP-40
- 0.02% Ficoll 400

Formalin

- Phosphate buffered saline (PBS) + 3.7% Formaldehyde

Homogenisation buffer (buffer H)

- 50mM NaCl
- 20mM Tris-HCL
- 1mM EGTA
- 2mM $MgCl_2$
- pH 7.5

Hybridisation buffer

- 50% formamide

- 5X SSC
- 1mg/ml Yeast RNA
- 100ug/ml Heparin
- Denharts solution
- 0.1% Chaps
- 10mM EDTA
- 0.1% Tween
- pH 7

Luria-Bertani (Lb) medium

- 10g/l Tryptone
- 5g/l Yeast
- 10g/l NaCl
- pH 7.4

Maleic acid Buffer (MAB)

- 100mM Maleic acid
- 150mM NaCl
- 0.1% Tween 20
- pH 7.8

MEMFA

- 100mM MOPS pH 7.4
- 2mM EGTA
- 1mM $MgSO_4$
- 3.7% formaldehyde

NAM

- 110mM NaCl
- 2mM KCl
- 1mM $Ca(NO_3)_2$
- 0.1mM EDTA

NAM/2

- NAM/2 + 0.25mM Bicarbonate + 25pg/ml Gentamycin

NAM/3 + Ficoll

- NAM/3 + 0.25mM Bicarbonate + 25pg/ml Gentamycin + 5% Ficoll

NAM/10

- NAM/10 + 25pg/ml Gentamycin

Modified ringer solution/9 (MRS/9)

- 11mM NaCl
- 0.2mM KCl
- 0.22mM CaCl2
- 0.11mM MgCl2
- 0.5mM Hepes

MRS/20

- 5mM NaCl
- 90µM KCl
- 0.1mM CaCl2
- 0.1mM MgCl2
- 5mM Hepes
- 100pg/ml Gentamycin

PBS

- 137mM NaCl
- 2.7mM KCl
- 10mM Na_2HPO_4
- 1.8mM KH_2PO4
- pH 7.4

PBST

- PBS + 0.1% Tween

Resolving gel

- 375mM Tris pH 8.8
- 10% Acrylamide mix
- 0.1% SDS
- 0.05% APS
- 0.05% TEMED

SDS page sample buffer

- 2% SDS
- 50mM Tris (pH6.8)
- 0.2mg/ml Bromophenol blue

- 0.1M DTT
- 10% Glycerol

SDS page non-reducing sample buffer

- 2% SDS
- 50mM Tris (pH6.8)
- 0.2mg/ml Bromophenol blue
- 10% Glycerol

Stacking gel

- 125mM Tris pH 6.8
- 4% Acrylamide mix
- 0.1% SDS
- *0.05% APS*
- 0.1% *TEMED*

Stripping buffer

- 19.4mM DTT
- 10mM Tris base
- 0.05% SDS
- pH 6.8

Tri-acetate-EDTA (TAE) buffer

- 40mM Tris base
- 0.1% Glacial acetic acid
- 1mM EDTA

Tris buffered saline (TBS)

- 137mM NaCl
- 2.7mM KCl
- 25mM Tris
- pH 7.4

Tris-glycine running buffer (running buffer)

- 12.4mM Tris base
- 96mM Glycine
- 0.05% SDS
- pH8.3

Tris-glycine transfer buffer (transfer buffer)

- 48mM Tris base
- 39mM Glycine
- pH 8.8

2.1.3 Summary of antibodies

In situ hybridisation

- Anti-DIG Fab fragments coupled to horse radish peroxidase (1/2000: Roche)

Western blot

- Primary Anti-β-catenin antibody (1/25,000: Sigma)
- Primary Anti-Diphospho-ERK antibody (DpERK: 1/4000: Sigma)
- Primary Anti-GAPDH antibody (1/100,000: Sigma)
- Primary Anti-GFP antibody (1/2,000: Invitrogen)
- Primary Anti-HA antibody (1/4,000: Sigma)
- Primary Anti-MCM3 antibody (1/25,000: J.Chong, The University of York)
- Primary Anti-Phospho-smad2 (Psmad2: 1/1,000: Millipore)
- Primary Anti-Total-ERK antibody (1/1,000,000: Sigma)
- Secondary Anti-mouse peroxidise antibody (Anti-mouse POD: 1/4,000: Amersham)
- Secondary Anti-rabbit POD antibody (1/8,000: Abcam)

2.2 Embryological methods

2.2.1 *Xenopus laevis in vitro* fertilisation and culture

Xenopus laevis females were primed by subcutaneous injection with 50 units of human chorionic gonadotropin hormone (HCG; Chorulon) a week before the experiment. Females were induced by injecting them with 250 units of HCG and incubating them in the dark, overnight (15 hours) at 19°C. Eggs were fertilised using a sperm suspension produced from freshly crushed testis from a

Xenopus laevis male. Embryos were cultured at 21°C in NAM/10 in 55mm petri dishes coated with 1% agarose (diluted in water for embryological methods). Embryos were de-jellied after 45 minutes of culture using cysteine.

2.2.2 *Xenopus tropicalis* in vitro fertilisation and culture

Xenopus tropicalis females were primed by subcutaneous injection with 10 units of Chorulon the night before (15 hours) the experiment. On the morning of the experiment females were injected with 100 units of Chorulon and then incubated in the dark at 27°C for three hours. Eggs were fertilised using a sperm suspension produced from male *Xenopus tropicalis* testis. Male *Xenopus tropicalis* were primed by subcutaneous injection of Chorulon 3 hours before fertilisation. Testis were stored and homogenised in 1ml of L15 + 10% foetal calf serum at 12°C. Embryos were cultured at 21°C in MRS/9 in 55mm petri dishes coated with 1% agarose. Embryos were de-jellied after 40 minutes using cysteine.

2.2.3 Microinjection

Xenopus laevis embryos were microinjected with the appropriate concentration of mRNA using either a pneumatic microinjector (Harvard apparatus/Narishige) or Drummond injector (Drummond Scientific Company) and glass pull needles. Microinjections were done in NAM/3 + 5% Ficoll and embryos were transferred to NAM/10 before gastrulation. For the axis duplication assay embryos were injected in the marginal zone of one ventral blastomere at the four cell stage. For animal cap assays embryos were injected bilaterally in the animal hemisphere at the 2 cell stage. Embryos were injected with 20nl per embryo, which equates to 10nl per blastomere at the 2 cell stage and 5nl per blastomere at the four cell stage. For Wnt-HA-GFP diffusion assays embryos were injected animally in either one or two blastomeres at the four cell stage.

2.2.4 Animal cap assays

Following microinjection, embryos were cultured until NF stage 8 in NAM/10. Embryos were transferred to NAM/2 and the vitelline membranes were removed from the vegetal pole of the embryo. Animal cap explants were taken using tungsten needles and allowed to rest for 15 minutes in NAM/2.

Convergent extension assays

Animal caps were transferred to Terasaki dishes and cultured in NAM/2 + 1ug/ml BSA in the presence or absence of recombinant activin (1/5000 dilution). Animal caps were cultured at 23°C until NF stage 19 and then fixed using formalin. Animal caps were then analysed for convergent extension.

Western blot

Animal caps were transferred to Tersaki dishes coated with 1% agrose and cultured in NAM/2 overnight at 12°C. Animal caps were cultured until NF stage 10.5 and then snap frozen for western blot.

Confocal microscopy

Following microinjection, embryos were cultured in NAM/10 overnight at 12°C. At NF stage 8 vitelline membranes were removed, animal caps were taken and transferred to 55mm petri dishes coated with 1% agarose. Animal caps were cultured in the dark at 21°C for four hours to allow the fluorophores cerulean, green fluorescent protein, Venus and red fluorescent protein to mature. Relief slides were generated by coating superfrost slides with two layers of PVC insulation tape. Following this a 14mm by 10mm rectangle was cut out of the tape to leave a chamber to mount animal caps in. Healed animal caps were mounted apical side up in the slide and covered using a No.1.5 cover slip. The glass cover slip was left to dry for 20 minutes and then sealed with nail varnish to prevent sample drift during imaging. Samples were imaged by confocal microscopy using the inverted laser scanning microscope LSM710 (Carl Zeiss) and Zen software (2008-2010, Carl Zeiss). Samples were imaged in lambda mode to minimise problems associated with sample drift. In lambda mode the

confocal microscope collects data from all of the florescent channels simultaneously. Once collected the image was unmixed to produce separate fluorophore channels. This was done using spectral traces collected for each of the florescent constructs used in isolation, prior to the experiment.

2.2.5 *In situ* hybridisation

Embryos were cultured until NF stage 10 or 10.5 in NAM/10 and the vitelline membranes were then removed. Embryos were fixed in MEMFA for 1 hour at room temperature and then dehydrated in 100% methanol and stored at -20°C. Embryos were rehydrated using a series of methanol and PBST washes and then treated with 10ug/ml proteinase K for 12 minutes at 37°C. Embryos were subsequently washed twice in trietholamine for 10 minutes, with acetic anhydride added to the second wash. Following this embryos were washed in PBST and re-fixed for 20 minutes in formalin. Embryos were washed again in PBST and then allowed to equilibrate at 60°C in hybridisation buffer. Embryos were then blocked in hybridisation buffer for two hours at 60°C. This was then replaced with hybridisation buffer containing DIG probe and embryos were left overnight at 60°C.

To remove excess probe embryos were washed twice in hybridisation buffer, three times in 2X SSC + 0.1% Tween and three times in 0.2XSSC + 0.1% Tween at 60°C. Embryos were then washed twice in MAB + 0.1% Tween and then blocked in MAB + 2% BMB + 20% heat treated lamb serum + 0.1% Tween for 2 hours at room temperature. Embryos were the incubated overnight in this blocking solution + Anti-DIG antibody. The following morning embryos were given 5 short washes in MAB followed by 3 one hour washes at room temperature. Embryos were washed in AP buffer and then the samples were developed using a 1/3 solution of BM purple in AP buffer for 12-48 hours. To stop the reaction embryos were washed twice in PBST and fixed and stored in formalin at room temperature.

2.2.6 Photography

Embryos were photographed using a SPOT 14.2 Colour Mosaic camera (Diagnositics Instruments Inc.) and SPOT Advanced software, with a Leica MZ FLIII microscope. Images were processed using Adobe Photoshop CS3 (64 Bit).

2.3 Molecular biology methods

2.3.1 Transformation

Subcloning Efficiency™ DH5α™ competent cells were used for heat shock transformation (90 seconds at 42°C then 90 seconds on ice). Cells were cultured in Lb media for one hour at 37°C and then plated on Lb-agar plates containing 100ug/ml ampicillin. Plates were cultured overnight at 37°C.

2.3.2 Colony PCR

The PCR reaction was set up in a sterile PCR tube as follows:

- 10µl of 2X PCR master mix
- 1µl of forward/reverse primer (10µM)
- 6µl of water

In addition 2µl of molecular grade water were used to disperse the selected colony. This water was then streaked on a patch plate and then added to the reaction above to increase the volume to 20µl. The PCR program was as follows:

5 minutes	95°C	
30 seconds	95°C	
30 seconds	55-65°C	**} X30**
30 seconds-2 minutes	72°C	
15 minute	72°C	

The annealing temperature varied depending on the requirements of the primers used. The extension time was dependent on the size of the gene being amplified, PCR master mix is capable of synthesising 1Kb per minute. Following the reaction, the size of the PCR products were checked on a 1% agarose gel by gel electrophoresis.

2.3.3 Agarose gel electrophoresis

DNA and RNA samples were run on an ethidium bromide stained 1-3% agarose gels in TAE buffer at 100-200mV. Samples were loaded using DNA loading buffer and run alongside 3µl of Kb ladder. For gel extractions, ultrapure agarose was used.

2.3.4 DNA minipreps

Plasmid DNA was amplified by inoculating a 5ml Lb + 100ug/ml ampicillin culture with a single colony from the PCR patch plate. The bacterial culture was grown at 37°C overnight in a shaker. On the following day 1.5ml of bacterial culture was spun at 13000 RPM for 5 minutes to pellet the bacteria. The liquid was discarded and the process repeated twice more to obtain the majority of the bacteria from the culture media. Bacterial DNA was then extracted using a QIAprep® Spin Miniprep kit™ as per instructions.

2.3.5 Quantification of DNA and RNA

DNA and RNA were quantified using the NanoDrop 2000/8000 spectrophotometer (Thermo Scientific) to measure the absorbance of samples at 260nm.

2.3.6 Sequencing

Plasmid DNA was sequenced by the genomics laboratory within the technology facility at The University of York using the 3130 genetic analyser (Applied Biosystems).

Table 2.1; Sequencing primers used

Primer used	**Sequence 5' to 3'**
SP6	AGGTGACACTATAGAATACTCGTCAAC
T7	GTAATACGACTCACTATAGGGCG
T3	CGCGAATTAACCCTCACTAAAGGG

2.3.7 Linearizing plasmid DNA

For the synthesis of RNA, DNA sequences were cloned into the plasmids $CS2^{+}$ or pGem Teasy. CS2+ contains an SV40 polyadneylation sequence, which gives mRNA an increased stability *in vivo*. Sp64 and CS107 vectors also contain a polyadenalyation sequence. pGem Teasy lacks the polyadenylation site and was used to synthesise RNA for *in situ* hybridisation probes. Linearization reactions were set up as follows:

5ug Plasmid DNA
10µl Appropriate 10X restriction enzyme buffer
3µl Appropriate restriction enzyme (Table 2.2)
Reaction made up to 100µl with molecular grade water

The reaction was incubated at 37°C for 3 hours and then a 10µl sample was checked on a 1% agarose gel against undigested plasmid DNA. Once linearized, plasmid DNA was purified via a phenol chloroform extraction.

Table 2.2; Plasmids used for RNA synthesis

Name	Vector	Linearization/ transcription	Source
Caveolin-GFP	$CS2^+$	Not1/SP6	De-Li Shi
Chordin (probe)	CMV	Sal1/T7	IMAGE 5161617
Dvl-GFP	Bluescript RN3	Sfi1/T3	J. Green
DN*FGFr4a	CS2+	Sal1/	I. Hongo
FGF4a	CS2+	Not1/SP6	(Isaacs et al., 1994)
Glypican4-Cerulean	CS2+	Not1/SP6	S. W. Fellgett
Frzb	Sp64R1	Sal1/SP6	M. Moos
LacZ	CS2+	Not1/SP6	(Illes et al., 2009)
mRFP	CS2+	Not1/SP6	R. Tsien
mCerulean	CS2+	Not1/SP6	S. W. Fellgett
Nuclear-GFP2	CS2+	Not1/SP6	J. C. Illes
Sulf1	CS2+	Not1/SP6	S. Freeman
Sulf1 C-A	CS2+	Not1/SP6	S. Ramsbottom
Wnt3a	$CS2^+$	Not1/SP6	R. T. Moon
Wnt4	$CS2^+$	Not1/SP6	S. W. Fellgett
Wnt8a	CS2+	Not1/SP6	R. Moon
Wnt11b	CS2+	Not1/SP6	S.W.Fellgett
Wnt8a-HA	$CS2^+$	Not1/SP6	M. E. Pownall
Wnt11b-HA	$CS2^+$	Not1/SP6	J. Heasman
Wnt4-HA-GFP	CS2+	Not1/SP6	R. J. Maguire
Wnt8a/Wnt11b-HA-GFP	CS2+	Not1/SP6	S. W. Fellgett
Wnt8a/Wnt11b-HA-Venus	CS2+	Not1/SP6	S. W. Fellgett
Wnt8a/Wnt11b-Venus	CS107	Asc1/SP6	M. Taira
Xnr1	Sp64T	Sma1/SP6	C. Hill
Xnr3 (probe)	Bluescript SK-	Pst1/T7	IMAGE 7297499

2.3.8 DNA purification

To purify linearized DNA, the reaction volume was made up to 200µl with molecular grade water. An equal volume of phenol chloroform was added and the mixture vortexed thoroughly before being centrifuged at 13000RPM for 5 minutes at 4°C. The aqueous phase of the reaction was then removed and placed in a new tube where 0.1 volumes of NaOAc and 2.5 volumes of 100% ethanol were added and the sample vortexed. The DNA was the precipitated

on dry ice for 30 minutes, or overnight at -20°C. Following this, the mixture was centrifuged at 13000RPM for 15 minutes at 4°C. The liquid was removed and the DNA washed in 70% ethanol before being centrifuged at 13000RPM for 5 minutes at 4°C. The pelleted DNA was then dried under a vacuum and resuspended in the required volume of molecular grade water. Purified DNA was checked on a 1% agarose gel and stored at -20°C until use.

2.3.9 *In vitro* transcription of functional mRNA

Functional mRNA was synthesised using either SP6 or T3 MEGAscript^{TM} kits. The manufacturer's instructions were adapted as follows.

- The concentration of GTP was reduced from 50mM to 5mM for the SP6 kit and 75mM to 7.5mM for the T3 kit.
- 2.5µl of methyl GTP cap analog was added to the SP6 reaction, with 3.75µl added to the T3 reaction.

The ratio of GTP to methyl GTP promotes the formation of capped mRNA, which is translated more efficiently. The transcription reaction was allowed to proceed at 37°C for 4 hours and then synthesised RNA was checked on a 2% agarose gel. The DNA template was then degraded by the addition of 1µl of RQ1DNAse at 37°C. The sample was extracted using phenol chloroform and then chloroform. Following this, an equal volume of isopropanol was added to the sample, which was then precipitated at -80°C for 30 minutes. After this the sample was centrifuged for 15 minutes at 13000RPM at 4°C to pellet the RNA. RNA was washed in 70% ethanol and then centrifuged for 5 minutes at 13000RPM at 4°C. The pelleted RNA was dried under a vacuum and then resuspended in the required volume of molecular grade water. The mRNA was run on a 2% agarose gel to check that it was intact. The concentration of mRNA was determined using the NanoDrop and a LiCl extraction was performed using the manufacturer's instructions if required. mRNA was stored at -80°C until use.

2.3.10 *In vitro* transcription of DIG RNA probes

DIG RNA probes were made for *in situ* hybridisation using the following reaction:

- 10µl 5X Transcription buffer
- 5µl 100mM DTT
- 2.5µl 10X DIG NTP mix
- 2µl RNAsin plus
- 3µl Polymerase
- 2µl Linearized template DNA
- Reaction made up to 50µl using molecular grade water

The reaction was incubated at 37°C for 2 hours at which point a 2µl sample was run on a 2% agarose gel. If required the reaction was left longer and/or more polymerase was added. Following this the template DNA was digested using RQ1DNAse at 37°C for 15 minutes. The sample was then precipitated overnight at -20°C using 100% ethanol and 3M NaAOc. The following day samples were centrifuged at 13000RPM for 30 minutes at 4°C to pellet the RNA probe. Samples were washed in 70% ethanol and the centrifuged for 5 minutes at 13000RPM at 4°C. The pelleted RNA was dried under a vacuum and then resuspended in the required volume of molecular grade water. RNA was checked on a 2% agarose gel and then stored at -80°C until required.

2.3.11 Total RNA extraction

RNA was extracted from 30 whole *Xenopus* tropicalis embryos to create cDNA to amplify *Xenopus* tropicalis Wnt4. Embryos were homogenised in 1ml of Tri reagent and then centrifuged at 13000 RPM for 10 minutes at 4°C. The aqueous layer was then removed and left to stand for 5 minutes in a fresh tube. 200µl of chloroform was added to the sample and then the sample was vortexed thoroughly and left to stand for 10 minutes. The sample was centrifuged for 15 minutes at 13000RPM at 4°C, the aqueous layer was removed and the RNA precipitated using 500µl of isopropanol at -20°C for 30 minutes. Following this, the sample was centrifuged at 13000RPM for 15

minutes at 4°C, the supernatant was discarded and the RNA pellet washed with 70% ethanol. Samples were centrifuged at 13000RPM for 5 minutes at 4°C and the pellet was then dried under vacuum. The RNA pellet was resuspended in 50µl of molecular grade water and 60µl of 7.5M LiCl/50mM EDTA and left to precipitate overnight at -80°C. The following day the samples were centrifuged at 13000RPM for 30 minutes at 4°C. The supernatant was discarded and the RNA pellet washed with 70% ethanol. Following this, the sample was centrifuged at 13000RPM for 5 minutes at 4°C and the RNA pellet was then dried under vacuum. The sample was resuspended in 20µl of molecular grade water and the concentration and quality of the RNA was analysed using the NanoDrop. Total RNA was stored at -80°C until use.

2.3.12 cDNA synthesis

cDNA synthesis was performed using the first strand synthesis kit. The following reaction was set up in a sterile PCR tube:

- 1µl Oligo dT primer
- 1ug RNA
- 0.83mM dNTPs
- Made up to 12µl with molecular grade water

The sample was mixed by pipetting and then incubated at 65°C for 5 minutes. Following this, the reaction was chilled on ice for 2 minutes and then centrifuged briefly to collect any condensation. Once chilled the following mixture was added to the sample:

- 4µl of 5X 1st strand buffer
- 10mM DTT
- Made up to 7µl using molecular grade water

The sample was mixed using a pipette and then incubated at 42°C for 2 minutes. 1µl (200 units) of SuperscriptII was added to the sample and the reaction was incubated at 42°C for one hour. The SuperscriptII was inactivated

by incubating the reaction at 70°C for 15 minutes. cDNA was stored at -20°C until use.

2.3.13 L8 PCR

To determine whether the cDNA synthesis had been successful a PCR was performed for the 'housekeeping gene' L8. The following reaction was set up in a sterile PCR tube:

- 12.5µl of 2X PCR Master mix
- 1.5µl of Forward/reverse L8 primers (10µM)
- 1µl of cDNA
- Made up to 25µl using molecular grade water

The PCR reaction was as follows:

5 minutes	95°C	
30 seconds	95°C	
30 seconds	62°C	} X30
45 seconds	72°C	
10 minutes	72°C	

At the end of the reaction, 5µl of DNA loading dye was added to the sample and 15µl of sample was then analysed on a 1% gel by gel electrophoresis.

Table 2.3; L8 primers

Primer name	**Sequence (5' to 3')**
L8 Forward	GGGCTRTCGACTTYGCTGAA
L8 Reverse	ATACGACCACCWCCAGCAAC

2.3.14 Luciferase protocol

The luciferase assay was performed using 5 whole embryos per reaction. All reagents used in this assay were from the Dual luciferase® reporter assay system kit. The luciferase reagents were prepared as described in the manufacturer's instructions. 100µl of luciferase assay reagent II was predispensed into the required number of 12x75 Polystyrene graduated tubes. Embryos were homogenised in 20µl of 1X passive lysis buffer using a pipette. The embryo lysate was then transferred to a 12x75 polystyrene tube containing the luciferase assay reagent and mixed by pipetting 10 times. The 12x75 polystyrene tube was then placed in the luminometer (Lumat LB9501: Berthold) and the levels of luminescence recorded. Following this, the 12x75 polystyrene tube was removed and 100µl of Stop and Glo reagent was added. The sample was mixed thoroughly by vortexing and then placed back in the luminometer. The second measurement detected the levels of renilla luciferase activity. The relative luciferase units were then calculated.

2.3.15 Western blot

Reducing and non-reducing western blots

Western blot was performed on 10 animal caps per condition. Animal caps were homogenised in 30µl of Phosphosafe® on ice by pipetting. Following this, samples were snap frozen on dry ice for 2 minutes before being thawed out and spun at 13000RPM for 20 minutes at 4°C. The supernatant was then removed from the samples and placed into a separate tube along with 7µl of SDS page sample buffer (reducing or non-reducing depending on the blot). Samples were incubated at 95°C for 5 minutes and then loaded onto a 10% SDS page gel. The gel consisted of 8ml of resolving gel, topped with 2ml of stacking gel. 15µl of each sample was run on the gels alongside a PagerulerTM pre-stained protein ladder. The gel was run for 10 minutes at 100mV and then for 90 minutes 200mV, or longer when required, in tris-glycine running buffer. Following this, a PDVF membrane was prepared by wetting with 100% methanol for 1 minute and then equilibrating it in tris-glycine transfer buffer. Samples were transferred onto the PDVF membrane for 90 minutes at 100mV.

Transfer took place in tri-glycine transfer buffer and the reaction was kept cool using an ice pack. The PDVF membrane was then washed twice in PBST and blocked for 1 hour in PBST + 5% non-fat milk powder at room temperature. After an hour this was replaced with PBST + 5% non-fat milk powder containing the required primary antibody and incubated overnight at 4°C.

The following day the PDVF membrane was washed 6 times in PBST over 45 minutes (3x5minutes and 3x10 minutes). The membrane was then incubated with PBST + 5% non-fat milk powder containing the appropriate secondary antibody for 2 hours at room temperature. After this the membrane was washed 6 times in PBST over 45 minutes and then developed using the BM® chemiluminescent substrate kit. Membranes were placed between two sheets of a plastic wallet and coated in the chemiluminescent ECL substrate kit. After applying the ECL, the membranes were left for one minute before the plastic wallet was closed. Excess ECL was then cleared away by wiping the plastic sheet with blue roll, until no more ECL was released. The membrane was exposed to pre-flashed HyperfilmTM ECL® and developed using an SRX-101A Xograph. The membrane was exposed to film for the length of time required to visualise the proteins being analysed. This varied depending on the experiment, but was always between 1 second and 20 minutes. The PDVF membrane was then stored in PBST at 4°C until required.

To determine how evenly the gels were loaded the PDVF membrane was stripped at 55°C for 30 minutes using stripping buffer. The PDVF membrane was then washed 6 times in PBST over 45 minutes and then blocked at room temperature in PBST + 5% non-fat milk powder for one hour. The PDVF membrane was incubated in PBST + 5% non-fat milk powder containing the appropriate primary antibody overnight at 4°C. The following day the membrane was washed 6 times for 45 minutes in PBST and then incubated for one hour in PBST + 5% non-fat milk powder containing the appropriate secondary antibody. The PDVF membrane was then washed 6 times in PBST over 45 minutes and developed using the BM® chemiluminescent substrate kit and HyperfilmTM ECL®. The visualisation of the loading control was performed as above (see paragraph 2, section 2.3.15).

Subcellular fractionation protocol

To determine the levels of β-catenin in *Xenopus* animal caps a subcellular fractionation protocol was performed prior to western blot. Animal caps were covered with 500µl of Buffer H and then homogenised using an end over end invertor (Rotamix RM1) at 4°C for 10 minutes. Samples were then centrifuged at 3000RPM for 10 minutes at room temperature. Following this the supernatant was decanted and placed in a separate tube. The supernatant was mixed thoroughly with a pipette and then a 25µl sample was taken. 6µl of SDS page sample buffer (reducing) was added to each of the 25ul samples and 15µl of each sample was loaded onto a 10% gel alongside a PagerulerTM pre-stained protein ladder. From this point onwards the western blot was carried out as described above, from mid-way through the paragraph 1, section 2.3.15.

Western blot for measuring the levels of Wnt8a and Wnt11b-HA in the axis duplication assay

To determine whether the ability of Sulf1 to enhance the axis inducing ability of Wnt11b was simply due to changes in the amount of protein present, a western blot was carried out using embryos that had been injected in the marginal zone (see 2.2.3). Using film, the linear range over which protein can be quantified is just over one order of magnitude. Detecting low levels of signal quantitatively using film is difficult as a certain threshold of signal must be reached before it becomes detectable. In addition, at high levels of signal film darkens, and an increase in signal from this point is not linear with respect to the amount of light produced. In contrast using a charge couple device (CCD) camera offers a much wider dynamic range for signal detection (Dickinson and Fowler, 2002). In order to carefully measure the amounts of Wnt8a and Wnt11b-HA protein present during the axis duplication assay, a western blot was performed on whole embryos. In addition to using a CCD camera, two different amounts of protein were used for each of the assays, to ensure that the detection of proteins was linear for the amounts tested.

Embryos were microinjected with 0.5, 5, and 600pg of Wnt8a-HA or 5pg, 600pg and 2ng of Wnt11b-HA mRNA into one ventral blastomere of a four cell embryo. The amounts of protein were selected so that the lower doses had no effect on

the embryo, whereas the middle doses caused the phenotypes assayed in chapter 3. The higher doses were toxic and induced gross malformation in the injected embryos. In addition Sulf1 (1ng) was injected, to examine whether Sulf1 caused any changes in the relative amounts of Wn8a or Wnt11b-HA protein detected in the embryo. Embryos were cultured until NF stage 10.5 and then snap frozen for western blot. Five embryos were frozen for each condition, with the remaining embryos left to develop until NF stage 36. The five embryos were homogenised in 100µl of Phosphosafe® before being spun at 13000RPM for 20 minutes at 4°C. The supernatant was then removed from the samples and placed into a separate tube along with 20µl of reducing SDS page sample buffer. Samples were incubated at 95°C for 5 minutes and then spun at 13000RPM for 5 minutes to pellet the extra yolk present in whole embryos. Either 25µl (equivalent of one embryo) or 12.5µl (equivalent of half an embryo) of each sample was loaded onto a 10% SDS page gel and run on the gels alongside a PagerulerTM pre-stained protein ladder. The western blot was transferred as described in paragraph 1 section 2.3.15 and the PDVF was cut into two pieces. The cut was made just below the 40Kda mark on the ladder and meant that the membrane could be simultaneously blotted for GAPDH 35Kda and Wnt8a/Wnt11b-HA 45Kda. The membranes were washed, blocked an incubated in primary antibody as described in paragraph 1 section 2.3.15.

The second day of the bot was carried out as described in paragraph 2 section 2.3.15. Analysis of the blots was done using a G:Box Chemi XT-16 (MAN) Chemisampler (Syngene) and Gene Snap image acquisition software. The blot was covered with ECL and then placed inside a plastic wallet. The blot was placed inside the G:Box and brought into focus using transmitted light and a 40 millisecond exposure on Gene Snap. Following this the transmitted light was turned off and the aperture on the CCD camera was opened up to its maximum. To image Wnt8a/Wnt11b-HA blots the membranes were exposed for 3 minutes, any longer caused the imaging software to crash. To image GAPDH the membranes were exposed for 2 minutes. After imaging a blot, the aperture on the CCD camera was closed to its minimum size, so that the next blot could be brought into focus. All of the images were saved as TIF's and then densitometry was analysed using image J.

The CCD camera was not able to detect Wnt11b-HA protein in the 0.5 embryo samples. Consequently the western blots were stripped and re-probed for Wnt8a and Wnt11b-HA protein. The membranes were stripped for 30 minutes at 55°C and processed as described in paragraph 3 of section 2.3.15. The only exception to this was that the blots were incubated in secondary antibody for two hours at room temperature rather than one hour. The blots were developed using an Xograph and pre-flashed film as described in paragraph 2 of section 2.3.15.

The protein bands detected where subjected to densitometry, in order to determine the relative amounts of Wnt8a and Wnt11b-HA protein present. The data on film was scanned onto a computer using a CanoScan LiDE 70 scanner. Images were saved as TIFs and then analysed for densitometry in Fiji image J. The images produced using the CCD camera were opened directly in Fiji image J. A 110x250 pixel box (width by height) was drawn over the first band being analysed using the rectangle tool in Fiji image J, this was then selected as the first lane. Each of the following lanes on the gel were then selected and plotted using the plot peak function. The line tool was then used to close of the area under each of the peaks, before the wand tool was used to calculate this area. The size of all of the bands was recorded and the relative amounts of Wnt8a and Wnt11b-HA were calculated by dividing the area recorded for each of the HA blots by the corresponding area for GAPDH.

2.4 Subcloning DNA constructs

2.4.1: Primers used

Table 2.4 Primers used for subcloning

Primer name	**Sequence (5' to 3')**
Glypican-Cerulean forward part1	AGAGAGGGATCCACCATGGATTGGATCTCCTTCTACCCC
Glypican-Cerulean reverse part1	CTCTCTGAATTCATTAATGATTCCAGTCTTCGGCAT
Glypican-Cerulean forward part 2	AGAGAGGAATTCATGGTGAGCAAGGGCGAGGAGCTG
Glypican-Cerulean reverse part 2	CTCTCTCTCGAGCTTGTACAGCTCGTCCATGCC
Glypican-Cerulean forward part 3	AGAGAGCTCGAGTTTGTCGAGAAGACACCTTCTGCA
Glypican-Cerulean reverse part 3	CTCTCTTCTAGATTATCTCCATTGCCTCACCAAGAA
mCerulean forward	AGAGAGGAATTCACCATGGTGAGCAAGGGCGAGGAGCTG
mCerulean reverse	CTCTCTTCCGGACTTGTACAGCTCGTCCATGCC
Wnt4 forward	AGAGAGATCGATACCATGGCCCCAGAGTACTTCTTGAGG
Wnt4 reverse	CTCTCTCTCGAGTCACCGGCATGTGTGCATTTCAAC
Wnt11b forward	AGAGAGGAATTCACCATGGCTCCGACCCGTCACTGGGTT
Wnt11b reverse	CTCTCTCTCGAGTTACTTGCAGACATACCTCTCCAC
Wnt8a-HA-GFP/Venus forward part 1	AGAGAGGGATCCACCATGGAAAACACCACTTTGTTCATC
Wnt8a-HA-GFP/Venus reverse part1	CTCTCTCTCGAGAGCATAATCTGGAACATCATATGG
Wnt11b-HA-GFP/Venus forward part 1	AGAGAGGAATTCACCATGGCTCCGACCCGTCACTGGGTT
Wnt11b-HA-GFP/Venus reverse part 1	CTCTCTCTCGAGTGCGTAGTCTGGGACGTCGTATGG
Wnt-HA-GFP/Venus forward part 2	AGAGAGCTCGAGATGGTGAGCAAGGGCGAGGAGCTG
Wnt-HA-GFP/Venus reverse part 2	CTCTCTTCTAGATTACTTGTACAGCTCGTCCATGCC

2.4.2 General cloning strategy

DNA constructs were amplified by PCR using Phusion® high fidelity DNA polymerase. Reactions were set up in sterile PCR tubes as follows:

- 0.5µl Phusion DNA polymerase (2000 units/ml)
- 2-5µl Template DNA
- 2.5µl Forward/reverse primers (10µM)
- 0.5µl dNTPs
- 5µl of 5X High fidelity buffer
- Made up to 50µl using molecular grade water

The amount of template DNA used varied based on the source of the DNA. If the DNA was from a plasmid mini prep it was diluted down to 1ng/µl and then 2µl were used. If the DNA was produced via cDNA synthesis, 5µl of the cDNA was used per reaction. The PCR was as follows:

2 minutes	98°C	
15 seconds	98°C	
15 seconds	55-65°C	**} X30**
15-40 seconds	72°C	
10 minutes	72°C	

The annealing temperature depended on the combination of primers being used. The extension time depended on the length of the construct being amplified, Phusion is able to synthesise DNA at a rate of 1Kb per 15 seconds. Following the reaction the PCR products were cleaned up using a QIAquick gel extraction kit. The clean-up was carried out using the manufacturer's instructions with the exception that the final elution was performed using 30µl of molecular grade water. Following this 2µl of PCR product were checked on a 1% agarose gel by gel electrophoresis. All of the PCR primers developed for subcloning contain unique restriction sites that are incorporated up and downstream of the gene being amplified. Following the PCR clean up the

remaining 28µl of PCR product was digested using the appropriate restriction enzymes. The reaction was set up as follows:

- 28µl PCR product
- 2µl Appropriate restriction enzymes
- 5µl 10X Restriction enzyme buffer
- Made up to 50µl using molecular grade water.

At the same time the vector $CS2^{+}$ was prepared via restriction digest so that the PCR products could be cloned directly into the vector. The reaction was set up as follows:

- 1.5ug $CS2^{+}$
- 2µl Appropriate restriction enzymes
- 5µl 10X Restriction enzyme buffer
- Made up to 50µl using molecular grade water

Reactions were placed at 37°C for 3 hours, after which 5µl of each reaction was checked on a 1% agarose gel. Once cut to completion, the restriction digests containing the PCR products were moved onto ice. The digests containing CS2+ had 1ul of calf alkaline intestinal phosphatase added and the reaction was kept at 37°C for 6 more minutes. Following this, the calf alkaline intestinal phosphatase was inactivated at 65°C for 15 minutes. The digests containing CS2+ were placed on ice; while a 1% ultrapure agarose gel was prepared for electrophoresis. DNA loading buffer was added to each of the samples and then the samples were run on the ultrapure gel for one hour at 120mV. Following this a gel extraction and clean-up was performed using the QIAquick gel extraction kit as instructed. Ligation reactions were then set up using CS2+ and the various PCR products. Ligation reactions were set up as follows:

- 1µl T4 polymerase
- 1µl T4 polymerase buffer
- 1µl $CS2^{+}$
- 2-3µl PCR products
- Made up to 10µl using molecular grade water

Ligation reactions were given 15 hours at 12°C before being frozen. Ligation reactions were kept at -20°C until use. When ready 5µl of each ligation reaction was transformed into DH5αTM competent cells and PCR screens/mini preps were carried out as described above. Where two or more PCR products were cloned into CS2^{+} this was done simultaneously, but the total reaction volume never exceeded 10µl.

2.4.3 Specific constructs

Glypican4-Cerulean

GPI anchor proteins contain a short C terminal sequence that is cleaved off to attach the GPI anchor. Consequently cerulean could not be fused directly to the C terminus of glypican4 (White et al., 2000). The target GPI anchor sequence was determined and then cerulean inserted into a region upstream of the GPI anchor sequence. This region is poorly conserved and only found in *Xenopus* glypican4. Three primer pairs were developed to subclone Glycpican4-Cerulean. Glypican4-Cerulean part 1 amplified the majority of glypican4 up to the poorly conserved C terminal sequence where cerulean was to be inserted. Glypican4-Cerulean part 2 amplified cerulean, the up and downstream regions of this PCR product contained complementary restriction enzymes sites to part 1 and 3. Glypican4-Cerulean part 3 amplified the C terminal section of glypican4, downstream of the poorly conserved region. The three PCR amplicons were then cloned into CS2^{+}, inserting cerulean into the glypican4 gene. A diagram of the Glypican4-Cerulen construct can be seen in the appendices.

mCerulean

mCerulean was developed from an existing mRFP construct. mRFP contains a C terminal farnesylation sequence that targets red fluorescent protein to the plasma membrane. Red fluorescent protein is fused to the farnesylation sequence using a BspE1 restriction site. The reverse primer used to amplify cerulean contained the BspE1 site. Red fluorescent protein was cut out of CS2+ leaving the farnesylation sequence behind and cerulean was inserted in

its place. A diagram of the mCerulean construct can be seen in the appendices.

Wnt8a and Wnt11b-HA-GFP/Venus

The fluorescent Wnt ligands were designed so that each of the ligands/ fluorophores could be easily interchanged. The first step was to PCR clone Wnt8a and Wnt11b-HA into CS2+ from existing Wnt8a and Wnt11b-HA constructs. This way the stop codons of Wnt8a and Wnt11b-HA were mutated. Green fluorescent protein was then fused to the HA tag to create Wnt8a and Wnt11b-HA-GFP. Wnt8a and Wnt11b-HA was used for this process so that the HA tag could act as a linker domain to put space between the larger Wnt and green fluorescent proteins. The N and C terminal regions of green fluorescent protein and Venus are identical, so once the Wnt-HA-GFP constructs were developed, the same green fluorescent protein primers could be used to amplify Venus and fuse it to Wnt8a and Wnt11b-HA. Diagrams of the Wnt8a-HA-GFP/Venus and Wnt11b-HA-GFP/Venus constructs can be seen in the appendices.

2.5 Statistics and data analysis

2.5.1 Statistical tests used

To analyse continuous data (the percentage of X colocalising with Y) the non-parametric test Mann-Whitney U was used (Dytham, 2005). All of the error bars shown in this thesis represent the standard error of the mean (s.e.m). The students t-test was not used because the majority of the data analysed was not normally distributed and the variance of each sample was not equal, reviewed by (Fay and Proschan, 2010). To analyse discontinuous data (number of embryos displaying a phenotype) the non-parametric Chi square test was used (Dytham, 2005).

2.5.2 Determining the percentage colocalisation of different fluorescent proteins with the plasma membrane using Matlab

In order to determine the percentage coloclaistion of different fluorescent proteins with the plasma membrane a programme was written in Matlab. The programme was written by Stephen Cross. The main script contains the variables for the program, which once initiated calls the functions that analyse the data. These were set by Stephen Cross when he initially wrote the programme. The programme was designed using four randomly selected fields of data. Stephen designed the programme without knowing what the experiment meant, in an attempt not to bias the analysis. All of the images are converted to image sequence documents before analysis. The main script initially calls a function that determines the pixels that correspond to the plasma membrane in the image based on a pixel threshold. Following this a second function creates a mask using the pixels that correspond to the plasma membrane. The number of pixels in this mask that are occupied by pixels from a different channel (ie the protein being examined) is then determined. Following this, the membrane mask inverts so that the pixels on the membrane are no longer analysed, instead the pixels in the cytoplasm now make up the mask. The final function then analyses the percentage of pixels in this second mask that colocaise with pixels from another channel. The output from the analysis is the percentage of the membrane and the percentage of the cytoplasm occupied by the fluorophore being analysed. This was then used to determine the relative amount of protein colocalised with the plasma membrane.

Matlab script

Location analysis

```
%This is the main script, which calls all the other functions.
%"locationAnalysis" is what needs to be put in the command window to get
%this to run.

%Any variables currently stored are cleared at the start of each run of the
%analysis script
clear
```

```
%PARAMETERS:
initial_threshold = 30;  %This is an intensity threshold against which the
%cell wall image is compared.  Any pixels in the image with an intensity
%(ranging from 0-255) above this threshold are classed as corresponding to
%the cell wall and are used as a mask

filter_threshold = 30;  %This intensity threshold determines which pixels
%are classed as corresponding to the protein being analysed.

bulk = 0;  %This defines the amount by which the width of cell walls in the
%cell wall mask are increased.  Setting this to "0" will not increase the
%width.  Changing this will increase the area around the cell walls in
%which proteins are classed as being colocalised with the cell wall

plot_condition = 1;  %This determines whether the system will display
%images.  Setting this to "1" will show images and setting to "0" will
%surpress images

%MAIN SCRIPT:
%Asking the user to enter the root filename of the two images to be
%analysed.  This name doesn't contain the "0000.tif" part of the name.  It
%is a "string" variable type (word), so is written in single inverted
%commas
root_filename = input('Enter filename root: ', 's');

%Displaying the current filename (as input by the user) in the command
%window
disp(['Analysing "',root_filename, '"']);

%Loading the two images for analysis.  "base_im" is the image showing the
%cell walls and "top_im" is the image showing the proteins of interest
base_im = imread(strcat([root_filename,'0001.tif']));
top_im = imread(strcat([root_filename,'0000.tif']));

%Displaying the cell wall image ("base_im") if the user set
%"plot_condition" to "1"
if plot_condition == 1
   %Opening a new figure window
   figure();

   %Populating the new figure window with "base_im" and telling it to
   %display in grayscale (the default colourmap is a visible colour
   %spectrum)
   image(base_im), colormap(gray);

   figure();
   image(top_im), colormap(gray);

end

%Calling the two main functions, which generate and apply the image masks.
%These take certain input variables (listed in brackets) and output other
%ones (in square brackets).  The variables are listed in detail at the
%beginning of each of the functions.  Both functions operate in a very
%similar manner.  One function is for analysing proteins colocalised with
%the cell wall and the other analyses how much protein isn't on the cell
%wall.

[cell_wall_im filt_cell_wall_im cell_wall_table] = cellWallAnalysis(...
   base_im, top_im, initial_threshold, bulk, filter_threshold);

[membrane_im filt_membrane_im membrane_table] = membraneAnalysis(...
```

```
    base_im, top_im, initial_threshold, bulk, filter_threshold);

%If the user specified "plot_condition = 1" this will execute and display a
%series of images.  In each case a new figure window is opened.
if plot_condition == 1
    %The protein image with only the cell wall region displayed
    figure();
    image(cell_wall_im), colormap(gray);

    %The protein image with only the cell wall region displayed and
    %thresholded, so only pixels with an intensity above "filter_threshold"
    %are displayed
    figure();
    image(filt_cell_wall_im), colormap(gray);

    %The protein image with only the membrane region displayed
    figure();
    image(membrane_im), colormap(gray);

    %The protein image with only the membrane region displayed and
    %thresholded, so only pixels with an intensity above "filter_threshold"
    %are displayed
    figure();
    image(filt_membrane_im), colormap(gray);

end

%ANALYSIS:
%Calculating the percentage of pixels in the cell wall region, which are
%above "filter_threshold".

%"cell_wall_table" contains all the pixels, which were determined
%previously to lie on a cell wall.  Measuring the number of rows in this
%table gives the total number of pixels on the cell wall.
cell_wall_num_total = size(cell_wall_table);

%Here, the number of pixels in the protein image, which lie on the cell
%wall and have an intensity above "filter_threshold" are counted.
cell_wall_num_populated = size(find(cell_wall_table(:,4)==255));

%This calculates the percentage of pixels that correspond with protein
%(populated) in the total number of possible pixels (area in pixels of the
%cell wall)
cell_wall_percentage = (cell_wall_num_populated(1,1)/cell_wall_num_total...
    (1,1))*100;

%The percentage is displayed in the command window
disp([num2str(cell_wall_percentage), '% of cell wall populated']);

%The same analysis is conducted for the protein on the membrane image
membrane_num_total = size(membrane_table);
membrane_num_populated = size(find(membrane_table(:,4)==255));
membrane_percentage = (membrane_num_populated(1,1)/...
    membrane_num_total(1,1))*100;
disp([num2str(membrane_percentage), '% of membrane populated']);

%A blank line is output to the command line to make the output look tidier
disp([' ']);
```

Make mask

```
%This function takes a greyscale image and applies a pixel intensity
```

```
%threshold.  Pixels above (or equal to) this threshold are set to "255" and
%those below are set to "0".  There is also the option to increase the area
%surrounding the pixels above "255".  With this "bulking" option all the
%pixels within a square region around each pixel above the threshold is set
%to "255" regardless of their initial intensity.

%INPUTS:
%"input_im" is the input image, which is to be thresholded and turned into
%a mask
%"threshold" is the threshold to be applied to the input image.  It has to
%have a value between "0" and "255"
%"bulk" is a distance in pixels, which determines the area around all
%pixels with initial intensity above the threshold in which all pixels will
%be set to "255". Setting this to "0" effectively turns the feature off.

%OUTPUTS:
%"mask" is the modified version of "input_im", which displays all regions
%above the threshold with intensity "255" and those below with intensity
%"0"

function [mask] = makeMask(input_im, threshold, bulk)

%Initialising the array "mask".  This will be the same size as "input_im",
%so mask is initially just set to be a copy of "input_im"
mask = input_im;

%Applying the threshold to "input_im".  All pixels in "mask" corresponding
%to pixels in "input_im" below the threshold are set to "0"
mask(find(input_im(:,:) < threshold)) = 0;

%Applying the other part of the threshold.  All pixels above "threshold"
%are set to "255"
mask(find(input_im(:,:) >= threshold)) = 255;

%Applying the bulking feature.  This will always run, but if "bulk" is set
%to "0" the image will be unaffected.

%Generating a table called "mask_table", which lists the pixel locations of
%all pixels, which were initially above the threshold (i.e. have thus far
%been assigned an intensity of "255")
[mask_table(:,1), mask_table(:,2)] = find(mask == 255);

%Measuring the size of "mask_table".  This will tell how many rows are in
%"mask_table" and thus is used to determine how many times the bulking loop
%needs to run
size_mask_table = size(mask_table);

%Once for each row in "mask_table" this loop will run.  At each iteration
%the value "i" will increase by "1".  This is used to access the current
%row in "mask_table"
for i = 1:size_mask_table(1,1)
   %It will try to access some pixels outside the image when bulking,
   %which would cause the system to crash.  By using a "try" statement
   %the system will skip any attempts at assigning a new intensity to
   %a pixel where it fails.
   try
      %This section accesses a square region of "mask" around each pixel,
      %which was initially above the threshold. The square region has the
      %width (2*bulk)+1 (i.e. "bulk" either side of the current pixel and
      %the pixel itself) and the same height.
      mask((mask_table(i,1)-bulk):(mask_table(i,1)+bulk),...
         (mask_table(i,2)-bulk):(mask_table(i,2)+bulk)) = 255;
```

```
    end

end

%Along two edges of the image (the edges with pixel locations not equal to
%"1") "mask" will be "bulk" wider than "input_im".  This can cause problems
%when applying the mask (trying to multiple matrices of different
%dimensions is not possible), so those extra rows and columns are deleted.

%To know which rows and columns to remove the size of "mask" must be known.
%The number of rows and columns is set to "rows" and "cols".
[rows, cols] = size(mask);

%This takes the extra rows and columns and sets them to "[]", which has the
%effect of removing those rows or columns.
mask(rows-bulk+1:rows,:) = [];
mask(:,cols-bulk+1:cols) = [];
```

Cell wall analysis

```
%This function calls the functions responsible for generating and applying
%the mask, such that only regions of the top image ("top_im") are
%accessible (all other regions being set to an intensity of "0").  The
%locations and intensities of all pixels classed as being in the cell wall
%are stored in "cell_wall_table" for analysis outside of the function.

%INPUTS:
%"base_im" is the image showing the cell walls, which will be turned into a
%mask for "top_im"
%"top_im" is the image showing the proteins to be analysed
%"initial_threshold" is an intensity threshold, which determines which
%regions of "base_im" will be classed as being cell walls or membrane
%"bulk" is the pixel width added to the cell walls to increase the area
%in which proteins are classed as being co-localised with the cell wall
%"filter_threshold" is an intensity threshold, which distinguishes between
%proteins and the background

%OUTPUTS:
%"cell_wall_im" is "top_im" with the cell wall mask applied
%"filt_cell_wall_im" is "top_im" with the cell wall mask applied and all
%pixels with intensities above "filter_threshold" set to 255 and those
%below set to "0"
%"cell_wall_table" is a 4 column table containing information for all
%pixels identified as being in the cell wall.  The columns are horizontal
%position, vertical position, intensity in "top_im" and post-filter
%intensity

function [cell_wall_im filt_cell_wall_im cell_wall_table] = ...
    cellWallAnalysis(base_im, top_im, initial_threshold, bulk, ...
    filter_threshold)

%This function generates the mask outlining the cell walls.  It also
%applies any cell wall bulking as defined by the user (in "bulk")
[cell_wall_mask] = makeMask(base_im, initial_threshold, bulk);

%Applying the mask to "top_im".  The mask is set as either "0" or "255", so
%for the purpose of applying the mask all values are divided by "255"
cell_wall_im = top_im.*(cell_wall_mask/255);

%Applying the filter to "cell_wall_im", which sets all pixels above
%"filter_threshold" to "255" and all those below it to "0".  The filtered
```

```
%image is set to "filt_cell_wall_im".
[filt_cell_wall_im] = makeMask(cell_wall_im, filter_threshold, 0);

%Setting the first two columns of "cell_wall_table" to the row and column
%of each pixel in the cell wall.  These are identified as all locations in
%"cell_wall_mask" with an intensity equal to 255
[cell_wall_table(:,1), cell_wall_table(:,2)] = find(cell_wall_mask == 255);

%The number of pixels in the cell wall is given by the size of
%"cell_wall_table"
num_px = size(cell_wall_table);

%For each pixel listed by its coordinates in "cell_wall_table" the
%pre-filtered intensity (actual intensity in "top_im") and the
%post-filtered intensity ("0" or "255") are added to columns 3 and 4 of
%"cell_wall_table" respectively.
for i = 1:num_px
   cell_wall_table(i,3) = cell_wall_im(cell_wall_table(i,1),...
      cell_wall_table(i,2));

   cell_wall_table(i,4) = filt_cell_wall_im(cell_wall_table(i,1),...
      cell_wall_table(i,2));

end
```

Invert mask

```
%This function takes a black and white image (pixel intensities either "0"
%or "255") and inverts it.

%INPUTS
%"im" is the input image, which is to be inverted

%OUTPUTS
%"im" is the output image.  It is the same as the input version, but with
%inverted pixel intensities.

function [im] = invertim(im)

%All pixels with initial intensity "0" are set to an intermediate value of
%"1".  The built-in MATLAB "find" function searches the entire image, with
%the command "im(:,:)" telling MATLAB to access all rows and columns of the
%array "im".  The "find" function outputs an array of all the pixel
%locations with the intensity "0".  These locations are used to tell MATLAB
%which pixels to access and assign the intensity "1" to.
im(find(im(:,:) == 0)) = 1;

%Using a similar method, all pixels with initial intensity "255" are set to
%"0"
im(find(im(:,:) == 255)) = 0;

%All pixels which originally had intensity "255" have now been changed to
%"0".  Therefore, the pixels which were originally "0" and were temporarily
%changed to "1" can be changed to their final value of "255".
im(find(im(:,:) == 1)) = 255;
```

Membrane analysis

```
%This function calls the functions responsible for generating and applying
%the mask, such that only regions of the top image ("top_im") are
```

```
%accessible (all other regions being set to an intensity of "0").  The
%locations and intensities of all pixels classed as being in the membrane
%are stored in "membrane_table" for analysis outside of the function.

%INPUTS:
%"base_im" is the image showing the cell walls, which will be turned into a
%mask for "top_im"
%"top_im" is the image showing the proteins to be analysed
%"initial_threshold" is an intensity threshold, which determines which
%regions of "base_im" will be classed as being cell walls or membrane
%"bulk" is the pixel width added to the cell walls to increase the area
%in which proteins are classed as being co-localised with the cell wall
%"filter_threshold" is an intensity threshold, which distinguishes between
%proteins and the background

%OUTPUTS:
%"membrane_im" is "top_im" with the membrane mask applied
%"filt_membrane_im" is "top_im" with the membrane mask applied and all
%pixels with intensities above "filter_threshold" set to 255 and those
%below set to "0"
%"membrane_table" is a 4 column table containing information for all
%pixels identified as being in the cell wall.  The columns are horizontal
%position, vertical position, intensity in "top_im" and post-filter
%intensity

function [membrane_im filt_membrane_im membrane_table] = ...
    membraneAnalysis(base_im, top_im, initial_threshold, bulk, ...
    filter_threshold)

%This function generates the mask outlining the cell walls.  It also
%applies any cell wall bulking as defined by the user (in "bulk")
[membrane_mask] = makeMask(base_im, initial_threshold, bulk);

%The mask generated by "makeMask" would only show pixels in the cell wall
%if applied now.  Instead, this function inverts the mask, so when applied,
%it is the pixels in the membrane that are accessible (non-"0").
[membrane_mask] = invertImage(membrane_mask);

%Applying the mask to "top_im".  The mask is set as either "0" or "255", so
%for the purpose of applying the mask all values are divided by "255"
membrane_im = top_im.*(membrane_mask/255);

%Applying the filter to "membrane_im", which sets all pixels above
%"filter_threshold" to "255" and all those below it to "0".  The filtered
%image is set to "filt_membrane_im".
[filt_membrane_im] = makeMask(membrane_im, filter_threshold, 0);

%Setting the first two columns of "membrane_table" to the row and column
%of each pixel in the membrane.  These are identified as all locations in
%"membrane_mask" with an intensity equal to 255
[membrane_table(:,1), membrane_table(:,2)] = find(membrane_mask ~= 0);

%The number of pixels in the membrane is given by the size of
%"membrane_table"
num_px = size(membrane_table);

%For each pixel listed by its coordinates in "membrane_table" the
%pre-filtered intensity (actual intensity in "top_im") and the
%post-filtered intensity ("0" or "255") are added to columns 3 and 4 of
%"membrane_table" respectively.
for i = 1:num_px
    membrane_table(i,3) = membrane_im(membrane_table(i,1),...
```

```
    membrane_table(i,2));
  membrane_table(i,4) = filt_membrane_im(membrane_table(i,1),...
    membrane_table(i,2));

end
```

Note that the names ‘Cell wall analysis’ and ‘Membrane analysis’ were incorrectly labelled during the writing of the programme. Cell wall analysis refers to the analysis of pixels colocalising with the plasma membrane. Membrane analysis actually refers to the percentage of pixels colocalising with the cytoplasm.

2.5.3 Particle analysis using Fiji Image J

To analyse the qualitative shape of Wnt4/Wnt8a/Wnt11b-HA-GFP puncta on the cell membrane, Fiji Image J was used. Confocal images were opened directly in Fiji Image J and images were split into magenta (membrane) and green (Wnt-HA-GFP) channels. The green and magenta channels were thresholded using the auto-threshold function of Image J. ‘Moments’ was used for Wnt8a-HA-GFP and ‘Max Entropy’ was used for Wnt4/Wnt11b-HA-GFP puncta. The threshold ‘Moments’ was used to threshold the magenta channels for each image. The particles in each image were then analysed using the particle analysis function. Particles with an area of 0.1-10um^2 and a circularity of 0.1-1 were analysed. Circularity is a measure of how spherical particular puncta are, with 1 being a perfect circle and 0.1 being a straight line. The magenta channel was used as a mask for the analysis so that only puncta on the cell membrane were analysed.

2.5.4 Measuring coloclaisation using Fiji image J

To determine the percentage colocalisation between Wnt8a-HA-GFP and Wnt11b-HA-Venus, the Coloc 2 function of Fiji image J was used. Images were opened in Fiji image J and split into magenta (membrane), green (Wnt8a-HA-GFP) and yellow (Wnt11b-HA-Venus) channels. The green and yellow channels had the contrast enhanced by 0.01% and the background levels of fluorescence reduced by 4 pixels. The green and yellow channels were then thresholded using ‘Max Entropy’ and the magenta channel was thresholded using ‘Moments’. Following this the Manders’ correlation for Wnt8a-HA-GFP

and Wnt11b-HA-Venus was performed using the membrane as a mask. This allowed the percentage of Wnt8a-HA-GFP colocalising Wnt11b-HA-Venus on the cell membrane to be analysed. The Manders's correlation allows both the percentage of the yellow channel colocaising with the green channel and the percentage of the green channel colocalising with the yellow channel to be analysed (Manders et al., 1993). The same methods were used to analyse the percentage of Wnt8a and Wnt11b-HA-Venus that colocalised with caveolin-GFP, the only difference being that 'Moments' function was used as the auto-threshold for Wnt8a and Wnt11b-HA-Venus and caveolin-GFP.

2.5.5 Measuring the distance of diffusion of Wnt8a and Wnt11b-HA-GFP away from a source

To analyse the distance that Wnt8a and Wnt11b-HA-GFP diffused away from a source, the images for each condition were opened in one Photoshop document. The images were all taken under the same conditions on the microscope as to not bias the outcome of the experiment. The images were orientated so that the maximum range of Wnt-HA-GFP diffusion could be measured along the horizontal axis from left to right. Following this, the magenta channel was set to 0, so that only the green channel remained; the brightness/contrast of the green channel were not altered. All of the images for each condition were exported as a single bitmap and transferred to Fiji Image J. The ROI manager function was selected and a box 650pixels X 100pixels was drawn on the first panel in the bitmap. The box was positioned so that the very left hand side of it was touching the right hand edge of the Wnt expressing cells. The box was then shifted 27 pixels to the left (10um) so that it overlapped with the last 10um of the Wnt expressing cell. Once in position the data from the box was added to the ROI manager and the box was moved to the next panel in bitmap. Once data had been collected from all of the panels, the Multi plot function was selected. This plotted the intensity of GFP signal for every pixel along the 650 pixel horizontal axis. The intensity for each pixel along the horizontal axis was the average intensity of GFP along the Y axis.

To analyse the range of diffusion of Wnt8a and Wnt11b-HA-GFP puncta, the laser power of the confocal microscope was increased. A side effect of this was

that Wnt8a and Wnt11b-HA-GFP secreting cells appear bright green due to background levels of green fluorescent protein. The first 20uM of each of the plots was discarded as it distorted the levels of Wnt8a and Wnt11b-HA-GFP signal intensity when plotted on a graph. The distance over which the diffusion of Wnt8a and Wnt11b-HA-GFP could be measured varied between experiments. Importantly due to the curved nature of animal caps, the maximum range of Wnt8a and Wnt11b-HA-GFP diffusion could not be measured. Instead the graphs illustrate the rate of Wnt8a and Wnt11b-HA-GFP signal reduction with increasing distance from the source.

Curves were fit to the data using the regression wizard in Sigmaplot 12.5. With the exception of Wnt11b-HA-GFP diffusing away from a region expressing Sulf1 C-A (Figure 5.25C), all the plots were fitted using a single exponential decay model with three parameters. The Wnt11b-HA-GFP diffusing away from a region expressing Sulf1 C-A, was fit with a hyperbolic decay model with two parameters. Models were selected based on producing the lowest residual some of squares and the highest r^2 correlation values for each of the data sets. In addition the ability of the data to satisfy the Shapiro-Wilk, constant variance and Durbin-Watson statistics was also analysed (Durbin and Watson, 1950, 1951; Dytham, 2005). Once fitted the equations of the curves were used to predict the half-lives of Wnt ligand intensity for each of the data sets. In addition to plotting the curves the regression wizard in Sigmaplot 12.5 calculated the 95% confidence intervals for each of the curves. Confidence intervals are a measure of the dispersion of the distribution of the data. 95% confidence intervals display the range in which it is 95% certain the true mean values of the data are present (Dytham, 2005).

3.0 The effects of Sulf1 on canonical Wnt signalling

3.1 Introduction

3.1.1 The organiser domain

In 1924 Hans Spemann and Hilda Mangold showed that a small fragment of dorsal mesoderm transplanted to the ventral mesoderm of a salamander gastrula embryo resulted in the formation of a twinned embryo. This embryo possessed a completely patterned secondary axis containing, neural tissue, somites and other axial tissues. These structures were formed from the host tissue rather than directly from the dorsal mesoderm that was transplanted. The ability of the dorsal mesoderm to induce a well patterned secondary axis from host tissue lead to it being termed 'the organiser', reviewed in (De Robertis, 2009; De Robertis and Kuroda, 2004).

The organiser is responsible for the dorsal dorsal/ventral patterning of the embryo. Replacing the organiser with a graft from the ventral mesoderm of another embryo leads to ventralization of the embryo and a loss of axial structure. This phenotype is similar to that of UV ventralized embryos in which the dorsal axis fail to form (Malacinski et al., 1977; De Robertis, 2009). The dorsal/ventral patterning of the *Xenopus* embryo is achieved through the antagonistic interactions between secreted proteins from the dorsal and ventral mesoderm (see Figure 3.0). The organiser secretes several proteins involved in dorsal axis and head induction. These include the BMP inhibitors, chordin, noggin and follistatin (Hemmati-Brivanlou and Melton, 1992; Sasai et al., 1994; Smith and Harland, 1992), the Wnt inhibitor Frzb (Wang et al., 1997a) and the Wnt, nodal and BMP inhibitor cerberus (Bouwmeester et al., 1996). Chordin, noggin and follistatin are secreted from the organiser and diffuse ventrally to bind and inhibit BMP ligands in the ventral mesoderm (Fainsod et al., 1997; Piccolo et al., 1996; Zimmerman et al., 1996). Microinjection of mRNA encoding *chordin/noggin* rescued axis formation in UV ventralized embryos (Sasai et al., 1994; Smith and Harland, 1992). In addition microinjection of mRNA encoding follistatin lead to dorsalization of *Xenopus* embryos and loss of

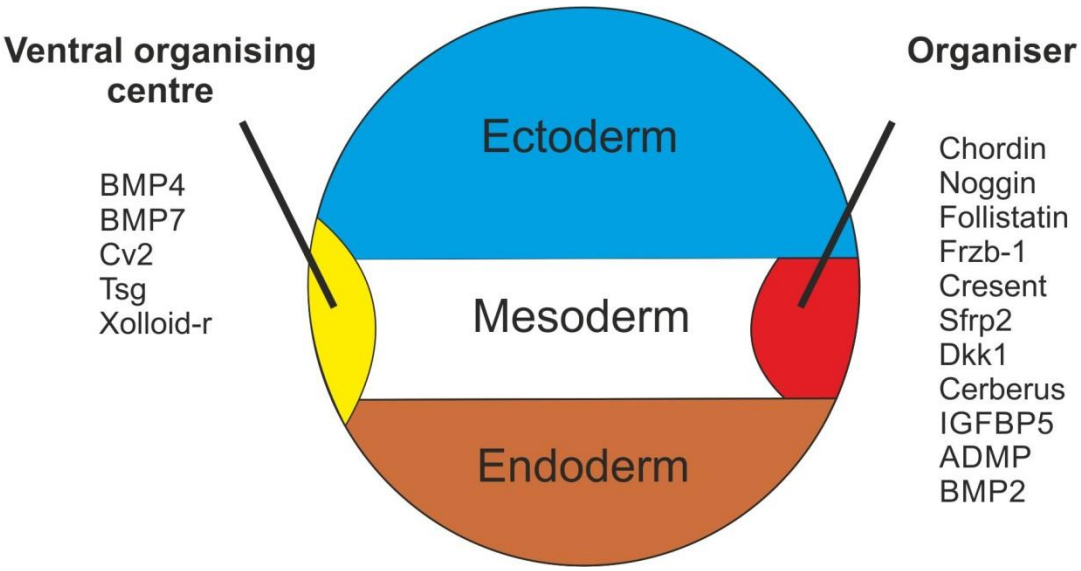

Figure 3.0; The organiser and ventral organising centre express secreted factors. The organiser and ventral organising centre secrete a variety of factors involved in the dorsal/ventral patterning of the embryo. BMP2/4/7 (bone morphogenetic protein2/4/7), Cv2 (crossveinless2), Tsg (twisted gastrulation), Xolloid-r (xolloid related), Sfrp2 (secreted frizzled related2), Dkk1 (dickopff1), IGFBP5 (insulin like growth factor binding protein 5), ADMP (anti dorsalizing morphogenetic protein). Figure adapted from (De Robertis, 2009).

axis formation (Fainsod et al., 1997). BMP4 and 7 are expressed in the VMZ of mesoderm in a region termed the 'ventral organiser' (Fainsod et al., 1994; Wang et al., 1997b). BMP4 and 7 act as ventralizing signals, over-expression of mRNA encoding *BMP4/7* in *Xenopus* embryos inhibited the formation of the dorsal axis (Jones et al., 1996; Wang et al., 1997b). In addition BMP4 was able to rescue axis formation in *Xenopus* embryos dorsalized by treatment with LiCl (Fainsod et al., 1994). BMP4/7 diffuse dorsally to inhibit the proteins secreted from the organiser. VMZ explants treated with increasing concentrations of chordin expressed markers of the dorsal mesoderm. Treatment of VMZ explants with BMP4 in addition to chordin blocked the dorsalizing effects of chordin (Piccolo et al., 1996).

Signals from the dorsal and ventral organising domains mutually antagonise each other to pattern the dorsal/ventral axis. RNAi mediated knockdown of *chordin, noggin* and *follistatin* leads to loss of neural plate formation. Chordin, noggin and follistatin show some redundancy in axis formation, as the neural plate formed when only two out of the three genes were inhibited. Interestingly if BMP4/7, chordin, noggin and follistatin were all inhibited the neural plate did form (Khokha et al., 2005). In contrast RNAi mediated knockdown of BMP4/7

resulted in dorsal/anteriorization of embryos. These embryos showed expanded domains of *otx2* (forebrain) and *krox20* (hindbrain) gene expression as well as an increase in the expression of myoD (marker of skeletal muscle in the somites) (Reversade et al., 2005). The actions of the dorsal and ventral organising centres lead to the formation of a correctly patterned dorsal/ventral axis in *Xenopus*.

3.1.2 The role of canonical Wnt signalling in establishing the organiser

Activation of the canonical Wnt pathway leads to the downstream stabilisation of β-catenin and its translocation into the nucleus to activate gene transcription. In *Drosophila*, the Wnt homologue Wg induces the stabilisation of the β-catenin homologue armadillo in order to activate gene transcription (see introduction). Both pathways require the presence of the canonical Wnt co-receptor LRP6/arrow (Pinson et al., 2000; Tamai et al., 2000; Wehrli et al., 2000). Wnt ligands can be broadly divided into two separate categories based on the effect of the ligand on cell signalling. Canonical Wnt ligands are able to rescue axis formation in UV ventralized embryos and induce the transformation C57MG cells in culture (Du et al., 1995; Shimizu et al., 1997). Non-canonical Wnt ligands cannot rescue axis formation in UV ventralized embryos, but over-expression leads to a severe shortening of the embryonic axis (Du et al., 1995).

The type of Wnt ligand used does not always determine which signalling pathway is activated. Over-expression of Wnt5a in the ventral blastomeres of embryos at the four cell stage causes axial defects, but does not induce axis duplication in *Xenopus* (Moon et al., 1993). In contrast ventral over-expression of Wnt5a together with Fz5 causes axis duplication, but not axial defects (He et al., 1997). In addition purified Wnt5a protein does not activate Topflash in HEK 293 cells transfected with *Fz4*. However Wnt5a is a potent activator of Topflash in cells transfected with both *Fz4* and *LRP5* (Mikels and Nusse, 2006). Wnt5a is able to activate canonical or non-canonical Wnt signalling depending on the presence of specific Wnt receptors.

In addition to rescuing UV ventralized embryos canonical Wnt ligands induce

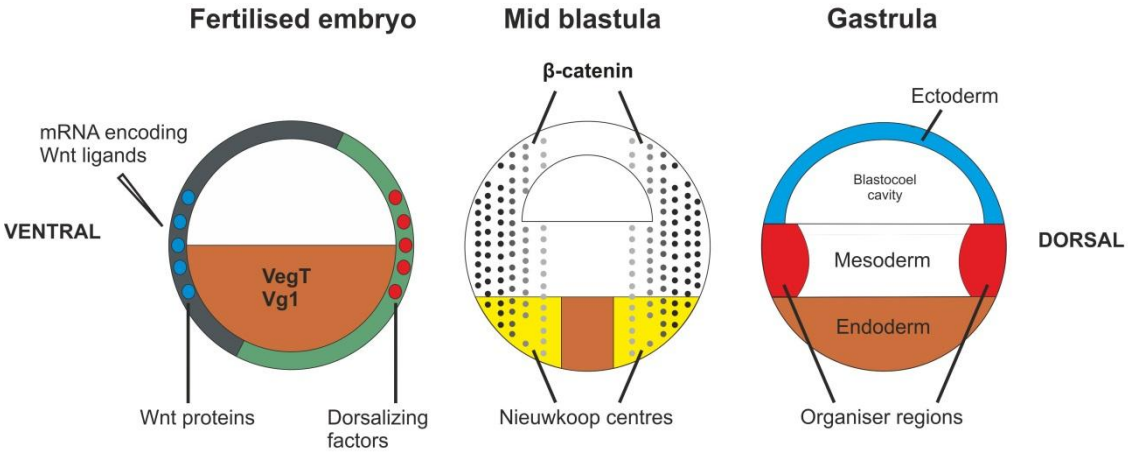

Figure 3.1; Microinjection of Wnt mRNA into the VMZ induces a secondary organiser. Microinjection of mRNA encoding *Wnt* ligands into the VMZ of the embryo leads to the over-expression of Wnt protein in this region. Wnt ligands activate the canonical Wnt signalling pathway leading to the induction of a secondary Nieuwkoop centre. High levels of nodals secreted from the two separate Nieuwkoop centres overlap with nuclear β-catenin leading to the formation of two separate organiser domains. Figure adapted from (De Robertis and Kuroda, 2004)

the formation of a secondary axis when over-expressed ventrally in *Xenopus* embryos (Christian et al., 1991; McMahon and Moon, 1989; Sokol et al., 1991; Wolda et al., 1993). Microinjection of mRNA encoding canonical Wnt ligands into a single ventral blastomeres at the four cell stage lead to the ectopic stabilisation of β-catenin. Ventrally stabilised β-catenin then overlaps with VegT and Vg1 to induce the formation of a secondary Nieuwkoop centre and subsequently a secondary organiser domain (see Figure 3.1). Over-expression of Wnt1 or Wnt3a induces the formation of a secondary axis that can be observed during neurala stages as a bifurcated neural tube (McMahon and Moon, 1989; Wolda et al., 1993). Over-expression of Wnt8a leads to the induction of a secondary axis with a full set of head and eyes. In addition histological sectioning of these embryos reveals the presence of a secondary notochord and secondary neural and muscle tissues (Sokol et al., 1991). Partial axis duplication can also be obtained by inhibiting BMP signalling on the ventral side of the embryo. Microinjection of mRNA encoding a *DN*BMP* receptor (*ΔmTRF11*) into both ventral blastomeres of embryos at the four cell stage induced the formation of a secondary axis. However unlike Wnt8a, the secondary axis induced by ΔmTRF11 did not have a full secondary head and eyes (Suzuki et al., 1994). Different proteins have qualitatively different effects on axis duplication in *Xenopus.*

Formation of the organiser requires the overlap of high levels of nodal signalling with nuclear localised β-catenin (Agius et al., 2000; Schneider et al., 1996; Stennard et al., 1996; Takahashi et al., 2000; Weeks and Melton, 1987). A particular subset of genes are expressed in the organiser, which include *Xnr3, siamois, goosecoid, noggin* and *chordin* (Cho et al., 1991; Lemaire et al., 1995; Sasai et al., 1994; Smith et al., 1995). Ectopic expression of these genes on the ventral side of the embryo will also lead to axis duplication. Over-expression of siamois at the four cell stage induces the formation of a secondary organiser, marked by the presence of a secondary blastopore lip. At later stages over-expressing siamois results in an embryo with a full secondary head and eyes (Lemaire et al., 1995). Ventral over-expression of goosecoid at the 4 cell stage leads to the formation of a secondary axis, but without complete head and eye duplication. Histological analysis of these embryos revealed the presence of a secondary notochord and secondary neural tissue (Cho et al., 1991).

Over-expression of chordin ventrally at the 32 cell stage leads to the induction of a secondary axis. In addition, chordin over-expression rescued the formation of the notochord and neural induction in UV irradiated embryos (Sasai et al., 1994). Noggin also rescued axis formation in UV ventralized embryos. Over-expression of Noggin in one ventral blastomere of a four cell stage embryo rescued dorsal axis induction including the formation of both head and eyes (Smith and Harland, 1992). In contrast Xnr3 was only able to rescue dorsal trunk induction in UV ventralized embryos. In addition over-expression of Xnr3 in wildtype embryos failed to induce axis duplication. Instead ectopic tube like protrusions formed in 20-30% of embryos (Smith et al., 1995). Different proteins expressed in the organiser region show differing abilities to induce axis duplication. Chordin, siamois and noggin show Wnt8a like activity inducing a full secondary axis with a complete set of head and eyes or completely rescuing axis formation in UV ventralized embryos (Lemaire et al., 1995; Sasai et al., 1994; Smith and Harland, 1992; Smith et al., 1995; Sokol et al., 1991). In contrast goosecoid and Xnr3 only have the ability to duplicate/rescue dorsal trunk formation when over-expressed in embryos (Cho et al., 1991; Smith et al., 1995).

Maternal depletion of β-catenin inhibited the expression of *chordin, siamois* and *Xnr3* in Xenopus embryos at NF stage 10.5 (Heasman et al., 2000). Ectopic expression of organiser genes can be induced by activating the canonical Wnt signalling pathway. LiCl, activates the canonical Wnt signalling pathway inducing ectopic expression of *chordin* and *siamois* (Klein and Melton, 1996; Lemaire et al., 1995; Sasai et al., 1994). In these experiments embryos were treated with LiCl at NF stages 6 and 7 before being analysed for *chordin* and *siamois* expression at NF stages 11.5 and 10 respectively. Over-expression of Wnt8a in the animal hemisphere of the embryo at the one cell stage expands the domain of *Xnr3* expression at NF stage 9 (Smith et al., 1995). Microinjection of mRNA encoding *β-catenin* induced the ectopic expression of *siamois* and *Xnr3* expression in animal cap tissue. In contrast culturing animal caps in either of bFGF or Activin did not induce *siamois* or *Xnr3* expression (Medina et al., 1997). One conclusion from this is that *siamois* and *Xnr3* are direct targets of canonical Wnt signalling and do not require FGF/nodal signalling or mesoderm induction (Slack et al., 1987; Smith, 1987).

Over-expression of β-catenin in the ventral blastomeres of 4 cell stage embryos leads to the ectopic induction of *chordin* RNA in ventral explants. However over-expression of Xnr1 and Xnr2 also caused ectopic *chordin* induction in ventral explants (Zorn et al., 1999). In addition over-expression of DN*FGF1r or DN*FGF4r inhibited *chordin* expression in *Xenopus* embryos at NF stage 10.5 (Branney et al., 2009). *Chordin* is a target of canonical Wnt signalling, however *Chordin* expression is also dependent on FGF/nodal signalling. The expression of *Chordin*, *siamois* and *Xnr3* in the embryo depends on the canonical Wnt signalling pathway. In addition ectopic activation of the canonical Wnt pathway causes the ectopic induction of all three genes. *Chordin, siamois* and *Xnr3* expression can be used to assay canonical Wnt signalling in the early *Xenopus* embryo.

3.1.3 Aims of this chapter

Sulf1 has been shown to enhance the ability of vertebrate Wnt ligands to activate canonical Wnt signalling in cell culture (Ai et al., 2003; Hayano et al., 2012; Tran et al., 2012). In contrast *Drosophila* Sulf1 inhibits Wg signalling in

the developing Wing disk (Kleinschmit et al., 2010; You et al., 2011). In addition Sulf1 has been found to enhance the ability of *Xenopus tropicalis* Wnt11b2 (XtWnt11b2) to induce axis duplication and *chordin* gene expression when both are over-expressed together (Freeman et al., 2008). Neither Sulf1, Wnt8a or Wnt3a have been shown to be expressed in the organiser region of the early *Xenopus* embryo (In der Rieden et al., 2010; Wolda et al., 1993) (Pownall laboratory unpublished data). Consequently this chapter will be concerned with investigating the effects of Sulf1 on canonical Wnt signalling rather than function of Sulf1 in the early *Xenopus* embryo.

mRNA encoding the ligands *Xenopus laevis Wnt3a* and *Wnt8a* were microinjected, with or without mRNA encoding *Xenopus tropicalis Sulf1*, into a single ventral blastomeres of a four cell stage embryo. The formation of a secondary axis and induction of an ectopic organiser were then investigated. In addition the same assays were used to determine the effects of Sulf1 on the non-canonical Wnt ligand *Xenopus laevis* Wnt11b (XlWnt11b). The results in this chapter show that Sulf1 differentially affects the ability of Wnt3a, Wnt8a and Wnt11b to activate canonical Wnt signalling. This cannot be explained simply by the previously proposed 'catch and present' model (Ai et al., 2003). The data suggests a more complex role for Sulf1 in regulating vertebrate Wnt signalling.

3.2 Results

3.2.1 Sulf1 inhibits the ability of Wnt8a to induce a secondary axis

The ability of Wnt8a to induce a second axis was used to examine the effects of Sulf1 on canonical Wnt signalling. Embryos were microinjected in the VMZ of one cell at the four cell stage, cultured until NF stage 36 and examined for phenotype. Injection of 1ng of mRNA encoding for *Sulf1* resulted in a failure of the blastopore to close in the majority of embryos (Figure 3.2B, red arrow marks exposed yolk, and see Figure 3.4B). Injection of 5pg of mRNA encoding for *Wnt8a* induced the formation of a secondary axis in 90% of embryos. Axis duplication was subdivided into embryos displaying duplicated cement glands, or a full set of head and eyes (Figure 3.2C, white arrowheads show full head duplication, Figure 3.2F red arrowheads mark duplicated cement glands). However when the same amount of *Wnt8a* is injected together with *Sulf1* the ability of Wnt8a to induce a secondary axis with a full set of head and eyes is abolished (compare Figure 3.2D-F to Figure 3.2C). The data from Figure 3.2 panels A-F is quantified in Figure 3.2G.

In addition to effects on axis induction, over-expression of Sulf1 together with Wnt8a lead to a notable truncation of the anterior/posterior axis (Figure 3.2D-F). To examine thisembryos were classified using the dorso-anterio axis (DAI) (see Figure 3.3) (Kao and Elinson, 1988). Injection of 1ng of mRNA encoding *Sulf1* caused axial defects in 95% of embryos (Figure 3.4A). Injection of 5pg of mRNA encoding *Wnt8a* had a similar effect to *Sulf1* on axis formation. Over-expression of Sulf1 and Wnt8a together enhanced axial defects with the majority of embryos displaying either a reduced or severely reduced posterior axis (Figure 3.4A). Embryos were also examined for how frequently the blastopore failed to close. Failure of the blastopore to close was analysed by the presence of exposed yolk in NF stage 36 embryos. Over-expression of Sulf1 resulted in the 88% of embryos displaying a failure of the blastopore to close correctly (Figure 3.4B). In contrast over-expression of

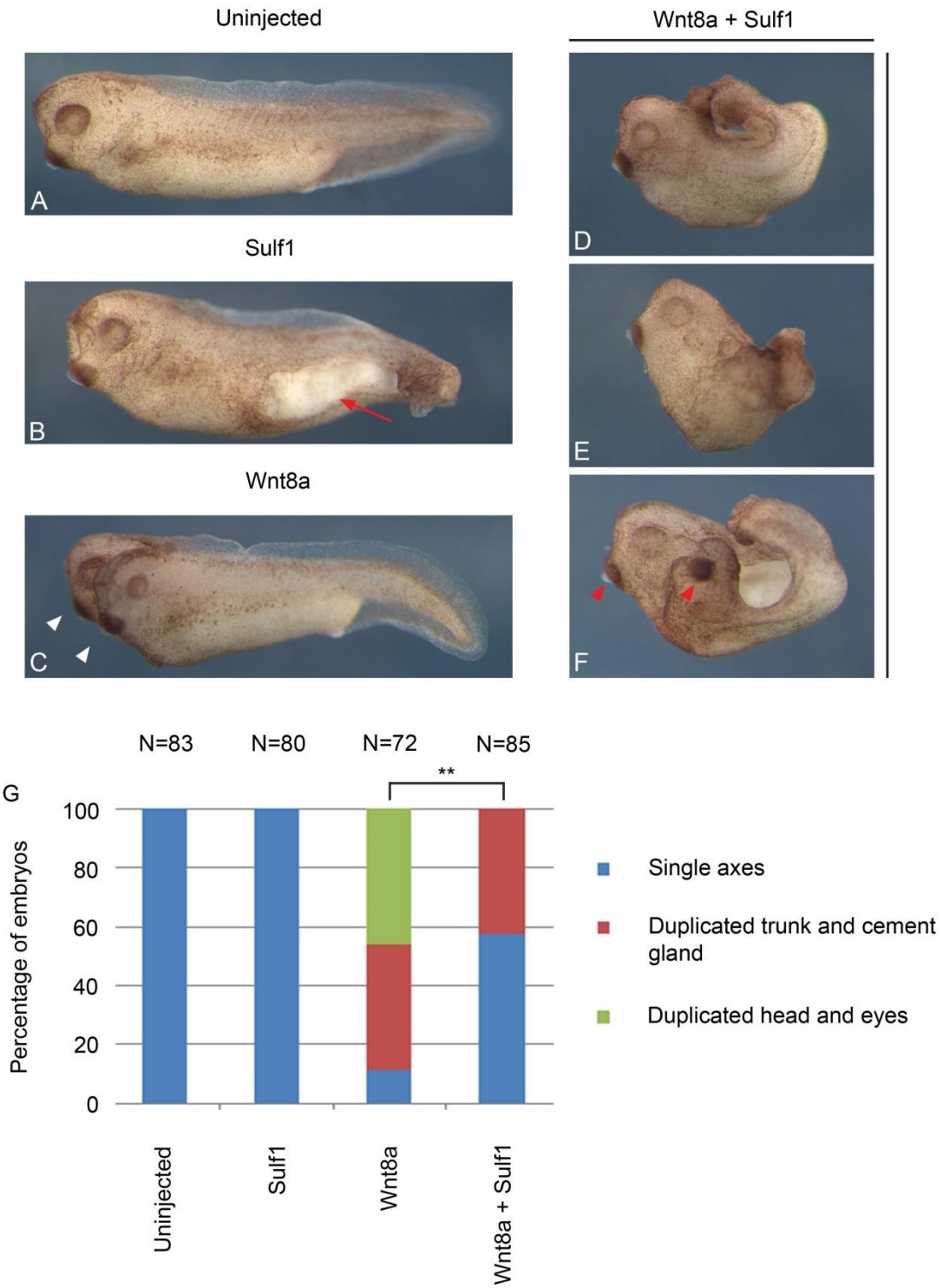

Figure 3.2; Sulf1 inhibits the ability of Wnt8a to induce axis duplication.
mRNA encoding *Sulf1* (1ng), *Wnt8a* (5pg) or both was injected into the VMZ of one cell of an embryo at the four cell stage. Embryos were cultured until NF stage 36 and then examined for phenotype. [A] Lateral view of an uninjected embryo. [B-C] lateral views of [B] *Sulf1* and [C] *Wnt8*a injected embryos. Over-expression of Sulf1 causes defects in gastrulation (red arrow marks exposed yolk), whereas Wnt8a over-expression results in axis duplication (white arrowheads show full head duplication). [D-F] Shows three different embryos coinjected with *Sulf1* and *Wnt8*a. Over-expression of both Sulf1 and Wnt8a enhances gastrulation defects, but inhibits the induction of a second head and eyes ([F] red arrowheads mark duplicated cement glands). [G] Graph quantifying the frequency of axis duplication in embryos injected with *Sulf1* and *Wnt8a.* Asterisks mark significant differences (**P<0.01) Chi-square test.

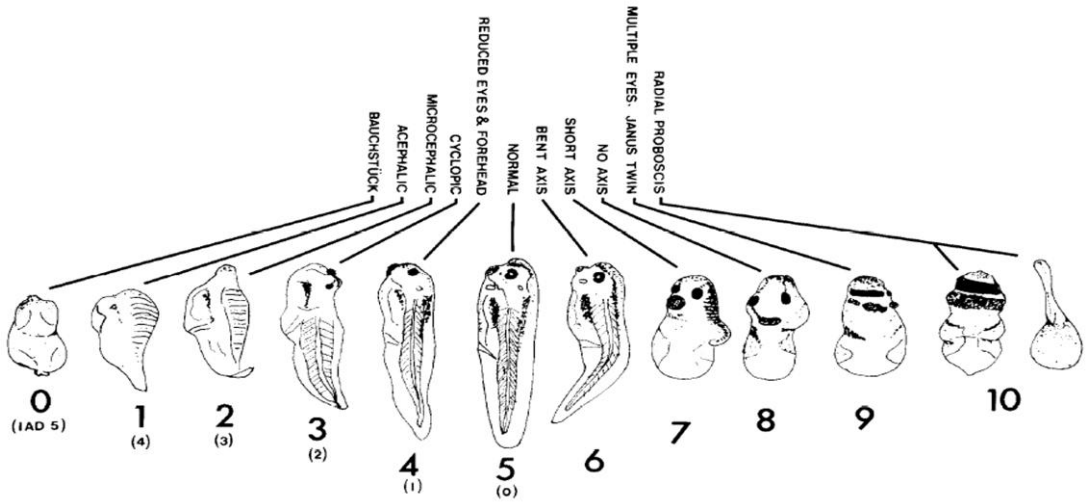

Figure 3.3; The dorso-anterior index.
Figure depicts the classification of axial defects using the dorso-anterior index (DAI) (Kao and Elinson, 1988). This system was used to classify axial defects seen in Figures 3.2 and 3.13. Embryos displaying reduced eyes and forehead with a relatively normal posterior axis are classified as DAI4. DAI5 embryos have a normal morphology. DAI6 embryos have normal head structures, but a slight bend in the posterior axis. DAI7 embryos have a severely reduced trunk although the somites are still visible. DAI8 embryos have a normal head structure, but lack other axial structures, no somites can be visualised. Figure from (Kao and Elinson, 1988).

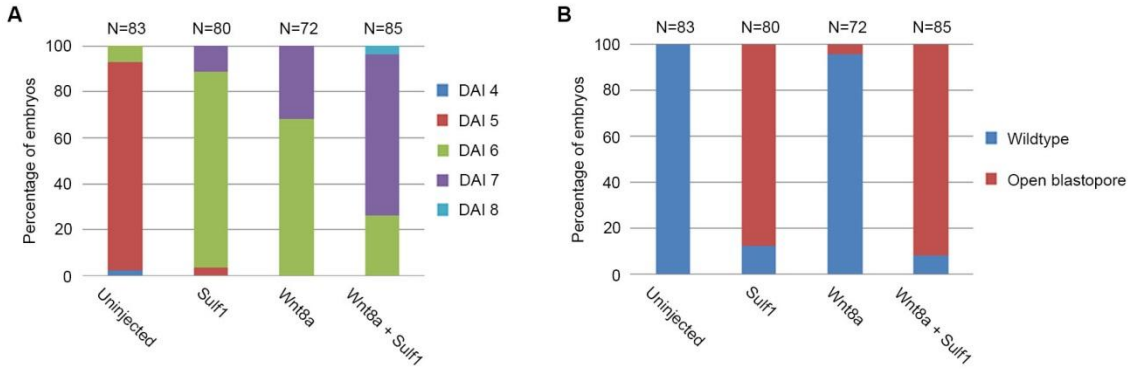

Figure 3.4; Over-expression of Sulf1 and Wnt8a enhanced embryonic axis defects.
mRNA encoding *Sulf1* (1ng), *Wnt8a* (5pg) or both was injected into the VMZ of one cell of an embryo at the four cell stage. Embryos were cultured until NF stage 36 and then examined for phenotype. [A] Over-expressing Sulf1 caused an increase in the number of embryos displaying a truncated posterior axis and this was enhanced by the over-expression Wnt8a alone. Over-expression of Sulf1 and Wnt8a together further enhanced axial defects, with the majority of embryos displaying either a reduced or severely reduced posterior axis. [B] Over-expression of Sulf1 resulted in a failure of blastopore closure in 90% of embryos, but over-expressing Wnt8a alone only caused this in 4% of embryos. Over-expression of Sulf1 and Wnt8a together did not enhance the number of embryos displaying a failure of blastopore closure.

Wnt8a alone did not affect blastopore closure. Over-expression of Sulf1 and Wnt8a together did not increase the frequency of embryos with defects in blastopore closure (Figure 3.4B). The data indicates that Sulf1 inhibits the ability of Wnt8a to induce an ectopic axis in *Xenopus* embryos, which suggests

that Sulf1 can inhibit the ability of Wnt8a to activate canonical Wnt signalling. In contrast *Sulf1* and *Wnt8a* synergise to enhance axial defects in injected embryos. One conclusion from this is that in the presence of Sulf1, Wnt8a is activating or inhibiting non-canonical Wnt signalling.

3.2.2 Sulf1 inhibits the ability of Wnt8a to induce ectopic *chordin* and *Xenopus nodal related 3* expression

Sulf1 inhibits the ability of Wnt8a to induce a secondary axis. One interpretation of this finding is that Sulf1 inhibits the ability of Wnt8a to activate canonical Wnt signalling. However there are other possible explanations: Sulf1 is a known inhibitor of BMP signalling and it has been shown that inhibiting BMP can result in a second axis (Freeman et al., 2008; Suzuki et al., 1994). In order to directly asses the effects of Sulf1 on canonical Wnt signalling, the expression of genes known to be targets of canonical Wnt signalling were analysed. *In situ* hybridisation analysis (Harland, 1991) was used to detect the expression of the organiser marker and direct canonical Wnt target gene *Xnr3.*

Embryos were microinjected with mRNAs encoding for *Sulf1* and *Wnt8a*, either individually or together, in the VMZ of one cell at the four cell stage and cultured until NF stage 10. Embryos were fixed and analysed for *Xnr3* gene expression by whole mount *in situ hybridisation*. Over-expression of Sulf1 alone did not affect *Xnr3* expression (compare Figure 3.5A to 3.5B). Over-expression of Wnt8a induced the formation of a second domain of *Xnr3* expression (see white arrowheads Figure 3.5C). Over-expression of Sulf1 together with Wnt8a completely inhibited the ability of Wnt8a to induce an additional domain of *Xnr3* expression (Figure 3.5D). The data from Figure 3.5A-F is quantified in Figure 3.5G.

C*hordin* gene expression in response to Wnt8a was similarly examined. Embryos were microinjected with mRNAs encoding for *Sulf1* and *Wnt8a*, either individually or together, in the VMZ of one cell at the four cell stage and cultured until NF stage 10.5. Embryos were fixed and analysed for *chordin* gene expression by whole mount *in situ hybridisation*. Over-expression of Sulf1 did not affect *chordin* expression (compare Figure 3.6A to 3.6B). Over-expression

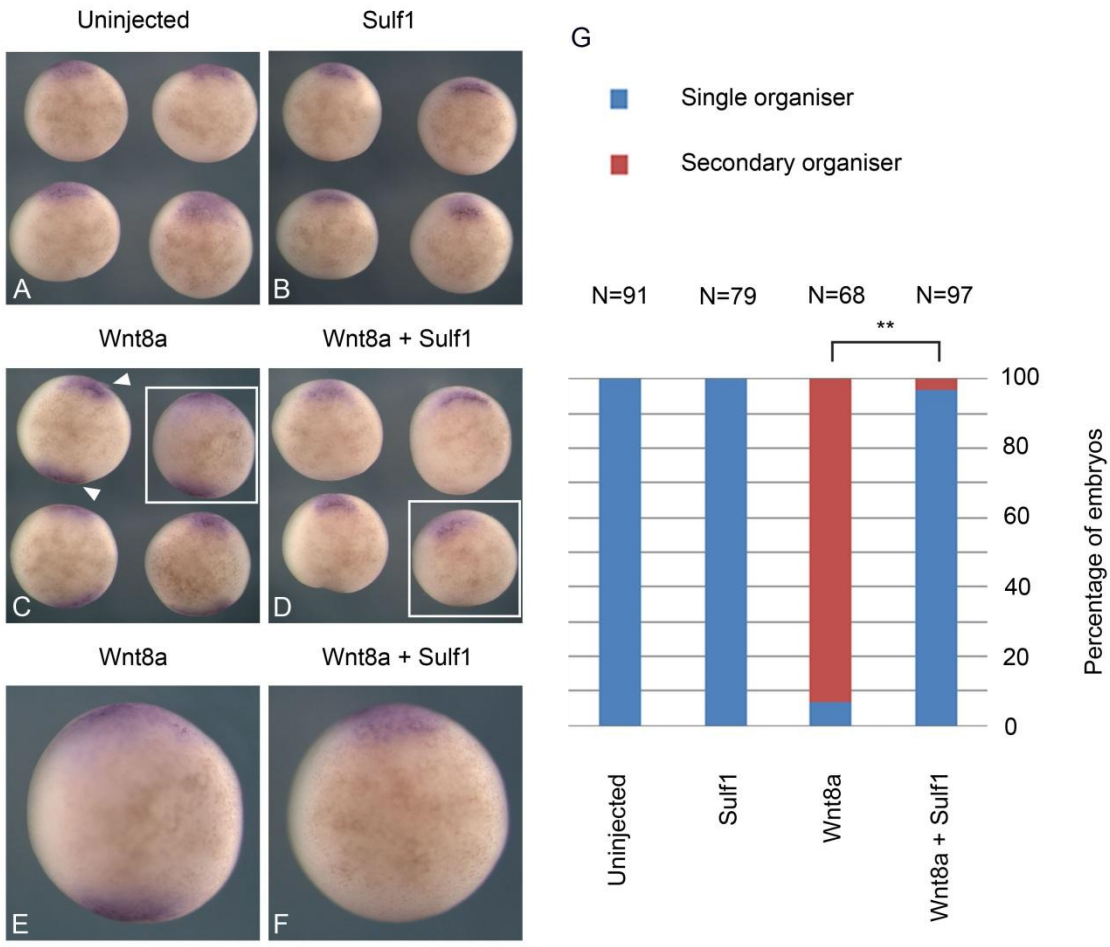

Figure 3.5; Sulf1 inhibits the ability of Wnt8a to induce ectopic *Xnr3* expression. mRNA encoding *Sulf1* (1ng), *Wnt8a* (5pg) or both was injected into the VMZ of one cell of an embryo at the four cell stage. Embryos were cultured until NF stage 10 and then analysed by whole mount *in situ hybridisation* for the expression of *Xnr3*. [A-F] Whole mount *in situ hybridisation* showing the expression of *Xnr3* in (A) uninjected embryos and embryos injected with [B] *Sulf1* [C and E] *Wnt8*a and [D and F] *Sulf1* and *Wnt8a*. The white boxes in [C] and [D] highlight the embryos used in [E] and [F] respectively. White arrowheads [C] mark the two regions of *Xnr3* expression. Over-expression of both Sulf1 and Wnt8a inhibits the ability of Wnt8a to induce an ectopic organiser [D]. [G] Graph quantifying the frequency of organiser induction in embryos injected with *Sulf1* and *Wnt8a.* Asterisks mark significant differences (**P<0.01) Chi-square test.

of Wnt8a induced the formation of a second domain of *chordin* expression (see white arrowheads Figure 3.6C). Over-expression of Sulf1 together with Wnt8a inhibited the ability of Wnt8a to induce an additional domain of *chordin* expression (Figure 3.6D). Ectopic *chordin* was still detected in these embryos; however it was no longer expressed as one broad domain lining the edge of the blastopore. Instead ectopic *chordin* expression was detected in either one or two small domains (compare Figure 3.6D to 3.6C). This qualitatively different type of chordin expression was classified as partial organiser induction (see Figure 3.6G). For embryos displaying two small domains of *chordin* expression

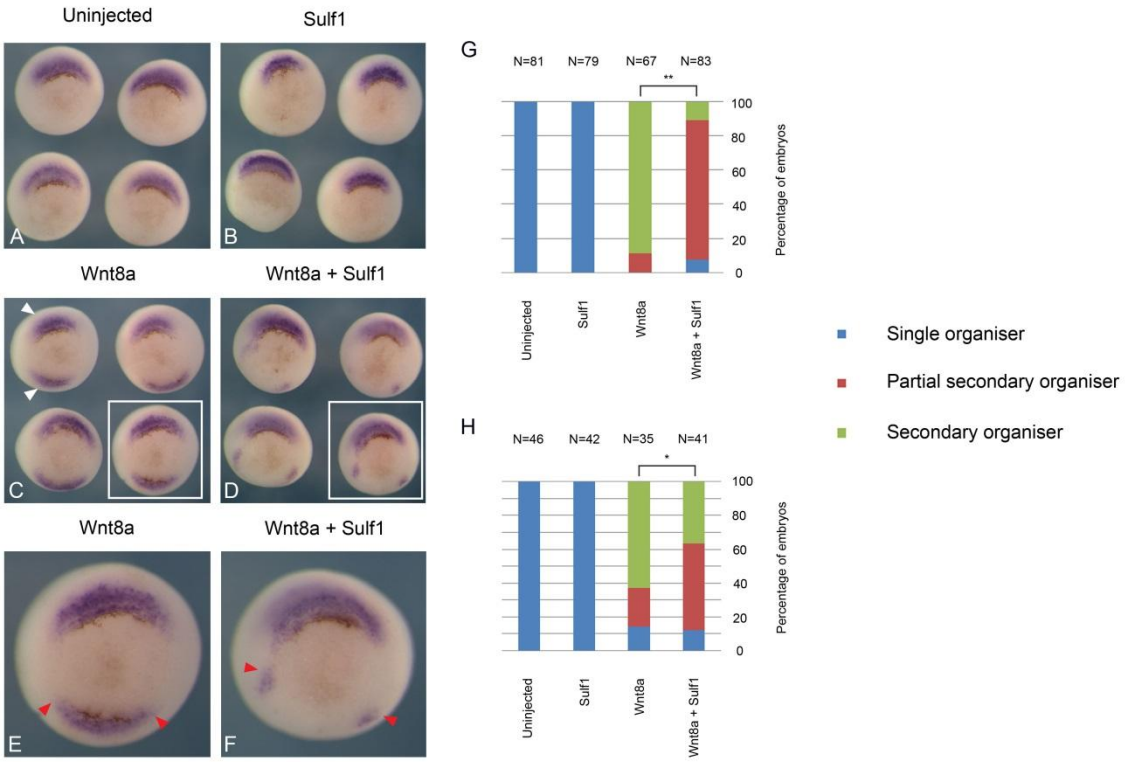

Figure 3.6; Sulf1 inhibits the ability of Wnt8a to induce ectopic *chordin* expression. mRNA encoding *Sulf1* (1ng), *Wnt8a* (5pg) or both was injected into the VMZ of one cell of an embryo at the four cell stage. Embryos were cultured until NF stage 10.5 and then analysed by whole mount *in situ hybridisation* for the expression of *chordin*. [A-F] Whole mount *in situ hybridisation* showing the expression of *chordin* in (A) uninjected embryos and embryos injected with [B] *Sulf1* [C and E] *Wnt8*a and [D and F] *Sulf1* and *Wnt8a*. The white boxes in [C] and [D] highlight the embryos used in [E] and [F] respectively. White arrowheads [C] mark the two regions of *chordin* expression. Over-expression of both Sulf1 and Wnt8a inhibits the ability of Wnt8a to induce ectopic *chordin* expression [D]. The red arrowheads [E] and [F] mark the very edges of the *chordin* domain. [G] Graph quantifying the frequency of organiser induction in embryos injected with *Sulf1* and *Wnt8a.* [H] Graph quantifying the frequency of organiser induction using 10pg of *Wnt8a* mRNA, the amount of *Sulf1* mRNA remained the same. Asterisks mark significant differences (*P<0.05 and **P<0.01) Chi-square test.

it appeared that the distance between these two domains was greater than the width of the ectopic *chordin* domain in embryos over-expressing Wnt8a alone. This is indicated by the red arrowheads in Figures 3.6E and 3.6F. The data from Figure 3.6A-F is quantified in Figure 3.6G. In addition the experiment was repeated using 10pg of *Wnt8a* mRNA to examine whether the effects of Sulf1 on Wnt8a signalling were dose specific (Figure 3.6H). Sulf1 significantly inhibits the ability of *Wnt8a* (5pg) to induce organiser induction at P<0.01. In contrast Sulf1 only inhibits the ability of *Wnt8a* (10pg) to induce organiser induction at P<0.05. Increasing the amount of *Wnt8a* mRNA reduced the ability of Sulf1 to inhibit Wnt8a signalling. Together the data shows that Sulf1 inhibits the ability of Wnt8a to induce the ectopic expression of the organiser genes *chordin* and

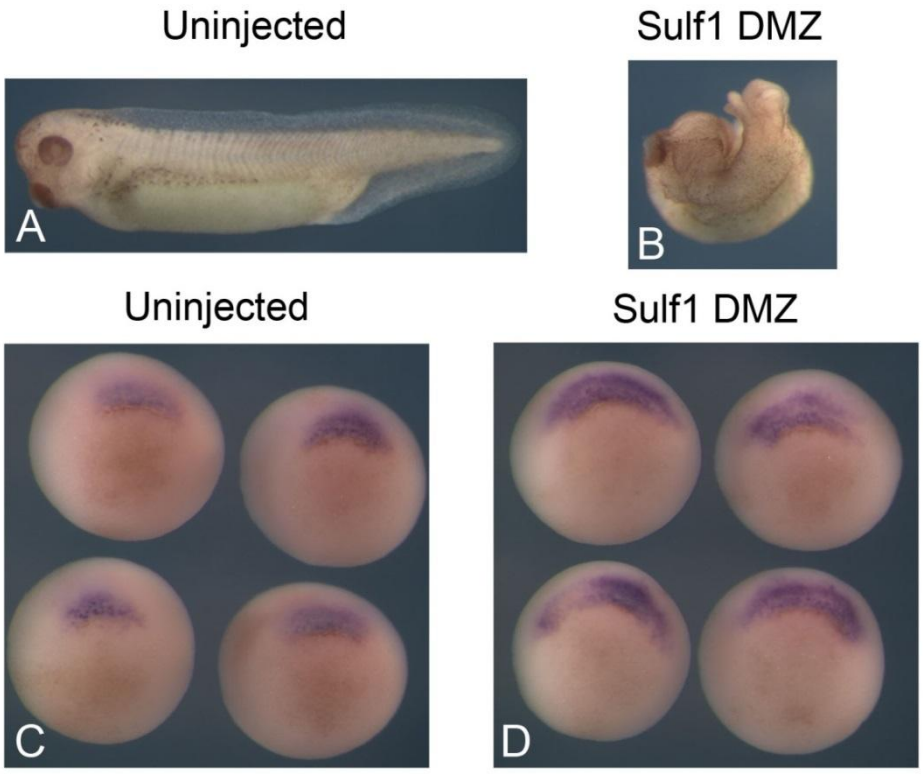

Figure 3.7; Over-expression of Sulf1 in the DMZ causes gastrulation defects, but does not inhibit *chordin* expression.
mRNA encoding *Sulf1* (4ng) was injected bi laterally into the DMZ of embryos at the four cell stage. Embryos were cultured until NF stage 10.5 and fixed for whole mount *in situ hybridisation* for *chordin* or NF stage 36 and analysed for phenotype. [A-B] Lateral view of [A] an uninjected embryo and [B] an embryo over-expressing Sulf1. [C-D] Vegetal views of *chordin* expression in [C] uninjected embryos and [D] embryos overexpressing Sulf1.

Xnr3.

Sulf1 inhibits the ability of Wnt8a to induce ectopic organiser gene expression. One prediction from this is that Sulf1 would affect the formation of the endogenous organiser. To investigate this mRNA encoding *Sulf1* was injected bilaterally in the DMZ of four cell stage embryos. Embryos were cultured until NF stage 10.5 and fixed for whole mount *in situ hybridisation* or NF stage 36 and analysed for phenotype. Over-expression of Sulf1 resulted in truncation of the embryonic axis (Figure 3.7B). However over-expression of Sulf1 did not inhibit endogenous *chordin* expression (compare Figure 3.7D to 3.7C). Over-expression of Sulf1 enhanced both the size and the width of the endogenous *chordin* domain. This contrasts with the ability of Sulf1 to inhibit Wnt8a induced *chordin* expression. One conclusion from this is that the function of Sulf1 *in vivo* is more complex than simply inhibiting the canonical Wnt signalling pathway.

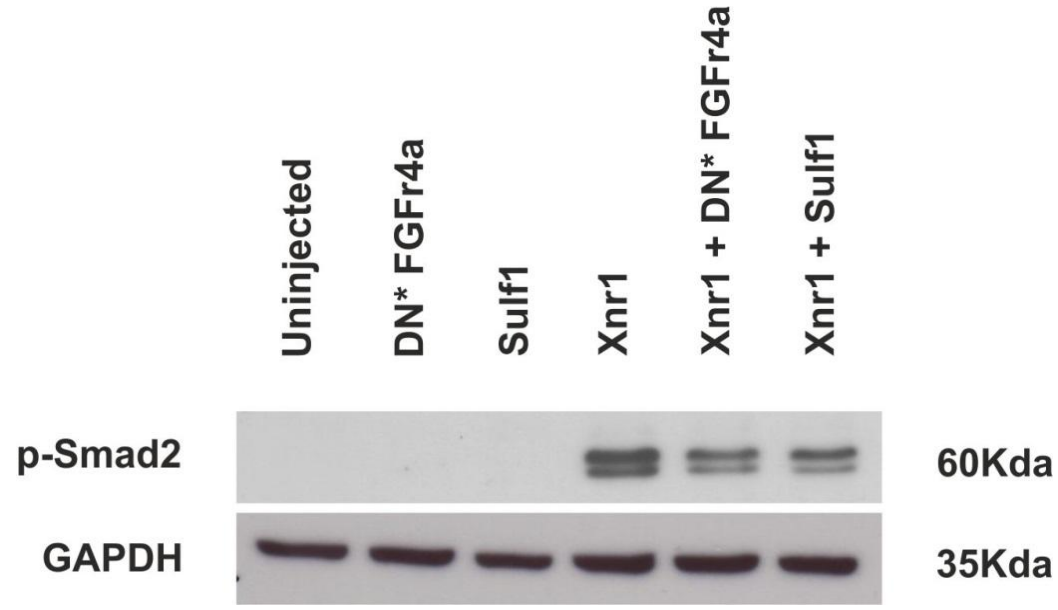

Figure 3.8; Sulf1 does not block Xnr1 induced activation of the nodal signalling pathway. mRNA coding for *Xnr1* (100pg), *DN*FGFr4a* (500pg) and *Sulf1* (4ng) was injected bilaterally into the animal hemisphere of embryos at the two cell stage. Embryos were cultured until NF stage 8 and then animal caps were taken and cultured until NF stage 10.5. Animal caps were then snap frozen for western blot. Over-expression of Xnr1 activates the nodal signalling pathway inducing pSmad2.

3.2.3 Sulf1 activity does not affect signalling by Xnr1

Nodal signalling, in addition to nuclear β-catenin is important for axis formation in *Xenopus*. Therefore it is possible that the effects seen on axis formation as a result of over-expressing Sulf1 could be due to its impact on nodal signalling in addition to or instead of effects on canonical Wnt signalling. Xnr1 is a protein expressed in the dorso-vegetal region of the embryo at NF stage 9 and is capable of inducing *chordin* expression in animal explants (Agius et al., 2000). Xnr1 is a member of the Transforming growth factor-β (TGF-β) family of growth factors and activation of nodal signalling results in phosphorylation of the transcription factor Smad2, reviewed by (Massague and Gomis, 2006). In order to directly asses the effects of Sullf1 on Xnr1, western blotting using an antibody specific to the phosphorylated form of Smad2 (pSmad2) was carried out on *Xenopus* animal caps. mRNA encoding *Xnr1, Sulf1* and *DN*FGFr4a* was microinjected bilaterally in the animal hemisphere at the two cell stage. Embryos were cultured until NF stage 8 and then animal caps were taken and cultured until NF stage 10.5. Animal caps were then snap frozen for western blot. Over-expression of Xnr1 activates the nodal signalling pathway inducing

pSmad2 (Figure 3.8). TGF-β and FGF signalling function synergistically in mesoderm induction (Kimelman and Kirschner, 1987; Mathieu et al., 2004; Slack et al., 1987). Over-expression of DN*FGFr1 or a dominant negative form of the activin receptor in the marginal zone of *Xenopus* embryos inhibits the induction of the pan mesodermal marker *brachyury* (Amaya et al., 1993; Hemmati-Brivanlou and Melton, 1992). In *Zebrafish* FGF signalling is downstream of nodal signalling and forms a positive feedback loop to amplify/propagate nodal signalling (Mathieu et al., 2004). Sulf1 inhibits FGF signalling in *Xenopus* embryos (Freeman et al., 2008; Wang et al., 2004). To rule out any indirect effects of Sulf1 on Xnr1 signalling due to inhibiting FGF signalling, mRNA encoding *DN*FGFr4a* was injected as a control. Over-expression of Xnr1 together with either DN(Freeman et al., 2008)*FGFr4a or Sulf1 caused a small reduction in pSmad2 induction (Figure 3.8). The effect of Sulf1 on Xnr1 signalling is no greater than that of DN*FGF4ra. One prediction from this is that if Sulf1 does inhibit nodal signalling then these effects are indirect. Over-expression of Sulf1 does not significantly block Xnr1 signalling and supports the notion that the effects of Sulf1 on axis induction are due to inhibiting the canonical Wnt signalling pathway.

3.2.4 Sulf1 inhibits β-catenin stabilisation in response to Wnt8a in *Xenopus* animal explants

Activation of the canonical Wnt pathway leads to the cytoplasmic stabilisation of β-catenin (Kikuchi et al., 2009; Shimizu et al., 1997). To investigate whether Sulf1 directly inhibited the ability of Wnt8a to activate canonical Wnt signalling the levels of β-catenin were detected by western blot. In addition to a role in the canonical Wnt signalling pathway, β-catenin also has a structural role in the cell and is found bound to the E-cadherin at the plasma membrane (Nagafuchi and Takeichi, 1988; Orsulic et al., 1999; Ozawa et al., 1989). In order to detect changes in β-catenin levels in response to canonical Wnt signalling, samples were prepared using a subcellular fractionation protocol to separate nuclear and supernatant fractions, prior to western blotting (see methods 2.3.15). The protocol was designed to examine the effects of Sulf1 on the total levels of Wnt induced β-catenin. The fractionation protocol was performed using a bench top

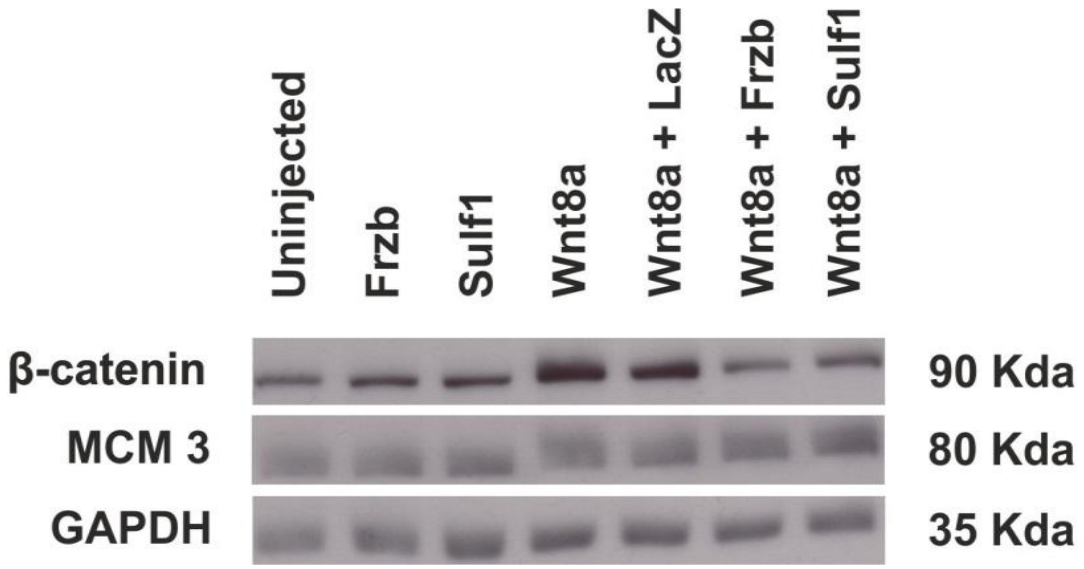

Figure 3.9; Sulf1 inhibits β-catenin signalling in response to Wnt8a.
mRNA encoding *Sulf1* (4ng), *Frzb* (2.5ng), *Wnt8a* (50pg) and *LacZ* (4ng) was injected bilaterally into the animal hemisphere of embryos at the two cell stage. Embryos were cultured until NF stage 8 and then animal caps were taken and cultured until NF stage 10.5. Animal caps were then snap frozen and then passed through a subcellular fractionation protocol to remove the nuclear fraction before western blot. Over-expression of Wnt8a activates the canonical Wnt signalling pathway resulting in the stabilisation of β-catenin. Over-expression of either Frzb or Sulf1 together with Wnt8a inhibits the stabilisation of β-catenin. Over-expression of Wnt8a together with the injection control LacZ has no effect on β-catenin stabilisation.

centrifuge instead of an ultracentrifuge. This meant that the nuclear and supernatant fractions produced were not pure. The nuclear fraction contained high molecular weight proteins from the *Xenopus* yolk that distorted the height at which β-catenin ran during western blotting. This made it impossible to reliably detect the levels of β-catenin in the nuclear fraction. The supernatant fraction represents the supernatant collected after the initial cell fractionation of *Xenopus* animal caps. This fraction was not purified, but was found to provide a reliable readout for β-catenin stabilisation in response to Wnt8a.

In order to directly asses the ability of Sulf1 to inhibit Wnt8a signalling, embryos were microinjected with mRNA into the animal hemispheres of both blastomeres at the two cell stage. Embryos were cultured until NF stage 8, animal caps were taken and then cultured until NF stage 10.5. At NF stage 10.5 animal caps were snap frozen and processed using the subcellular fractionation protocol. Over-expression of Wnt8a induced the stabilisation of β-catenin in the supernatant fraction of animal caps (Figure 3.9). Frzb inhibits the ability of Wnt8a to induce an ectopic axis in Xenopus (Wang et al., 1997a).

Frzb was used as a positive control to inhibit canonical Wnt signalling in this assay. Over-expression of either Sulf1 or Frzb together with Wnt8a inhibited the ability of Wnt8a to stabilise β-catenin. The injection control LacZ has no effect on Wnt8a induced β-catenin stabilisation (Figure 3.9). Because the supernatant fraction was not pure, both MCM3 and GAPDH were used as loading controls. This result shows that Sulf1 activity can directly inhibit the ability of Wnt8a to activate canonical Wnt signalling in animal cap explants.

3.2.5 Sulf1 does not alter the ability of Wnt3a to induce ectopic *chordin* expression

Wnt1, Wnt3a and Wnt8a are all classified as canonical Wnt ligands as over-expression of these ligands rescues UV ventralized embryos and causes axis duplication in *Xenopus* (Du et al., 1995). Studies in cell culture have measured the effects of Sulf1 on Wnt signalling using the ligands Wnt1 (Ai et al., 2003; Dhoot et al., 2001) and Wnt3a (Tang and Rosen, 2009), while the studies here used Wnt8a. To determine whether the effects of Sulf1 on the canonical Wnt pathway were ligand specific, the axis duplication experiments were repeated using Wnt3a as a second canonical Wnt ligand. Over-expression of Wnt3a in a single ventral blastomere of an embryo at the four cell stage lead to duplication of the dorsal axis at NF stage 20 (Figure 3.10B, see white arrows). At NF stage 36 the over-expression of Wnt3a had induced a second trunk, but no duplicated eyes or cement gland were present (Figure 3.10E). This is qualitatively different to the axis duplication induced by Wnt8a (compare Figure 3.10E to Figure 3.2C) and the effects of Sulf1 on head induction could not be analysed.

To investigate the effects of Sulf1 on the ability of Wnt3a to activate canonical Wnt signalling ectopic *chordin* induction was examined. Embryos were injected in the VMZ of one cell at the four cell stage and cultured until NF stage 10.5. Embryos were fixed and analysed for *chordin* gene expression by whole mount *in situ hybridisation*. Over-expression of Wnt3a induced an ectopic region of *chordin* expression around the edge of the blastopore (Figure 3.11C). Over-expression of Sulf1 together with Wnt3a did not inhibit the ability of Wnt3a to induce *chordin* expression (Figure 3.11D). The data from Figure 3.11 panels A-F is quantified in Figure 3.11G. Over-expression of Sulf1 and Wnt3a together

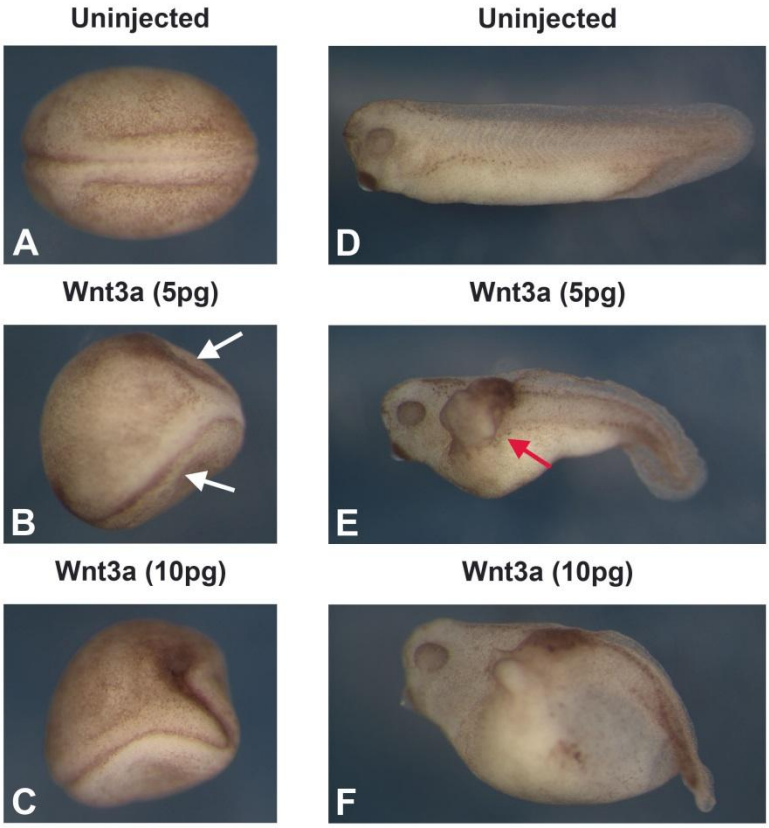

Figure 3.10; Wnt3a induces axis duplication but also posteriorization of the embryo. mRNA encoding *Wnt3a* (5 or 10pg) was injected into the VMZ of one cell of an embryo at the four cell stage. Embryos were cultured until either NF stage 20 or NF stage 36 and then examined for phenotype. [A] Animal view of an uninjected NF stage 20 embryo. [B-C] Animal views of NFstage 20 embryos injected with [B] *Wnt3a* (5pg) or [C] *Wnt3a* (10pg). [D] Lateral view of an uninjected NF stage 36 embryo. [E-F] Lateral views of NF stage 36 embryos injected with [E] *Wnt3a* (5pg) or [F] *Wnt3a* (10pg). Over-expression of Wnt3a leads to duplication of the neural tube at NF stage 20 (see white arrows [B]). Over-expression of Wnt3a leads to duplication of the trunk at stage 36, however these embryos lack duplicated eyes and cement glands (see red arrow [E]).

did appear to increase the width of the ectopic *chordin* domain compared to over-expressing Wnt3a alone (compare Figure 3.11F to E). To examine whether Sulf1 affects the ability of Wnt3a to activate canonical Wnt signalling, the amount of *Wnt3a* mRNA injected was titrated down until the induction of ectopic *chordin* occurred at a low frequency. 0.1pg of *Wnt3a* mRNA induced ectopic *chordin* in only 20% of embryos (Figure 3.12C). Sulf1 did not affect the ability of Wnt3a to induce ectopic *chordin* expression (Figure 3.12D). The data from Figure 3.12 panels A-F is quantified in Figure 3.12G. The width of the ectopic *chordin* domains induced appeared wider in embryos over-expressing Sulf1 and Wnt3a compared to embryos only over-expressing Wnt3a (compare

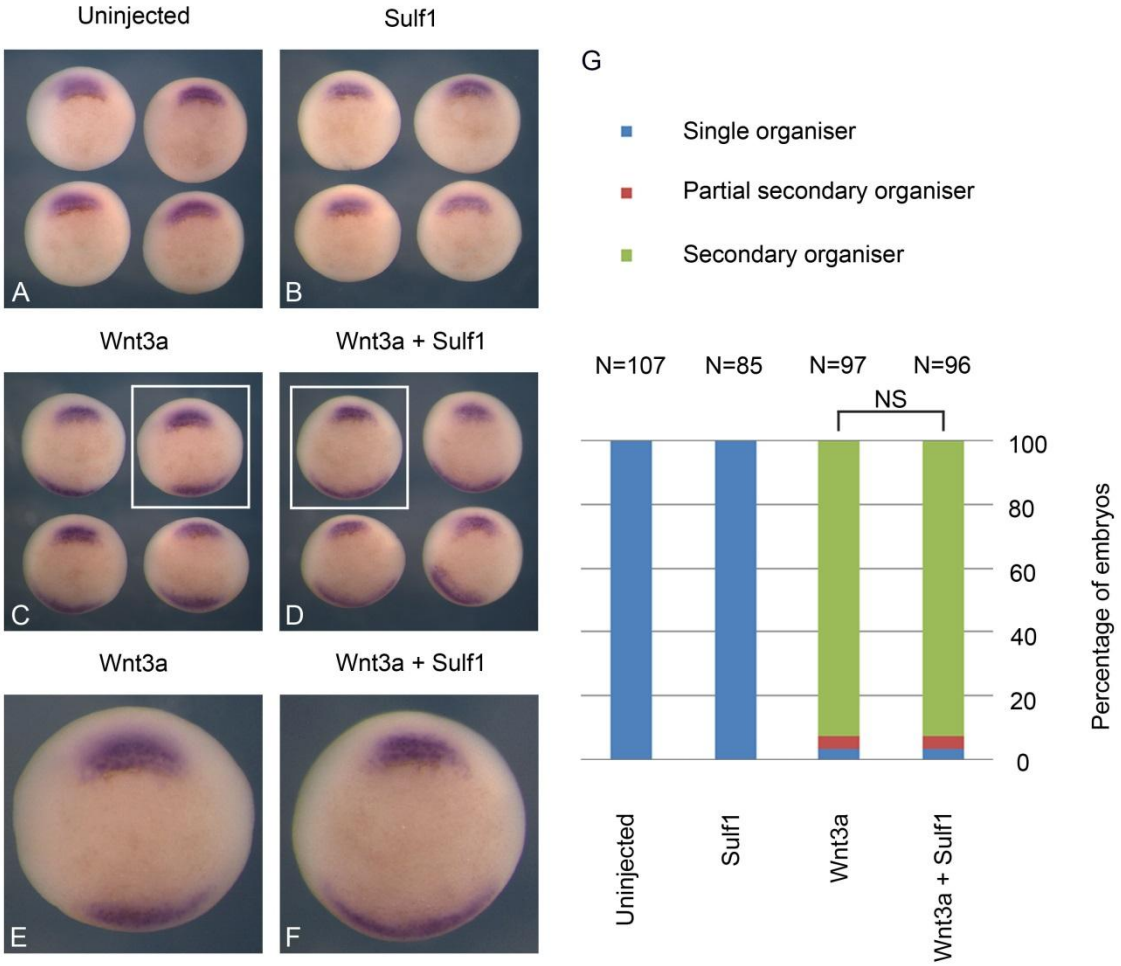

Figure 3.11; Sulf1 does not inhibit the ability of Wnt3a to induce ectopic *chordin* expression.
mRNA encoding *Sulf1* (1ng), *Wnt3a* (5pg) or both was injected into the VMZ of one cell of an embryo at the four cell stage. Embryos were cultured until NF stage 10.5 and then analysed by whole mount *in situ hybridisation* for *chordin* expression. [A-F] Whole mount *in situ hybridisation* showing the expression of *chordin* in (A) uninjected embryos and embryos injected with [B] *Sulf1* [C and E] *Wnt3*a and [D and F] *Sulf1* and *Wnt3a*. The white boxes in [C] and [D] highlight the embryos used in [E] and [F] respectively. Over-expression of Wnt3a induces ectopic *chordin* expression and this is not inhibited by Sulf1. [G] Graph quantifying the frequency of organiser induction in embryos injected with *Sulf1* and *Wnt3a.* No significant difference (NS) is detected between embryos over-expressing Wnt3a and Wnt3a and Sulf1, Chi-square test.

Figure 3.12F to 3.12E). Together the data demonstrates that Sulf1 does not affect the ability of Wnt3a to activate canonical Wnt signalling.

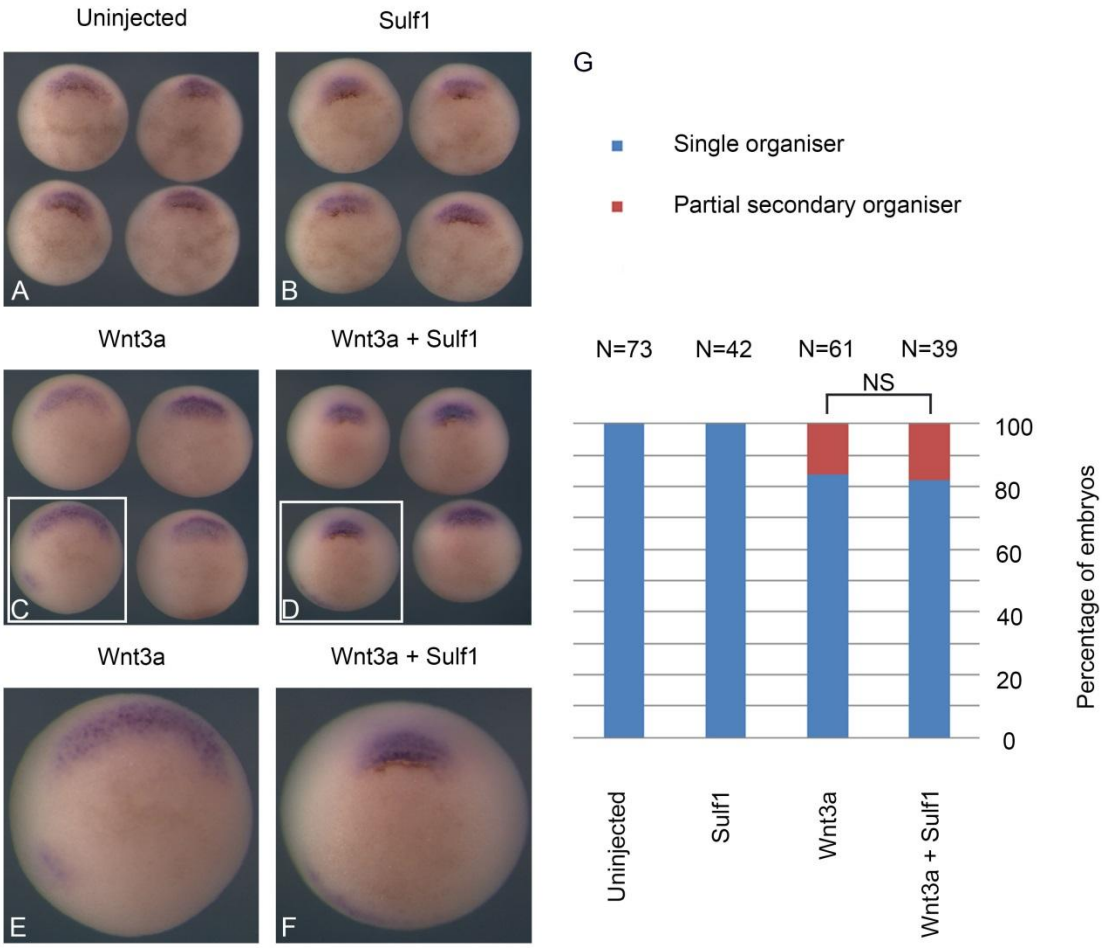

Figure 3.12; Sulf1 does not alter the ability of Wnt3a to induce ectopic *chordin* expression.
mRNA encoding *Sulf1* (1ng), *Wnt3a* (0.1pg) or both was injected into the VMZ of one cell of an embryo at the four cell stage. Embryos were cultured until NF stage 10.5 and then analysed by whole mount *in situ hybridisation* for *chordin* expression. [A-F] Whole mount *in situ hybridisation* showing the expression of *chordin* in (A) uninjected embryos and embryos injected with [B] *Sulf1* [C and E] *Wnt3*a and [D and F] *Sulf1* and *Wnt3a*. The white boxes in [C] and [D] highlight the embryos used in [E] and [F] respectively. Over-expression of Wnt3a induces a low frequency of ectopic *chordin* expression and this is not inhibited by Sulf1. [G] Graph quantifying the frequency of organiser induction in embryos injected with *Sulf1* and *Wnt3a.* No significant difference (NS) is detected between embryos over-expressing Wnt3a and Wnt3a and Sulf1, Chi-square test.

3.2.6 Sulf1 enhances the ability of Wnt11b to induce ectopic *chordin* expression

Sulf1 has previously been shown to enhance the ability of XtWntllb2 to induce ectopic *chordin* expression and a partial secondary axis (Freeman et al., 2008). XtWnt11b2 is the homologue of *Xenopus laevis* Wnt11b (Wnt11b), which was classified as a non-canonical Wnt ligand (Du et al., 1995). In this thesis XtWnt11b2 was found to be hypomorphic when analysed in two separate non-canonical Wnt signalling assays (see Chapter 4). In order to investigate whether Sulf1 had similar effects on Wnt11b the, axis inducing ability of Wnt11b was examined. mRNA coding for *Wnt11b* was microinjected into one ventral blastomeres at the four cell stage. Embryos were cultured until NF stage 36 and examined for phenotype. Over-expression of Sulf1 and Wnt11b individually failed to induce axis duplication (Figure 3.13B-C). Over-expression of Sulf1 and Wnt11b together did not appear to induce the formation of a secondary axis. The small deformity seen in Figure 13.3D could represent a partial secondary axis as seen in (Freeman et al., 2008). Alternatively the deformation could be caused due to a failure of the blastopore to close in these embryos. The data from Figure 3.13 panels A-D is quantified in Figure 3.13E.

Over-expression of Sulf1 and Wnt11b lead to defects in the embryonic axis. Injection of 1ng of mRNA encoding *Sulf1* caused axial defects in 98% of embryos. Injection of mRNA encoding *Wnt11b* caused axial defects, which were more severe than the injecting *Sulf1.* Over-expression of Sulf1 and Wnt11b together further disrupted the development of the dorsal axis and resulted in a failure to complete gastrulation (Figure 3.14A). Embryos were also examined for how frequently the blastopore failed to close. Over-expression of Sulf1 resulted in a failure of blastopore closure in 78% of embryos, whereas over-expression Wnt11b caused this in 36% of embryos. Over-expression of Sulf1 and Wnt11b together enhanced the number of embryos displaying a failure of blastopore closure to 98% (Figure 3.14B).

To determine more directly whether Sulf1 enhanced the ability of Wnt11b to activate canonical Wnt signalling, *chordin* induction was examined. Embryos were injected in the VMZ of one cell at the four cell stage and cultured until NF

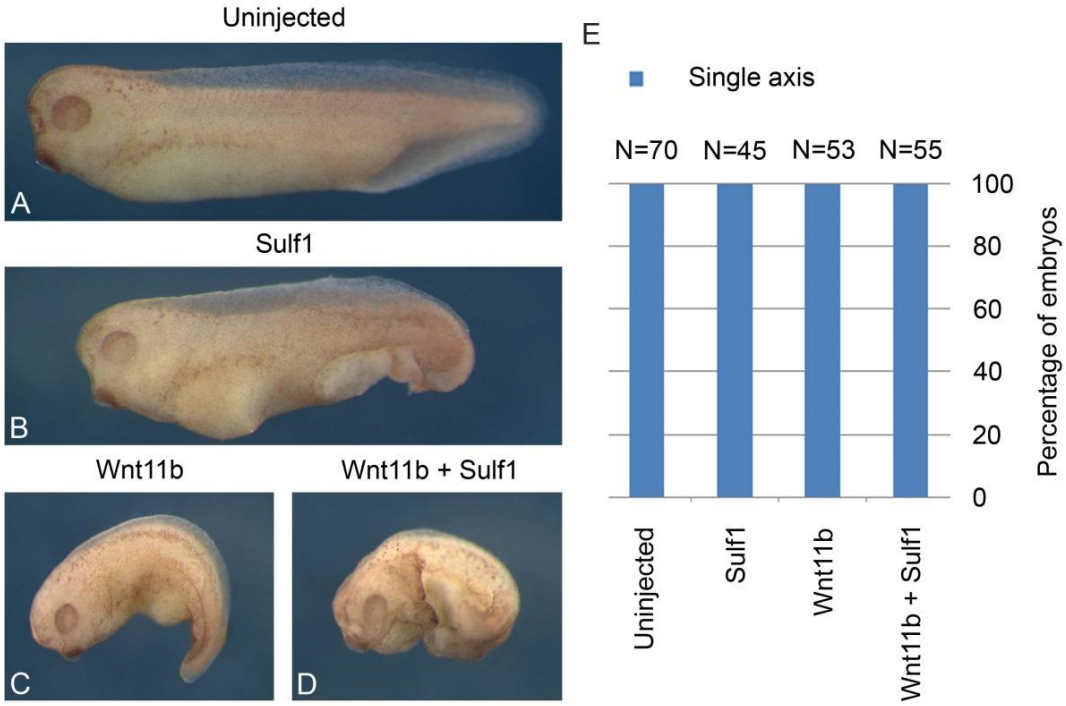

Figure 3.13; Sulf1 does not affect the ability of Wnt11b to induce axis duplication. mRNA encoding *Sulf1* (1ng), *Wnt11b* (600pg) or both was injected into the VMZ of one cell of an embryo at the four cell stage. Embryos were cultured until NF stage 36 and then examined for phenotype. [A] Lateral view of an uninjected embryo. [B-D] lateral views of embryos injected with [B] *Sulf1*, [C] *Wnt11b* or [D] *Sulf1* and *Wnt11b*. Over-expression of Sulf1 and Wnt11b either individually or together caused axial defects, but not axis duplication. [E] Graph quantifying the frequency of axis duplication in embryos injected with *Sulf1* and *Wnt11b.*

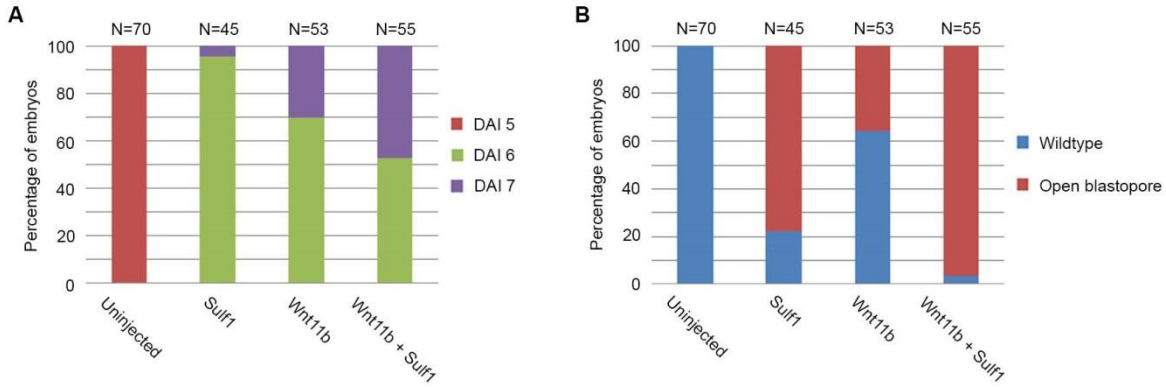

Figure 3.14; Over-expression of Sulf1 and Wnt11b enhanced embryonic axis defects. mRNA encoding *Sulf1* (1ng), *Wnt11b* (600pg) or both was injected into the VMZ of one cell of an embryo at the four cell stage. Embryos were cultured until NF stage 36 and then examined for phenotype. [A] Over-expressing Sulf1 caused an increase in the number of embryos displaying a truncated posterior axis and this was enhanced by the over-expression of Wnt11b alone. Over-expression of Sulf1 and Wnt11b together further enhanced axial defects. [B] Over-expression of Sulf1 resulted in a failure of blastopore closure in 78% of embryos, whereas over-expression Wnt11b alone caused this in 36% of embryos. Over-expression of Sulf1 and Wnt11b together enhanced the number of embryos displaying a failure of blastopore closure to 98%.

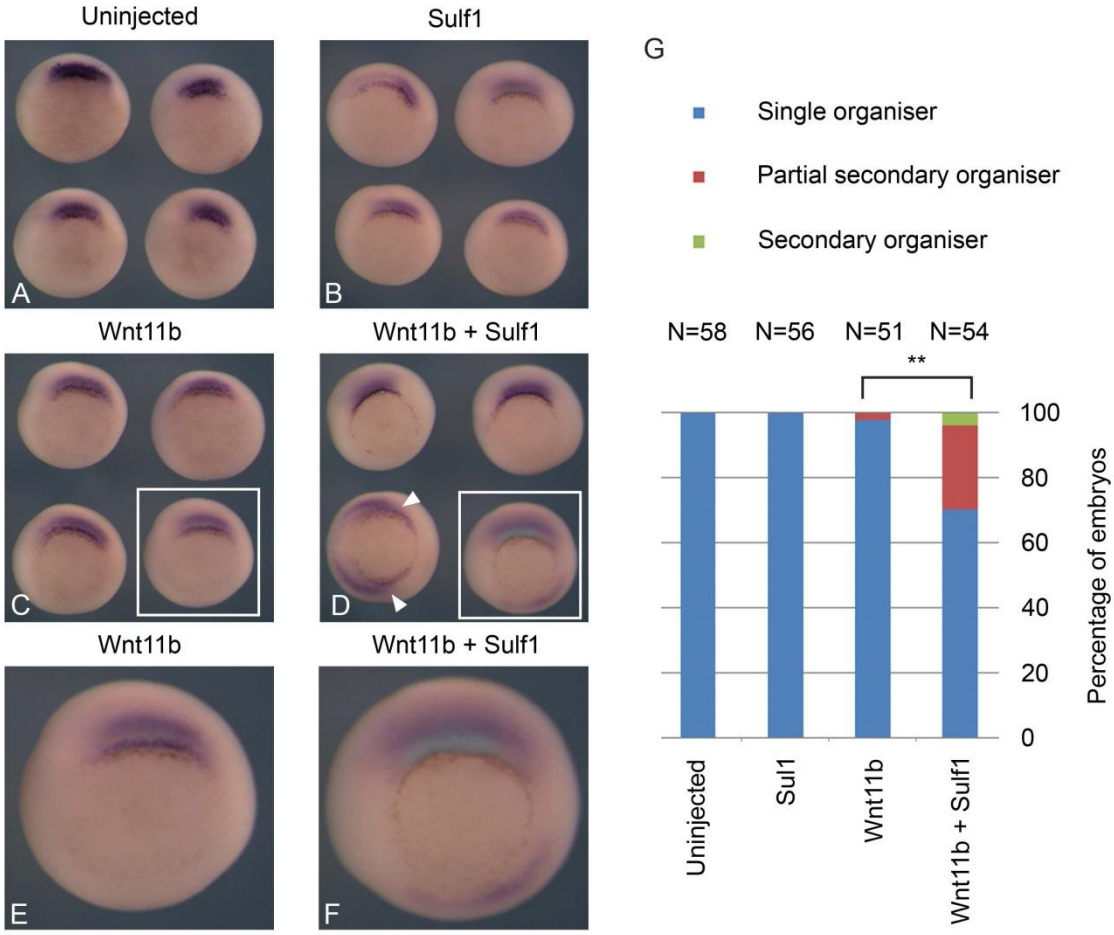

Figure 3.15; Sulf1 enhances the ability of Wnt11b to induce ectopic *chordin* expression. mRNA encoding *Sulf1* (1ng), *Wnt11b* (600pg) or both was injected into the VMZ of one cell of an embryo at the four cell stage. Embryos were cultured until NF stage 10.5 and then analysed by whole mount *in situ hybridisation* for *chordin* expression. [A-F] Whole mount *in situ hybridisation* showing the expression of *Chordin* in (A) uninjected embryos and embryos injected with [B] *Sulf1* [C and E] *Wnt11b* and [D and F] *Sulf1* and *Wnt11b*. The white boxes in [C] and [D] highlight the embryos used in [E] and [F] respectively. Over-expression of Wnt11b alone induces ectopic *chordin* expression at a low frequency, but this enhanced by over-expressing both Wnt11b and Sulf1 (compare [C and E] to [D and F]). [G] Graph quantifying the frequency of organiser induction in embryos injected with *Sulf1* and *Wnt11b.* Asterisks mark significant differences (**P<0.01) Chi-square test.

stage 10.5. Embryos were fixed and analysed for *chordin* gene expression by whole mount *in situ* hybridisation. Over-expression of Wnt11b failed to induce ectopic *chordin* expression (Figure 3.15C). Over-expression of Sulf1 and Wnt11b together induced ectopic *chordin* expression in 25% of embryos (Figure 3.15D). The data from Figure 3.15 panels A-F is quantified in Figure 3.15G. Sulf1 enhanced the ability of Wnt11b to induce ectopic *chordin* expression. These data suggest that Sulf1 enhanced the ability of Wnt11b to activate canonical Wnt signalling and that Sulf1 and Wnt11b synergise to cause axial defects. This is consistent with data produced by (Freeman et al., 2008).

3.3 Discussion

The aim of this chapter was to investigate the effects of Sulf1 on canonical Wnt signalling in *Xenopus laevis*. Sulf1 was originally shown to enhance the ability of Wnt1 to activate the canonical Wnt reporter Topflash when transfected in C2C12 cells (Dhoot et al., 2001). Following this Ai, et al., (2003) showed that Sulf1 enhanced the ability Wnt1 to activate Topflash in the same cell line. In addition the authors demonstrated that Sulf1 reduced the ability of Wnt8a to bind to recombinant heparin and glypican1, although importantly the effects of Sulf1 on Wnt8a signalling were not investigated. The ability Sulf1 to inhibit the binding of Wnt8a to HS, but enhance Wnt1 signalling, lead to the creation of the 'catch and present' model for the effects of Sulf1 on Wnt signalling. In this model, Sulf1 promotes the release of Wnt ligands from the cell surface allowing activation of the canonical Wnt signalling pathway (Ai et al., 2003). This model is supported by data from HEK 293, myoblast and odontoblast cell lines (Frese et al., 2009; Hayano et al., 2012; Tran et al., 2012) The data presented in this chapter demonstrates that Sulf1 differentially regulates the abilities of Wnt3a, 8a and 11b to activate canonical Wnt signalling. This data cannot be explained simply by the 'catch and present' model alone.

3.3.1 Sulf1 inhibits the ability of Wnt8a to activate canonical Wnt signalling

Sulf1 inhibits the ability of Wnt8a to activate canonical Wnt signalling in *Xenopus laevis*. Sulf1 inhibited the ability of Wnt8a to induce an ectopic axis as measured by head induction and organiser gene expression using two separate doses of *Wnt8a* mRNA. Increasing the dose of *Wnt8a* mRNA from 5-10pg reduced the ability of Sulf1 to inhibit axis induction. High levels of Wnt8a are able to overcome the inhibitory effects of Sulf1 on Wbt8a signalling. This is consistent with Sulf1 having a regulatory role during development (Ai et al., 2007; Holst et al., 2007; Ratzka et al., 2008). In addition Sulf1 blocked the ability of Wnt8a to stabilise β-catenin in animal caps. Work on ligand receptor interactions has shown that Sulf1 reduces the interaction between Wnt8a and LRP6 (Pownall laboratory unpublished communication). These findings are not

what would have been predicted based on work in cell culture (Ai et al., 2003; Dhoot et al., 2001; Hayano et al., 2012; Tang and Rosen, 2009; Tran et al., 2012).

One important difference between the work in this thesis and the experiments done by (Ai et al., 2003; Dhoot et al., 2001; Tang and Rosen, 2009) is where Sulf1 and the canonical Wnt ligands were expressed. In all three previous experiments one population of cells were transfected with Sulf1 and Topflash and a second population of cells with the Wnt ligands. The different populations were then cultured together and the effects on Topflash analysed. This experimental setup is designed to analyse the effects of Sulf1 on the reception of Wnt ligands. In contrast the work in this chapter has centred around the effect of Sulf1 on Wnt signalling when Wnt and Sulf1 are expressed in the same cells. In this setup Sulf1 could affect the reception, but also the secretion and oligomerization of Wnt ligands. It is possible that Sulf1 could inhibit the secretion/oligomerization of Wnt8a in Wnt secreting cells, masking any effects of Sulf1 in Wnt receiving cells. However this is not what would be predicted based on data in Figure 3.6. Separating the effects of Sulf1 in Wnt producing cells from those in Wnt receiving cells will be addressed in chapter 5.

Work on the *Drosophila* homologue of Sulf1, has provided similar findings to those for Sulf1 and Wnt8a in *Xenopus*. Over-expression of Sulf1 in the *Drosophila* wing disk inhibited the formation of both chemosensory and mechanosensory bristles (Kleinschmit et al., 2010), a phenotype consistent with the inhibition of Wg signalling (Phillips and Whittle, 1993). In addition over-expression of Sulf1 inhibits the expression of distaless, a low threshold Wg target gene (Kleinschmit et al., 2010; Neumann and Cohen, 1997; Zecca et al., 1996). In contrast Sulf1 LOF mutant *Drosophila* show an increase in the number of chemosensory and mechanosensory bristles and an increase in the expression of distaless, consistent with enhanced Wg signalling (Cadigan et al., 1998; Gerlitz and Basler, 2002; Kleinschmit et al., 2010; You et al., 2011). This is consistent with Sulf1 inhibiting Wg signalling in *Drosophila.* The findings on the effects of Sulf1 on Wnt8a signalling shown here are consistent with those of Sulf1 on Wg in *Drosophila*, but not those of Sulf1 on Wnt signalling in cell culture.

3.3.2 Sulf1 does not alter the ability of Wnt3a to activate canonical Wnt signalling

Sulf1 does not alter the ability of Wnt3a to activate canonical Wnt signalling in the *chordin* induction assay. This finding is different to that for Wnt8a and not what would have been predicted from either work in *Drosophila* or cell culture (Ai et al., 2003; Dhoot et al., 2001; Kleinschmit et al., 2010; You et al., 2011). Wnt3a and Wnt8a are both canonical Wnt ligands, as they induce ectopic organiser formation and axis duplication when over-expressed ventrally in embryos. However, the effects of Wnt3a and Wnt8a on axis duplication are qualitatively different. Over-expression of Wnt8a leads to the duplication of head and eyes in the embryo. Over-expression of Wnt3a leads to axis duplication, but also posteriorization of the secondary axis, which appears as a duplicated trunk. Wnt3a and Wnt8a have different effects on neuralized animal cap tissue. Wnt8a has no effect on gene expression in neuralized animal caps, but Wnt3a induces the expression of hindbrain and neural crest markers at the expense of forebrain markers (Saint-Jeannet et al., 1997). Despite both activating canonical Wnt signalling, Wnt3a and Wnt8a have different effects on cell fate specification during development.

There are many different types of HSPG in vertebrates. One prediction from this is that different HSPGs will have specific roles in regulating the ability of different Wnt ligands and receptors to activate Wnt signalling. For example dally and dlp are members of the glypican family of HSPGs expressed in *Drosophila*. Over-expression of dally in *Drosophila* increased the levels of armadillo protein present in *Drosophila* larva (Tsuda et al., 1999). In addition loss of function (LOF) mutants for dally display a loss of chemosensory and mechanosensory bristles in the wing, characteristic of a loss of high threshold Wg signalling (Phillips and Whittle, 1993; Tsuda et al., 1999). In contrast LOF mutants for dlp displayed an increase in the expression of sensless (a high threshold target gene for Wg signalling) and an increase in bristle formation in the developing wing (Franch-Marro et al., 2005; Nolo et al., 2000; Phillips and Whittle, 1993). Dally and dlp have different effects on Wg signalling during *Drosophila* development. One prediction from this, is that Sulf1 could have

different effects on Wg signalling depending on which glypican is being modified.

A context specific for the role of Sulf1 in cell signalling is supported by work investigating the effects of Sulf1 on Hh signalling in *Drosophila*. Over-expression of Sulf1 in the posterior compartment of the developing wing disk enhances Hh signalling in the anterior compartment. However over-expression of Sulf1 in the anterior compartment inhibits the activation of Hh signalling here (Wojcinski et al., 2011). The ability of Wnt5a to activate canonical or non-canonical Wnt signalling is context specific. Over-expression of Wnt5a in the VMZ of *Xenopus* embryos has no effect on axis duplication. However over-expression of Wnt5a together with Fz5 caused the induction of a full secondary axis (He et al., 1997). In addition Wnt5a was unable to activate Topflash expression in HEK 293 cells unless the cells had been transfected with Fz4 and LRP5 (Mikels and Nusse, 2006). The effects of Wn5a on canonical Wnt signalling depend on the complement of co-receptors present in the tissue. The ability of Sulf1 to regulate canonical Wnt signalling is likely context specific and will depend on the individual Wnt ligands, receptors and HSPGs present in the environment.

3.3.3 Sulf1 enhances the ability of Wnt11b to activate canonical Wnt signalling

Sulf1 enhanced the ability of Wnt11b to activate canonical signalling. Wnt11b is defined as a non-canonical Wnt ligand because it induces gastrulation defects instead of axis duplication when over-expressed in embryos (Du et al., 1995). This is consistent with data in Figures 3.13-3.15, which showed that over-expression of Wnt11b caused a shortening of the posterior axis, but not axis duplication. It is unclear how different Wnt ligands specifically activate canonical and non-canonical signalling pathways, although the presence of particular receptors is important. Wnt5a is a non-canonical Wnt ligand, which in the right context can activate canonical Wnt signalling (Du et al., 1995; He et al., 1997; Mikels and Nusse, 2006). One prediction from this is that in the presence of a specific subset of receptors Wnt11b activates canonical Wnt signalling. Sulf1 enhances the ability of Wnt11b to induce ectopic *chordin* expression. In

addition, Sulf1 enhances the ability of Wnt11b to associate with the canonical Wnt co-receptor LRP6 (Freeman et al., 2008). This contrasts with the ability of Sulf1 to inhibit Wnt8a-LRP6 interactions (Pownall laboratory unpublished data). A change in the abilities of Wnt8a and Wnt11b to interact with LRP6 could provide a mechanism for the effects of Sulf1 on canonical Wnt signalling described in this chapter.

Over-expression of Sulf1 in the DMZ of four cell stage embryos leads to an increase in the size and width of the endogenous *chordin* domain. Formation of the embryonic axis requires the presence of maternally deposited dorsal determinants in the oocyte, reviewed in (De Robertis and Kuroda, 2004). Dvl and the GSK3β inhibitory protein GBK have both been proposed as candidates for the dorsal determinants (Miller et al., 1999; Weaver et al., 2003). In addition the non-canonical Wnt ligands Wnt5a and Wnt11b have also been proposed (Cha et al., 2008; Tao et al., 2005). Knockdown of maternal *Wnt11b* blocks the formation of the embryonic axis and this can be rescued by the over-expression β-catenin. mRNA encoding *Wnt11b* is found in the vegetal hemisphere at the eight cell stage and Wnt11b protein is expressed in the dorsal half of the embryo at the 64 cell stage (Ku and Melton, 1993; Schroeder et al., 1999). *Sulf1* RNA is also localised to the vegetal hemisphere during early cleavage divisions and colocalises with *Wnt11* (Freeman et al., 2008). Sulf1 enhances the ability of Wnt11b to activate canonical Wnt signalling. One prediction from this is that the enlarged domain of *chordin* expression in Figure 3.7 is due to Sulf1 potentiating the endogenous axis specifying activity of Wnt11b. Interestingly, Tao et al., (2005) also showed a requirement for the gene EXT1 in axis specification. *EXT1* codes for a HS polymerase and knockdown of *EXT1* inhibits axis formation in Xenopus embryos (Lind et al., 1998; McCormick et al., 1998; Tao et al., 2005). It is tempting to speculate that maternal Sulf1 may have a role in endogenous axis specification in *Xenopus* by enhancing the ability of maternal Wnt11 to activate canonical Wnt signalling.

3.3.4 Sulf1 and Wnt synergise to broaden the domain of ectopic chordin expression

Over-expression of Sulf1 and Wnt8a together inhibited the ability of Wnt8a to induce an ectopic domain of *chordin,* leading to the induction of either one or two small domains of *chordin* expression (Figure 3.3D and F). In Figure 3.3F it appears that Sulf1 inhibits Wnt8a signalling cell autonomously, but that Wnt8a can diffuse out of the domain expressing Sulf1 and induce ectopic *chordin*. Similar findings have been discovered for other extracellular inhibitors of Wnt/Wg signalling. Secreted frizzled related proteins (Sfrp) are a family of secreted Wnt antagonists that bind directly to Wnt proteins via a CRD, which bares homology to the Fz CRD, reviewed by (Kawano and Kypta, 2003). Sfrp3 (Frzb) inhibits the ability of Wnt8a to induce axis duplication in Xenopus (Wang et al., 1997a). However the effects of Sfrps on Wnt signalling are not always inhibitory. Work by Mii and Taira (2009) has shown that Sfrp3 can enhance the range of diffusion of a fluorescently tagged Wnt8a constructs in Xenopus. Sfrp3 is expressed in the DMZ during gastrula stages and interestingly knockdown of *Sfrp3* reduced the distance from the marginal zone at which nuclear β-catenin could be detected (Mii and Taira, 2009; Wang et al., 1997a). Similarly Sfrp1/2 are required for the activation of canonical Wnt signalling in the mouse optic cup. *Sfrp1/2* knockout caused a reduction in the levels of active β-catenin in the developing optic cup. In addition *Sfrp1/2* knockout decreased the range of distribution of fluorescently labelled Wnt11b in the developing retina, which was rescued by the over-expression of Sfrp1 (Esteve et al., 2011). Rather than simply inhibiting Wnt signalling, Sfrp1-3 extended the range of Wnt signalling in these systems. One conclusion from these experiments is that by inhibiting the binding of Wnt ligands to their receptors, Sfrps enhance the range of Wnt signalling in the embryo.

Context dependent inhibition of Wnt signalling is a property shown by other Wnt antagonists. In the *Drosophila* wing disc dlp has been shown to enhance the range of Wg diffusion, but inhibit the activation of high threshold Wg target genes (Franch-Marro et al., 2005; Yan et al., 2009). The extracellular Wnt binding protein (Swim) shows similar properties to Dlp. Over-expression of Swim enhances the range of diffusion of extracellular Wg, inhibiting senseless,

but activating distaless expression. RNAi mediated knockdown of *Swim* decreases the levels of extracellular wingless, inhibiting distaless, but not senseless expression (Mulligan et al., 2012). In addition, the cytoplasmic proteins reggie/flotillin have similar effects on Wg signalling as Swim and dlp (Katanaev et al., 2008). One conclusion from these data, is that proteins which inhibit the activation of high threshold Wnt/Wg target genes, can also have important roles in maintaining long range Wnt/Wg signalling. Sulf1 may have a role in promoting the long range diffusion of Wnt8a at the expense of short range targets in *Xenopus* embryos.

Over-expression of Sulf1 and Wnt3a or Wnt11b induced a broad domain of ectopic *chordin* expression. This was different to *chordin* expression induced by Wnt3a or Wnt8a alone. The ability of Sulf1 to increase the width of the ectopic *chordin* domain in response to Wnt3a is independent of its ability to repress/activate *chordin* expression. Sulf1 expression in the posterior compartment of the *Drosophila* wing disk enhances the range over which Hh activates gene expression in the anterior compartment (Wojcinski et al., 2011). It is possible that Sulf1 may have a role in enhancing the range of Wnt3a signalling without inhibiting short range targets. The role of Sulf1 in modulating the diffusion of Wnt8a and Wnt11b will be examined further in chapter 5.

This chapter has been concerned with investigating the effects of Sulf1 on canonical Wnt signalling. Sulf1 has no effect on Wnt3a, inhibits the ability of Wnt8a and enhances the ability of Wnt11b to activate canonical Wnt signalling. The data indicates that the effects of Sulf1 on canonical Wnt signalling are ligand specific in *Xenopus.* In addition over-expression of Sulf1 and Wnt8a/Wnt11b enhances the axial defects seen in embryos. Defects in the embryonic axis are often a result of problems that occur during gastrulation. The non-canonical Wnt signalling pathway is important in regulating the complex cell-cell rearrangements that occur during gastrulation (see introduction). This suggests that Sulf1 may have a role in regulating non-canonical Wnt signalling in addition to canonical Wnt signalling. A role for Sulf1 in regulating non-canonical Wnt signalling will be the subject of the following chapter.

4.0 Sulf1 potentiates non-canonical Wnt signalling

4.1 Introduction

4.1.1 The vertebrate homologues of Wnt11

The Wnt11 subfamily of Wnt ligands are highly conserved during development. The mammalian genome contains only one Wnt11 gene, whereas two Wnt11 genes can be found in *Chick, Xenopus* and *Zebrafish* (Garriock et al., 2007). *Wnt11* is found expressed in multiple tissues including the node, somites, developing heart and the meso/metanephros during *Mouse* development (Kispert et al., 1996). *Wnt11* knockout mice die either during embryogenesis or perinatally. Although the cause of death was not investigated, *Wnt11* knockout mice had smaller kidneys than *Wnt11* heterozygous mice (Majumdar et al., 2003). This is similar to the phenotype seen in *Sulf1/2* double knockout mice (Holst et al., 2007). There is strong expression of Wnt11 during uteric branching in the developing kidney (Kispert et al., 1996) and branching is inhibited in *Wnt11* knockout mice (Majumdar et al., 2003). Wnt11 has an important role during kidney formation in mammals and LOF mutations in *Wnt11* cause lethality.

There are two genes encoding *Wnt11* in *Chick, Xenopus* and *Zebrafish* and these are known as *Wnt11 related (Wnt11r)* and *Wnt11b*. Wnt11r is more closely related to mammalian Wnt11 than Wnt11b (see Figure 4.0A) (Garriock et al., 2007). In *Xenopus, Wnt11r* is expressed in the somites, neural tube and heart during development (Garriock et al., 2005). *Wnt11b* is maternally deposited in the vegetal region of the oocyte and is found dorsally during early development (Ku and Melton, 1993; Schroeder et al., 1999). Zygotically *Wnt11b* is expressed in the DMZ at the start of gastrulation and in a ring around the blastopore as gastrulation proceeds. At later stages *Wnt11b* is expressed in the somites and brachial arches (Ku and Melton, 1993). Targeted knockdown of *Wnt11r* in the developing heart field inhibits heart morphogenesis, but not heart induction (Garriock et al., 2005). In *Zebrafish,* mutations in *Wnt11b/Slb* causes defects in convergent extension and axis elongation during gastrulation (Heisenberg et al., 2000). In *Xenopus tropicalis,* a further gene duplication

A

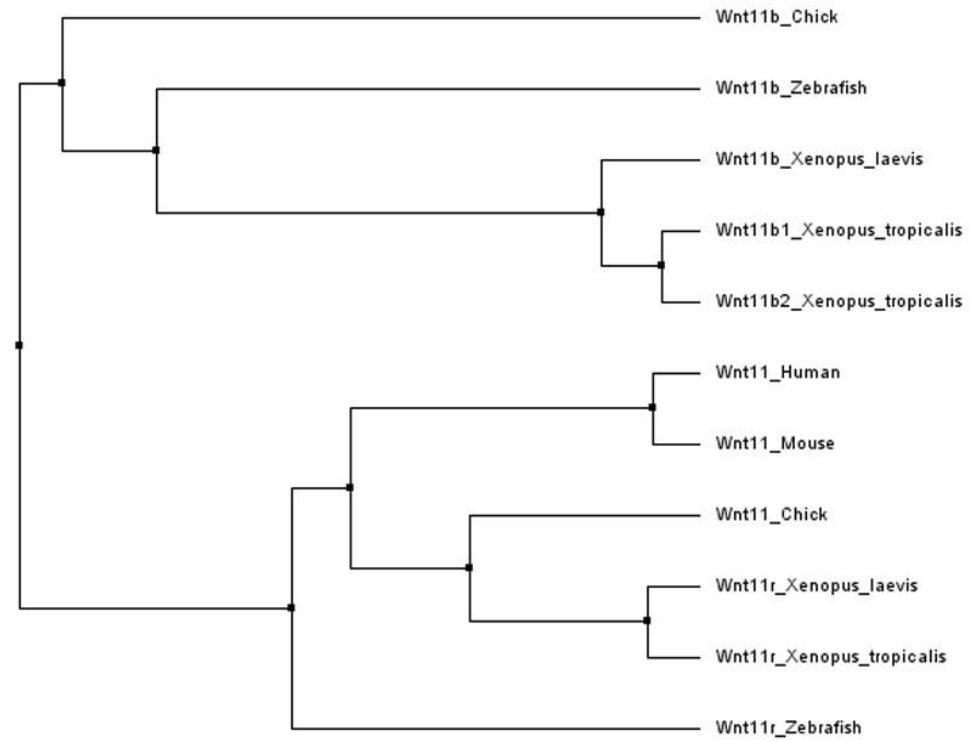

B

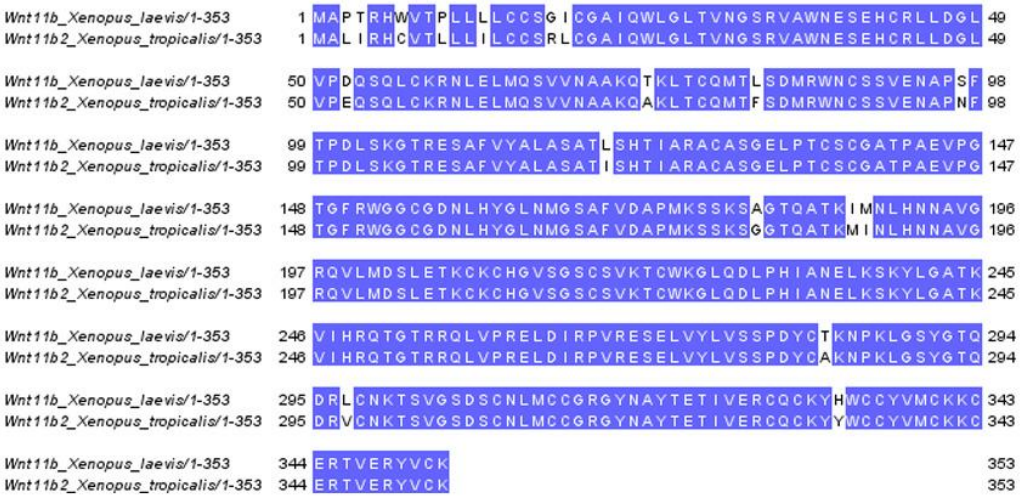

Figure 4.0; XtWnt11b2 is a paralogue of XlWnt11b.
[A] Tree displaying the percentage identity of Wnt11 proteins from different species after sequence alignment using 'Muscle' with default settings. There is one Wnt11 gene in mammals compared to at least two in *Chick*, *Zebrafish* and *Xenopus*. In Xenopus the closest paralogue of Human Wnt11 is annotated as Wnt11 related (Wnt11r), with the other paralogue annotated as Wnt11b. [B] Protein sequence alignment of Xenopus laevis Wnt11b and Xenopus tropicalis Wnt11b2. The two proteins are highly similar and the majority of the differences are concentrated at the N terminus.

event has occurred to generate *XtWnt11b1* and *XtWnt11b2*. XTWnt11b1/2 show 97% identity at the nucleotide level and both proteins are highly identical to Wnt11b (see Figure 4.0A) (Garriock et al., 2007). *Wnt11* is expressed in the mesoderm during development and is important in both heart and kidney formation. Loss of Wnt11 function during development blocks uteric branching in the kidneys and inhibits the cell-cell interactions required for the formation of the dorsal-ventral axis and vertebrate heart (Garriock et al., 2005; Majumdar et al., 2003; Tada and Smith, 2000).

4.1.2 Activating the non-canonical Wnt signalling pathway

Non-canonical Wnt signalling has important roles in regulating cell fate, migration and polarity during development (see introduction). One problem with investigating the effects of non-canonical Wnt signalling is that over and under activation of non-canonical Wnt signalling can result in the same phenotype. For example, over-expression of wildtype or dominant negative Wnt11b inhibits gastrulation leading to truncations in the anterior/posterior axis of *Xenopus* embryos (Du et al., 1995; Tada and Smith, 2000). To complicate matters this is essentially the same phenotype produced by inhibiting FGF signalling (Amaya et al., 1991). Gastrulation is a complex process, so to dissect the roles of individual signalling pathways, simpler explant models can be used to evaluate the cell behaviours that occur during gastrulation.

Activin is a member of the TGF-β family of signalling proteins. Activin signals by the same pathway as nodal, leading to the phosphorylation of Smad2. Activin differs from nodal siganlling as it does not require members of the EGF-CFC family to act as co-receptors and is not inhibited by lefty, reviewed by (Shen, 2007). Activin treatment of animal cap tissue induces the formation of dorsal mesoderm, which undergoes the same convergent extension behaviour seen by the dorsal mesoderm during gastrulation (Asashima, 1990; Smith, 1987). This leads to the convergence and extension of animal cap tissue that forms an elongated structure. In contrast, animal caps cultured in the absence of activin round up to form spherical balls of epithelium (see Figure 4.1). Over-expression of wildtype or dominant negative Wnt11b inhibits activin induced

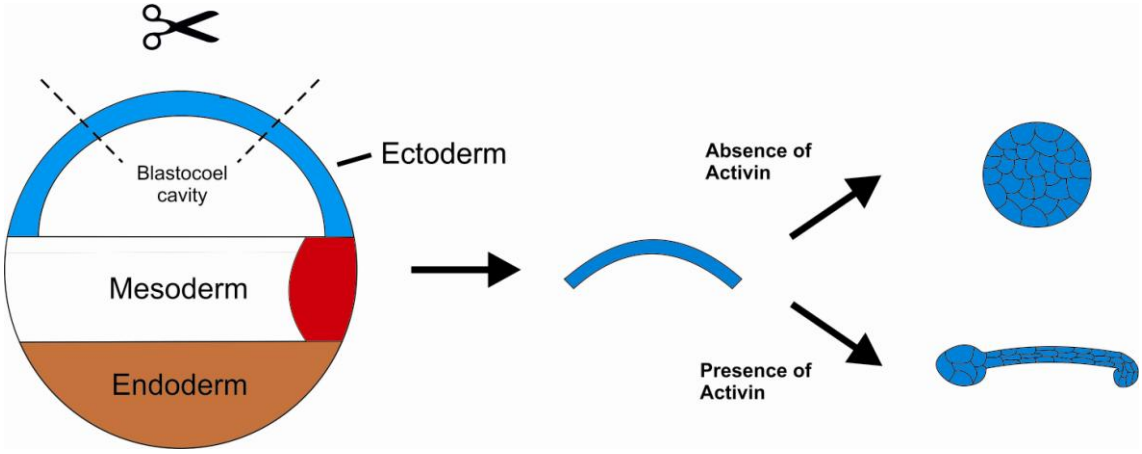

Figure 4.1; Animal cap tissue explants.
Animal cap tissue is isolated from the animal pole of embryos at NF stage 7-8. Culturing animal cap tissue in isolation leads to the formation of a spherical ball of cells. In the presence of activin animal cap tissue transforms into dorsal mesoderm and undergoes medial/lateral convergent extension.

convergent extension, preventing animal caps from elongating (Hikasa et al., 2002; Tada and Smith, 2000). Activin induced convergent extension can be used to model the effects of non-canonical Wnt signalling on cell behaviour *in vitro.*

Dvl (vertebrate dishevelled) is essential for both canonical and non-canonical Wnt signalling (see introduction). In *Drosophila* PCP signalling Dsh (*Drosophila* dishevelled) asymmetrically localises to the distal membrane of polarized epithelial together with *DFz* (Axelrod, 2001). The fusion protein Dsh-GFP (green fluorescent protein) can be visualised by confocal microscopy in live *Xenopus* animal caps. Dsh-GFP displays as discrete puncta that are evenly distributed throughout the cytoplasm, when over-expressed in *Xenopus*. Over-expression of DFz together with Dsh-GFP results in the translocation of Dsh-GFP to the plasma membrane. Membrane recruitment of Dsh-GFP by DFz requires the DEP domain of Dsh, which is necessary for activating PCP signalling in *Drosophila* (Axelrod et al., 1998) and non-canonical Wnt signalling in vertebrates, reviewed by (Wallingford and Habas, 2005). Vertebrate Dvl-GFP shows similar properties to *Drosophila* Dsh-GFP in animal cap tissue. Dvl-GFP occupies a punctate expression pattern in the cytoplasm when over-expressed in animal cap tissue. Over-expression of Fz1 induces the translocation of Dvl-GFP to the plasma membrane and this requires the DEP domain of Dvl (Rothbacher et al., 2000). Dvl-GFP is also recruited to the plasma membrane in

response to Wnt11b (Yamanaka and Nishida, 2007). Dvl-GFP translocates to the cell membrane in response to non-canonical Wnt signalling. The localisation of Dvl-GFP can be used to investigate the effects of Sulf1 on non-canonical Wnt signalling in *Xenopus.*

4.1.3 Cross talk between non-canonical Wnt signalling and FGF signalling during gastrulation

FGF signalling is required for medial/lateral convergence of the dorsal mesoderm that results in anterior/posterior extension during gastrulation. Blocking FGF signalling in *Xenopus* embryos inhibits convergent extension, resulting in a failure of embryos to gastrulate (Amaya et al., 1991; Isaacs et al., 1994). In addition over-expression of FGF3 inhibits notochord convergent extension in *Ciona intestinalis* embryos (Shi et al., 2009). Dvl-GFP is recruited to the plasma membrane in DMZ explants undergoing convergent extension. One prediction from this is that the polarised accumulation of Dvl is required for correct cell behaviour during gastrulation. Dvl-GFP membrane recruitment is inhibited by treating DMZ explants with SU5402 (a chemical inhibitor of FGF receptor signalling) (Mohammadi et al., 1997; Shi et al., 2009). FGF signalling is required for the membrane recruitment of Dvl-GFP during convergent extension in DMZ explants. The FGF and non-canonical Wnt signalling pathways are both able to regulate the subcellular localisation of Dvl-GFP.

PKCδ also plays an important role during gastrulation. Microinjection of morpholinos encoding PKCδ causes gastrulation defects in *Xenopus* embryos and inhibits medial/lateral convergent extension in DMZ explants (Kinoshita et al., 2003). In addition PKCδ translocates to the plasma membrane, along with Dvl, in response to Fz7 (Kinoshita et al., 2003). The membrane localisation of PKCδ depends on FGF signalling as well as non-canonical Wnt signalling. PKCδ-GFP translocates to the membrane in response to bFGF in *Xenopus* animal cap tissue (Sivak et al., 2005). PKCδ-YFP (yellow fluorescent protein) is recruited to the membrane in DMZ explants undergoing convergent extension, but this is inhibited by SU5402 (Shi et al., 2009). The non-canonical Wnt and FGF signalling pathways interact at the level of Dvl and PKCδ during gastrulation. This can make it difficult to dissect out the effects on non-

canonical Wnt signalling from those on FGF signalling. It is important that any assays designed to investigate the effects of Sulf1 on non-canonical Wnt signalling take this into account.

4.1.4 Aims of this chapter

Microinjection of mRNA encoding *Sulf1* into the marginal zone of *Xenopus* embryos causes gastrulation defects (chapter 3) (Freeman et al., 2008). In addition over-expression of Sulf1 together with either Wnt8a or Wnt11b in the ventral blastomere of *Xenopus* embryos enhances gastrulation defects (see chapter 3). One prediction from this is that Sulf1 has a role in regulating non-canonical Wnt signalling. The effects of Sulf1 on non-canonical Wnt signalling have not been explored in any detail. Work by (Tran et al., 2012) showed that Wnt7a could induce a greater activation of CamKII in *Sulf1/2* knockout myoblasts compared to control myoblasts, suggesting that Sulf1 plays an inhibitory role in the Wnt/Ca^{2+} pathway. This chapter will investigate the effects of Sulf1 on non-canonical Wnt signalling in animal cap assays and whole embryos. In addition the effects of Sulf1 on the ability of the canonical Wnt ligand Wnt8a to activate non-canonical signalling will be assessed.

mRNA encoding *Xenopus tropicalis Wnt4 (Wnt4)* and *Xenopus laevis Wnt11b* were microinjected, with or without *Xenopus tropicalis Sulf1* into the animal hemisphere of *Xenopus* embryos. The ability of Sulf1 and Wnt4/Wnt11b to regulate activin induced convergent extension and Dvl-GFP localisation in animal caps was investigated. The same assays were used to investigate the effects of Sulf1 on the canonical ligand *Xenopus laevis* Wnt8a. The results in this chapter show that Sulf1 enhances the ability Wnt4 and Wnt11b to activate non-canonical Wnt signalling. In contrast, Sulf1 has no effect on the ability of Wnt8a to activate non-canonical Wnt signalling. The ability of Sulf1 to enhance non-canonical Wnt signalling is opposed to previous findings (Tran et al., 2012), but supported by data in whole embryos (chapter 3).

4.2.0 Results

4.2.1 XtWnt11b2 is hypomorphic in non-canonical Wnt signalling

XtWnt11b2 was previously used in this laboratory as a non-canonical ligand to investigate the effects of Sulf1 on Wnt signalling (Freeman et al., 2008). The initial studies in this thesis used this same cDNA to investigate the role of Sulf1 in non-canonical Wnt signalling assays.

Wnt11b has previously been shown to inhibit activin induced convergent extension when over-expressed in animal caps (Hikasa et al., 2002). However the activity of XtWnt11b2 in this assay has not been investigated before. Embryos were microinjected bilaterally in the animal hemisphere with mRNA encoding *XtWnt11b2* and *Sulf1.* Embryos were cultured until NF stage 8 and then animal cap explants were taken and cultured in either the presence or absence of activin until NF stage 19. In the absence of activin animal caps round up into spherical balls epithelial of tissue (Figure 4.2A). In the presence of activin animal caps undergo convergent extension to form elongated structures (Figure 4.2B). Over-expression of XtWnt11b2 had no effect on the convergent extension of *Xenopus* animal caps (Figure 4.2C), in contrast to previous studies using Wnt11b (Hikasa et al., 2002). In contrast over-expression of Sulf1 inhibited animal cap elongation (compare Figure 4.2D to 4.2B). The effects of Sulf1 were not altered by the presence or absence of XtWnt11b2 (compare Figure 4.2E to 4.2D). XtWnt11b2 is unable to inhibit activin induced convergent extension in *Xenopus* animal caps.

Over-expression of Wnt11b results in the translocation of Dvl-GFP to the plasma membrane (Yamanaka and Nishida, 2007). Embryos were microinjected bilaterally in the animal hemisphere with mRNA encoding *farnesylated red fluorescent protein (mRFP)* and *Dvl-GFP*. In addition embryos were injected with mRNA encoding *XtWnt11b2*. Embryos were cultured until NF stage 8 and then animal cap explants were taken. Animal caps were

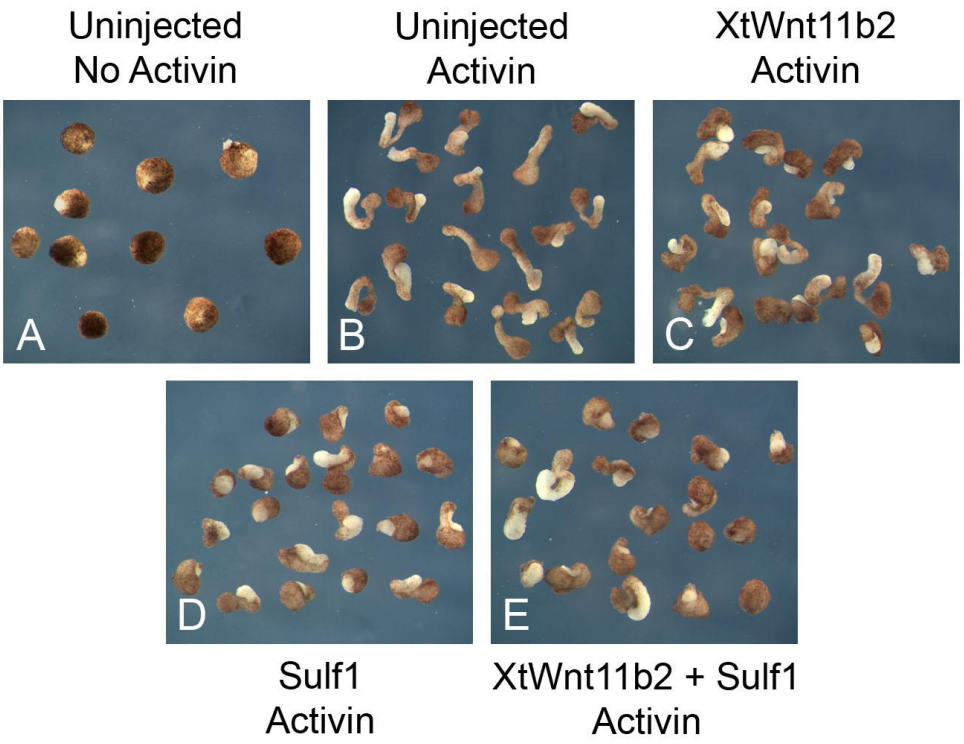

Figure 4.2; XtWnt11b2 does not inhibit activin induced convergent extension of Xenopus laevis animal explants.
mRNA encoding *XtWnt11b2* (600pg), *Sulf1* (500pg) or both was injected bilaterally into the animal hemisphere of embryos at the two cell stage. Embryos were cultured until NF stage 8 and then animal cap explants were taken. Animal explants were cultured in either the presence or absence of activin until NF stage 19. [A-B] Uninjected animal explants cultured in either the absence [A] or presence [B] of activin. [C-E] Embryos injected with [C] *XtWnt11b2*, [D] *Sulf1* or [E] *XtWnt11b2* and *Sulf1* and cultured in the presence of activin. Over-expression of Sulf1 or XtWnt11b2 and Sulf1 inhibited activin induced convergent extension to a similar extent.

cultured in the dark for four hours at 21˚C prior to imaging by confocal microscopy. In control animal caps Dvl-GFP occupies a punctate pattern in the cytoplasm (Figure 4.3A-D). Over-expression of XtWnt11b2 had no effect on the distribution of Dvl-GFP (Figure 4.3E-H). As a positive control the *Xenopus laevis* homologue of XtWnt11b2, Wnt11b, was able to induce Dvl-GFP translocation to the cell membrane (see Figure 4.10). XtWnt11b2 is unable to inhibit activin induced convergent extension or induce the translocation of Dvl-GFP to the cell membrane. XtWnt11b2 is not a suitable ligand for investigating the effects of Sulf1 on non-canonical Wnt signalling.

Wnt11b is the *Xenopus laevis* paralogue of XtWnt11b2 and has been shown to function in the non-canonical Wnt signalling pathway (Du et al., 1995; Hikasa et al., 2002; Yamanaka and Nishida, 2007). Comparison of the amino acid

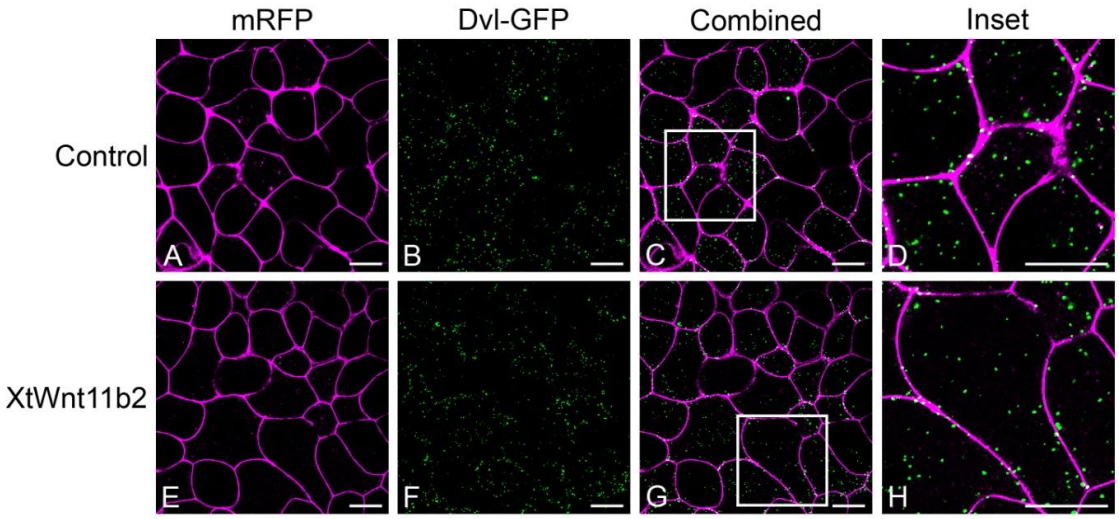

Figure 4.3; XtWnt11b2 does not induce Dvl-GFP translocation to the cell membrane. mRNA encoding *mRFP* (500pg) and *Dvl-GFP* (500pg) was injected bilaterally into the animal hemisphere of embryos at the two cell stage. In addition embryos were also injected with *XtWnt11b2* (600pg). Embryos were cultured until NF stage 8 and then animal cap explants were taken. Animal caps were cultured in the dark for four hours at 21˚C prior to imaging by confocal microscopy. [A-D] Control animal caps over-expressing mRFP and Dvl-GFP and [E-H] animal caps over-expressing mRFP, Dvl-GFP and XtWnt11b2. The white boxes in [C] and [G] mark the areas used to create panels [D] and [H] respectively. In control conditions Dvl-GFP is present as puncta evenly distributed in the cytoplasm. Over-expression of XtWnt11b2 had no effect on the distribution of Dvl-GFP in animal caps. mRFP (magenta), Dvl-GFP (green), scale bars represent 20µm.

sequences of Wnt11b and XtWnt11b2 reveals a high degree of homology between them (Figure 4.0B). Another Wnt11 cDNA, Wnt11b-HA had also been previously used in this laboratory (Freeman et al., 2008) and was tested for activity in the activin animal cap assay. Embryos were microinjected bilaterally in the animal hemisphere with mRNA encoding *Wnt11b-HA* and *Sulf1.* Embryos were cultured until NF stage 8 and then animal cap explants were taken. Animal caps were cultured in either the presence or absence of activin until NF stage 19. Over-expression of Wnt11b-HA inhibits activin induced convergent extension in animal caps (compare Figure 4.4C to 4.4B). Wnt11b-HA and Sulf1 inhibit convergent extension in an additive manner over-expressed together (compare Figure 4.4E to 4.4C and 4.4D). Inhibition of convergent extension by Wnt11b-HA and Sulf1 could be due to a reduction or excess of non-canonoical Wnt signalling, but in this case is likely to be excess (see Figure 4.11). Wnt11b is a suitable ligand to investigate the effects of Sulf1 on non-canonical Wnt signalling.

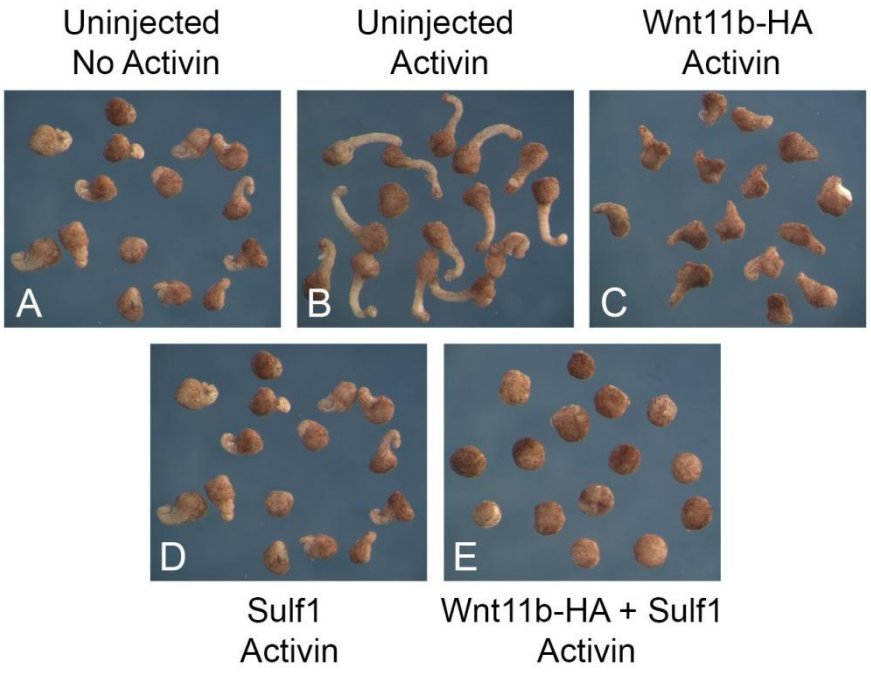

Figure 4.4; Sulf1 synergises with XlWnt11b-HA to inhibit convergent extension. mRNA encoding *Sulf1* (500pg), *XlWnt11b-HA* (250pg) or both was injected bilaterally into the animal hemisphere of embryos at the two cell stage. Embryos were cultured until NF stage 8 and then animal cap explants were taken. Animal caps were cultured in either the presence or absence of activin until NF stage 19. [A-B] Uninjected animal explants cultured in either the absence [A] or presence [B] of activin. [C-E] Embryos injected with [C] *Wnt11b-HA*, [D] *Sulf1* or [E] *Wnt11b-HA* and *Sulf1* and cultured in the presence of activin. Over-expression of Wnt11b-HA inhibits activin induced convergent extension. In addition Wnt11b-HA and Sulf1 synergise to inhibit convergent extension.

4.2.2 Sulf1 synergises with Wnt11b, but not Wnt8a to inhibit activin induced convergent extension in animal caps

Wnt11b-HA activates non-canonical Wnt signalling in activin animal cap assays. The coding region of *Wnt11b* was subcloned from *Wnt11-HA* by PCR amplification. *Wnt11b* was then ligated into the expression vector CS2+, together with a Kozak sequence in order to enhance the levels of *Wnt11b* mRNA translation, review by (Kozak, 1994). To be able score animal cap convergent extension, the levels of animal cap elongation in response to activin were classified. Figure 4.5 shows the varying degrees of animal cap elongation induced by activin. Complete failure of animal caps to converge and extend was defined as class 0 (Figure 4.5A). If the overall animal cap morphology remained spherical; however a clear protrusion could be seen this was defined as class 1 (Figure 4.5B). Class 2 animal caps were no longer spherical, but had

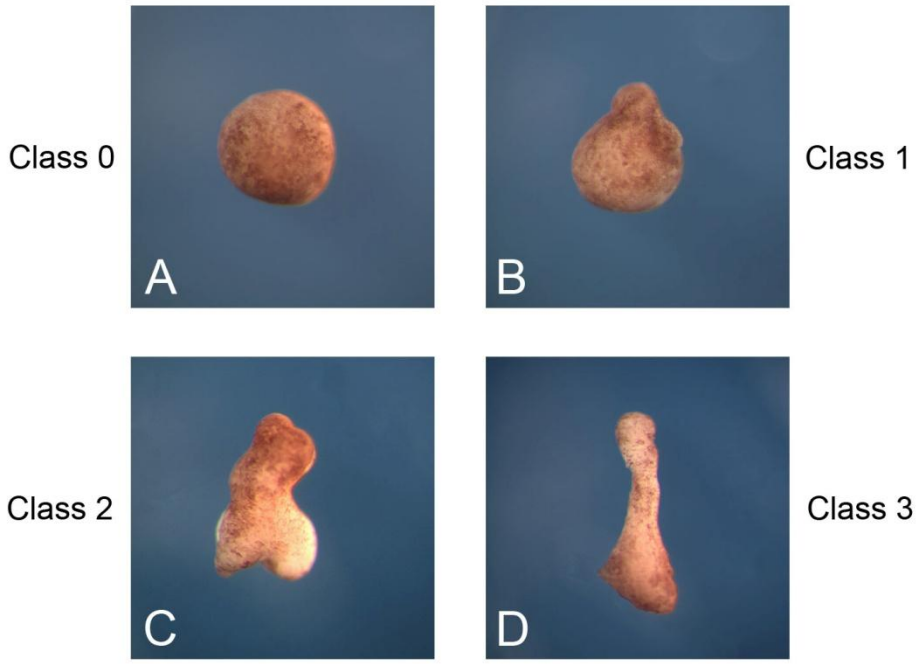

Figure 4.5; Classifying the level of convergent extension in uninjected animal explants treated with activin.
Uninjected embryos were cultured until NF stage 8 and then animal caps explants were taken and cultured in the presence of activin until NF stage 19. The level of convergent extension undergone by the animal caps was classified as one of four categories. [A] Class 0, [B] Class 1, [C] Class 2, [D] Class 3.

not undergone convergent extension along a single axis (Figure 4.5C). Animal caps that had undergone convergent extension and elongated along a specific axis were defined as class 3 (Figure 4.5D)

Embryos were microinjected bilaterally in the animal hemisphere with mRNA encoding *Wnt11b* and *Sulf1.* Embryos were cultured until NF stage 8 and then animal cap explants were taken. Animal caps were cultured in either the presence or absence of activin until NF stage 19. Over-expression of Wnt11b or Sulf1 inhibited activin induced convergent extension (compare Figure 4.6C and 4.6D to 4.6B). Over-expression of Wnt11b and Sulf1 together enhances the inhibition of convergent extension (compare Figure 4.6E to 4.6C and 4.6D). The data from figure 4.6A-E is quantified in Figure 4.6F. Sulf1 and Wnt11b synergise to inhibit activin induced convergent extension in *Xenopus* animal caps.

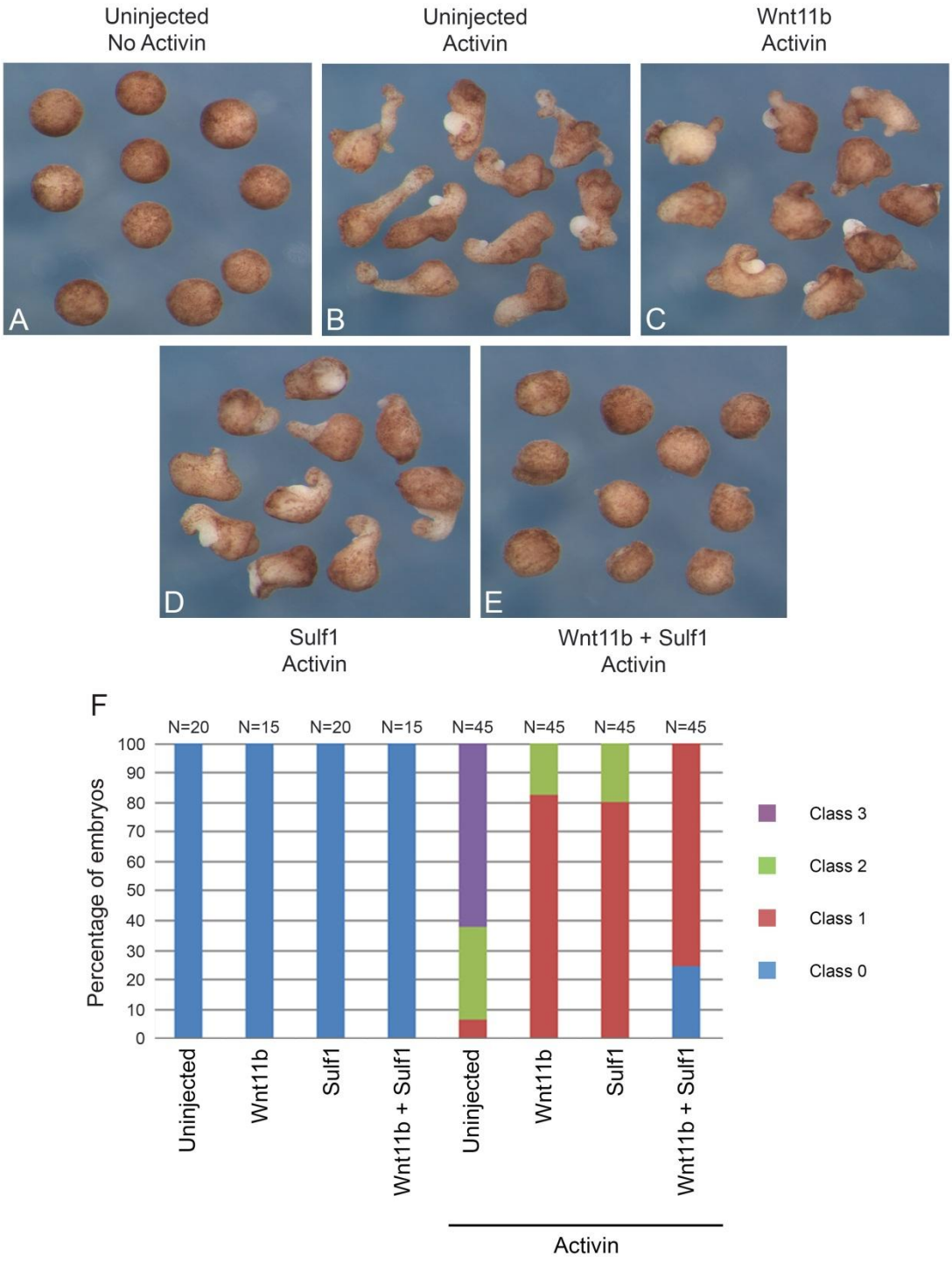

Figure 4.6; Sulf1 synergises with Wnt11b to inhibit convergent extension.
mRNA encoding *Sulf1* (500pg), *Wnt11b* (50pg) or both was injected bilaterally into the animal hemisphere of embryos at the two cell stage. Embryos were cultured until NF stage 8 and then animal cap explants were taken. Animal caps were cultured in either the presence or absence of activin until NF stage 19. [A-B] Uninjected animal explants cultured in either the absence [A] or presence [B] of activin. [C-E] Embryos injected with [C] *Wnt11b*, [D] *Sulf1* or [E] *Wnt11b* and *Sulf1* and cultured in the presence of activin. Over-expression of either Wnt11b or Sulf1 inhibits activin induced convergent extension. Wnt11b and Sulf1 synergise to further inhibit convergent extension when over-expressed together. [F] Graph quantifying the level of convergent extension in each condition, N = number of embryos.

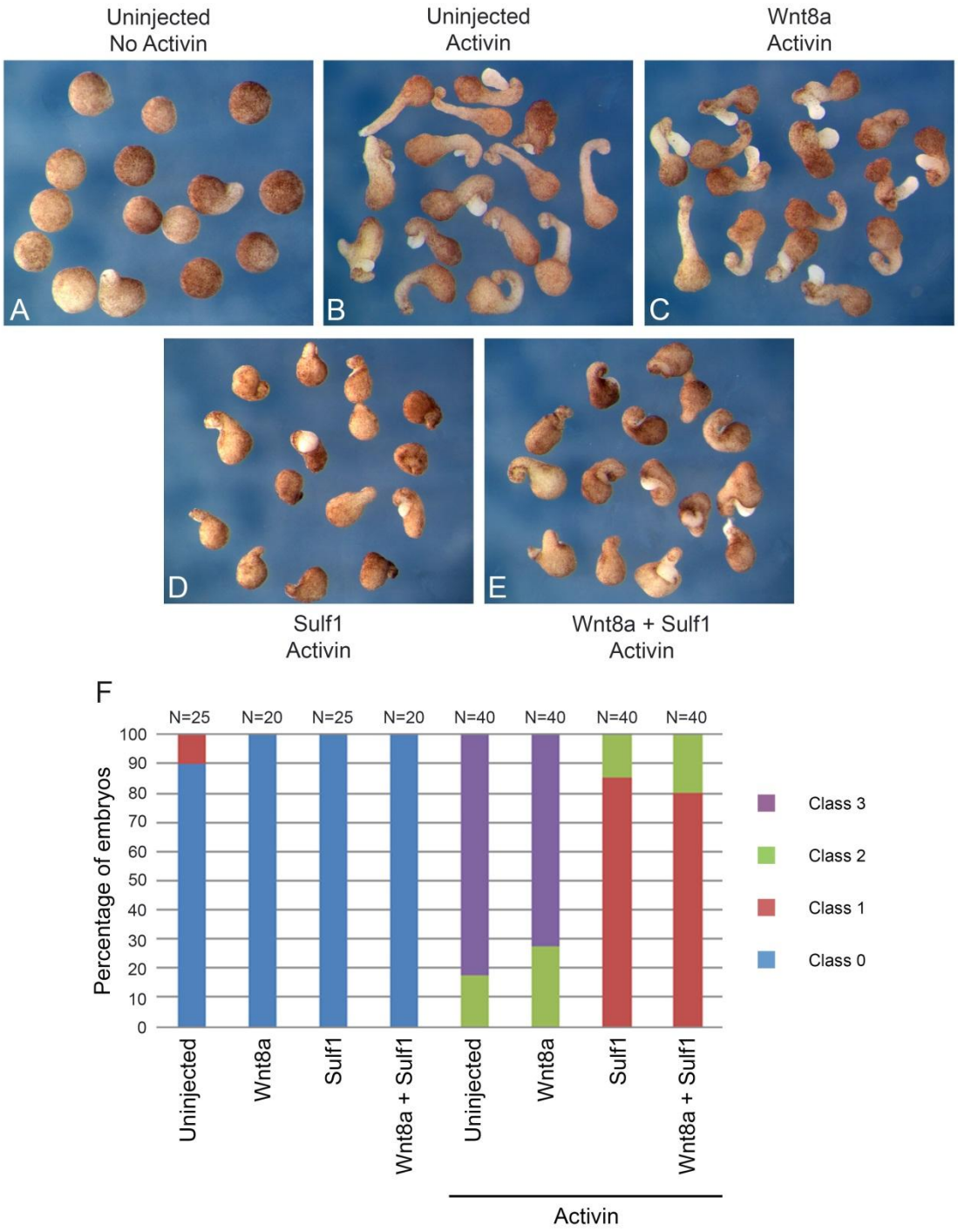

Figure 4.7; Sulf1 does not synergise with Wnt8a to inhibit activin induced convergent extension.
mRNA encoding *Sulf1* (500pg), *Wnt8a* (20pg) or both was injected bilaterally into the animal hemisphere of embryos at the two cell stage. Embryos were cultured until NF stage 8 and then animal cap explants were taken. Animal caps were cultured in either the presence or absence of activin until NF stage 19. [A-B] Uninjected animal explants cultured in either the absence [A] or presence [B] of activin. [C-E] Embryos injected with [C] *Wnt8a*, [D] *Sulf1* or [E] *Wnt8a* and *Sulf1* and cultured in the presence of activin. Over-expression of Wnt8a does not inhibit activin induced convergent extension. Embryos over-expressing Sulf1 or Sulf1 and Wnt8a inhibited convergent extension to a similar extent. [F] Graph quantifying the level of convergent extension in each condition, N = number of embryos.

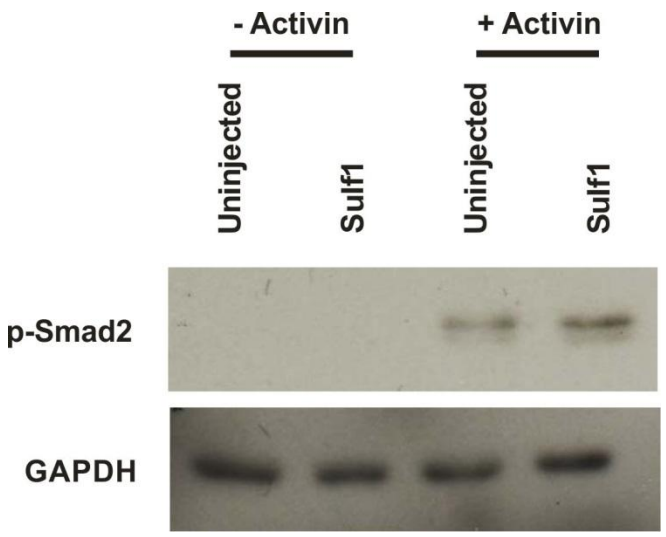

Figure 4.8; Sulf1 does not inhibit activin induced activation of the activin/TGF-β signalling pathway.
mRNA encoding *Sulf1* (4ng) was injected bilaterally into the animal hemisphere of embryos at the two cell stage. Embryos were cultured until NF stage 8 and then animal cap explants were taken. Animal caps were cultured in either the presence or absence of activin for two hours at 21˚C and then snap frozen for western blot. Activin treatment activates the activin/TGFβ signalling pathway inducing pSmad2 and this is unaffected by the over-expression of Sulf1.

Chapter 3 discussed how Sulf1 enhanced the ability of Wnt11b to activate the canonical Wnt signalling pathway. To investigate whether Sulf1 could alter the effects of Wnt8a on non-canonical Wnt signalling, Wnt8a and Sulf1 were over-expressed in animal caps. Embryos were microinjected bilaterally in the animal hemisphere with mRNA encoding *Wnt8a* and *Sulf1.* Embryos were cultured until NF stage 8 and then animal cap explants were taken. Animal caps were cultured in either the presence or absence of activin until NF stage 19. Over-expression of Wnt8a had no effect on activin induced convergent extension (compare Figure 4.7C to 4.7B). Wnt8a did not synergise with Sulf1 to enhance the inhibition of animal cap elongation (compare Figure 4.7E to 4.7D). The data from Figures 4.7A-E is quantified in Figure 4.7F. Sulf1 does not enhance the ability of Wnt8a to inhibit convergent extension in *Xenopus* animal caps.

Activin treatment transforms animal cap tissue in to dorsal mesoderm (Smith, 1987). It is possible that Sulf1 inhibits activin signalling directly. To test this a Western blot for pSmad2 was performed. mRNA encoding *Sulf1* was microinjected bilaterally in the animal hemisphere of embryos at the two cell stage. Embryos were cultured until NF stage 8 and then animal caps explants were taken. Animal caps were cultured in either the presence or absence of

activin for two hours at 21˚C and then snap frozen for western blot. Activin treatment of animal caps results in the induction of pSmad2 and this was unaffected by over-expressing Sulf1 (Figure 4.8). Sulf1 does not inhibit activin induced activation of pSmad2. Sulf1 synergises with the non-canonical ligand Wnt11b, but not the canonical ligand Wnt8a to inhibit activin induced convergent extension in animal caps.

4.2.3 Characterising the Sulf1 C-A mutant

Sulf1 is a member of an evolutionarily conserved family of sulfatases that undergo a specific posttranslational modification essential for enzymatic activity. A conserved cysteine in the amino terminal of the sulfatase is converted to formylglycine and this is essential for catalytic activity (Schmidt, et al, 1995; Selmer, et al, 1996). In *Human* Sulf1, this conserved residue is cysteine 87 and mutation of this residue to an alanine results in a catalytically inactive mutant (Morimoto-Tomita, et al, 2002). *Quail* Sulf1has conserved residues at cysteines 89 and 90. Mutations of both of these residues to alanine produced the Sulf1 C-A mutant that was unable to potentiate Wnt1 activation of Topflash in C2C12 cells (Dhoot et al., 2001). To generate the *Xenopus tropicalis* Sulf1 C-A mutant the conserved cysteine residues at positions 86 an 87 of *Xenopus tropicalis* Sulf1 were converted to alanines by PCR based mutagenesis (Figure 4.9A). This prevents formylglycine modification and inhibits Sulf1 C-A catalytic activity.

To investigate the functional activity of Sulf1 C-A, mRNA encoding *Sulf1* and *Sulf1 C-A* was microinjected bilaterally in the marginal zone of embryos at the two cell stage. Embryos were cultured until the desired stage and analysed for phenotype. At NF stage 14, uninjected embryos have entered neurulation (Figure 4.9B). Over-expression of either Sulf1 or Sulf1 C-A delays entry to neurulation and inhibits blastopore closure (see white arrows Figure 4.9C and 4.9D). At NF stage 36, embryos over-expressing either Sulf1 or Sulf1 C-A have severely truncated anterior/posterior axes and show failure of the blastopore to close (compare 4.9H and 4.9I to 4.9E). Microinjection of mRNA encoding Sulf1 C-A or Sulf1 into the animal hemispheres of *Xenopus* embryos produces a different phenotype. Over-expression of Sulf1 or Sulf1 C-A resulted in minor axial defects, but caused the cement glands of injected embryos to enlarge

Figure 4.9; The Sulf1 C-A mutant.
Figure illustrating the development and testing of the Sulf1 C-A mutant. [A] Diagram depicting the portion of the Sulf1 catalytic site that undergoes formylglycine modification. The Sulf1 C-A mutant was created by PCR based cloning, where the cysteine residues at positions 86 and 87 were converted to alanines, preventing the formylglycine modification (marked in red). [C-D] mRNA encoding *Sulf1* or the *Sulf1 C-A mutant* (4ng) was injected bilaterally into the marginal zone of *Xenopus* embryos at the two cell stage and cultured until controls reached NF stage 14. [E-I] mRNA encoding *Sulf1* or the *Sulf1 C-A* mutant (4ng) was injected bilaterally into the [F-G] animal hemisphere or [H-I] marginal zone (MZ) of embryos at the two cell stage. Embryos were cultured until NF stage 36. [B] Animal view of an uninjected embryo at NF stage 14. [C-D] Vegetal views of embryos over expressing [C] the Sulf1 C-A mutant and [D] Sulf1. Over expression of either protein causes gastrulation defects (see white arrows [C-D]). [E] Lateral view of an NF stage 36 embryo. [F-G] Lateral views of embryos over expressing [F] the Sulf1 C-A mutant and [G] Sulf1 in the animal hemisphere. Over expression of either protein resulted in axial defects as the embryos fail to elongate correctly and caused the cement gland to enlarge (see red arrowheads [F-G]). [H-I] Lateral views of embryos over expressing [H] the Sulf1 C-A mutant [I] Sulf1 in the marginal zone. Over expression of either protein caused severe axial defects and enlarged cement glands. [J] mRNA encoding *Sulf1* (4ng), *Sulf1 C-A* mutant (4ng), *FGF4a* (10pg), *LacZ* (4ng) and *DN*FGFr4a* (500pg) was injected bilaterally into the animal hemisphere of embryos at the two cell stage. Embryos were cultured until NF stage 8 and then animal cap explants were taken and cultured until NF stage 10.5. Animal caps were then snap frozen for western blot. Over expression of FGF4a activates the FGF signalling pathway inducing dpERK and this is completely inhibited by over expressing DN*FGFr4a. Over expression of Sulf1 causes a greater reduction in dpERK than Sulf1C-A.

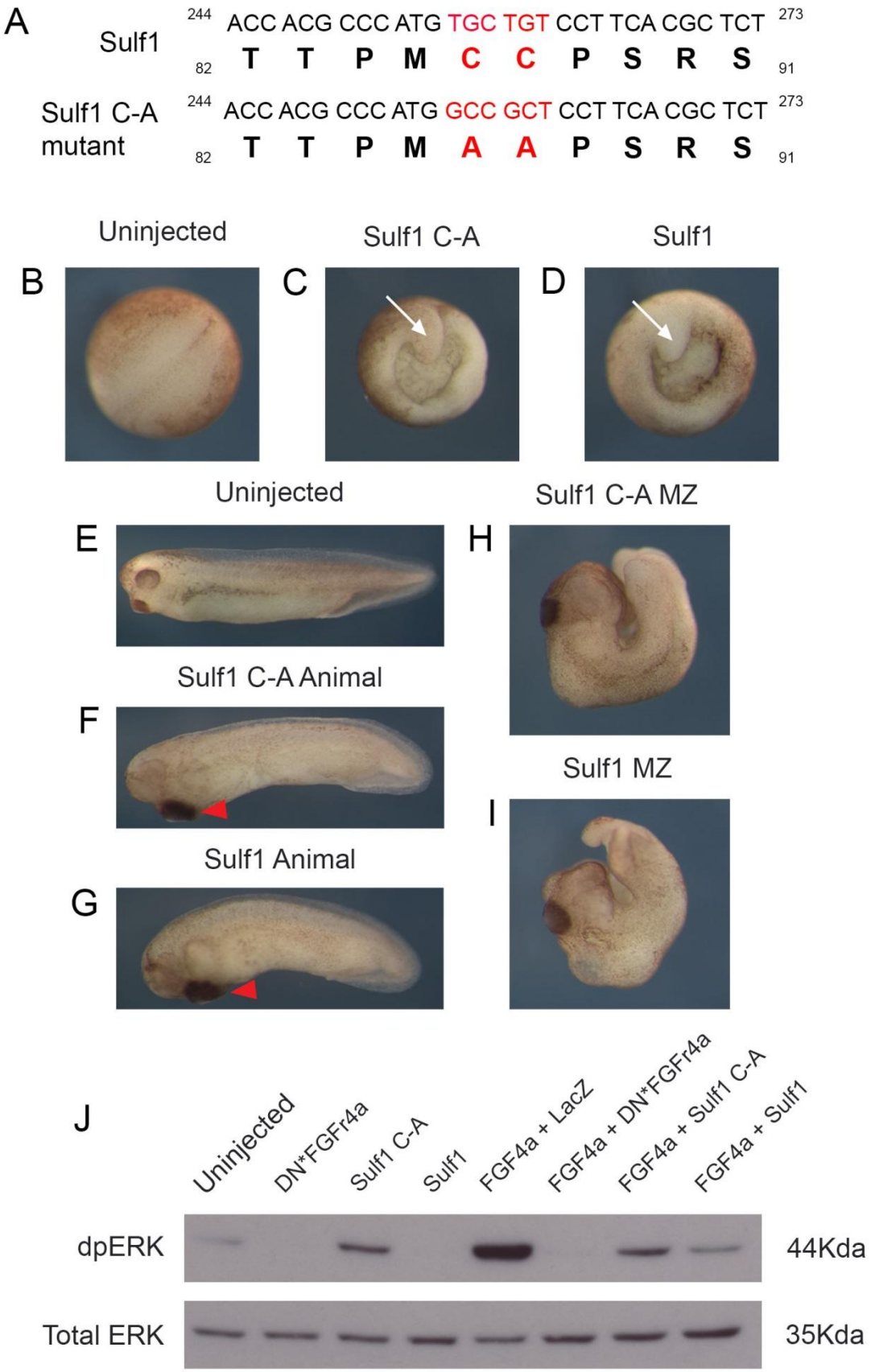
A
Sulf1
244 ACC ACG CCC ATG TGC TGT CCT TCA CGC TCT 273
82 T T P M C C P S R S 91
Sulf1 C-A mutant
244 ACC ACG CCC ATG GCC GCT CCT TCA CGC TCT 273
82 T T P M A A P S R S 91
Uninjected
Sulf1 C-A
Sulf1
B
C
D
Uninjected
Sulf1 C-A MZ
E
H
Sulf1 C-A Animal
F
Sulf1 MZ
I
Sulf1 Animal
G
J
Uninjected
DN*FGFr4a
Sulf1 C-A
Sulf1
FGF4a + LacZ
FGF4a + DN*FGFr4a
FGF4a + Sulf1 C-A
FGF4a + Sulf1
dpERK
44Kda
Total ERK
35Kda

(compare 4.9F and 4.9G to 4.9E). The Sulf1 C-A mutant produced similar phenotypes to Sulf1 when over-expressed in *Xenopus* embryos.

To analyse the signalling activity of the Sulf1 C-A mutant a western blot was performed for the induction of dpERK. Sulf1 has previously been shown to inhibit FGF signalling in animal caps (Freeman et al., 2008; Wang et al., 2004). mRNA encoding *Sulf1, Sulf1 C-A, DN*FGFr4a, LacZ* and *FGF4a* was microinjected bilaterally into the animal hemisphere of embryos at the two cell stage. Embryos were cultured until NF stage 8 and then animal caps explants were taken. Animal caps were cultured until NF stage 10.5 and then snap frozen for western blot. Over-expression of Sulf1 or DN*FGFr4a, but not Sulf1 C-A inhibits endogenous dpERK in animal caps (Figure 4.9J). Over-expression of FGF4a activates FGF signalling increasing the levels of dpERK. Over-expression of DN*FGFr4a completely abolishes the induction of dpERK by FGF4a. Both Sulf1 and Sulf1 C-A reduce the induction of dpERK, but the effects of Sulf1 are stronger than those of the Sulf1 C-A mutant (Figure 4.9J).

Despite mutating both of the conserved residues required for formylglycine modification, the Sulf1 C-A mutant can still function in *Xenopus.* Sulf1 C-A produces similar phenotypes to Sulf1 and inhibits FGF signalling, although to a lesser extent than Sulf1. Sulf1 C-A is a hypomorphic mutant and as such can still be used as an injection control for analysing the effects of the catalytic activity of Sulf1 on non-canonical Wnt signalling.

4.2.4 Sulf1 enhances the ability of Wnt11b to induce Dvl-GFP translocation to the cell membrane

Sulf1 and Wnt11b synergise to inhibit convergent extension in *Xenopus* animal caps. To look more directly at the effects of Sulf1 on non-canonical Wnt signalling, the localisation of Dvl-GFP was investigated in animal caps. Embryos were injected bilaterally in the animal hemisphere with mRNA encoding *mRFP* and *Dvl-GFP.* In addition embryos were injected with increasing amounts of *Wnt11b* mRNA. Embryos were cultured until NF stage 8 and then animal cap explants were taken. Animal caps were cultured in the dark for four hours at 21˚C prior to imaging by confocal microscopy. In control

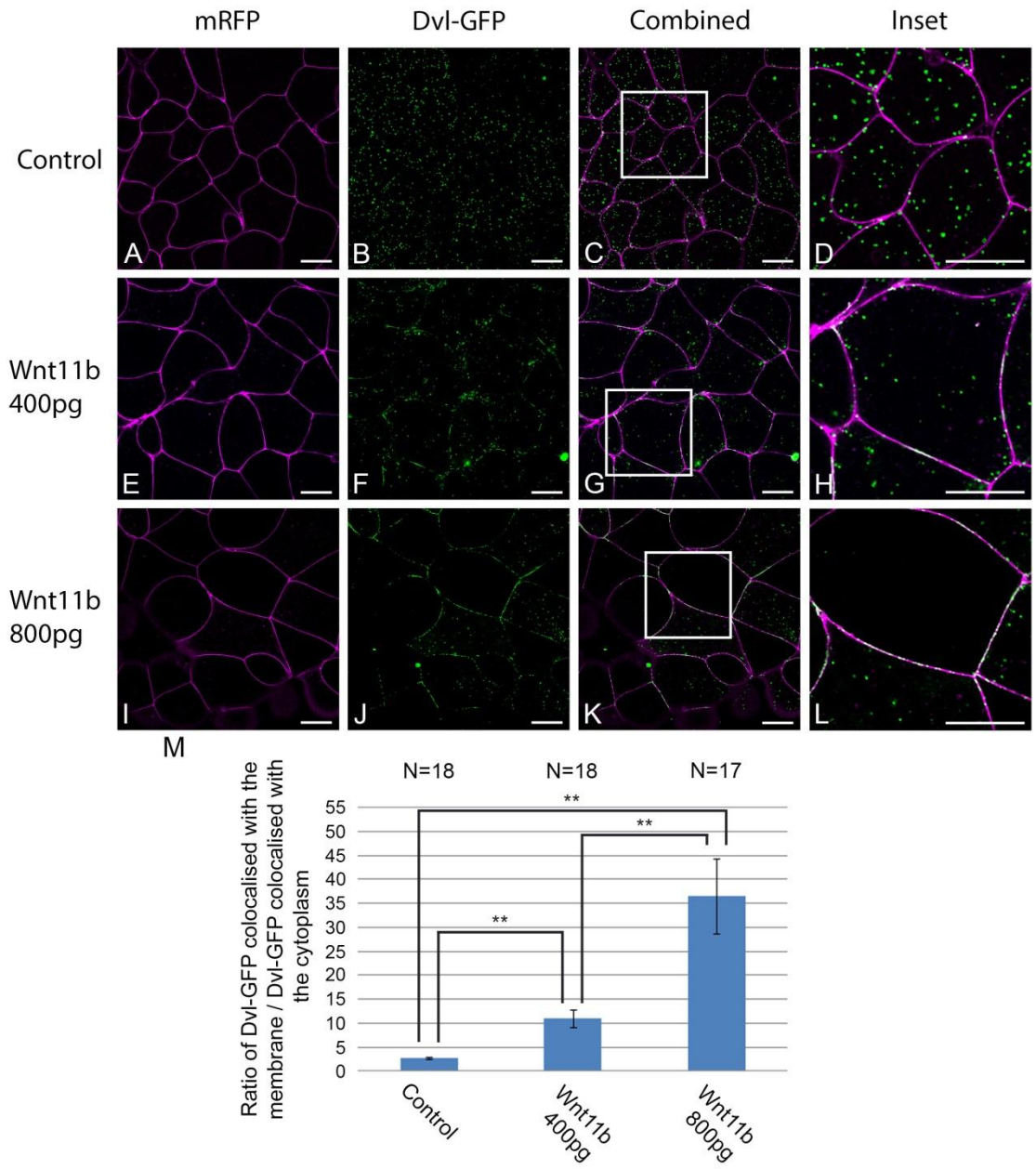

Figure 4.10; Wnt11b causes the translocation of Dvl-GFP to the cell membrane. mRNA encoding *mRFP* (500pg) and *Dvl-GFP* (500pg) was injected bilaterally into the animal hemisphere of embryos at the two cell stage. In addition embryos were injected with increasing amounts of *Wnt11b* mRNA. Embryos were cultured until NF stage 8 and then animal cap explants were taken and cultured for four hours at 21˚C prior to imaging by confocal microscopy. [A-D] Control animal caps over-expressing mRFP and Dvl-GFP. Animal caps injected with [E-H] 400pg or [I-L] 800pg of *Wnt11b* mRNA in addition to *mRFP* and *Dvl-GFP*. The white boxes in [C], [G] and [K] mark the areas used to create panels [D], [H] and [L] respectively. Over-expression of 400pg of Wnt11b caused Dvl-GFP to translocate to the cell membrane where it appeared both as aggregates and spherical puncta. Increasing the dose of Wnt11b to 800pg increased the amount of Dvl-GFP that translocated to the cell membrane. [M] Graph quantifying the effects of increasing Wnt11b levels on Dvl-GFP translocation. Data obtained using a programme written in MATLAB see methods 2.5.2 for details. Asterisks mark significant differences (**P<0.01) Mann-Whitney U, error bars represent s.e.m. mRFP (magenta), Dvl-GFP (green), scale bars represent 20µm, N = number of embryos.

animal caps Dvl-GFP occupies a punctate pattern in the cytoplasm (Figure 4.10A-D). Over-expression of Wnt11b causes Dvl-GFP to translocate to the plasma membrane. At the cell membrane Dvl-GFP appears as spherical puncta, but also begins to form longer aggregates (compare Figure 4.10E-H to 4.10A-D). Increasing the amount of *Wnt11b* injected, increased the translocation of Dvl-GFP to the membrane. At high doses of Wnt11b, the majority of Dvl-GFP is colocalised with the cell membrane, with little left in the cytoplasm. In addition Dvl-GFP at the membrane has formed larger aggregates, with less spherical puncta visible (compare Figure 4.10I-L to 4.10E-H). The data from Figure 4.10A-L is quantified in Figure 4.10M. The data was quantified using a programme written in Matlab (see methods 2.5.2 for details). Briefly the programme calculates the percentage of Dvl-GFP pixels colocalising with mRFP pixels, removes these pixels and then calculates the percentage of black (cytoplasmic) pixels occupied by Dvl-GFP. The ratio of Dvl-GFP colocalised with mRFP/Dvl-GFP colocalised with black pixels creates an arbitrary value for the amount of Dvl-GFP colocalised with the cell membrane. Increasing the expression of Wnt11b enhances the level of Dvl-GFP colocalising with the cell membrane. This assay can be used to investigate the effects of Sulf1 on non-canonical Wnt signalling.

Embryos were microinjected bilaterally in the animal hemisphere with mRNA encoding *mRFP* and *Dvl-GFP*. In addition embryos were microinjected with mRNA encoding *Sulf1, Sulf1 C-A, Wnt11b* or a mixture of the three. Embryos were cultured until NF stage 8 and then animal cap explants were taken. Animal caps were cultured in the dark for four hours at 21˚C prior to imaging by confocal microscopy. Over-expression of either Sulf1 or Sulf1 C-A had no effect on the localisation of Dvl-GFP (compare Figure 4.11E-H and 4.11I-L to 4.11A-D). Over-expression of Wnt11b induced the translocation of Dvl-GFP to the plasma membrane (compare Figure 4.11M-P to 4.11A-D). Over-expression of Sulf1 C-A together with Wnt11b caused a small increase in the translocation of Dvl-GFP to the plasma membrane (compare Figure 4.11Q-T to Figure 4.11M-P). However over-expression of Sulf1 together with Wnt11b produced a dramatic increase in the translocation of Dvl-GFP to the cell membrane. In this condition, only a small amount of Dvl-GFP remained in the cytoplasm with

Figure 4.11; Sulf1 enhances Wnt11b induced Dvl-GFP translocation to the cell membrane.
mRNA encoding *mRFP* (500pg) and *Dvl-GFP* (500pg) was injected bilaterally into the animal hemisphere of embryos at the two cell stage. In addition embryos were injected with mRNA encoding *Sulf1* (4ng), *Sulf1 C-A* (4ng), *Wnt11b* (400pg) or a mixture of the three. Embryos were cultured until NF stage 8 and then animal cap explants were taken and cultured for four hours at 21˚C prior to imaging by confocal microscopy. [A-D] Control animal caps over expressing mRFP and Dvl-GFP. Animal explants over expressing [E-H] Sulf1 C-A, [I-L] Sulf1, [M-P] Wnt11b [Q-T] Sulf1 C-A and Wnt11b and [U-X] Sulf1 and Wnt11b. The white boxes in [C], [G], [K], [O], [S] and [W] mark the areas used to create panels [D], [H], [L], [P], [T] and [X] respectively. Over expression of Wnt11b caused Dvl-GFP to translocate to the cell membrane. Sulf1 C-A enhanced the effects of Wnt11b on Dvl-GFP localisation, but Sulf1 had a much greater effect on Wnt11b signalling (compare [U-X] to [Q-T]). mRFP (magenta), Dvl-GFP (green), scale bars represent 20μm.

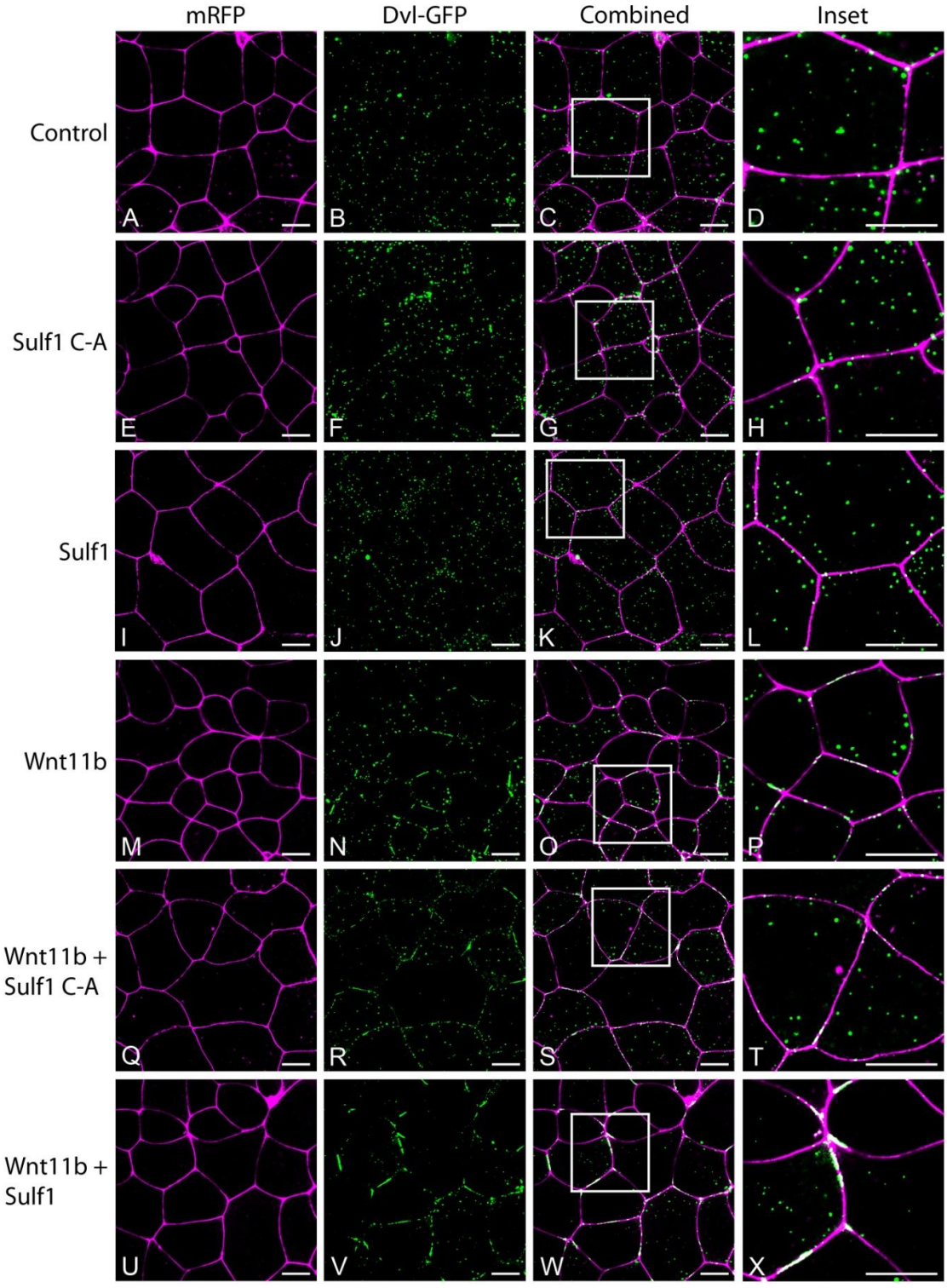
mRFP
Dvl-GFP
Combined
Inset
Control
Sulf1 C-A
Sulf1
Wnt11b
Wnt11b +
Sulf1 C-A
Wnt11b +
Sulf1
A
B
C
D
E
F
G
H
I
J
K
L
M
N
O
P
Q
R
S
T
U
V
W
X

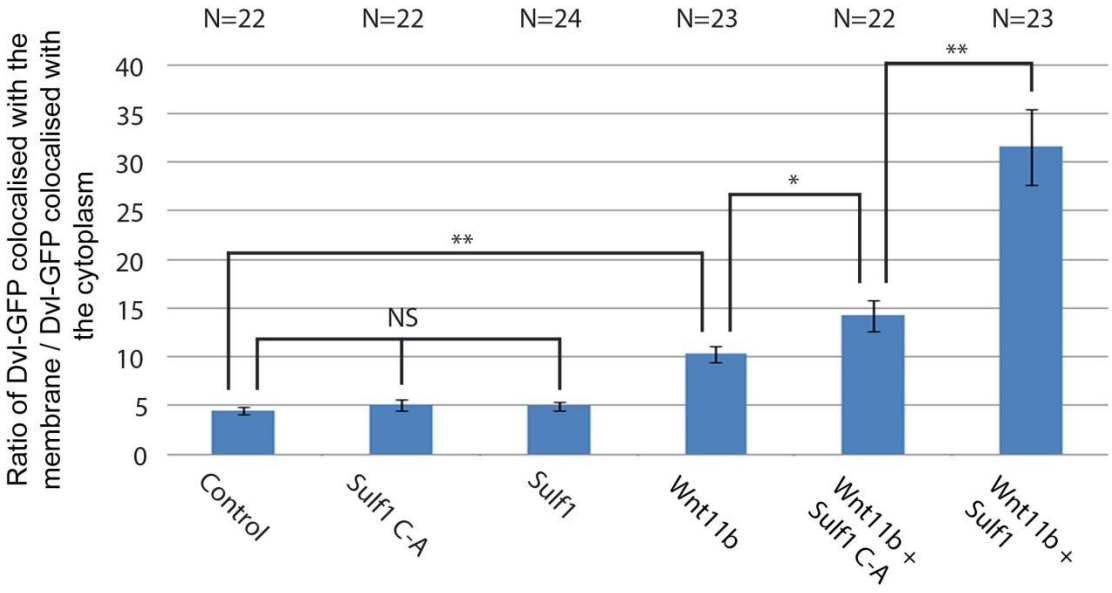

Figure 4.12; Graph illustrating the effects of Sulf1 on Wnt11b induced Dvl-GFP translocation to the cell membrane.
Graph illustrating the data shown in Figure 4.11, data quantified by a programme written in Matlab. Over-expression of Wnt11b induced the translocation of Dvl-GFP to the plasma membrane compared to control conditions. Sulf1 C-A enhanced the effects of Wnt11b on Dvl-GFP translocation, but to a much weaker extent than Sulf1. Asterisks mark significant differences (*P<0.05 and **P<0.01), NS marks non-significant differences, Mann-Whitney U, error bars represent s.e.m, N = number of embryos.

Dvl-GFP forming thick aggregates on the cell membrane (compare Figure 4.11U-X to 4.11M-P and 11Q-T). The data from Figure 4.11 is quantified in Figure 4.12. Over-expression of Sulf1 C-A together with Wnt11b caused a slight increase in the level of Dvl-GFP associating with the plasma membrane compared to Wnt11b alone. Over-expression of Sulf1 and Wnt11b lead to a dramatic increase in the levels of Dvl-GFP colocalising with the cell membrane. Sulf1 C-A is acting as a hypomorphic mutant in this assay, similar to its effects on FGF signalling. Sulf1 enhances the ability of Wnt11b to induce Dvl-GFP translocation to the cell membrane. The data suggests that Sulf1 enhances the ability of Wnt11b to activate non-canonical Wnt signalling.

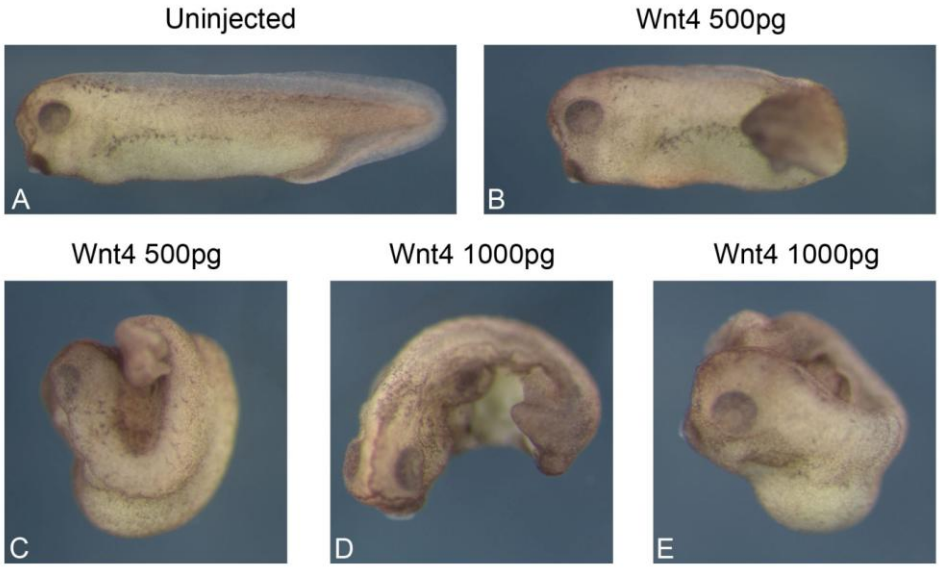

Figure 4.13; Wnt4 does not induce axis duplication in *Xenopus*.
mRNA encoding *Wnt4* was injected into the VMZ of one cell of at the four cell stage. Embryos were cultured until NF stage 36 and then examined for phenotype. [A] Lateral view of an uninjected embryo. Lateral views of embryos injected with [B-C] 500pg and [D-E] 1ng of *Wnt4* mRNA. Over-expression of Wnt4 caused gastrulation defects, but did not induce axis duplication.

4.2.5 Sulf1 enhances the ability of Wnt4, but not Wnt8a to induce Dvl-GFP translocation to the cell membrane

Wnt4 is classified as a non-canonical Wnt ligand as it induces axial defects when over-expressed dorsally in *Xenopus* embryos (Du et al., 1995). In addition Wnt4 did not induce axis duplication when over-expressed in *Xenopus* embryos (Figure 4.13). Embryos were microinjected in one ventral blastomere at the four cell stage with mRNA encoding *Wnt4* and cultured until NF stage 36. Over-expression of Wnt4 did not induce axis duplication, but instead caused truncations in the anterior/posterior axis (compare 4.13B and 4.13C to 4.13A). At higher concentrations *Wnt4* inhibited blastopore closure (see exposed yolk Figure 4.13D), consistent with the classification of Wnt4 as a non-canonical Wnt ligand (Du et al., 1995).

To determine whether the effects of Sulf1 on Wnt signalling were specific to the ligand Wnt11b, the Dvl-GFP assay was repeated using Wnt4. The Sulf1 C-A mutant was used as an injection control in this experiment. Embryos were microinjected bilaterally in the animal hemisphere with mRNA encoding *mRFP* and *Dvl-GFP*. In addition embryos were microinjected with mRNA encoding

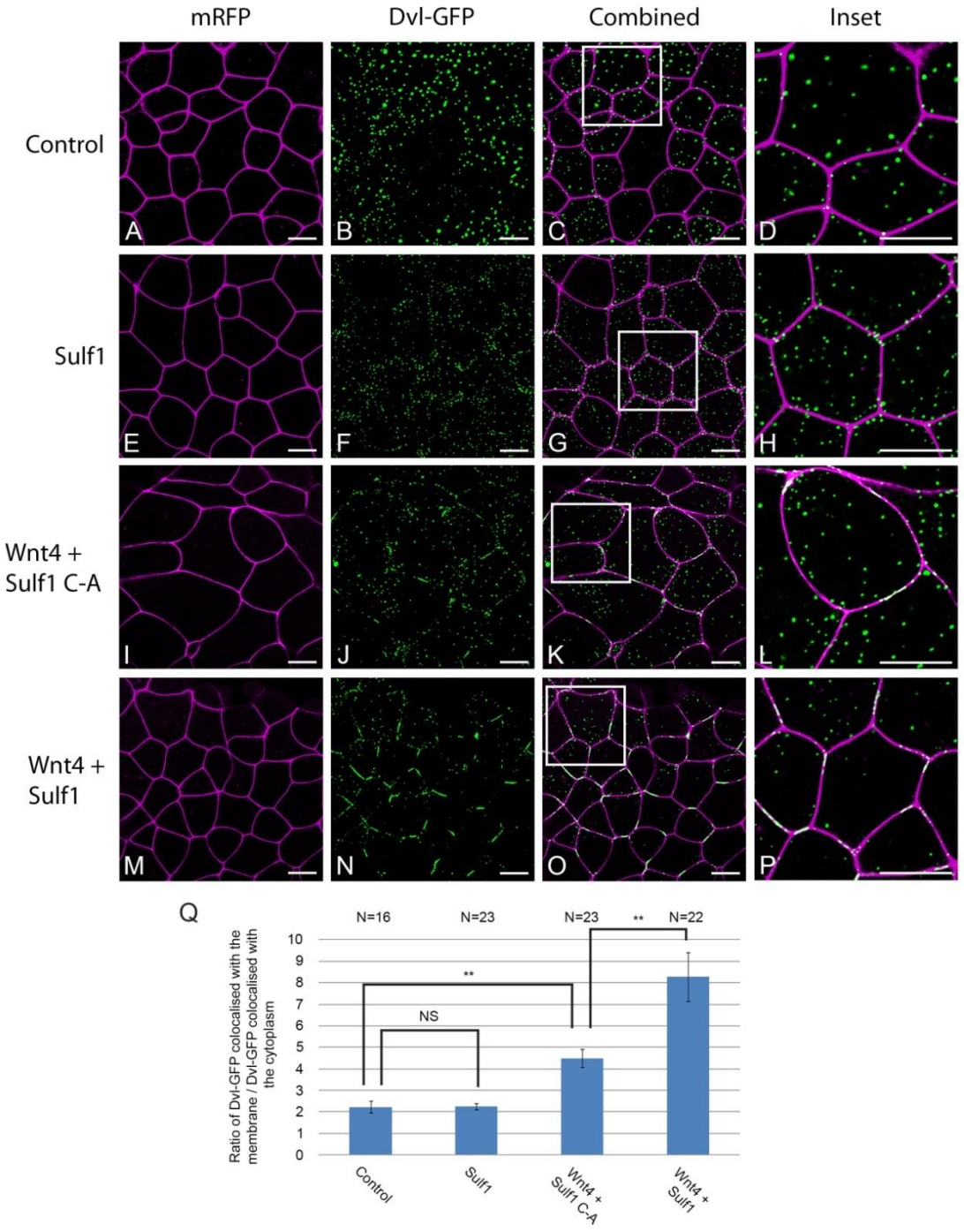

Figure 4.14; Sulf1 enhances Wnt4 induced Dvl-GFP translocation to the cell membrane. mRNA encoding *mRFP* (500pg) and *Dvl-GFP* (500pg) was injected bilaterally into the animal hemisphere of embryos at the two cell stage. In addition embryos were injected with mRNA encoding *Sulf1* (4ng), *Wnt4* (400pg) or both together. Embryos were cultured until NF stage 8 and then animal cap explants were taken and cultured for four hours at 21˚C prior to imaging by confocal microscopy. [A-D] Control animal caps over-expressing mRFP and Dvl-GFP. Animal caps over-expressing [E-H] Sulf1, [I-L] Sulf1 C-A and Wnt4 and [M-P] Sulf1 and Wnt4. The white boxes in [C], [G], [K] and [O] mark the areas used to create panels [D], [H], [L] and [P] respectively. Over-expression of Sulf1 C-A and Wnt4 induced the translocation of Dvl-GFP to the plasma membrane and this was enhanced by over-expressing Sulf1 with Wnt4. [Q] Graph quantifying the effects on Dvl-GFP translocation to the cell membrane. Asterisks mark significant differences (**P<0.01), NS marks non-significant differences, Mann-Whitney U, error bars represent s.e.m. mRFP (magenta), Dvl-GFP (green), scale bars represent 20µm, N = number of embryos.

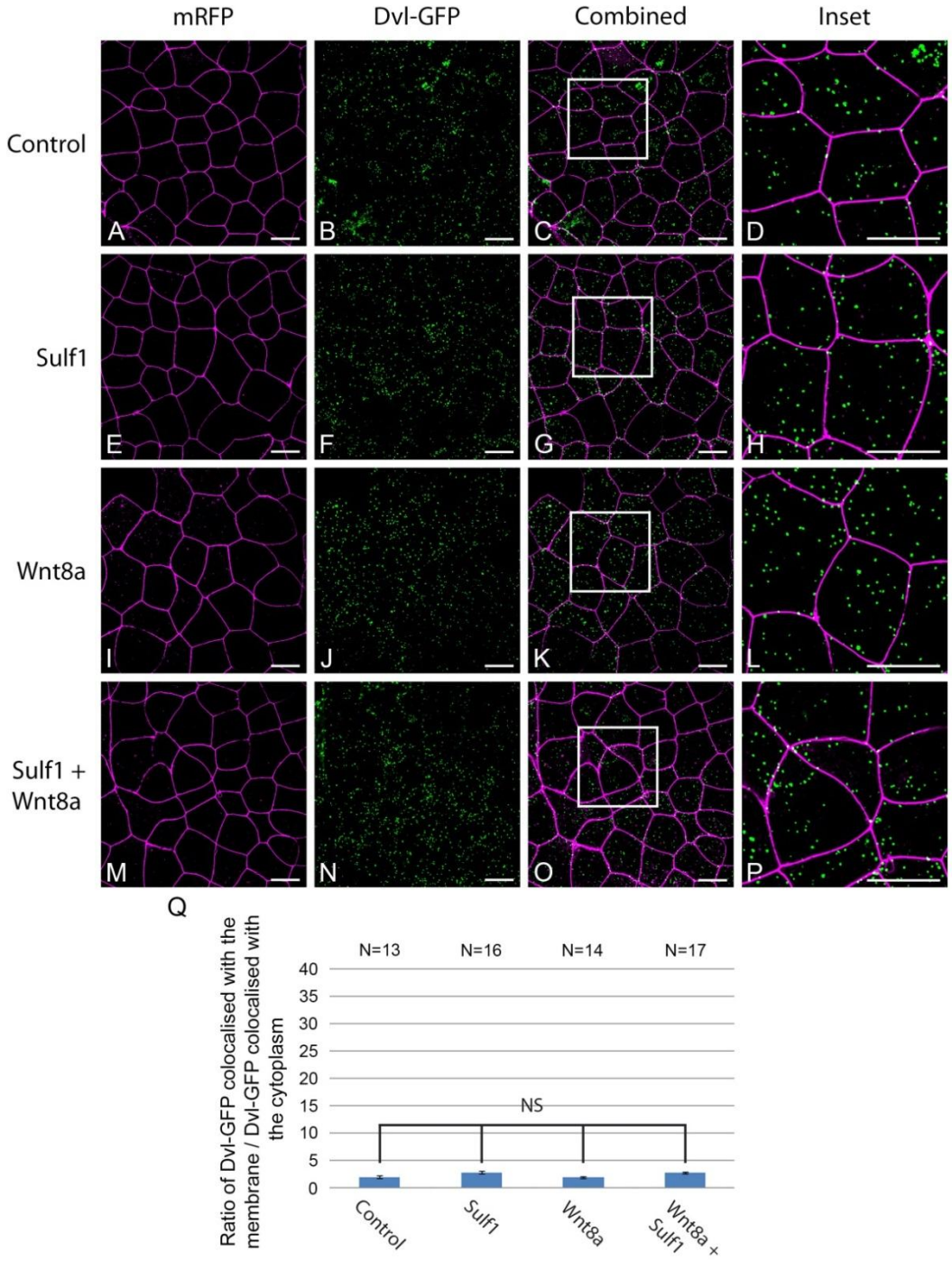

Figure 4.15; Sulf1 and Wnt8a do not induce Dvl-GFP translocation to the cell membrane. mRNA encoding *mRFP* (500pg) and *Dvl-GFP* (500pg) was injected bilaterally into the animal hemisphere of embryos at the two cell stage. In addition embryos were injected with mRNA encoding *Sulf1* (4ng), *Wnt8a* (20pg) or both together. Embryos were cultured until NF stage 8 and then animal caps were taken and cultured for four hours at 21˚C prior to imaging by confocal microscopy. [A-D] Control animal caps over-expressing mRFP and Dvl-GFP. Animal caps over-expressing [E-H] Sulf1, [I-L] Wnt8a or [M-P] Sulf1 and Wnt8a. The white boxes in [C], [G], [K] and [O] mark the areas used to create panels [D], [H], [L] and [P] respectively. Over-expression of Sulf1, Wnt8a or both together had no effect on Dvl-GFP localisation (compare [I-L] and [M-P] to [A-D]). [Q] Graph quantifying the effects on Dvl-GFP translocation to the cell membrane. NS marks non-significant differences, Mann-Whitney U, error bars represent s.e.m. mRFP (magenta), Dvl-GFP (green), scale bars represent 20μm, N = number of embryos.

Sulf1, Sulf1 C-A, Wnt4 or a mixture of the three. Embryos were cultured until NF stage 8 and then animal cap explants were taken. Animal caps were cultured in the dark for four hours at 21˚C prior to imaging by confocal microscopy. Over-expression of Sulf1 C-A and Wnt4 together resulted in Dvl-GFP trafficking to the cell membrane (compare Figure 4.14I-L to 4.14A-D). Over-expression of Sulf1 and Wnt4 together enhanced the translocation of Dvl-GFP to the cell membrane (compare Figure 4.14M-P to 4.14I-L). The data from Figure 4.14A-P is quantified in Figure 4.14Q. Sulf1 enhances the ability of Wnt4 to induce Dvl-GFP translocation to the cell membrane.

To investigate whether Sulf1 could alter the ability of Wnt8a to activate canonical Wnt signalling the localisation of Dvl-GFP was examined. Embryos were microinjected bilaterally in the animal hemisphere with mRNA encoding *mRFP* and *Dvl-GFP*. In addition embryos were microinjected with mRNA encoding *Sulf1, Sulf1 C-A, Wnt8a* or a mixture of the three. Embryos were cultured until NF stage 8 and then animal cap explants were taken. Animal caps were cultured in the dark for four hours at 21˚C prior to imaging by confocal microscopy. Over-expression of Wnt8a had no effect on the localisation of Dvl-GFP (compare Figure 4.15I-L to 4.15A-D). In addition over-expression of Sulf1 did not alter the effects of Wnt8a on Dvl-GFP localisation (compare Figure 4.15M-P to 4.15A-D). The data from Figure 4.15A-P is quantified in Figure 4.15Q. Together these data show that Sulf1 enhances the ability of Wnt4 and Wnt11b, but not Wnt8a, to activate non-canonical Wnt signalling.

4.2.6 Sulf1 enhances the ability of Wnt11b to activate an ATF2 reporter

The data in this chapter has shown that Sulf1 enhances the ability of Wnt4 and Wnt11b to activate non-canonical Wnt signalling. (Ohkawara and Niehrs, 2010) showed that a 33 base pair region of the CHOP promoter known as the C/EBP-ATF site could act as a reliable reporter of non-canonical Wnt signalling in *Xenopus*. The CHOP sites are similar to the consensus binding sequences for the CCAAT/enhancer-binding (C/EBP) and the activating transcription factor/cyclic AMP response element (ATF/CRE). The C/EBP-ATF site is

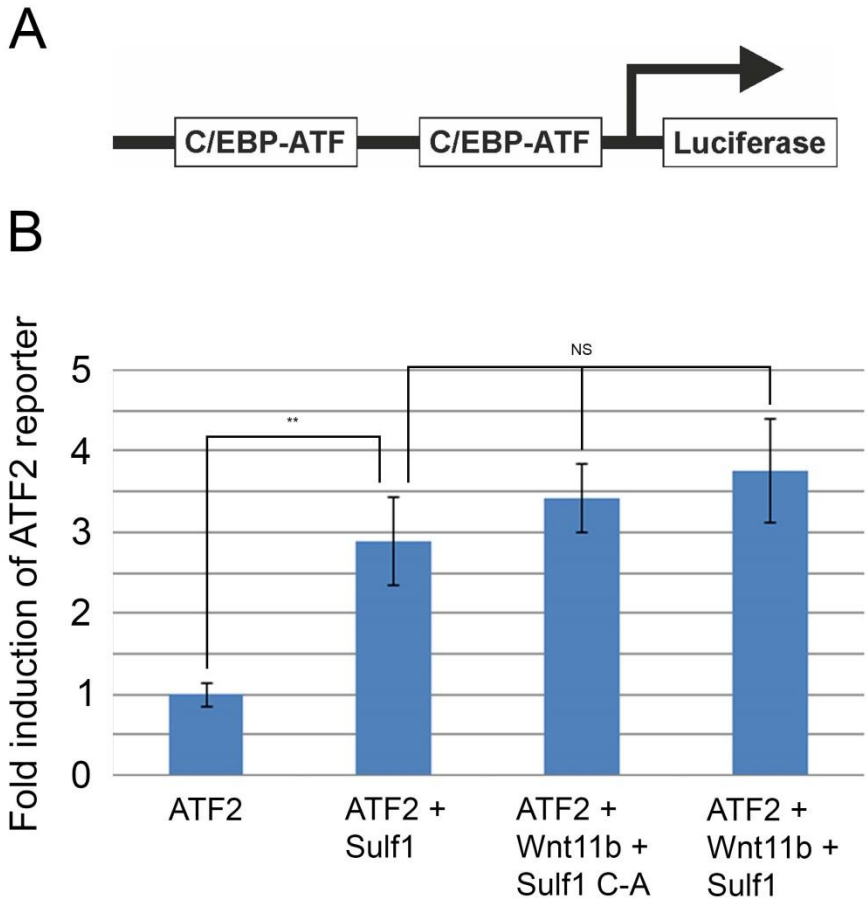

Figure 4.16; Sulf1 and Wnt11b do not synergise to activate the non-canonical Wnt signalling reporter ATF2.
[A] Diagram of the ATF2 reporter used for this assay (adapted from Van de Sanden, et al, 2004). [B] Plasmid DNA encoding the *ATF reporter construct* (100pg) was injected into the marginal zone of all four cells in a four cell stage embryo. In addition embryos were injected with mRNA encoding *Sulf1* (4ng), *Sulf1 C-A* (4ng), *Wnt11b* (200pg) or a mixture of the three. Graph illustrating the effects of Sulf1 and Wnt11b on the activation of the ATF reporter. The experiment was repeated eight times using a minimum of five embryos per condition. Asterisks mark significant differences (**P<0.01), NS marks non-significant differences, Mann-Whitney U, error bars represent s.e.m.

directly upstream of a thymidine kinase promoter that drives the expression of a leuciferase reporter (Bruhat, et al, 2000; Van der Sanden, et al 2004). A diagram of the reporter (ATF2) can be seen (Figure 4.16A). Previous work has shown that microinjection of *Wnt11* together with the ATF2 reporter resulted in a fourfold increase in luciferase activity (Ohkawara and Niehrs, 2010).

Plasmid DNA encoding the *ATF2 reporter construct* (100pg) was injected into the marginal zone of all four cells in a four cell stage *Xenopus* embryo. In addition embryos were injected with mRNA encoding *Sulf1* (4ng), *Sulf1 C-A*

(4ng), *Wnt11b* (200pg) or a mixture of the three. Over-expression of Sulf1 caused a two and a half fold up regulation of luciferase activity compared to control conditions. Over-expression of either Sulf1C-A and Wnt11b, or Sulf1 and Wnt11b failed to produce a significant increase in reporter activation compared to Sulf1 alone (Figure 4.16B). The experiment was repeated eight times using five embryos per condition. Sulf1 and Wnt11b did not synergise to enhance the activation of the ATF2 reporter.

4.3.0 Discussion

The aim of this chapter was to investigate the effects of Sulf1 on non-canonical Wnt signalling. One previous experiment has shown that Wnt7a is more effective at activating CamKII in *Sulf1/2* knockout myoblasts (Tran et al., 2012). In this experiment *Sulf1/2* knockout myoblasts were treated with Wnt7a, so that the role of Sulf1 in cells receiving Wnt7a was analysed. As with chapter 3, all of the experiments in chapter 4 looked at the effects of Sulf1 when Sulf1 and Wnt were expressed in the same cells. Sulf1 potentiated the ability of Wnt4 and Wnt11b to activate non-canonical Wnt signalling. In contrast Sulf1 did not alter the ability of Wnt8a to activate non-canonical Wnt signalling. Together the data suggests that Sulf1 potentiates the ability of non-canonical Wnt ligands to activate signalling, but has no effect on canonical Wnt ligand Wnt8a.

4.3.1 XtWnt11b2 and Wnt11b show different activities in *Xenopus laevis*

XtWnt11b2 was previously used to investigate the effects of Sulf1 on canonical Wnt signalling (Freeman et al., 2008). However, in the current analysis XtWnt11b2 was unable to inhibit activin induced convergent extension, or induce Dvl-GFP translocation in animal cap cells. In contrast, Wnt11b is a potent inhibitor of animal cap elongation and activator of Dvl-GFP translocation. Sulf1 enhances the ability of Wnt11b to induce ectopic *chordin* expression in *Xenopus* embryos (chapter 3, Figure 3.15). This is similar to the effects of XtWnt11b2 reported by (Freeman et al., 2008). The ability of Sulf1 to potentiate the canonical activity of XtWnt11b2 is much greater than that of Wnt11b. In contrast Wnt11b was able to synergise with Sulf1 to activate non-canonical Wnt signalling in this chapter. Sequence alignments show that XtWnt1b2 and Wnt11b are 97% identical (Figure 4.0B), which leaves the reason for the difference in signalling activities unclear. It is important to investigate the individual signalling activities of different Wnt ligands, regardless of the levels of homology between the protein sequences.

4.3.2 The Sulf1 C-A mutant retains some signalling activity

The Sulf1 C-A mutant has had the conserved cysteine residues at positions 86 and 87 converted to alanines, preventing formylglycine modification and inhibiting sulfatase activity (Schmidt et al., 1995; Selmer et al., 1996). Mutation of the conserved cysteine residues in *Quail* Sulf1 and *Human* Sulf1 blocks the ability of these mutants to remove the 6-O sulphate group from IdoA2S-GlcNS6S disaccharides (Ai et al., 2003; Frese et al., 2009). Unpublished data from the Pownall laboratory has shown that Sulf1 C-A is unable to catalyse the removal of 6-O sulphates from IdoA2-GlcNS6S relative to wildtype Sulf1. One conclusion from this, is that the Sulf1 C-A mutant is able to modulate cell signalling independent of its role as a sulfatase. (Dhoot et al., 2001) demonstrated that *Quail* Sulf1 C-A was unable to potentiate canonical Wnt signalling in C2C12 cells in response to Wnt1. However, *Quail* Sulf1 C-A did inhibit the induction of *brachyury* in response to FGF2 in *Xenopus* animal caps, indicating that the *Quail* Sulf1 C-A may have some biological activity (Wang et al., 2004). Sulf1 may have a catalytic independent role in regulating cell signalling.

The hydrophilic domain of Sulf1 is important for its activity. Deletion of the hydrophilic domain of Sulf1 results in the loss of Sulf1 from the surface of cells and inhibits it catalytic activity (Dhoot et al., 2001; Frese et al., 2009). The hydrophilic domain of Sulf1 is intact in the Sulf1 C-A mutant. One prediction from this is that Sulf1 C-A may act as a dominant negative construct associating with HS, but being unable to catalyse the removal of 6-O sulphate. Sulf1 C-A was able to inhibit dpERK induction in response to FGF4a and cause an increase in Wnt11b induced Dvl-GFP translocation to the cell membrane. This suggests that Sulf1 C-A functions as a hypomorphic, rather than a dominant negative mutant. Sulf1 C-A-GFP associates with the cell membrane in a similar manner to Sulf1-GFP in *Xenopus* animal caps (Pownall laboratory unpublished data). One conclusion from this is that Sulf1 may have a catalytically independent role in organising HSPGs or receptors into specific microdomains on the cell surface. To further characterise the activity of Sulf1, it will be

important to determine exactly what roles are played by each of its individual domains.

As far as I am aware, this is the first time a catalytically independent activity of Sulf1/2 has been described. This project was undertaken to investigate the effects of 6-O sulphate modification on Wnt signalling. Consequently the Sulf1 C-A mutant is an important control, as it controls for the catalytically independent activity of Sulf1. However, care must be taken when comparing the effects of Sulf1 to Sulf1 C-A. Knockout studies in *Mouse* have shown that Sulf1 is a modulator, rather than being absolutely required for cell signalling (Ai et al., 2007; Holst et al., 2007; Ratzka et al., 2008). It is possible that differences in Wnt signalling detected between wildtype and Sulf1 conditions may not be detected when comparing Sulf1 C-A and Sulf1 conditions.

4.3.3 Sulf1 potentiates the ability of Wnt11b to activate non-canonical Wnt signalling

Sulf1 synergises with Wnt11b to inhibit activin induced convergent extension and induce Dvl-GFP translocation to the cell membrane in *Xenopus* animal caps. This is consistent with data from chapter 3, which showed that Sulf1 and Wnt11b enhanced gastrulation defects when over-expressed together in whole embryos. The data indicates that Sulf1 potentiates non-canonical Wnt signalling in *Xenopus.* This is opposite to findings in (Tran et al., 2012), which showed that loss of Sulf1/2 potentiated Wnt7a activation of CamKII activity. It is possible that the effects of Sulf1 in *Xenopus* are not due to effects on the Wnt/Ca^{2+} pathway. In addition, based on chapter 3, it is likely that the effects of Sulf1 on Wnt signalling are ligand specific.

Sulf1 enhances the ability of Wnt11b to induce the formation of Fz7-Ror2 complexes in *Xenopus* (Pownall laboratory unpublished data). This provides a possible mechanism to explain the effects of Sulf1 on non-canonical Wnt signalling. Cthrc1 has previously been shown to enhance non-canonical Wnt signalling. Cthrc1 functions in the PCP pathway in mice and enhances the formation of Wnt3a/5a-Fz-Ror2 complexes (Yamamoto et al., 2008). One prediction from this, is that regulating the formation of Wnt-receptor complexes

may serve as a common mechanism for activating specific Wnt signalling pathways.

LRP6 may play a role in activating non-canonical Wnt signalling in *Xenopus*. Microinjection of a morpholino targeting *LRP6* into *Xenopus* embryos resulted in gastrulation defects. These defects were not accompanied by alterations in cell fate (Tahinci et al., 2007). Interestingly, these defects are similar to those of embryos microinjected with *Sulf1* (Freeman et al., 2008). Knockdown of *LRP6* in DMZ explants inhibited the medial/lateral elongation and protrusive activity of DMZ cells (Tahinci et al., 2007). In addition, knockdown of *LRP6* caused the translocation of Dvl-GFP from the cytoplasm to the cell membrane in *Xenopus* animal caps (Tahinci et al., 2007). Sulf1 enhances the formation of Wnt11b-LRP6 complexes in whole embryos (Freeman et al., 2008). One prediction from this, is that enhanced binding of Wnt11b to LRP6 may lead to the turnover of LRP6 protein in addition to activating the canonical Wnt pathway (chapter 3). This could be an alternative explanation for the ability of Sulf1 to enhance the Wnt11b induced Dvl-GFP translocation to the cell membrane.

4.3.4 Sulf1 potentiates the ability of Wnt4 to activate non-canonical Wnt signalling

Wnt4 was selected as a second non-canonical Wnt ligand to use in the Dvl-GFP assay. Dorsal over-expression of Wnt4 causes gastrulation defects in *Xenopus* embryos (Du et al., 1995). However, work by Lyons et al., (2004) has shown that Wnt4 can activate Topflash in the MDCK kidney cell line. Wnt4 was not able to induce axis duplication in *Xenopus* (Figure 4.13), suggesting that it is unable to activate canonical Wnt signalling in whole embryos. Wnt4 is vital for kidney tubulogenesis in vertebrates as *Wnt4* knockout mice die perinatally with small kidneys. Histological analysis of these kidneys revealed that the kidney mesenchyme fails to condense to form tubules (Stark et al., 1994). The reduction in kidney size and perinatal lethality is similar to the phenotypes seen in *Wnt11* knockout and Sulf1/2 double knockout mice (Holst et al., 2007; Majumdar et al., 2003). In mammals the adult kidney is known as the metanephros, reviewed by (Wessely and Tran, 2011). Co-culture of metanephric mesenchyme with NIH3T3 cells expressing *Wnt4* triggers

tubulogenesis. Treatment of isolated metanephric mesenchyme with chlorate blocks the ability of Wnt4 to induce tubulogenesis (Kispert et al., 1998), indicating the importance of HSPGs for Wnt4 induced kidney tubulogenesis during development.

The pronephros is the earliest form of the embryonic kidney, which is present in all vertebrates, reviewed by (Wessely and Tran, 2011). Microinjection of a morpholino targeting Wnt4 specifically inhibits pronephros tubulogenesis in *Xenopus,* without affecting pronephros induction or pronephric duct formation (Saulnier et al., 2002). In *Xenopus, Sulf1* is expressed in the early pronephric kidney (Freeman et al., 2008). As Sulf1 potentiates the ability of Wnt4 to activate non-canonical Wnt signalling in *Xenopus,* it is possible that Sulf1 promotes Wnt4 signalling during kidney tubulogenesis.

4.3.5 Sulf1 does not alter the ability of Wnt8a to activate non-canonical Wnt signalling

Sulf1 does not alter the ability of Wnt8a to activate non-canonical Wnt signalling in convergent extension and Dvl-GFP translocation assays. This is not what would have been predicted based on the effects of Sulf1 and Wnt8a on gastrulation in whole embryos (chapter 3). Previous work has shown that components of the canonical Wnt pathway are unable to alter non-canonical Wnt signalling. Over-expression of β-catenin does not inhibit convergent extension in *Xenopus* animal caps. In addition, Wnt8a is unable to induce Dvl-GFP translocation to the cell membrane when over-expressed in animal caps (Tahinci et al., 2007). Sulf1 inhibits Wnt8a activation of canonical and has no effect on the activation of non-canonical Wnt signalling.

4.3.6 The effects of Sulf1 on non-canonical Wnt signalling are not due to alterations in FGF signalling

Over-expression of DN*FGFr1 inhibits activin induced mesoderm induction and convergent extension in *Xenopus* animal caps (Cornell and Kimelman, 1994). In addition, FGF signalling is required for the polarised accumulation of Dvl-GFP and PKCδ-YFP in DMZ explants (Shi et al., 2009). Sulf1 inhibits FGF signalling

in *Xenopus* and cell culture (Freeman et al., 2008; Lamanna et al., 2008; Wang et al., 2004) and therefore it is not surprising that Sulf1 inhibits convergent extension in animal caps, as this requires FGF signalling. Sulf1 potentiates the ability of Wnt4 and Wnt11b to induce Dvl-GFP translocation to the cell membrane. One prediction from this is that Sulf1 can inhibit convergent extension in animal cap explants by altering non-canonical Wnt signalling, independent of any effects on FGF signalling.

This chapter has been concerned with investigating the effects of Sulf1 on non-canonical Wnt signalling. Sulf1 potentiates the ability of Wnt4 and Wnt11 to activate non-canonical Wnt signalling. In addition, Sulf1 does not alter the ability of Wnt8a to activate non-canonical Wnt signalling. The thesis thus far has focused on establishing the effects of Sulf1 on the activation of canonical and non-canonical Wnt signalling in *Xenopus.* Chapter 5 will address possible mechanisms by how these may occur.

5.0 The effects of Sulf1 on Wnt8a and Wnt11b diffusion

5.1 Introduction

5.1.1 HSPGs shape morphogen gradients

Wg is expressed at the dorsal/ventral boundary of the wing disc and Wg protein diffuses away from the boundary forming a morphogen gradient (Cadigan et al., 1998). The Wg morphogen gradient activates distinct genes in different regions of the wing disc, depending on its local concentration. *Senseless* and *hindsight* are activated close to the source of Wg, either side of the dorsal ventral boundary, while *distaless* is activated more broadly across the wing disc (Neumann and Cohen, 1997; Nolo et al., 2000; Phillips and Whittle, 1993; Zecca et al., 1996). A diagram of Wg signalling in the *Drosophila* wing disc is shown (Figure 5.0A-B). Mutations in genes required for HSPG biosynthesis disrupt the formation of morphogen gradients in *Drosophila*. *LOF* mutations in the enzymes required for HS polymerisation, *Ttv, botv* or *sotv,* cause a reduction in the levels of Hh, Wg and Dpp in the *Drosophila* wing disc (Bellaiche et al., 1998; Bornemann et al., 2004; Han et al., 2004; Takei et al., 2004). In addition LOF mutations in the nucleotide-sugar transporter *fringe connection* or the gene *sulfateless* result in a loss of Wg protein in *Drosophila* (Baeg et al., 2001; Selva et al., 2001).

Ttv, botv and sotv are differentially required for Wg signalling in *Drosophila*. LOF mutations in either *ttv* or *sotv* reduce the activation of the long range Wg target *distaless* at a distance, but not near to the source of Wg. In contrast LOF mutations in *botv* leads to a reduction in *distaless* expression both near to and at a distance from the source of Wg (Han et al., 2004; Takei et al., 2004). *Senseless* expression is unaffected in *ttv* and *sotv* mutants, but reduced in *Drosophila* with LOF mutations in *botv* (Han et al., 2004). Mutations in *ttv* or *sotv* affect the range of Wg signalling, whereas mutations in *botv* affect both the range and activity of Wg. *botv* encodes the HS polymerase required to initiate HS chain polymerisation, in contrast *ttv* and *sotv* encode the *Drosophila* homologues of EXT1 and 2 respectively (Bellaiche et al., 1998; Bornemann et al., 2004; Han et al., 2004). In vertebrates both EXT1 and EXT2 can catalyse

the addition of HS individually, whereas EXTL2 (the homologue of botv) is required for the initiation of polymerisation (Kim et al., 2001; Lind et al., 1998; McCormick et al., 1998, 2000; Senay et al., 2000). This may explain the different effects of botv, ttv and sotv on Wg signalling in *Drosophila.* Mutations in genes required for HSPG biosynthesis affect the levels of Wg protein and the shape of the Wg morphogen gradient in *Drosophila*.

The Drosophila glypicans dally and dlp regulate the Wg morphogen gradient during wing disc development. Over-expression dlp expands the range of *distaless* expression, but inhibits *senseless* expression in *Drosophila*. LOF mutations in *dlp* causes a decrease in the range of *distaless* expression without altering *sensless* expression (Franch-Marro et al., 2005; Yan et al., 2009). In contrast, LOF mutations in *Dally* causes a loss of expression of the high threshold Wg target gene *Hindsight* (Han et al., 2005; Phillips and Whittle, 1993). Dally is required for the activation of short range Wg target genes, whereas Dlp activates the expression of long range Wg target genes at the expense of short range targets. LOF mutations in *dally* cause a reduction in the levels of Wg protein diffusing away from the dorsal/ventral boundary. Over-expression of dally leads to an increase in Wg protein at the dorsal/ventral boundary, but does not alter the overall shape of the Wg morphogen gradient (Han et al., 2005). In contrast LOF mutations in *dlp* result in a decrease in extracellular Wg, but only at a distance from the dorsal/ventral boundary (Han et al., 2005). Over-expression of Dlp increases the levels of extracellular wingless in cells away from the dorsal/ventral boundary (Baeg et al., 2001; Franch-Marro et al., 2005; Han et al., 2005). The effect of this is to expand the range, but reduce the steepness of the Wg gradient. A diagram illustrating the location of dally/dlp in the developing wing disc can be seen (Figure 5.0C-D).

Two models have been produced to describe the biphasic action of dlp on Wg signalling. The first involves the secreted α/β-hydroxylase notum. Notum is expressed along the dorsal/ventral boundary of the wing disc, Giráldez et al., (2002) in a similar pattern to Wg (Zecca et al., 1996). Notum cleaves the GPI anchor domain of dlp allowing it to be secreted from the cell surface (Kreuger et al., 2004). GOF mutations in *notum* inhibit Wg signalling in *Drosophila*; in contrast LOF mutations in Notum cause an increase in the levels of extracellular

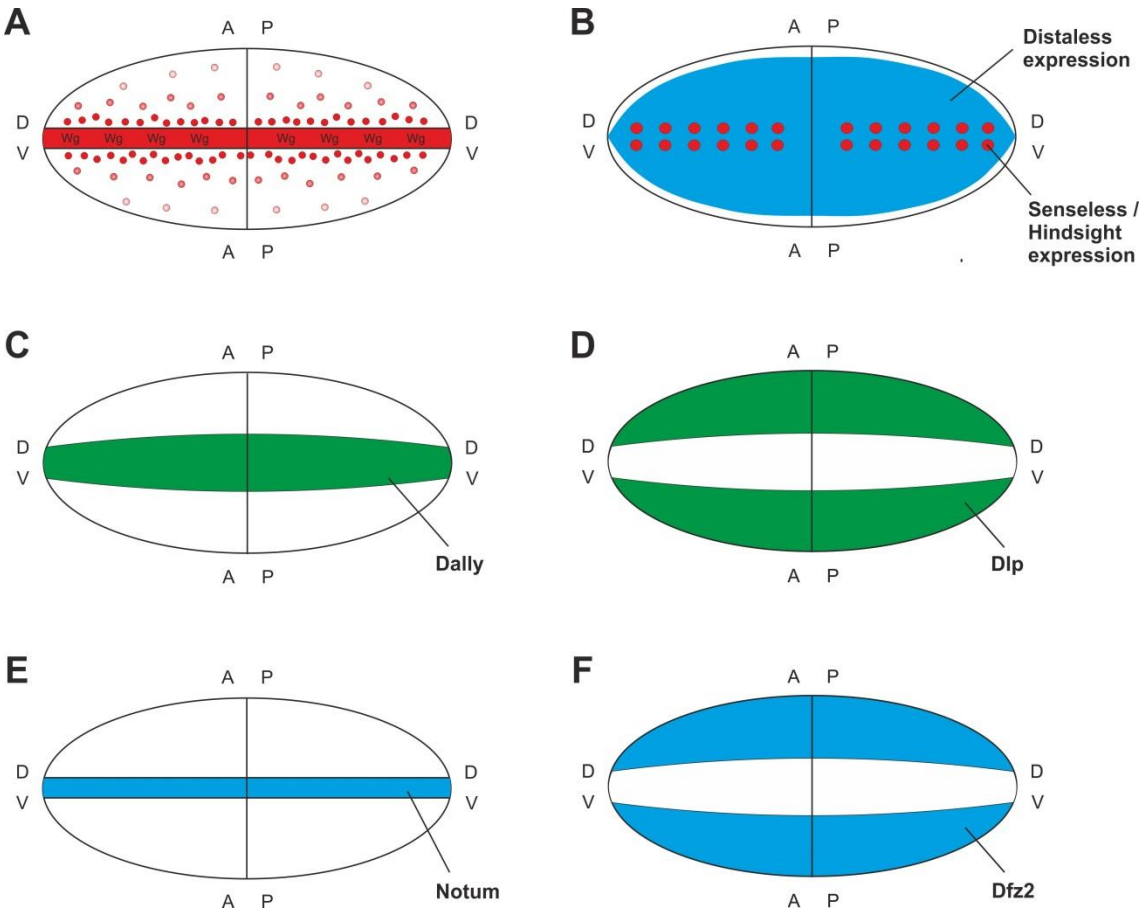

Figure 5.0; The *Drosophila* wing disc.
Figure illustrating the expression patterns of various genes during wing disc development. [A] *Wg* is expressed along the dorsal/ventral boundary of the wing disc and Wg protein diffuses away from this region forming a morphogen gradient (Cadigan et al., 1998; Zecca et al., 1996). [B] High levels of Wg induce the expression of proneural genes in a region adjacent to the dorsal/ventral boundary. This region goes on to form the sensory organ precursors, which express genes including senseless and *hindsight*. Lower concentrations of Wg induce distaless expression (Giráldez et al., 2002; Nolo et al., 2000; Phillips and Whittle, 1993; Zecca et al., 1996). [C-D] The expression patterns of dally and dlp during wing disc development (Han et al., 2005). [E-F] The expression patterns of notum (Giráldez et al., 2002) and DFz2 (Cadigan et al., 1998) during wing disc development. A (anterior), P (posterior), D (dorsal) and V (ventral).

Wg and *hindsight* expression (Giráldez et al., 2002). Dlp is absent from cells at the dorsal/ventral boundary, but is present throughout the rest of the wing disc (Han et al., 2005). Notum and dlp synergise to inhibit Wg signalling at the dorsal/ventral boundary of the wing disc, when over-expressed together (Kreuger et al., 2004). Over-expression of notum inhibits the accumulation of Wg in response to over-expressing dlp in the *Drosophila* wing disc (Giráldez et al., 2002). In this model Wg binds to dlp, which is then shed from the surface of the wing disc by the actions of notum. This prevents the accumulation of Wg protein at the dorsal/ventral boundary, broadening the Wg morphogen gradient. The ability of a secreted form of dlp to enhance long range Wg signalling would

be similar to the effects of Swim in *Drosophila,* Mulligan et al., (2012) and Sfrp1/2 in *Mouse* (Esteve et al., 2011). A diagram illustrating the location of notum can be seen (Figure 5.0E).

The second model developed to explain the effects of dlp on Wg signalling, examined the role of Dfz2 in the wing disc. *DFz2* expression is repressed by Wg signalling and shows a similar expression pattern to that of dlp (Figure 5.0F) (Cadigan et al., 1998). DFz2 and dlp synergise to induce *senseless* expression when over-expressed together in the *Drosophila* wing disc. In S2 cells a 1:1 or 2:1 ratio of dlp to Dfz2 enhances the binding of DFz2 to Wg. However increasing the ratio of dlp:DFz2 inhibits the binding of Wg to DFz2 (Yan et al., 2009). High ratios of dlp to DFz2 represses Wg signalling, however as the distance from the dorsal/ventral boundary and the concentration of DFz2 increase dlp enhances Dfz2-Wg binding. The role of dlp in activating/repressing Wg signalling depends on the levels of dlp and DFz2. In contrast to the first model, the study by, Yan et al., (2009) indicated that the biphasic activity of dlp was independent of the GPI anchor domain and so did not require notum.

5.1.2 Wnt/Wg ligands are not freely diffusible

The addition of palmitate and palmitoleic acid to Wnt/Wg ligands makes these ligands highly hydrophobic and not freely diffusible (Franch-Marro et al., 2008; Takada et al., 2006; Willert et al., 2003). However Wnt/Wg ligands are morphogens and involved in long range signalling during development. One prediction from this is that the diffusion of Wnt/Wg must be facilitated. Several different mechanisms have been proposed to explain the facilitation of Wg/Wnt diffusion *in vivo*. Greco et al., (2001) identified the secretion of exo-vesicles from cells in the *Drosophila* wing disc. These exo-vesicles (known as argosomes) were produced throughout the imaginal disc and could be observed diffusing intracellulalry through adjacent cells. Argosomes diffused rapidly away from cells secreting them and stained positively for Wg. This lead to the suggestion that these exo-vesicular structures were facilitating the diffusion of Wg in the wing disc (Greco et al., 2001). Active Wnt ligands have been found associated with exosomes in cell culture. Wnt3a fractionates together with exosomes in HEK293 cells and L cells. In addition the Wnt3a-exosome fraction

is able to activate canonical Wnt signalling. Interestingly, shRNA mediated knockdown of *Evi* disrupts the fractionation of Wnt3a with exosomes (Gross et al., 2012). In the *Drosophila* wing disc both Wg and Evi are found colocalised with secreted exosomes (Gross et al., 2012). Evi may be required to load Wnt/Wg onto exosomes for extracellular diffusion.

Panáková et al., (2005) found that Wg cofractionated together with apolipophorin II in *Drosophila* larva and Wg coloclaised with liphophorin in the wing imaginal disc. Wg was not found to colocalise with exosomes in *Drosophila* larva. RNAi mediated depletion of liphophorin inhibited Wg diffusion and reduced *distaless* expression in the wing disc (Panáková et al., 2005). This suggests that the long range diffusion of Wg requires lipophorin particles, but not exosomes. In addition, Neumann et al., (2009) demonstrated that active Wnt3a was secreted from L cells on high density lipoproteins. Wnt3a failed to cofractionate with exosomes in this study.

The reggie/flotillin proteins are present in almost every cell type in both vertebrates and invertebrates. They localise to the cytoplasmic portion of the plasma membrane and associate with lipid rafts (Stuermer et al., 2001). Reggie1/flotillin2 regulate Wg signalling in the *Drosophila* wing disc. Over-expression of reggie1 enhances the secretion and increases the range of Wg diffusion, inhibiting of *senseless* expression (Katanaev et al., 2008). In contrast LOF mutations in *reggie1* inhibit Wg secretion, shortening the Wg morphogen gradient and reducing the range of *distaless* expression. Reggie1 was also able to regulate the secretion and range of diffusion of Hh in the wing disc (Katanaev et al., 2008). Reggie/flotillin potentiate the secretion of Wg and Hh, enhancing the range of ligand diffusion to facilitate long range patterning in the embryo.

5.1.3 Secreted inhibitors of Wnt/Wg signalling are important for the formation of long range morphogen gradients

Members of the Sfrp family are important for regulating Wnt/Wg signalling. Members of the Sfrp family were originally identified as secreted proteins that

were able to bind and antagonise Wnt signalling, reviewed by (Kawano and Kypta, 2003). However Sfrp's have a more complex role in regulating Wnt signalling *in vivo.* Wg and Sfrp1 are both able to bind heparan sulphate (Reichsman et al., 1996; Uren et al., 2000). In addition, recombinant heparin stimulates the binding of Wg to Sfrp1 *in vitro*. Wg induces the stabilisation of armadillo in *Drosophila* S2 cells transfected with *DFz2* and treatment of these cells with small doses of recombinant Sfrp1 enhances the ability of Wg to stabilise armadillo (Reichsman et al., 1996). In *Mouse* embryos, Sfrp1/2 are required to maintain long range Wnt diffusion in order to pattern the optic cup. Knockout of *Sfrp1/2* leads to patterning defects in the dorsal optic cup, resulting in a reduction in the size of the eyes (Esteve et al., 2011). In *Xenopus,* Sfrp3 enhances the distance from the organiser that nuclear β-catenin can be detected during gastrulation (Mii and Taira, 2009).

In *Drosophila,* the secreted protein Swim inhibits the activation of high threshold Wg target genes, but enhances the range of Wg diffusion. Over-expression of Swim enhances the size of the *distaless* domain, but inhibits *senseless* expression. RNAi mediated knockdown of *Swim* reduced the range of *distaless* expression, but had no effect on *senseless* (Mulligan et al., 2012). Swim and the Sfrp's show a similar activity towards Wnt/Wg signalling as dlp in Drosophila (Yan et al., 2009). Secreted inhibitors of Wnt/Wg signalling extend the range of the Wnt/Wg morphogen gradient, reducing the concentration of Wnt/Wg close to the source.

5.1.4 Sulf1 regulates the diffusion of Wg in *Drosophila*

In *Drosophila, Sulf1* is expressed either side of the dorsal/ventral and anterior/posterior boundaries (Figure 5.1) (Kleinschmit et al., 2010). This positions it immediately outside of the region expressing *Wg* (Figure 5.0A) (Cadigan et al., 1998; Zecca et al., 1996). Over-expression of Sulf1 inhibits *senseless* expression in the wing disc (Kleinschmit et al., 2010). Analysis of Wg distribution reveals that over-expression of Sulf1 causes a reduction in the levels of extracellular Wg (Kleinschmit et al., 2010; You et al., 2011). In addition, LOF mutations in *Sulf1* increase the levels of extracellular Wg and enhance *senseless* and *distaless* expression in the *Drosophila* wing disc

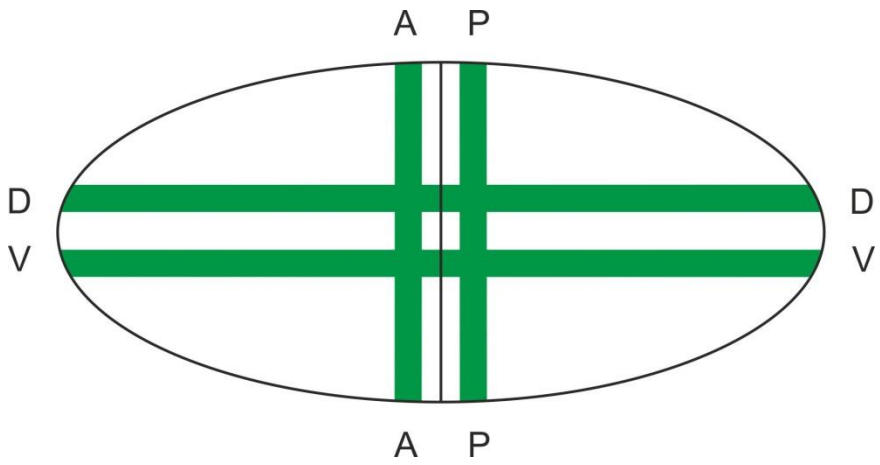

Figure 5.1; The expression pattern of *Sulf1* in the *Drosophila* wing disc.
Diagram illustrating the expression pattern of Sulf1 in *Drosophila*. *Sulf1* is expressed either side of the *Wg* expression domain at the dorsal/ventral boundary. Sulf1 expression in green, figure adapted from (Kleinschmit et al., 2010).

(Kleinschmit et al., 2010). Over-expression of dally leads to the accumulation of Wg in a band around the dorsal/ventral boundary in the wing disc. In contrast, over-expression of dlp leads to the accumulation of lower levels of Wg throughout the *Drosophila* wing disc. Over-expression of Sulf1 together with either dally or dlp blocks the accumulation of Wg protein (Kleinschmit et al., 2010). The 6-O sulphate group of dally and dlp is required for the stabilisation of Wg on the surface of the *Drosophila* wing disc. Sulf1 inhibits the diffusion of Wg in *Drosophila* regulating the formation of the Wg morphogen gradient

5.1.5 Aims of this chapter

So far, this thesis has shown that Sulf1 can differentially regulate the abilities of Wnt3a, Wnt8a and Wnt11b to activate canonical Wnt signalling. In addition, Sulf1 enhances the abilities of Wnt4 and Wnt11b to activate non-canonical Wnt signalling. These effects cannot be explained simply by the 'catch and present' model (Ai et al., 2003). Sulf1 regulates the diffusion of Wg, Kleinschmit et al., (2010); You et al., (2011) and the localisation of Hh protein, Wojcinski et al., (2011) during *Drosophila* development. In addition, Sulf1 regulates the diffusion of Shh in *Xenopus* embryos (Pownall laboratory unpublished data). The aim of this chapter is to determine a mechanism for the effects of Sulf1 on Wnt signalling. This focuses on analysing the diffusion of fluorescently tagged Wnt ligands in *Xenopus* animal cap explants. The ability of Sulf1 to modulate Wnt

ligand diffusion provides an explanation for the effects of Sulf1 on canonical and non-canonical Wnt signalling.

Fluorescently tagged *Xenopus tropicalis Wnt4* and *Xenopus laevis Wnt8a* and *Wnt11b* were constructed and shown to be biologically active. Following this, the behaviour of the three ligands was analysed in the presence or absence of *Xenopus tropicalis* Sulf1. Sulf1 enhanced the stability of Wnt4/Wnt11b-HA-GFP on the cell membrane. Sulf1 increased the range of diffusion of Wnt8a in animal caps reducing the overall concentration of the ligand. In contrast Sulf1 enhanced both the levels and the diffusion of Wnt11b-HA-GFP in animal cap explants. These results go some way to explaining how Sulf1 potentiates the ability of Wnt11b to activate both canonical and non-canonical Wnt signalling. Sulf1 has specific roles in regulating the formation of Wnt morphogen gradients in *Xenopus.* These findings are important for understanding the role of Sulf1 during development and in disease.

5.2 Results

5.2.1 Wnt11b inhibits Wnt8a activation of canonical Wnt signalling

Sulf1 inhibits the ability of Wnt8a to activate canonical Wnt signalling, but potentiates the ability of Wnt11b to activate both canonical and non-canonical Wnt signalling (see chapters 3 and 4). One possible explanation for this, is that the inhibitory effects of Sulf1 on Wnt8a could be due to the activation of non-canonical Wnt signalling. To investigate this embryos were microinjected with mRNA encoding *Wnt8a, Wnt11b* and *GFP* into one ventral blastomere at the four cell stage. Embryos were cultured until NF stage 36/37 and analysed for axis duplication. Over-expression of Wnt8a alone or together with GFP induced the formation of a secondary axis in more than 90% of embryos (Figure 5.2B and 5.2C). Over-expression of Wnt11b inhibited the ability of Wnt8a to induce a secondary axis (compare Figure 5.2D to 5.2B and 5.2C). The data from Figure 5.2A-D is quantified in Figure 5.2E. Wnt11b inhibits the ability of Wnt8a to activate canonical Wnt signalling. This is consistent with the findings of Torres et al., (1996), which showed that Wnt4, Wnt5a and Wnt11b were all able to supress Wnt8a induced axis duplication. The non-canonical ligands Wnt4, Wnt5a and Wnt11b are able to inhibit the ability of Wnt1 and Wnt8a to activate canonical Wnt signalling in the early *Xenopus* embryo.

The data in Figure 5.2 was described previously Torres et al., (1996), however the ability of canonical Wnt ligands to inhibit non-canonical Wnt signalling has not been described. To examine whether Wnt8a inhibits Wnt11b signalling, activin induced convergent extension and Dvl-GFP localisation assays were analysed. Embryos were microinjected bilaterally in the animal hemisphere with mRNA encoding *Wnt11b* and *Wnt8a.* Embryos were cultured until NF stage 8 and then animal cap explants were taken. Animal caps were cultured in either the presence or absence of activin until NF stage 19. Over-expression of Wnt11b inhibited activin induced convergent extension in animal caps (Figure 5.3C). Microinjection of either 20pg or 400pg of *Wnt8a* mRNA had no effect on

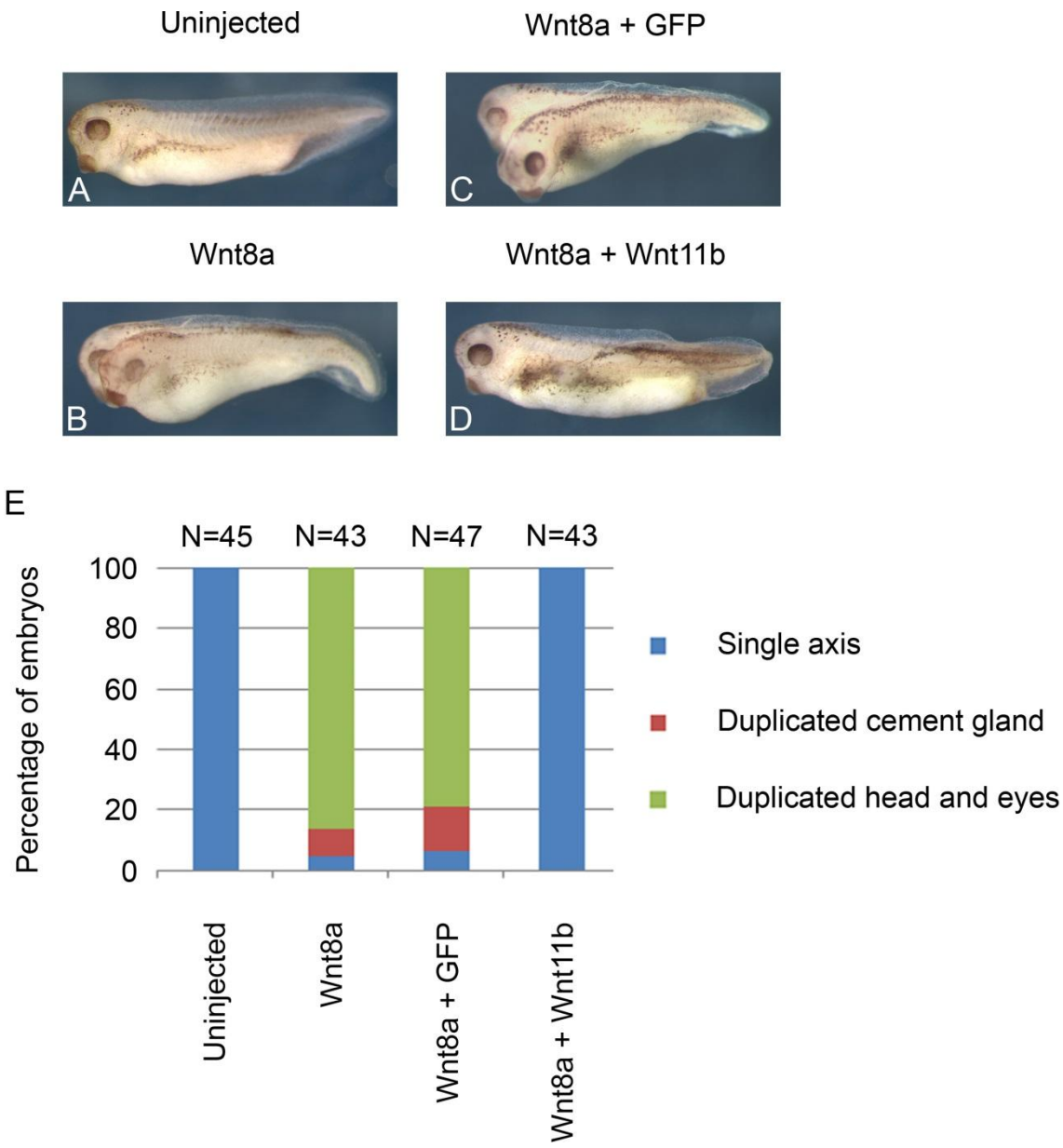

Figure 5.2; Wnt11b inhibits the axis inducing ability of Wnt8a.
mRNA encoding *Wnt11b* (100pg), *Wnt8a* (5pg), *GFP* (100pg) or a mixture of the three was injected into the VMZ of one cell of an embryo at the four cell stage. Embryos were cultured until NF stage 36/37 and then examined for phenotype. [A] Lateral view of an uninjected embryo. [B-D] Lateral view of embryos injected with [B] *Wnt8a*, [C] *Wnt8a* and *GFP* and [D] *Wnt8a* and *Wnt11b*. Over-expression of Wnt8a induced the formation of a secondary axis, but this was inhibited by Wnt11b. [E] Graph quantifying the frequency of axis duplication in embryos injected with *Wnt8a, Wnt11b and GFP*, N = number of embryos.

the ability of *Wnt11b* to inhibit convergent extension (compare Figures 5.3D and 5.3E to 5.3C). The data from Figure 5.3A-E is quantified in Figure 5.3F. Wnt8a did not reduce the ability of Wnt11b to inhibit convergent extension in animal cap explants. To investigate whether Wnt8a inhibited Wnt11b induced Dvl-GFP translocation, embryos were microinjected bilaterally in the animal hemisphere

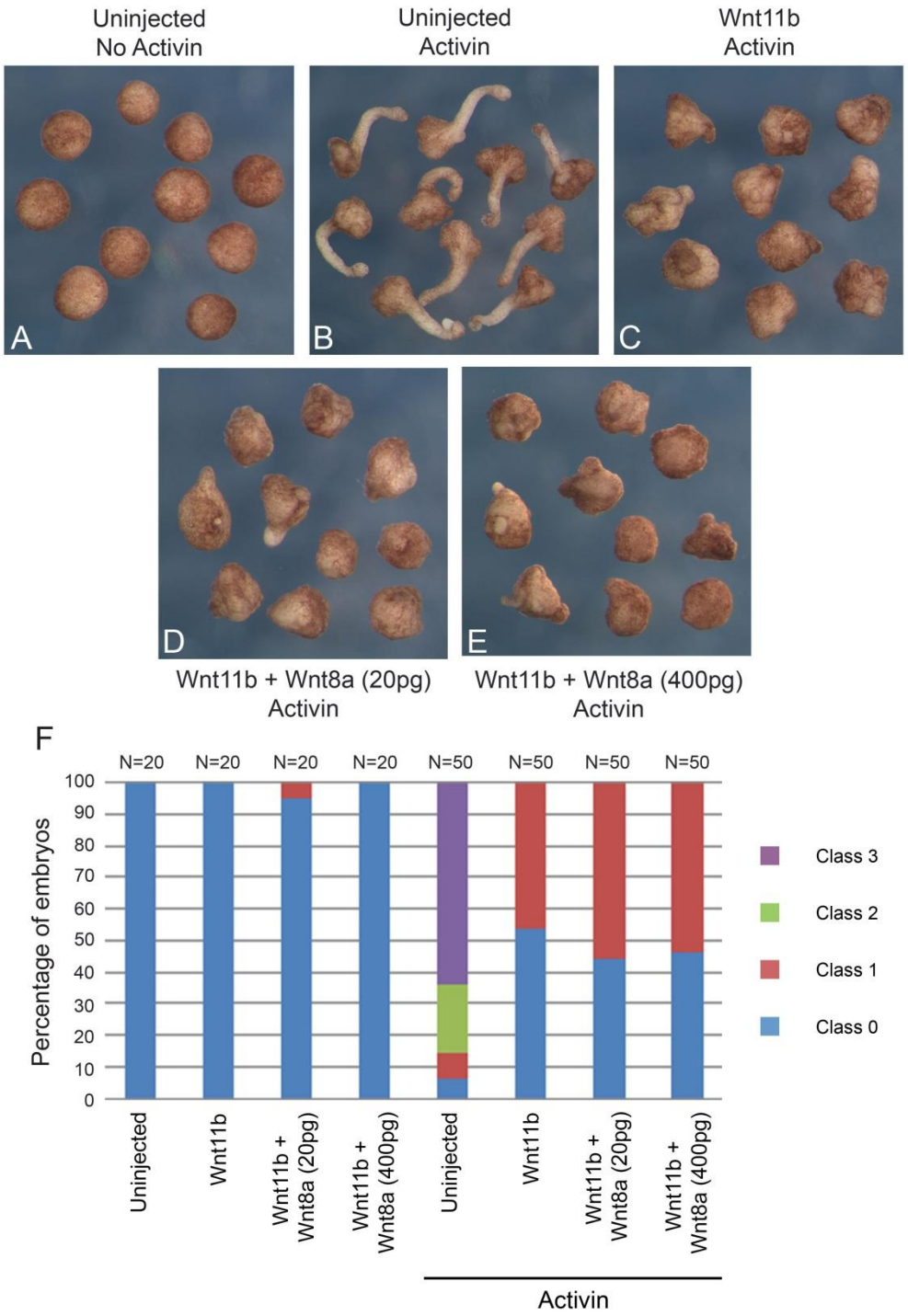

Figure 5.3; Wnt8a does not block the ability of Wnt11b to inhibit activin induced convergent extension.
mRNA encoding *Wnt11b* (250pg), *Wnt8a* (20pg or 400pg) or both was injected bilaterally into the animal hemisphere of embryos at the two cell stage. Embryos were cultured until NF stage 8 and then animal cap explants were taken. Animal caps were cultured in either the presence or absence of activin until NF stage 19. [A-B] Uninjected animal caps cultured in either the absence [A] or presence [B] of activin. [C-E] Embryos injected with [C] *Wnt11b*, [D] *Wnt11b* and *Wnt8a* (20pg) or [E] *Wnt11b* and *Wnt8a* (400pg) and cultured in the presence of activin. Over-expression of Wnt11b inhibited activin induced convergent extension. Wnt8a does not block the ability of Wnt11b to inhibit activin induced convergent extension. [F] Graph quantifying the level of convergent extension in each condition, N = number of embryos.

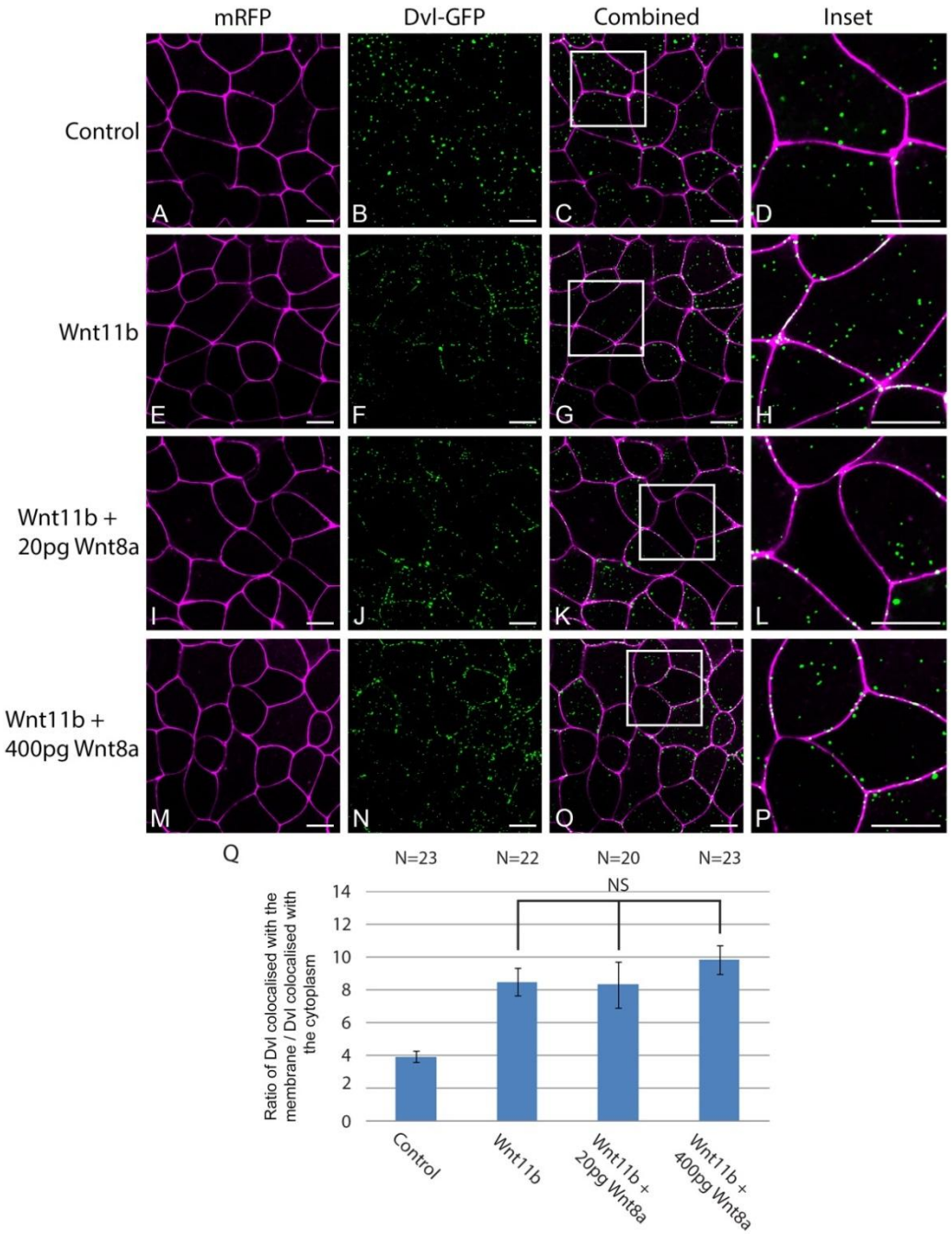

Figure 5.4; Wnt8a does not inhibit Wnt11b induced Dvl-GFP translocation to the cell membrane.
mRNA encoding *mRFP* (500pg) and *Dvl-GFP* (500pg) was injected bilaterally into the animal hemisphere of embryos at the two cell stage. In addition embryos were injected with mRNA encoding *Wnt11b* (400pg), *Wnt8a* (20pg or 400pg) or both together. Embryos were cultured until NF stage 8 and then animal cap explants were taken and cultured for four hours at 21˚C prior to imaging by confocal microscopy. [A-D] Control animal caps over-expressing mRFP and Dvl-GFP. Animal caps over-expressing [E-H] Wnt11b, [I-L] Wnt11b and Wnt8a (20pg) and [M-P] Wnt11b and Wnt8a (400pg). The white boxes in [C], [G], [K] and [O] mark the areas used to create panels [D], [H], [L] and [P] respectively. Over-expression of Wnt11b induced the translocation of Dvl-GFP to the cell membrane and this was not affected by the over-expression of Wnt8a. [Q] Graph quantifying the effects on Dvl-GFP translocation to the cell membrane. Data obtained using a programme written in Matlab, see methods 2.5.2 for details. NS marks non-significant differences, Mann-Whitney U, error bars represent s.e.m. mRFP (magenta), Dvl-GFP (green), scale bars represent 20um, N = number of embryos.

with mRNA encoding *mRFP* and *Dvl-GFP*. In addition embryos were microinjected with mRNA encoding *Wnt8a, Wnt11b* or a mixture of the two. Embryos were cultured until NF stage 8 and then animal cap explants were taken. Animal caps were cultured in the dark for four hours at 21˚C prior to imaging by confocal microscopy. Over-expression of Wnt11b induced the translocation of Dvl-GFP to the plasma membrane (Figure 5.4E-H). Microinjection of 20pg or 400pg of *Wnt8a* mRNA together with *Wnt11b* did not inhibit the ability of Wnt11b to activate Dvl-GFP translocation (compare Figures 5.4I-L and 5.4M-P to 5.4E-H). The data from Figure 5.4A-P is quantified in Figure 5.4Q. Wnt8a did not inhibit the ability of Wnt11b to induce Dvl-GFP translocation to the cell membrane.

Wnt11b inhibits the ability of Wnt8a to activate canonical Wnt signalling. In contrast Wnt8a has no effect on Wnt11b induced non-canonical Wnt signalling. As shown in chapter 3, Sulf1 potentiates the ability of the non-canonical Wnt ligands Wnt4 and Wnt11b to activate non-canonical Wnt signalling. It is possible that Sulf1 enhancement of endogenous non-canonical Wnt activity could be the mechanism by which Sulf1 inhibits canonical Wnt signalling in axis duplication assays.

5.2.2 Investigating the levels of Wnt8a and Wnt11b-HA protein in *Xenopus* embryos

Sulf1 alters the abilities of Wnt8a and Wnt11b to activate Wnt signalling. To determine whether the effects of Sulf1 were due to changes in the amount of protein present, a western blot was carried out using embryos that had been injected in the marginal zone. Using film, the linear range over which protein can be quantified is approximately one order of magnitude. Detecting low levels of signal quantitatively using film is difficult, as a minimum threshold of signal must be reached before it is detectable. In addition, at high levels of signal film darkens, and an increase in signal from this point is not linear with respect to the amount of light produced. In contrast, using a charge couple device (CCD) camera offers a much wider dynamic range for signal detection (Dickinson and Fowler, 2002). In order to carefully measure the amounts of Wnt8a and Wnt11b-HA protein present during the axis duplication assay, a western blot

was performed on whole embryos. In addition to using a CCD camera, two different amounts of protein were examined for each of the assays, to ensure that the transfer of proteins was linear for the amounts tested.

Embryos were microinjected with 0.5, 5, and 600pg of Wnt8a-HA or 5pg, 600pg and 2ng of Wnt11b-HA mRNA into one ventral blastomere of a four cell embryo. The amounts of protein were selected so that the lower doses had no effect on the embryo, whereas the middle doses caused the phenotypes assayed in chapter 3. The higher doses were toxic and induced gross malformation in the injected embryos. In addition Sulf1 (1ng) was injected, to examine whether Sulf1 caused any changes in the relative amounts of Wn8a or Wnt11b-HA protein detected in the embryo. Embryos were cultured until NF stage 10.5 and then snap frozen for western blot or NF stage 36 and analysed for phenotype (see methods 2.3.15 for details).

Over-expression of 0.5pg of Wnt8a-HA mRNA had no effect on axis duplication in Xenopus (Figure 5.5B). Increasing the amount of Wnt8a-HA mRNA to 5pg resulted in axis duplication, with embryos displaying a fully duplicated set of head and eyes (Figure 5.5C). Increasing the levels of Wnt8a-HA mRNA to 600pg, resulted in the truncation of the embryo, with the posterior axis failing to form (Figure 5.5E). In contrast, over-expression of 5pg of Wnt11b-HA mRNA failed to cause a phenotype (Figure 5.5D). Increasing the dose of mRNA to 600pg, caused a shortening of the anterior/posterior axis of the embryo, but no effects on axis duplication were detected (Figure 5.5F). Raising the dose of Wnt11b-HA mRNA to 2ng resulted in a severe shortening of the anterior/posterior axis of the embryo. In addition, the blastopore failed to close, however no obvious effect on axis duplication were detected (Figure 5.5G).

Analysis of the levels of Wnt8a and Wnt11b-HA protein in each of the conditions revealed that Wnt8a-HA is able to induce axis duplication at levels that cannot be detected by western blot (see 5pg dose in Figures 5.5H and 5.7A). Over-expression of 600pg of Wnt8a or Wnt11b-HA mRNA produces completely different phenotypes in Xenopus. Interestingly there appears to be approximately 6 times more Wnt8a-HA protein present than Wnt11b-HA at this dose (compare relative levels of protein from 1 embryo, Figures 5.6A and 5.6B).

Figure 5.5; Detecting the levels of Wnt8a and Wnt11b-HA protein using a CCD camera.
mRNA encoding *Sulf1* (1ng), *Wnt8a-HA* (0.5pg-600pg), *Wnt11b-HA* (5pg-2ng) or a mixture of the three was injected into the VMZ of one cell of an embryo at the four cell stage. [A-G] Embryos were cultured until NF stage 36 and then examined for phenotype. [A] Uninjected embryo, [B-G] embryos injected with [B] 0.5pg *Wnt8a-HA*, [C] 5pg *Wnt8a-HA*, [D] 5pg *Wnt11b-HA*, [E] 600pg *Wnt8a-HA*, [F] 600pg *Wnt11b-HA* or [G] 2ng *Wnt11b-HA*. [H-K] Embryos were cultured until NF stage 10.5 and then snap frozen for western blot. Two different amounts of protein were run for Wnt8a and Wnt11b-HA to investigate whether or not the blots were transferring linearly. For this figure all western blots were developed using a CCD camera.

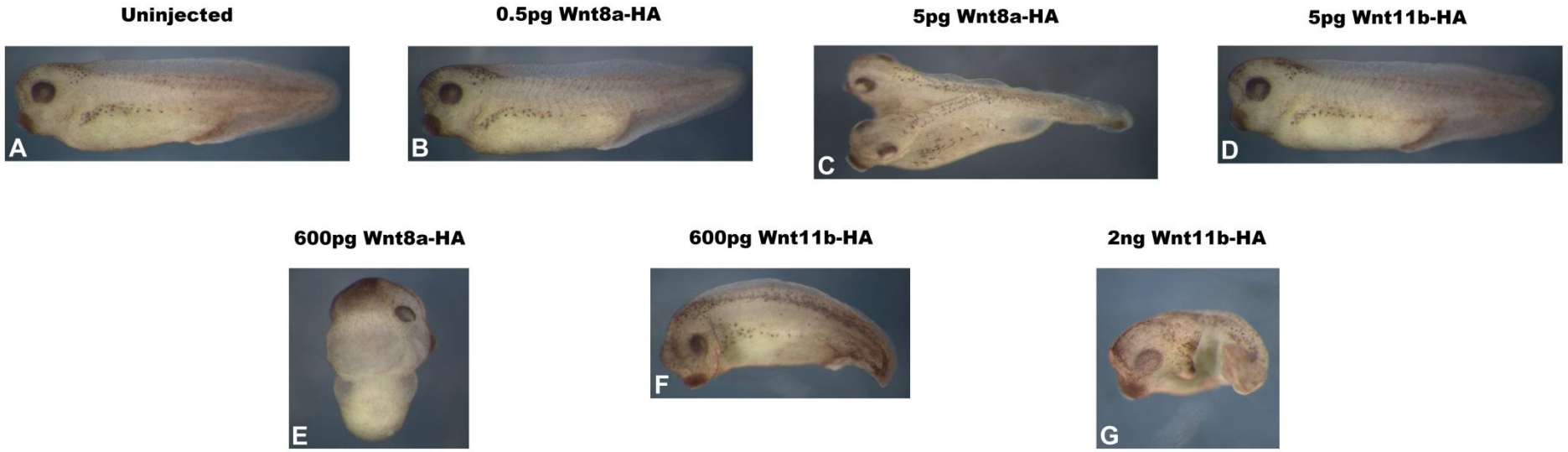

H
Uninjected
0.5pg Wnt8a-HA
0.5pg Wnt8a-HA + Sulf1
5pg Wnt8a-HA
5pg Wnt8a-HA + Sulf1
600pg Wnt8a-HA
600pg Wnt8a-HA + Sulf1
1 Embryo
45Kda
35Kda
I
Uninjected
5pg Wnt11b-HA
5pg Wnt11b-HA + Sulf1
600pg Wnt11b-HA
600pg Wnt11b-HA + Sulf1
2ng Wnt11b-HA
2ng Wnt11b-HA + Sulf1
1 Embryo
45Kda
35Kda
J
Uninjected
0.5pg Wnt8a-HA
0.5pg Wnt8a-HA + Sulf1
5pg Wnt8a-HA
5pg Wnt8a-HA + Sulf1
600pg Wnt8a-HA
600pg Wnt8a-HA + Sulf1
0.5 Embryos
45Kda
35Kda
K
Uninjected
5pg Wnt11b-HA
5pg Wnt11b-HA + Sulf1
600pg Wnt11b-HA
600pg Wnt11b-HA + Sulf1
2ng Wnt11b-HA
2ng Wnt11b-HA + Sulf1
0.5 Embryos
45Kda
35Kda

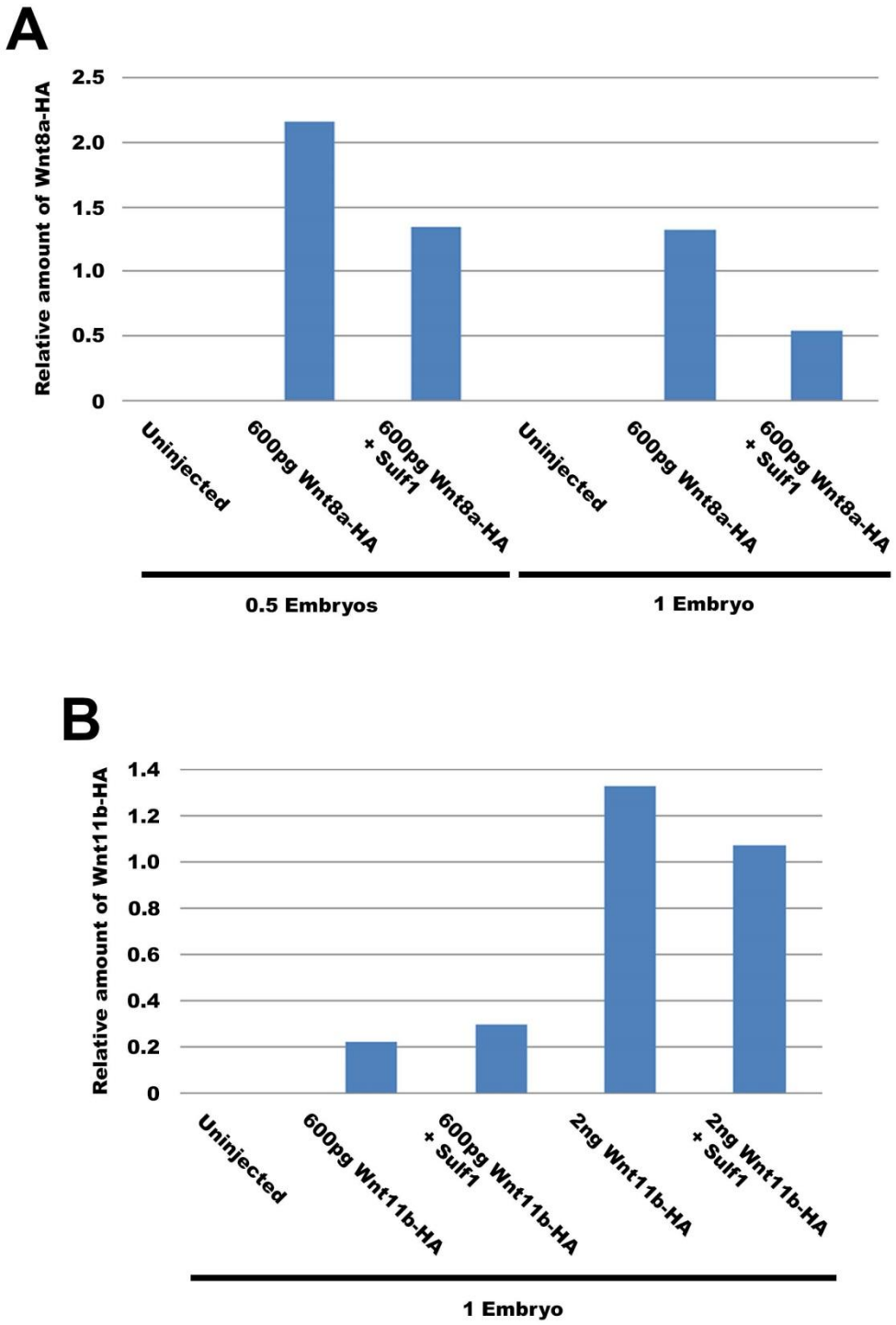

Figure 5.6; Quantifying the relative amounts of Wnt8a and Wnt11b-HA protein visualised using a CCD camera.
Graphs illustrating the data shown in Figures 5.5H-5.5K. The relative amounts of Wnt8a and Wnt11b-HA were calculated using Fiji image J. The graph in [A] represents the data from [5.5H] and [5.5J]. The graph in [B] represents the data from [5.5I]. With the exception of the uninjected lanes, the conditions in which no Wnt8a/Wnt11b-HA protein was detected were not plotted.

Increasing the amount of Wnt11b-HA mRNA injected to 2ng, brings the relative amount of Wnt11b-HA protein present in the embryo to a similar level as 600pg of Wnt8a-HA (compare relative levels of protein from 1 embryo, Figures 5.6A and 5.6B). Importantly though 2ng of Wnt11b-HA mRNA produces a qualitatively different phenotype from 600pg Wnt8a-HA. Embryos over-expressing Wnt11b-HA show a severe shortening of the anterior/posterior axis, but the somites and other posterior axial structures are still present. In contrast embryos over-expressing Wnt8a-HA display a failure of the posterior axis of the embryo to form, but gastrulation defects such as an exposed yolk are not seen (compare Figures 5.5E and 5.5G). One prediction from this, is that the qualitatively different effects produced by Wnt8a-HA and Wnt11b-HA are not due to the total levels of protein in the embryo. Over-expression of Sulf1 causes approximately a 40% reduction in the relative amount of Wnt8a-HA protein, when the protein from half an embryo was analysed, and a 60% decrease when the protein from a whole embryo was analysed. One conclusion from this is that the ability of Sulf1 to inhibit Wnt8a signalling may simply be due to a decrease in the amount of Wnt8a protein present in the embryo. However this is inconsistent with data presented in chapter 3. In Figure 3.6D and 3.6F, Sulf1 appears to inhibit canonical Wnt signalling inside the domain of Sulf1 expression, but Wnt8a that could diffuse away from this region was able to induce small ectopic domains of chordin expression. If Sulf1 was simply reducing the total levels of Wnt8a protein, then these small ectopic domains would not be induced.

Over-expression of Sulf1 together with Wnt11b induces the formation of a secondary axis (see Figure 3.15). Sulf1 increased the relative amount of Wnt11b-HA protein by approximately 35% when 600pg of Wnt11b-HA mRNA was injected. In contrast, Sulf1 reduced the relative amount of Wnt11b-HA protein when 2ng of Wnt11b-HA mRNA was injected (Figure 5.5I). An increase in the relative amount of Wnt11b protein could be responsible for the ability of Sulf1 to enhance Wnt11b activation of canonical Wnt signalling. Importantly though, the ectopic domains of chordin expression induced by Wnt11b and Sulf1 are much broader than those induced by either Wnt3a or Wnt8a alone (see Figures 3.6, 3.11 and 3.15). This suggests that Sulf1 is causing a qualitative change in the range of Wnt11b diffusion, in addition to any increases

in the amount of Wnt11b protein present. In addition it only takes 5pg of Wnt8a-HA mRNA to induce axis duplication in Xenopus. In contrast 600pg (120 times the amount) of Wnt11b-HA mRNA does not induce axis duplication. The predicted ratio between the relative amounts of Wnt8a-HA and Wnt11b-HA protein, when injecting 600pg of mRNA, is 6:1. If this difference is conserved using different amounts of mRNA, then 600pg of Wnt11b-HA mRNA should still produce approximately 20 times more protein than 5pg of Wnt8a mRNA. One conclusion from this is that the difference between the activities of Wnt8a and Wnt11b is not due to the total amounts of protein present.

In order to examine whether or not different amounts of protein transferred linearly during the western blot, both Wnt8a and Wnt11b-HA western blots were carried out using protein from half and protein from a whole embryo. If too much protein is present then the western blot transfer will become saturated, and differences between conditions may not be visible. The relative amount of Wnt8a-HA protein present is 40% less when analysing a whole embryo sample, compared to a half embryo sample (Figure 5.6A). One prediction from this is that increasing the amount of protein used from 0.5 embryos to 1 embryo does not produce a linear increase in the amount of Wnt8a-HA protein that is transferred. Importantly though, the ability of Sulf1 to reduce the relative amount of Wnt8a-HA protein present is conserved when using either amount of protein.

Wnt11b-HA could not be detected using a CCD camera when protein from half an embryo was analysed. To investigate whether linear transfer was occurring when using different amounts of Wnt11b-HA protein, the western blots were stripped and re-analysed using film (see Figures 5.7B and 5.7D). Sulf1 produced an increase in the relative amounts of Wnt11b-HA protein when either 600pg or 2ng of *Wnt11b-HA* mRNA was injected (Figure 5.8B). For the 600pg doses of *Wnt11b-HA*, increasing the amount of protein used from half an embryo to a whole embryo reduced the relative amount of Wnt11b-HA protein detected in control conditions. However in the presence of Sulf1, more Wnt11b-HA protein was detected using protein from a whole embryo, compared to half an embryo. The reverse was true when analysing the 2ng doses of *Wnt11b-HA* mRNA (Figure 5.8B). One conclusion from this is that the differences in the

Figure 5.7; Detecting the levels of Wnt8a and Wnt11b-HA protein using film.
mRNA encoding *Sulf1* (1ng), *Wnt8a-HA* (0.5pg-600pg), *Wnt11b-HA* (5pg-2ng) or a mixture of the three was injected into the VMZ of one cell of an embryo at the four cell stage. Embryos were cultured until NF stage 10.5 and then snap frozen for western blot. Two different amounts of protein were run for Wnt8a and Wnt11b-HA to investigate whether or not the blots were transferring linearly. [A and C] Western blots for Wnt8a-HA using protein from either one embryo [A] or half an embryo [C]. [B and D] Western blots for Wnt11b-HA using protein from either one embryo [I] or half an embryo [K]. For this figure all western blots were developed using an Xograph and film.

A
Uninjected
0.5pg Wnt8a-HA
0.5pg Wnt8a-HA + Sulf1
5pg Wnt8a-HA
5pg Wnt8a-HA + Sulf1
600pg Wnt8a-HA
600pg Wnt8a-HA + Sulf1
1 Embryo
45Kda
35Kda
B
Uninjected
5pg Wnt11b-HA
5pg Wnt11b-HA + Sulf1
600pg Wnt11b-HA
600pg Wnt11b-HA + Sulf1
2ng Wnt11b-HA
2ng Wnt11b-HA + Sulf1
1 Embryo
45Kda
35Kda
C
Uninjected
0.5pg Wnt8a-HA
0.5pg Wnt8a-HA + Sulf1
5pg Wnt8a-HA
5pg Wnt8a-HA + Sulf1
600pg Wnt8a-HA
600pg Wnt8a-HA + Sulf1
0.5 Embryos
45Kda
35Kda
D
Uninjected
5pg Wnt11b-HA
5pg Wnt11b-HA + Sulf1
600pg Wnt11b-HA
600pg Wnt11b-HA + Sulf1
2ng Wnt11b-HA
2ng Wnt11b-HA + Sulf1
0.5 Embryos
45Kda
35Kda

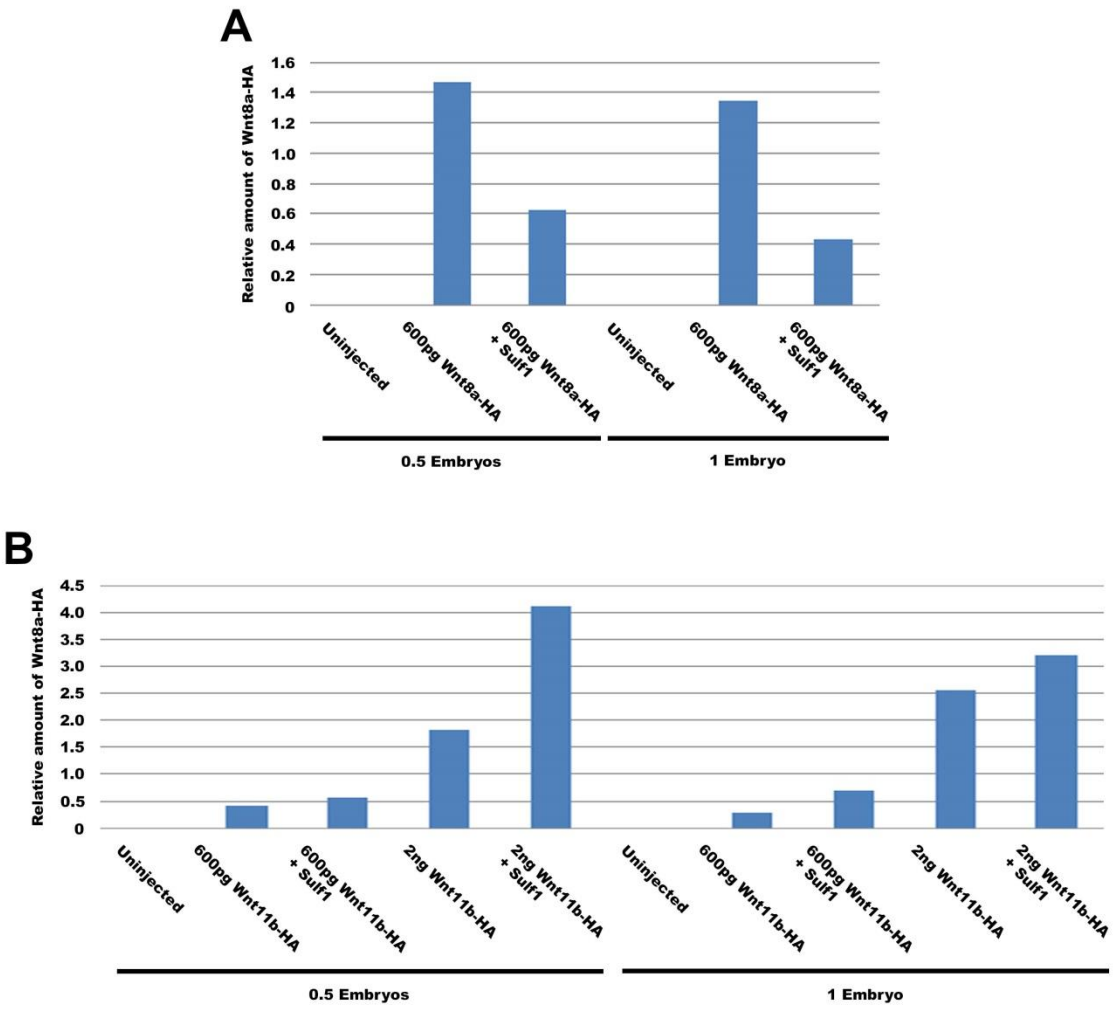

Figure 5.8; Quantifying the relative amounts of Wnt8a and Wnt11b-HA protein visualised using film.
Graphs illustrating the data shown in Figures 5.7A-5.7D. The relative amounts of Wnt8a and Wnt11b-HA were calculated using image J. The graph in [A] represents the data from [5.5A] and [5.5C]. The graph in [B] represents the data from [5.5B] and [5.5D]. With the exception of the uninjected lanes, the conditions in which no Wnt8a/Wnt11b-HA protein was detected were not plotted.

relative amounts of protein detected when using protein from half and embryo, compared to a whole embryo, are not solely due to saturation of the transfer process. When comparing the linear transfer of Wnt8a-HA protein using film, the differences between using protein from half an embryo, compared to protein from a whole embryo, were smaller than those seen using the CCD camera. As the CCD camera has a better dynamic range than film, Dickinson and Fowler, (2002), the results obtained using the CCD camera are likely to be more reliable than those obtained by film. Importantly though, the effects of Sulf1 on the relative levels of Wnt8a-HA protein are conserved when using protein from either half or a whole embryo (Figure 5.8A).

The data presented in Figures 5.5-5.8 suggest that there is a difference in the relative amounts of Wnt8a and Wnt11b protein produced by the embryo. However, when this is combined with data from chapter 3, it is unlikely that the ability of Sulf1 to alter Wnt8a and Wnt11b signalling is solely due to changes in the total amounts of Wnt8a and Wnt11b protein present.

5.2.3 Developing Wnt8a-HA-GFP and Wnt11b-HA-GFP

To investigate the effects of Sulf1 on Wnt8a and Wnt11b diffusion, Wnt8a and Wnt11b-HA-GFP constructs were developed. The GFP tag was subcloned onto the C terminus of existing Wnt8a and Wnt11b-HA constructs. Mii and Taira, (2009), previously published work using Wnt8a and Wnt11b tagged N terminally with Venus, to model the effects of Sfrp3 and crescent on Wnt diffusion. To ensure Wnt8a and Wnt11b-Venus were secreted efficiently, the signal peptide sequence of TGF-β1 was cloned N terminally to the Venus tag. A diagram of Wnt8a and Wnt11b-HA-GFP/Venus constructs are shown (Figure 5.9).

Before investigating Wnt ligand diffusion, the biological activities of the Wnt8a and Wnt11b-HA-GFP/Venus constructs were assessed. Embryos were microinjected with mRNA encoding *Wnt8a, Wnt8a-HA-GFP* and *Wnt8a-Venus* into one ventral blastomere at the four cell stage. Embryos were cultured until NF stage 37/38 and analysed for axis duplication. The majority of embryos over-expressing Wnt8a or Wnt8a-HA-GFP showed a fully duplicated set of head and eyes (Figure 5.10C and 5.10E). In contrast, the majority of embryos over-expressing Wnt8a-Venus only displayed duplications of the trunk (Figure 5.10F and 5.10G). The data in Figure 5.10A-G is quantified in Figure 5.10H. Wnt8a-HA-GFP displayed similar axis inducing properties to Wnt8a, while Wnt8a-Venus was less active. Wnt8a-HA-GFP was selected to model Wnt ligand diffusion in *Xenopus.*

To investigate the biological activities of the Wnt11b constructs, embryos were microinjected bilaterally in the animal hemisphere with mRNA encoding *Wnt11b-HA, Wnt11b-HA-GFP* and *Wnt11b-Venus.* Embryos were cultured until NF stage 8 and then animal cap explants were taken. Animal caps were

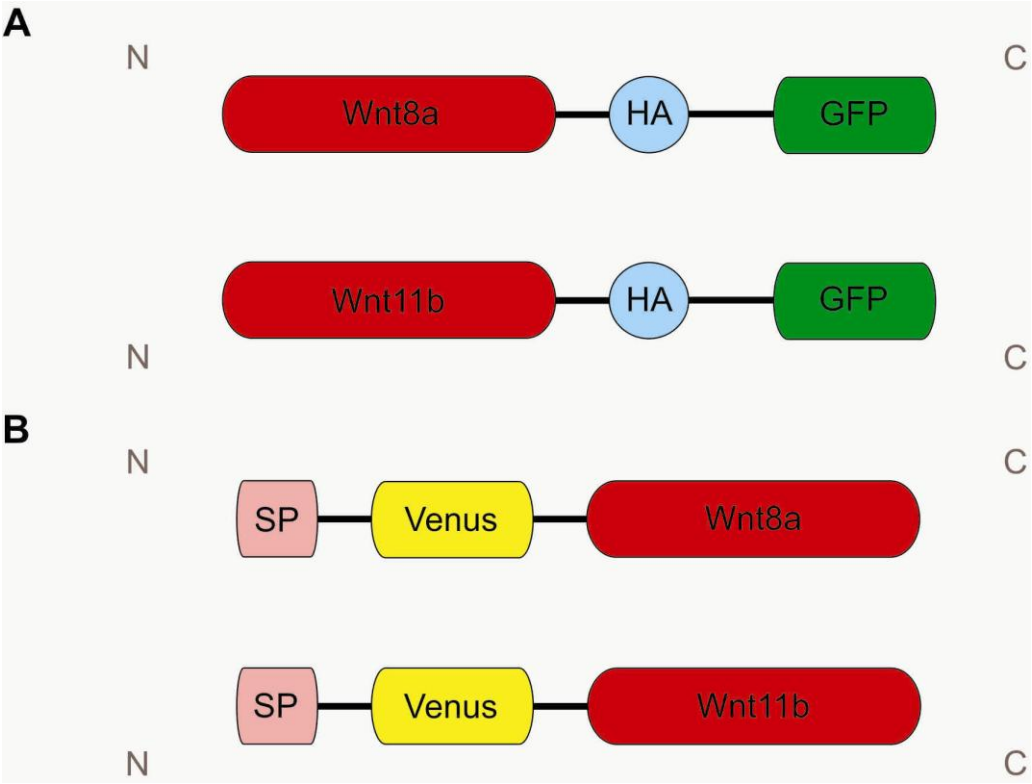

Figure 5.9; Development of fluorescent Wnt constructs.
Diagram depicting the fluorescent Wnt constructs subcloned in this thesis and those obtained from (Mii and Taira, 2009). [A] Diagram of fluorescent Wnt ligands created by GFP tagging existing Wnt8a and Wnt11b-HA constructs. The HA and GFP tags are both fused to the C terminus of Wnt8a and Wnt11b in series. [B] Diagram of fluorescent Wnt constructs that have been used to follow Wnt ligand diffusion (Mii and Taira 2009). The Venus constructs are fused to the N terminus of Wnt8a and Wnt11b and the TGF-β1 signal peptide is fused N terminally to Venus.

cultured in either the presence or absence of activin until NF stage 19. Wnt11b-HA inhibited activin induced convergent extension in a dose dependent manner (compare Figure 5.11C-E to 5.11B). Over-expression of increasing amounts of Wnt11b-HA-GFP or Wnt11b-Venus inhibited activin induced convergent extension to similar levels (compare Figure 5.11F-H to 5.11I-K). Wnt11b-HA-GFP was selected to model Wnt ligand diffusion in *Xenopus* animal caps for consistency with Wnt8a-HA-GFP.

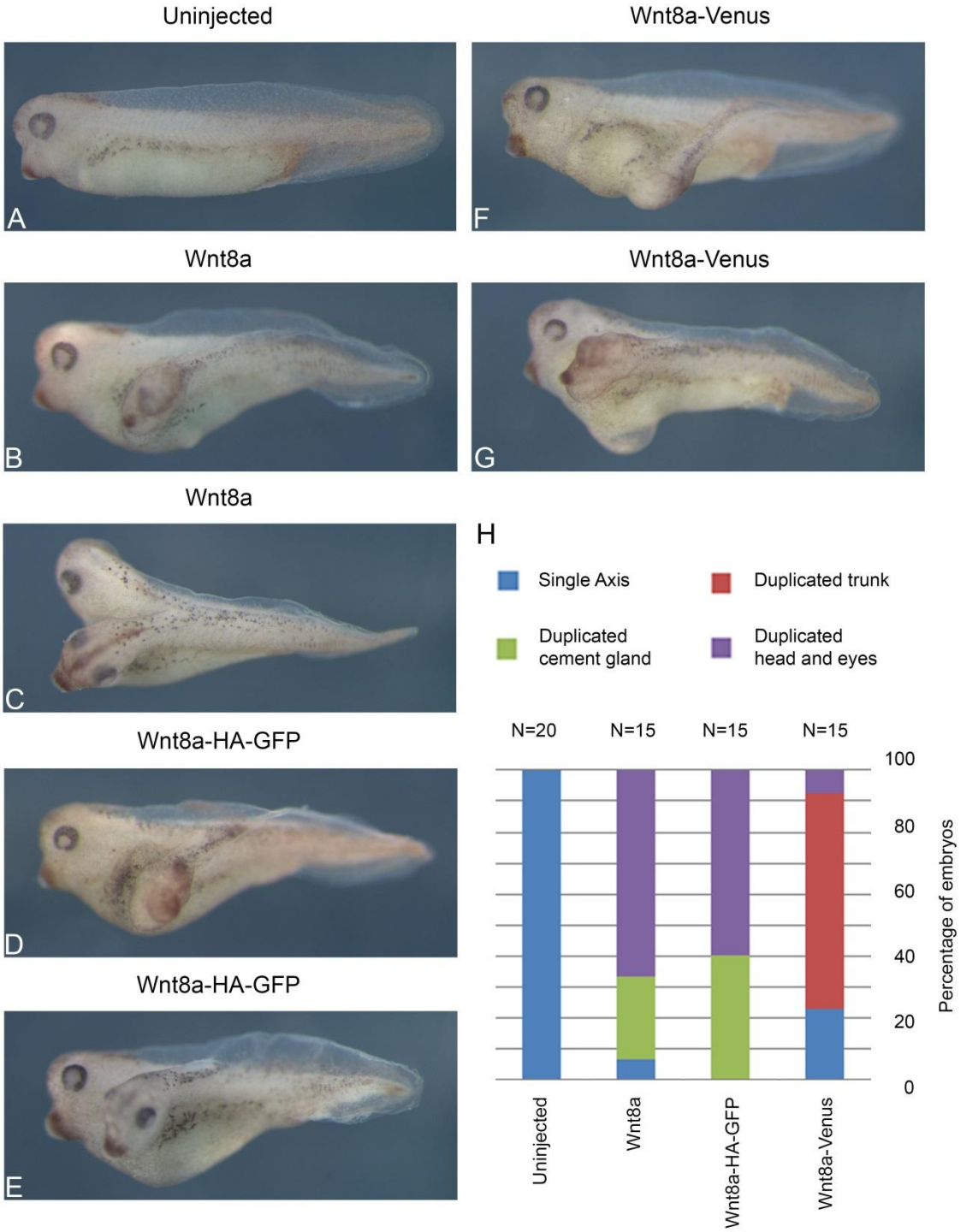

Figure 5.10; Wnt8a-HA-GFP and Wnt8a-Venus are biologically active.
mRNA encoding *Wnt8a* (10pg), *Wnt8a-HA-GFP* (10pg) or *Wnt8a-Venus* (10pg) was injected into one ventral blastomere of an embryo at the four cell stage. Embryos were cultured until NF stage 37/38 and then examined for phenotype. [A] Lateral view of an uninjected embryo. Lateral views of embryos over-expressing [B-C] Wnt8a, [D-E] Wnt8a-HA-GFP and [F-G] Wnt8a-Venus. [H] Graph quantifying the frequency of axis duplication in embryos over-expressing Wnt8a, Wnt8a-HA-GFP and Wnt8a-Venus. Wnt8a-HA-GFP showed a similar level of activity to Wnt8a in axis duplication assays and was selected to analyse Wnt ligand diffusion.

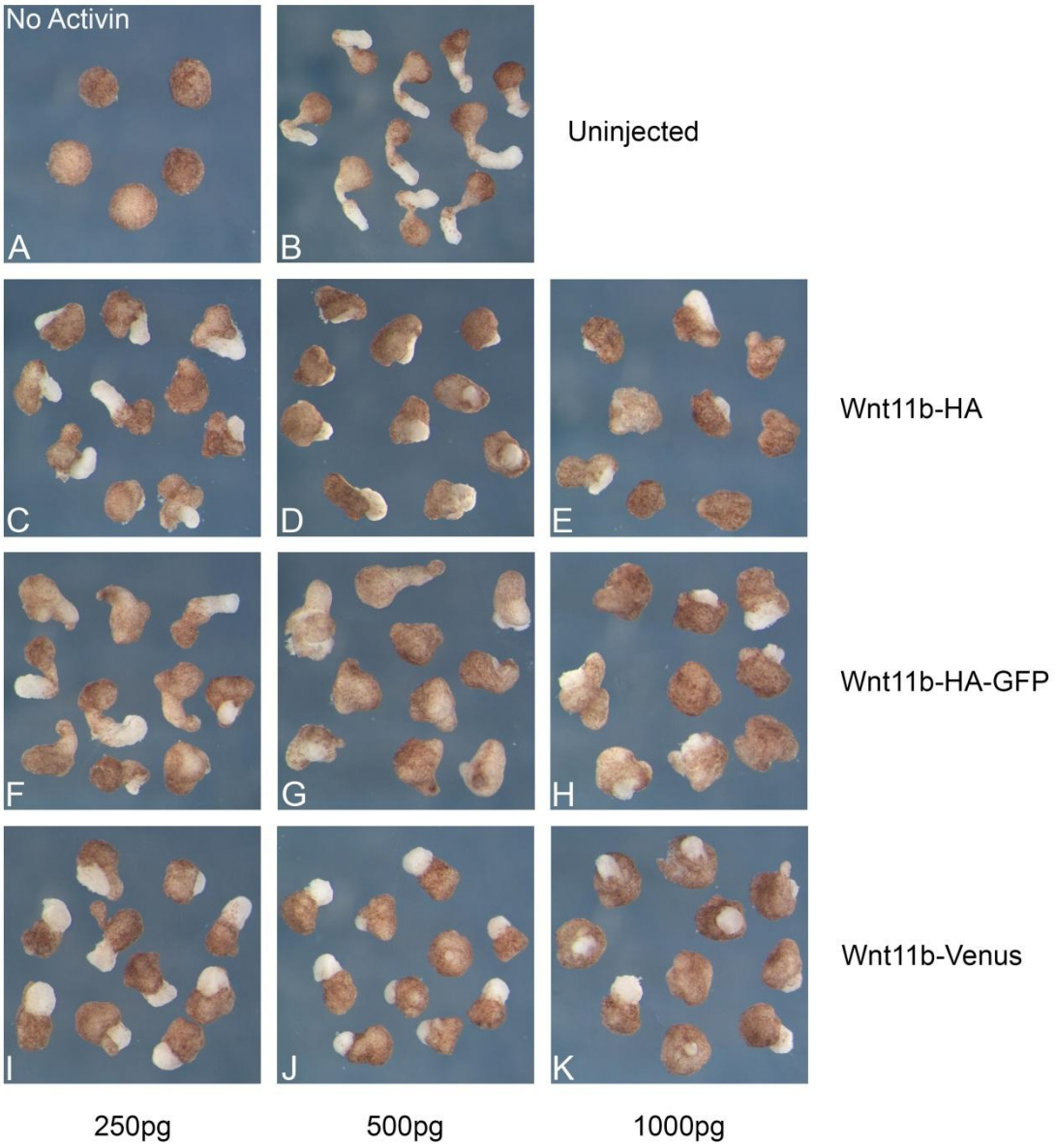

Figure 5.11; Wnt11b-HA-GFP and Wnt11b-Venus are biologically active.
mRNA encoding *Wnt11-HA*, *Wnt11-HA-GFP* or *Wnt11b-Venus* was injected bilaterally into the animal hemisphere of embryos at the two cell stage. Embryos were cultured until NF stage 8 and then animal cap explants were taken and cultured in either the presence or absence of activin until NF stage 19. [A-B] Uninjected animal caps cultured in either the absence [A] or presence [B] of activin. [C-K] Animal caps injected with increasing amounts of [C-E] *Wnt11b-HA*, [F-H] *Wnt11b-HA-GFP* and [I-K] *Wnt11b-Venus* mRNA. Over-expression of increasing amounts of Wnt11-HA inhibited activin induced convergent extension of animal caps. Over-expression of either Wnt11b-HA-GFP or Wnt11b-Venus inhibited activin induced convergent extension to a similar extent. Wnt11b-HA-GFP and Wnt11-Venus showed similar levels of biological activity. Wnt11b-HA-GFP was used instead of Wnt11b-Venus to analyse Wnt ligand diffusion.

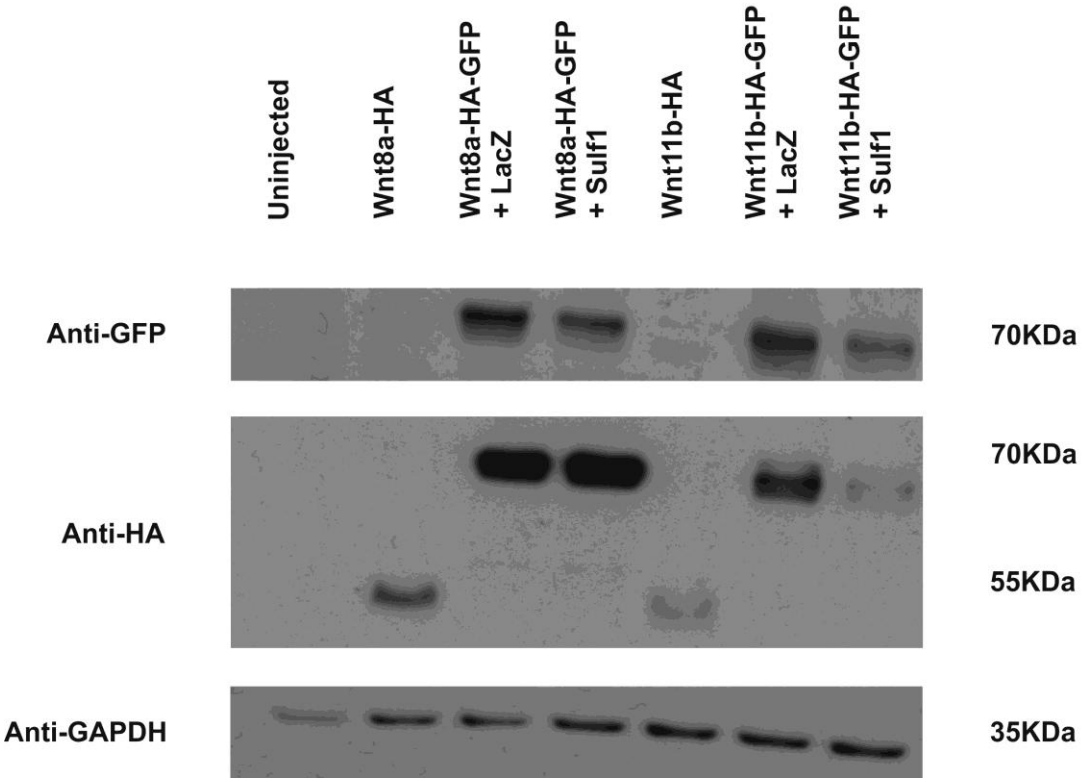

Figure 5.12; The expression of Wnt8a-HA-GFP and Wnt11b-HA-GFP in *Xenopus* animal caps.
mRNA encoding for *Wnt8a-HA* (400pg), *Wnt8a*-HA-GFP (400pg), *Wnt11b-HA* (400pg), *Wnt11b-HA-GFP* (400pg), *LacZ* (4ng) and *Sulf1* (4ng) was injected bilaterally into the animal hemisphere of embryos at the two cell stage. Embryos were cultured until NF stage 8 and then animal cap explants were taken and cultured until NF stage 10.5. Animal caps were then snap frozen for western blot. Anti-HA and anti-GFP antibodies were used to examine the expression of Wnt8a and Wnt11b-HA-GFP in animal caps, anti GAPDH was used as a loading control.

To investigate whether Sulf1 altered the level of expression of either Wnt8a or Wnt11b-HA-GFP, embryos were microinjected bilaterally with mRNA encoding *Wnt8a/Wnt11b-HA, Wnt8/Wnt11b*-HA-GFP, *LacZ* and *Sulf1* in the animal hemisphere at the two cell stage. Embryos were cultured until NF stage 8 and then animal caps were taken and cultured until NF stage 10.5. Animal caps were then snap frozen for western blot, to determine the levels of protein present. The expression Wnt8a and Wnt11b-HA-GFP in animal caps was detected using anti-HA and anti-GFP antibodies. Wnt8a and Wnt11b-HA present as a single band at approximately 45-50Kda (Figure 5.12). The predicted size of GFP is 27Kda, therefore Wnt8a and Wnt11b-HA-GFP should run at approximately 75Kda. Consistent with this, blotting with either anti-HA or anti-GFP produces a single band for Wnt8a/Wnt11b-HA-GFP at approximately 70Kda. Over-expression of Sulf1 caused a reduction in the levels of Wnt11b-

HA-GFP protein, but had no effect on Wnt8a-HA-GFP (Figure 5.12). Similar results were obtained using Sulf1 C-A rather than LacZ as an injection control (data not shown). Together these data show that Wnt8a and Wnt11b-HA-GFP are biologically active constructs that can be detected using either the HA or GFP tags. Wnt8a and Wnt11b-HA-GFP were used to investigate a potential role for Sulf1 in regulating Wnt ligand diffusion.

5.2.4 Sulf1 alters the expression of Wnt8a and Wnt11b-HA-GFP on the cell membrane

The effects of Sulf1 on the levels of cell surface Wnt8a and Wnt11b-HA-GFP were examined in *Xenopus* animal cap explants. Embryos were microinjected bilaterally in the animal hemisphere with mRNA encoding *mRFP*. In addition embryos were microinjected with mRNA encoding *Sulf1, LacZ, Wnt8a/Wnt11b-HA-GFP* or a mixture of the four. Embryos were cultured until NF stage 8 and then animal cap explants were taken. Animal caps were cultured in the dark for four hours at 21˚C prior to imaging by confocal microscopy. The dose of mRNA used for the Wnt ligands in this experiment was 500pg and 1000pg for *Wnt8a* and *Wnt11b-HA-GFP* respectively. For Wnt8a-HA-GFP especially, this was much higher than the doses of mRNA used for the phenotype experiments in chapters 3 and 4. The high doses of Wnt8a and Wnt11b-HA-GFP were required to visualise the proteins. Although Sulf1 was found to have distinct effects on Wnt8a and Wnt11b-HA-GFP puncta in this assay, this does not mean that the data will represent exactly the phenotypes seen in chapters 3 and 4, or Sulf1's effects in vivo. This is a common limitation of any over-expression assay.

In control conditions (LacZ expressing), Wnt8a-HA-GFP displayed a punctate expression pattern on the cell membrane (Figure 5.13A-D). Over-expression of Wnt8a-HA-GFP together with Sulf1 had no effect on the amount of Wnt8a-HA-GFP colocalising with the cell membrane (compare Figure 5.13E-H to 5.13A-D). The amount of detectable Wnt11b-HA-GFP is lower than that of Wnt8a-HA-GFP in control conditions (LacZ). In addition Wnt11b-HA-GFP puncta are more elongated than Wnt8a-HA-GFP puncta on the cell membrane (compare Figure 5.13I-L to 5.13A-D). Over-expression of Sulf1 increased the overall levels of

Figure 5.13; Sulf1 enhances the levels of Wnt11b-HA-GFP present on the cell surface. mRNA encoding *mRFP* (500pg) was injected bilaterally into the animal hemisphere of embryos at the two cell stage. In addition embryos were injected with mRNA encoding *LacZ* (4ng), *Sulf1* (4ng), *Wnt8a-HA-GFP* (500pg), *Wnt11b-HA-GFP* (1ng) or a mixture of the four. Embryos were cultured until NF stage 8 and then animal cap explants were taken and cultured for four hours at 21˚C prior to imaging by confocal microscopy. [A-D] Control animal caps over-expressing LacZ and Wnt8a-HA-GFP. [E-H] Animal caps over-expressing Sulf1 and Wnt8a-HA-GFP. [I-L] Control animal caps over-expressing LacZ and Wnt11b-HA-GFP. [M-P] Animal caps over-expressing Sulf1 and Wnt11b-HA-GFP. The white boxes in [C], [G], [K] and [O] mark the areas used to create panels [D], [H], [L] and [P] respectively. Over-expression of Sulf1 did not alter the overall levels of Wnt8a-HA-GFP colocalising with the cell membrane. Over-expression of Sulf1 increased the levels of Wnt11b-HA-GFP on the cell membrane. Graphs quantifying the relative levels of [Q] Wnt8a-HA-GFP and [R] Wnt11b-HA-GFP on the cell membrane. Data obtained using a programme written in Matlab see methods 2.5.2 for details. Asterisks mark significant differences (**P<0.01), NS marks non-significant differences, Mann-Whitney U, error bars represent s.e.m. mRFP (magenta), Wnt8a/Wnt11b-HA-GFP (green), scale bars represent 20μm, N = number of embryos.

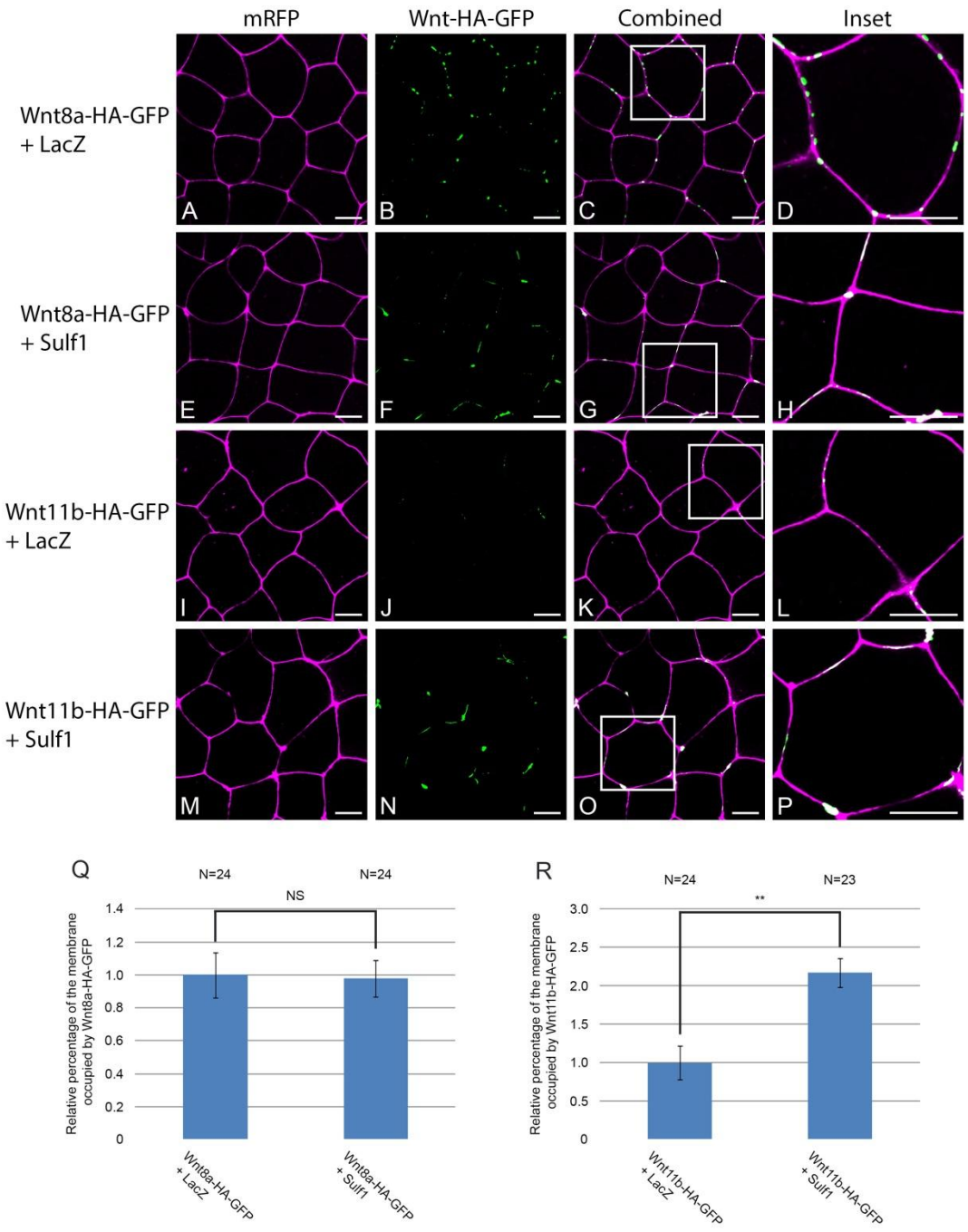
mRFP
Wnt-HA-GFP
Combined
Inset
Wnt8a-HA-GFP
+ LacZ
Wnt8a-HA-GFP
+ Sulf1
Wnt11b-HA-GFP
+ LacZ
Wnt11b-HA-GFP
+ Sulf1
A
B
C
D
E
F
G
H
I
J
K
L
M
N
O
P
Q
N=24
N=24
NS
Relative percentage of the membrane occupied by Wnt8a-HA-GFP
1.4
1.2
1.0
0.8
0.6
0.4
0.2
0
Wnt8a-HA-GFP + LacZ
Wnt8a-HA-GFP + Sulf1
R
N=24
N=23
**
Relative percentage of the membrane occupied by Wnt11b-HA-GFP
3.0
2.5
2.0
1.5
1.0
0.5
0
Wnt11b-HA-GFP + LacZ
Wnt11b-HA-GFP + Sulf1

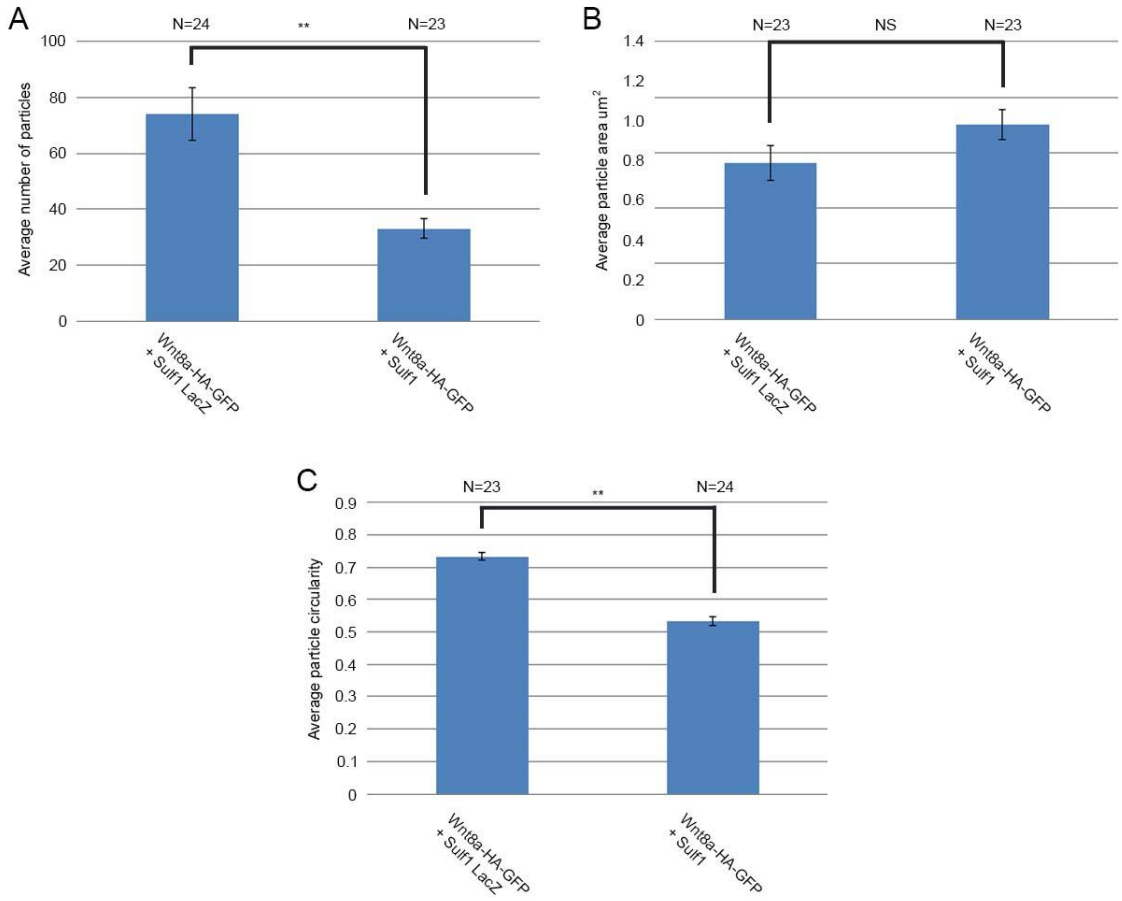

Figure 5.14; Sulf1 causes an increase in the number of and change in shape of Wnt8a-HA-GFP particles on the cell membrane.
Graphs illustrating the data shown in Figure 5.13. Images were analysed using the particle analysis function in Fiji Image J (see methods 2.5.3 for details). [A] Over-expression of Sulf1 caused a decrease in the average number of Wnt8a-HA-GFP particles present on the cell membrane compared to control conditions. [B] Over-expression of Sulf1 had no effect on the average size of Wnt8a-HA-GFP particles compared to control conditions. [C] Over-expression of Sulf1 caused a reduction in the average circularity of Wnt8a-HA-GFP particles on the cell membrane shifting them from spherical puncta towards more elongated non-circular aggregates. Asterisks mark significant differences (**P<0.01), NS marks non-significant differences, Mann-Whitney U, error bars represent s.e.m, N = number of embryos.

Wnt11b-HA-GFP on the cell membrane (compare Figure 5.13M-P to 5.13I-L). The data in Figures 5.13A-H and 5.13I-P is quantified in Figures 5.13Q and 5.13R respectively. The data was quantified using the same Matlab programme as for the Dvl-GFP analysis (see methods 2.5.2 for details). Briefly the programme calculates the percentage of Wnt8a/Wnt11b-HA-GFP pixels colocalising with mRFP pixels. This value can then be compared between different conditions. Over-expression of Sulf1 enhances the levels of Wnt11b-HA-GFP, but not Wnt8a-HA-GFP colocalising with the cell membrane.

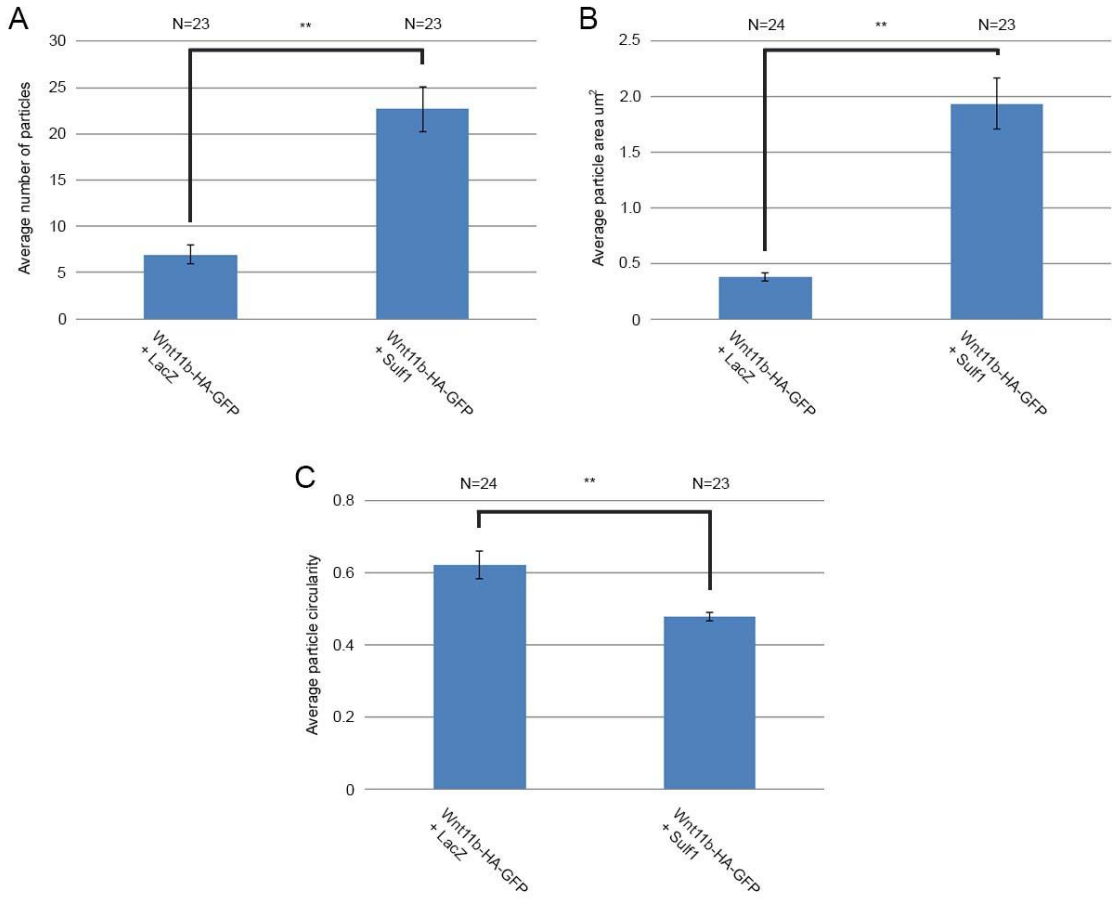

Figure 5.15; Sulf1 causes an increase in the number and size of and a change in shape of Wnt11b-HA-GFP particles on the cell membrane.
Graph illustrating the data shown in Figure 5.13, images were analysed using Fiji Image J. [A] Over-expression of Sulf1 caused an increase in the number of Wnt11b-HA-GFP particles on the cell membrane compared to control conditions. [B] Over-expression of Sulf1 caused an increase in the average size of Wnt11b-HA-GFP particles on the cell membrane compared to control conditions. [C] Sulf1 caused a reduction in circularity of Wnt11b-HA-GFP particles on the cell membrane compared to control conditions. Asterisks mark significant differences (**P<0.01), NS marks non-significant differences, Mann-Whitney U, error bars represent s.e.m, N = number of embryos.

To investigate the qualitative changes in Wnt8a and Wnt11b-HA-GFP puncta, the particle analysis function of Fiji image J was used (see methods 2.5.3 for details). Briefly, the images in Figure 5.13 were converted to black and white images using the Auto threshold function in image J. The images were then analysed for Wnt-HA-GFP particle number, size and circularity using the Analyse particles function in image J. Circularity is a measure of how closely an object resembles a perfect circle, with 1 representing a perfect circle and 0.1 an elongated non-circular shape. Over-expression of Sulf1 lead to an increase in the number of Wnt8a-HA-GFP particles colocalised with the cell membrane (Figure 5.14A). However Sulf1 had no significant effect on the average

Table 5.1; Summary of Wnt8a and Wnt11b-HA-GFP particle analysis

Ligand	**Average number of particles**	**Average particle size**	**Average particle circularity**
Wnt8a-HA-GFP	Sulf1 reduces average particle number	Sulf1 does not alter average particle size	Sulf1 reduces average particle circularity
Wnt11b-HA-GFP	Sulf1 increase average particle number	Sulf1 increases average particle size	Sulf1 reduces average particle circularity

size of Wnt8a-HA-GFP puncta (Figure 5.14B). In addition, Sulf1 caused a decarese in the average circularity of Wnt8a-HA-GFP puncta (Figure 5.14C). In control conditions, fewer Wnt11b-HA-GFP particles are present on the cell membrane than Wnt8a-HA-GFP particles (compare Figure 5.15A-B to 5.14A-B). In addition Wnt11b-HA-GFP particles are less spherical than Wnt8a-HA-GFP particles in control conditions (compare Figure 5.15C to 5.14C). Over-expression of Sulf1 resulted in an increase in the number and average size of Wnt11b-HA-GFP particles (Figure 5.15A and B). Over-expression of Sulf1 also lead to a decrease in Wnt11b-HA-GFP particle circularity, similar to the effects of Sulf1 on Wnt8a-HA-GFP. Sulf1 increases the amount of Wnt11b-HA-GFP colocalised with the cell membrane. In addition Sulf1 causes a qualitative change in the shape of both Wnt8a and Wnt11b-HA-GFP particles. A summary table for the effects of Sulf1 on Wnt8a and Wnt11b-HA-GFP particles can be seen (Table 5.1).

5.2.5 Sulf1 alters the expression of Wnt4-HA-GFP on the cell membrane

Sulf1 potentiates the ability of Wnt4 to activate non-canonical Wnt signalling (chapter 4). To investigate whether Sulf1 would have a similar effect on Wnt4 localisation to that of Wnt11b, Wnt4 was C terminally tagged with HA and GFP in a similar manner to Wnt8a and Wnt11b-HA-GFP. Embryos were microinjected bilaterally in the animal hemisphere with mRNA encoding *mRFP*. In addition, embryos were microinjected with mRNA encoding *Sulf1, Sulf1 C-A, Wnt4-HA-GFP* or a mixture of the four. Embryos were cultured until NF stage

Figure 5.16; Sulf1 enhances the level of Wnt4-HA-GFP on the cell membrane.
mRNA encoding *mRFP* (500pg) was injected bilaterally into the animal hemisphere of embryos at the two cell stage. In addition embryos were injected with mRNA encoding *Sulf1* (4ng), *Sulf1 C-A* (4ng), *Wnt4-HA-GFP* (500pg), or a mixture of the three. Embryos were cultured until NF stage 8 and then animal cap explants were taken and cultured for four hours at 21˚C prior to imaging by confocal microscopy. [A-D] Control animal caps over-expressing Sulf1 C-A and Wnt4-HA-GFP. [E-H] Animal caps over-expressing Sulf1 and Wnt4-HA-GFP. The white boxes in [C] and [G] mark the areas used to create panels [D] and [H] respectively. Over-expression of Sulf1 increased the levels of Wnt4-HA-GFP on the cell membrane. [I] Graph quantifying the relative levels of Wnt4-HA-GFP on the cell membrane. [J-L] Graphs illustrating the qualitative change in Wnt4-HA-GFP puncta in response to Sulf1, images were analysed using Fiji Image J. [J] Over-expression of Sulf1 caused an increase in the number of Wnt4-HA-GFP particles on the cell membrane compared to control conditions. [K] Over-expression of Sulf1 did not affect the average size of Wnt4-HA-GFP particles compared to control conditions. [L] Over-expression of Sulf1 caused an increase in the average circularity of Wnt4-HA-GFP particles on the cell membrane. Asterisks mark significant differences (**P<0.01), NS marks non-significant differences, Mann-Whitney U, error bars represent s.e.m. mRFP (magenta), Wnt4-HA-GFP (green), scale bars represent 20μm, N = number of embryos.

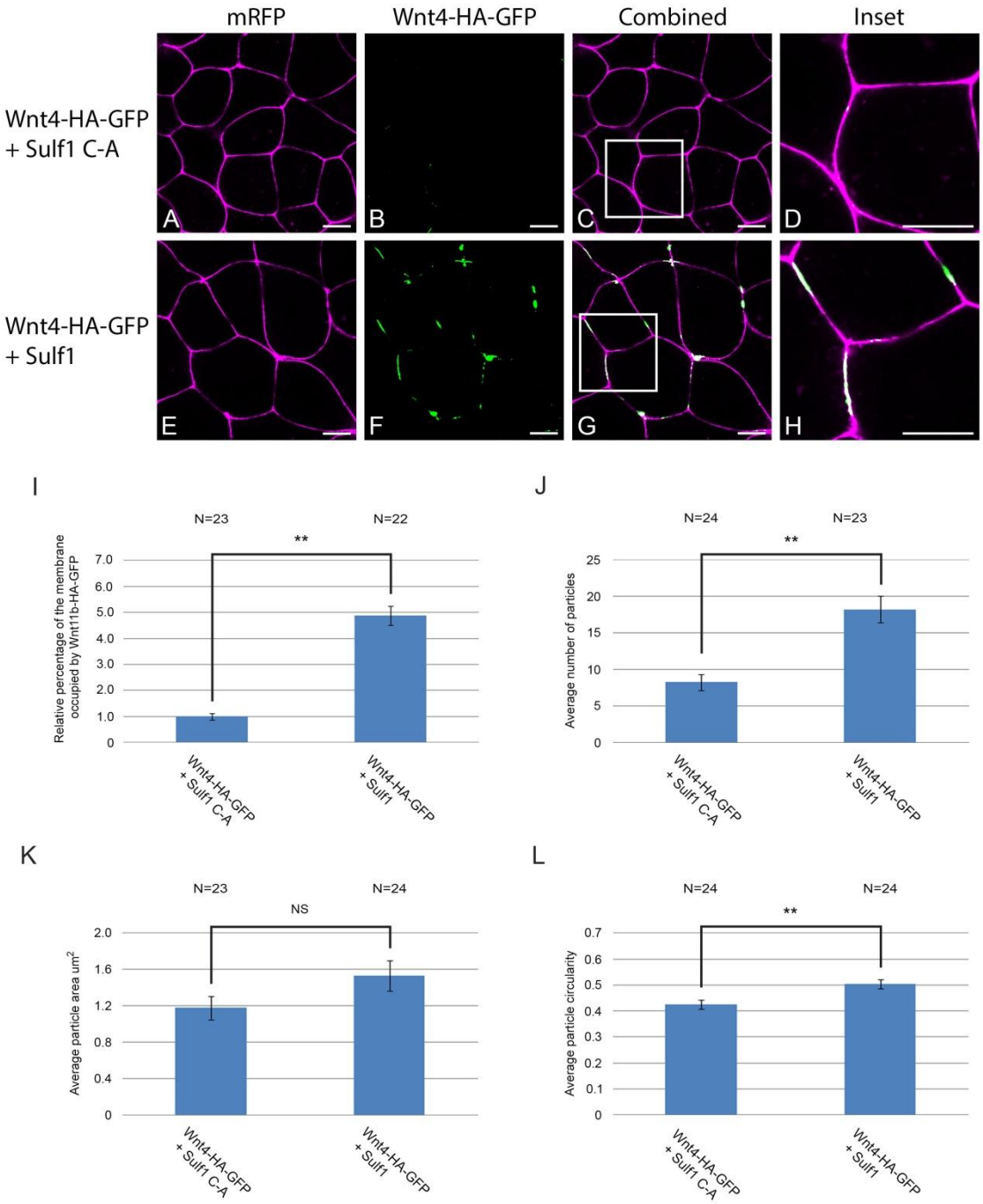
mRFP
Wnt4-HA-GFP
Combined
Inset
Wnt4-HA-GFP
+ Sulf1 C-A
Wnt4-HA-GFP
+ Sulf1
A
B
C
D
E
F
G
H
I
N=23
N=22
**
Relative percentage of the membrane occupied by Wnt11b-HA-GFP
7.0
6.0
5.0
4.0
3.0
2.0
1.0
0
Wnt4-HA-GFP + Sulf1 C-A
Wnt4-HA-GFP + Sulf1
J
N=24
N=23
**
Average number of particles
25
20
15
10
5
0
Wnt4-HA-GFP + Sulf1 C-A
Wnt4-HA-GFP + Sulf1
K
N=23
N=24
NS
Average particle area um2
2.0
1.6
1.2
0.8
0.4
0
Wnt4-HA-GFP + Sulf1 C-A
Wnt4-HA-GFP + Sulf1
L
N=24
N=24
**
Average particle circularity
0.7
0.6
0.5
0.4
0.3
0.2
0.1
0
Wnt4-HA-GFP + Sulf1 C-A
Wnt4-HA-GFP + Sulf1

and then animal cap explants were taken. Animal caps were cultured in the dark for four hours at 21˚C prior to imaging by confocal microscopy. In control conditions (Sulf1 C-A), Wnt4-HA-GFP was found at low levels on the cell membrane. Wnt4-HA-GFP puncta appeared as aggregates, similar to Wnt11b-HA-GFP (compare Figure 5.16A-D to 5.13I-L). Over-expression of Sulf1 enhanced the levels of Wnt4-HA-GFP on the cell membrane. Wnt4-HA-GFP particles presented as aggregates on the cell membrane, which were concentrated at the junctions between cells (Figure 5.16E-H). The data in Figure 5.16A-H is quantified in Figure 5.16I. The data was quantified using a program written in Matlab. The effects of Sulf1 on Wnt4-HA-GFP are similar to those on Wnt11b-HA-GFP.

To investigate the qualitative changes in Wnt4-HA-GFP, the particle analysis function of Fiji Image J was used. In control conditions a similar number of Wnt4-HA-GFP puncta were present as were detected for Wnt11b-HA-GFP (compare Figure 5.16J to 5.15A). However, in control conditions the average size of the Wnt4-HA-GFP puncta was greater and the average circularity lower than that of either Wnt8a-HA-GFP or Wnt11b-HA-GFP puncta (compare Figures 5.16J-K to 5.13B-C and 5.14B-C). Over-expression of Sulf1 increased both the number and average circularity of Wnt4-HA-GFP puncta (Figure 5.16J and 5.16L). However, it is unclear whether Wnt4-HA-GFP aggregates became more spherical when Sulf1 was over-expressed. Sulf1 enhanced the accumulation of Wnt4-HA-GFP, around cell junctions. This may have led to several Wnt4-HA-GFP aggregates being detected as large particles that appeared ‘more spherical’ (Figure 5.16F). Sulf1 enhances the average number of particles and overall levels of Wnt4-HA-GFP colocalising with the cell membrane. This is similar to the effects of Sulf1 on Wnt11b-HA-GFP, suggesting Sulf1 may play a similar role in regulating these two non-canonical ligands.

5.2.6 Sulf1 enhances the colocalisation of caveolin-GFP with Wnt11b-HA-Venus, but not Wnt8a-HA-Venus

Work in cell culture has shown that caveolin dependent endocytosis is required for canonical Wnt signalling (Bilic et al., 2007; Yamamoto et al., 2006), while

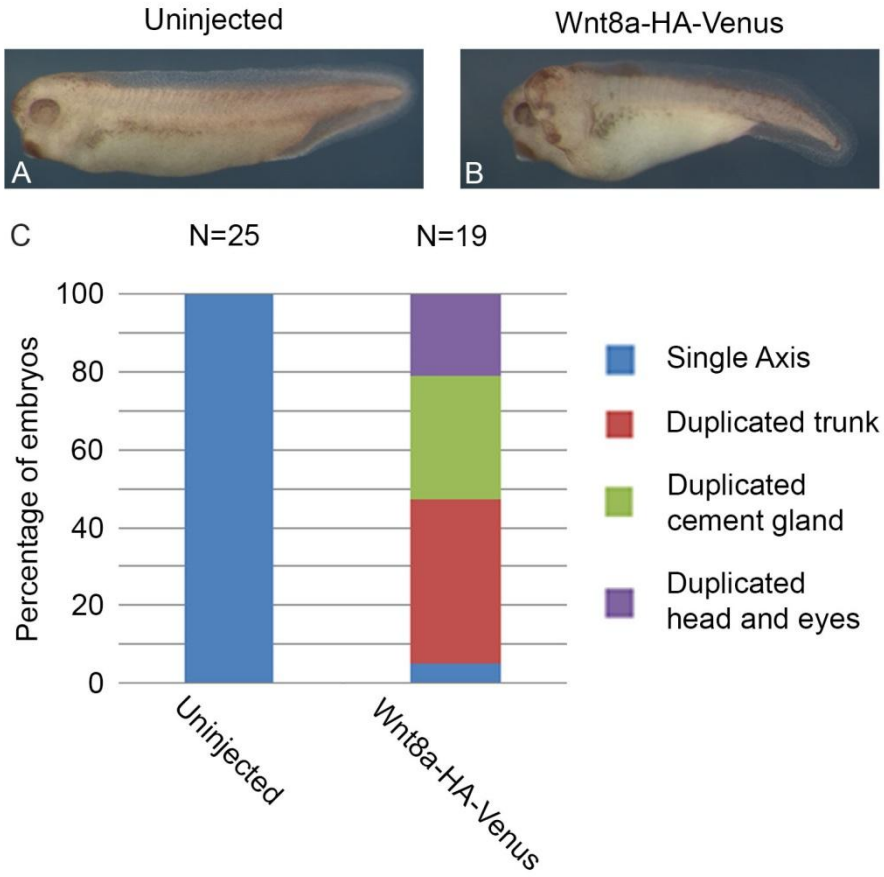

Figure 5.17; Wnt8a-HA-Venus is biologically active.
mRNA encoding *Wnt8a-HA-Venus* (10pg) was injected into one ventral blastomere of an embryo at the four cell stage. Embryos were cultured until NF stage 36/37 and then examined for phenotype. Lateral views of a [A] an uninjected embryo and [B] an embryo injected with *Wnt8a-HA-Venus*. Wnt8a-HA-Venus induces axis duplication in *Xenopus*. [C] Graph quantifying the frequency of axis duplication in embryos over-expressing Wnt8a-HA-Venus, N = number of embryos.

clathrin dependent endocytosis is important for non-canonical Wnt signalling (Kim and Han, 2007; Sato et al., 2009). To examine whether Sulf1 could alter the caveolin dependent internalisation of Wnt ligands, *Wnt8a* and *Wnt11b-HA-Venus* constructs were developed. These constructs were used instead of those published by Mii and Taira, (2009) as they have the same overall structure as Wnt8a and Wnt11b-HA-GFP, except Venus was used as the fluorescent tag. To investigate whether Wnt8a-HA-Venus was biologically active mRNA encoding *Wnt8a-HA-Venus* was microinjected into one ventral blastomere of an embryo at the four cell stage. Embryos were cultured until NF stage 36/37 and assessed for axis duplication. Over-expression of Wnt8a-HA-venus induced axis duplication (Figure 5.17B). The data from Figure 5.17A-B is

quantified in Figure 5.17C. Embryos injected with *Wnt8a-HA-Venus* predominantly displayed either trunk or cement gland duplication. In approximately 20% of cases, a full secondary head and eyes were detected. Wnt8a-HA-Venus is biologically active, although weaker in axis duplication assays than Wnt8a-HA-GFP (compare Figure 5.17 to Figure 5.10).

To determine the biological activity of Wnt11b-HA-Venus the Dvl-GFP localisation assay was performed. Embryos were microinjected bilaterally in the animal hemisphere with mRNA encoding *mRFP* and *Dvl-GFP*. In addition, embryos were microinjected with mRNA encoding *Sulf1, Sulf1 C-A, Wnt11b-HA-Venus* or a mixture of the three. Embryos were cultured until NF stage 8 and then animal cap explants were taken. Animal caps were cultured in the dark for four hours at 21˚C prior to imaging by confocal microscopy. Over-expression of Sulf1 C-A and Wnt11b-HA-Venus lead to the translocation of Dvl-GFP from the cytoplasm to the plasma membrane (Figure 5.18K-N). At the plasma membrane, Dvl-GFP puncta overlap with Wnt11-HA-Venus particles. Interestingly Dvl-GFP puncta do not always form aggregates opposite Wnt11b-HA-Venus particles, instead discreet spherical Dvl-GFP puncta were seen where Wnt11b-HA-Venus was not detected (Figure 5.18N). Over-expression of Sulf1 enhanced both the level of Wnt11b-HA-Venus colocalising with the cell membrane and Wnt11b-HA-Venus induced Dvl-GFP translocation (compare Figure 5.18K-N to 5.18O-S). In the presence of Sulf1, Dvl-GFP can be seen beginning to aggregate opposite Wnt11b-HA-Venus on the cell membrane. The data from Figure 5.18 is quantified in Figure 5.19. Wnt11b-HA-Venus is biologically active, but hypomorphic, similar to Wnt8a-HA-Venus. Sulf1 enhances the ability of Wnt11b-HA-Venus to activate non-canonical Wnt signalling.

Figure 5.18; Sulf1 enhances Wnt11b-HA-Venus induced Dvl-GFP translocation to the cell membrane.
mRNA encoding *mRFP* (500pg) and *Dvl-GFP* (500pg) was injected bilaterally into the animal hemisphere of embryos at the two cell stage. In addition embryos were injected with mRNA encoding *Sulf1* (4ng), *Sulf1 C-A* (4ng), *Wnt11b-HA-Venus* (1ng) or a mixture of the three. Embryos were cultured until NF stage 8 and then animal cap explants were taken and cultured for four hours at 21˚C prior to imaging by confocal microscopy. [A-E] Control animal caps over-expressing mRFP and Dvl-GFP. Animal caps over-expressing [F-J] Sulf1, [K-N] Sulf1 C-A and Wnt11b-HA-Venus and [O-S] Sulf1 and Wnt11b-HA-Venus. The white boxes in [D], [I], [N] and [S] mark the areas used to create panels [E], [J], [O] and [T] respectively. Over-expression of Sulf1 C-A and Wnt11b-HA-Venus caused Dvl-GFP to translocate to the cell membrane and this was enhanced by the over-expression Sulf1. mRFP (magenta), Dvl-GFP (green), Wnt11b-HA-Venus (yellow), scale bars represent 20µm.

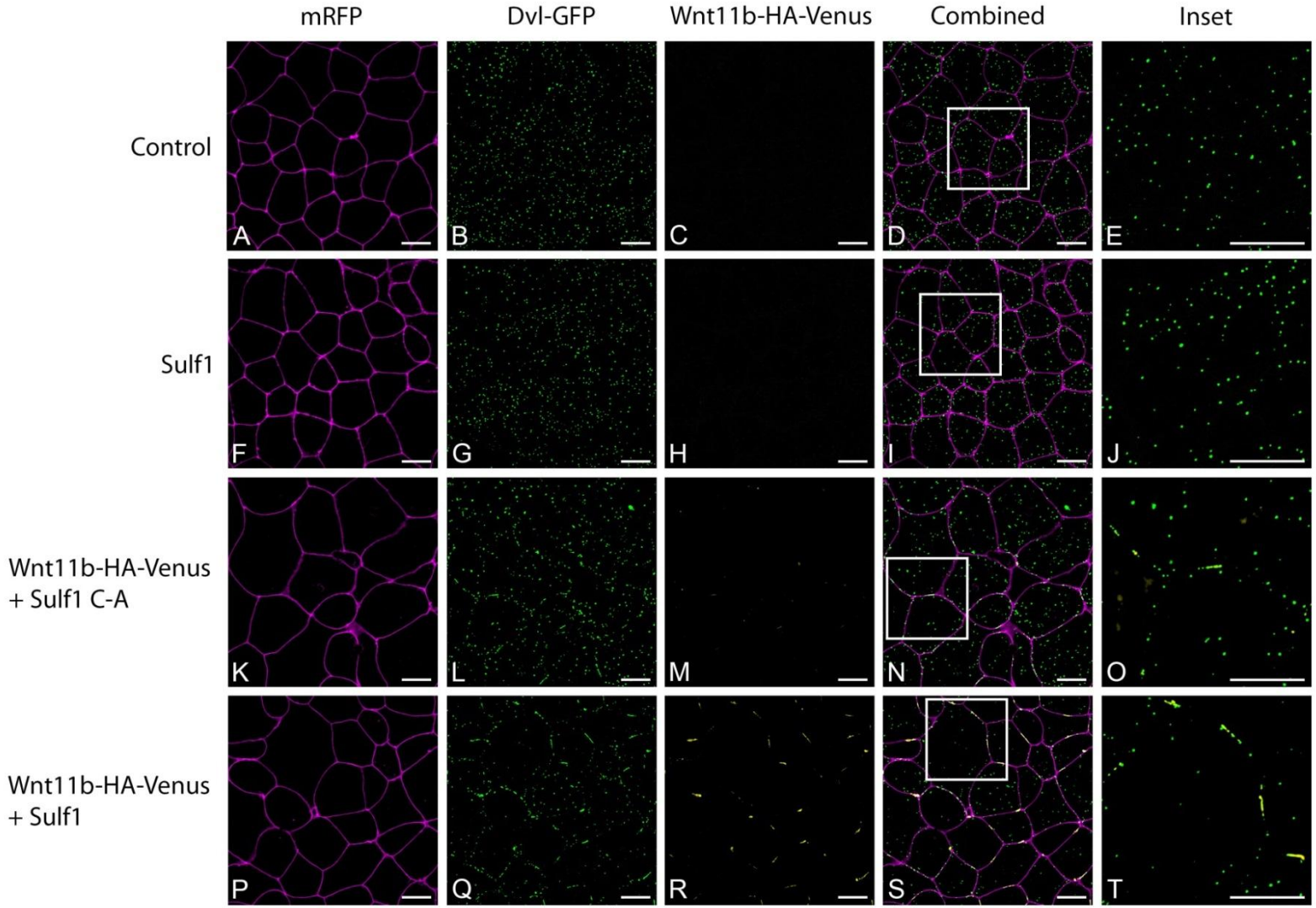
mRFP
Dvl-GFP
Wnt11b-HA-Venus
Combined
Inset
Control
Sulf1
Wnt11b-HA-Venus
+ Sulf1 C-A
Wnt11b-HA-Venus
+ Sulf1
A
B
C
D
E
F
G
H
I
J
K
L
M
N
O
P
Q
R
S
T

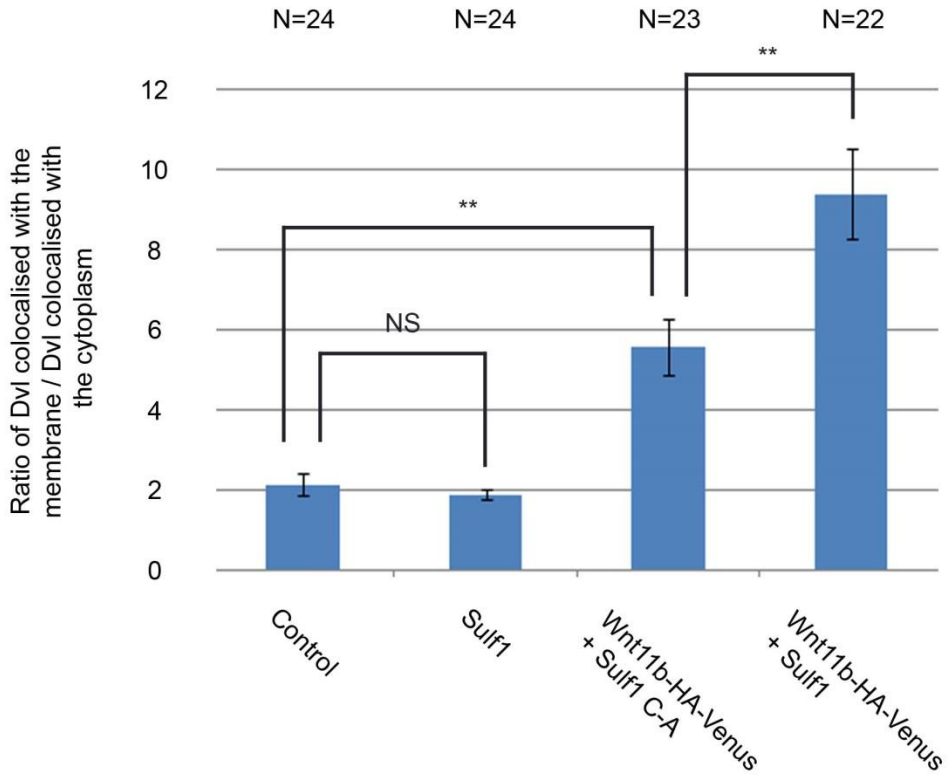

Figure 5.19; Graph illustrating the effects of Sulf1 on Wnt11b-HA-Venus induced Dvl-GFP translocation to the cell membrane.
Graph illustrating the data shown in Figure 5.18. Over-expression of Sulf1 C-A and Wnt11b-HA-Venus induced Dvl-GFP translocation to the plasma membrane and this was enhanced by the over-expression Sulf1. Asterisks mark significant differences (**P<0.01), NS marks non-significant differences, Mann-Whitney U, error bars represent s.e.m, N = number of embryos.

To examine whether Sulf1 altered the localisation of caveolin-GFP, embryos were microinjected bilaterally in the animal hemisphere with mRNA encoding *mRFP* and *caveolin-GFP*. In addition, embryos were microinjected with mRNA encoding *Sulf1 or Sulf1 C-A.* Embryos were prepared for confocal microscopy as describe previously. In the presence of Sulf1 C-A, caveolin-GFP is found in specific domains on the cell membrane and as spherical vesicles in the cytoplasm (Figure 5.20A-D). Over-expression of Sulf1 did not alter the distribution of caveolin-GFP (compare Figure 5.20E-H to 5.20A-D).

To investigate a potential role for Sulf1 in regulating the caveolin dependent internalisation of Wnt ligands, embryos were microinjected bilaterally in the animal hemisphere with mRNA encoding *mRFP* and *caveolin-GFP*. In addition, embryos were microinjected with mRNA encoding *Sulf1, Sulf1 C-A, Wnt8a/Wnt11b-HA-Venus* or a mixture of the four. Embryos were prepared for

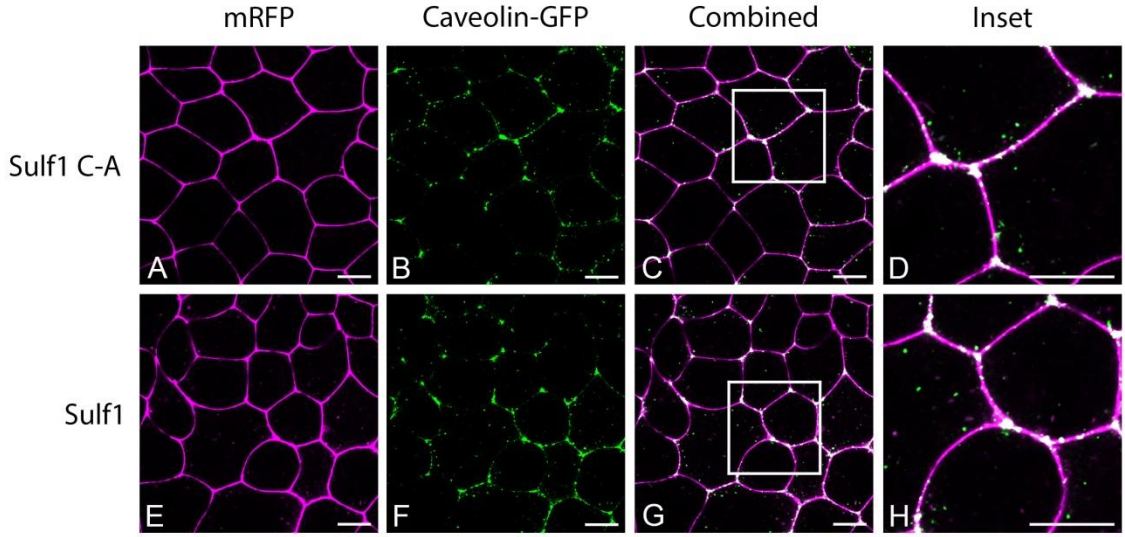

Figure 5.20; Sulf1 does not affect the localisation of caveolin-GFP.
mRNA encoding *mRFP* (500pg) and *caveolin-GFP* (500pg) was injected bilaterally into the animal hemisphere of embryos at the two cell stage. In addition embryos were injected with mRNA encoding *Sulf1* (4ng) or *Sulf1 C-A* (4ng). Embryos were cultured until NF stage 8 and then animal cap explants were taken and cultured for four hours at 21˚C prior to imaging by confocal microscopy. [A-D] Control animal caps over-expressing Sulf1 C-A, [E-H] animal caps over-expressing Sulf1. The white boxes in [C] and [G] mark the areas used to create panels [D] and [H] respectively. Over-expression of Sulf1 did not alter the pattern of caveolin-GFP in *Xenopus* animal caps compared to control conditions. mRFP (magenta), caveolin-GFP (green), scale bars represent 20μm.

confocal microscopy as describe previously. In control conditions Wnt8a-HA-Venus colocalised with caveolin-GFP on the cell membrane (Figure 5.21A-E). Over-expression of Sulf1 did not alter the proportion of Wnt8a-HA-Venus overlapping with caveolin-GFP on the cell surface (compare Figure 5.21F-J to 5.21A-E). Wnt11b-HA-Venus was present at low levels on the cell surface in control conditions. Wnt11b-HA-Venus puncta did colocalise with caveolin-GFP on the membrane, but at a lower frequency than was found for Wnt8a-HA-Venus (compare Figure 5.21K-O to 5.21A-E). Over-expression of Sulf1 increased the levels of Wnt11b-HA-Venus on the membrane and the colocalisation of Wnt11b-HA-Venus and caveolin-GFP (compare Figure 5.21P-T to 5.21K-O).

The data from Figure 5.21 is quantified in Figure 5.22. Fiji image J was used to calculate the Manders coefficients for the colocalisation Wnt8a/Wnt11b-HA-Venus with caveolin-GFP (see methods 2.5.4 for details). Briefly, each image was split into separate channels and thresholded using the Auto threshold function. Images were then analysed using the Coloc 2 function in image J.

Figure 5.21; Sulf1 does not affect the colocalisation of Wnt8a-HA-Venus or Wnt11b-HA-Venus with caveolin-GFP.
mRNA encoding mRFP (500pg) and caveolin-GFP (500pg) were injected bilaterally into the animal hemisphere of embryos at the two cell stage. Embryos were also injected with mRNA encoding *Wnt8a-HA-Venus* (1ng), *Wnt11b-HA-Venus* (1ng), *Sulf1 C-A* (4ng), *Sulf1* (4ng) or a mixture of the four. Embryos were cultured until NF stage 8 and then animal cap explants were taken and cultured for four hours at 21˚C prior to imaging by confocal microscopy. [A-J] Animal caps over-expressing Wnt8a-HA-Venus and [A-E] Sulf1 C-A or [F-J] Sulf1. [K-T] Animal caps over-expressing Wnt11b-HA-Venus and [K-O] Sulf1 C-A or [P-T] Sulf1. The white boxes in [D], [I], [N] and [S] mark the areas used to created [E], [J], [O] and [T] respectively. Sulf1 does not affect the colocalisation of Wnt8a-HA-Venus, or Wnt11b-HA-Venus with caveolin-GFP. mRFP (magenta), caveolin-GFP (green), Wnt-HA-Venus (yellow), scale bars represent 20μm.

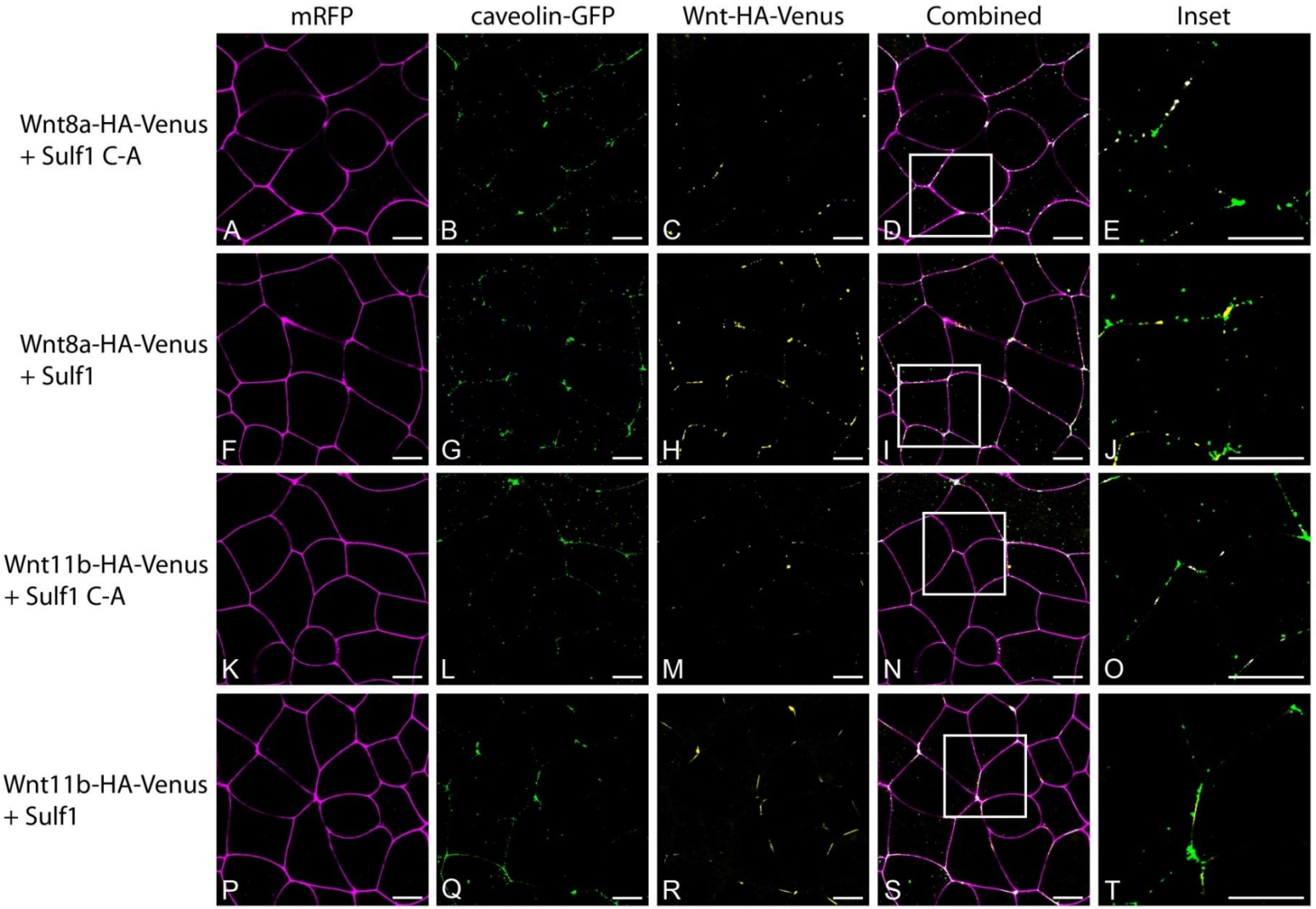
mRFP
caveolin-GFP
Wnt-HA-Venus
Combined
Inset
Wnt8a-HA-Venus
+ Sulf1 C-A
Wnt8a-HA-Venus
+ Sulf1
Wnt11b-HA-Venus
+ Sulf1 C-A
Wnt11b-HA-Venus
+ Sulf1
A
B
C
D
E
F
G
H
I
J
K
L
M
N
O
P
Q
R
S
T

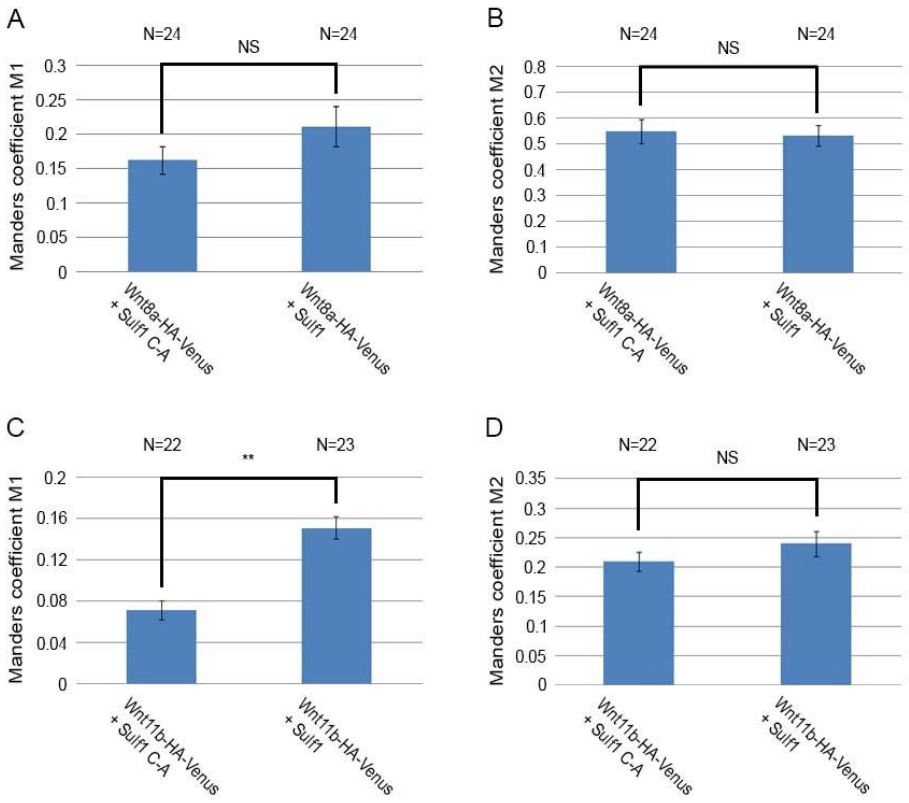

Figure 5.22; Graphs illustrating the effects of Sulf1 on the colocalisation of Wnt8a-HA-Venus and Wnt11b-HA-Venus with caveolin-GFP.
Graph illustrating the data shown in figure 5.21. Fiji image J was used to calculate the Manders coefficients for the colocalisation for Wnt8a-HA-Venus and Wnt11b-HA-Venus (see methods 2.5.4 for details). [A and C] Colocalisation of caveolin-GFP with [A] Wnt8a-HA-Venus and [C] Wnt11b-HA-Venus. [B and D] Colocalisation of [B] Wnt8a-HA-Venus and [D] Wnt1b-HA-Venus with caveolin-GFP. Asterisks mark significant differences ($P<0.01$), NS marks non-significant differences, Mann-Whitney U, error bars represent s.e.m, N = number of embryos.

The values plotted represent the colocalisation of Wnt8a/Wnt11b-HA-Venus with caveolin-GFP. Colocalisation between caveolin-GFP and Wnt8a and Wnt11b-HA-Venus was determined using the Manders coefficients M1 and M2. It was important to use Manders coefficients, as the total number of objects being analysed in the caveolin-GFP and Wnt8a/Wnt11b-HA-Venus channels was not equal. Pearson's correlation coefficient can also be used to describe colocalisation, however it is less useful when the numbers of objects being analysed are unequal. For example if you have 20 red dots and 20 green dots with 10 dots from each category colocalising then the pearson's correlation coefficient is 0.5. However if you have 20 red dots, but only 5 green dots and all of the green dots overlap with red dots then the pearson's correlation coefficient still comes out at 0.5. In contrast using Manders coefficients you get a value for the colocalisation of red with green

(M1 = 0.25) and a value for the colocalisation of green with red (M2 = 1). In this scenario using Manders correlation coefficients provides more information about the data being analysed.

In control conditions approximately 15% of caveolin-GFP pixels colocalised with Wnt8a-HA-Venus (M1) and 50% of Wnt8a-HA-Venus pixels colocalised with caveolin-GFP (M2, Figure 5.22A-B). In contrast only 8% of caveolin-GFP pixels colocalised with Wnt11b-HA-Venus (M1) and 20% of Wnt11b-HA-Venus pixels colocalised with caveolin-GFP (M2, Figure 5.22C-D). Over-expression of Sulf1 did not alter either M1 or M2 for Wn8a-HA-Venus. In contrast over-expression of Sulf1 lead to an increase in M1, but not M2, for Wnt11b-HA-Venus. Over-expression of Sulf1 increased the percentage of caveolin-GFP colocalising with Wnt11b-HA-Venus.

5.2.7 Sulf1 does not affect the colocalisation of Wnt8a-HA-GFP and Wnt11b-HA-Venus

Work by Cha et al., (2008) demonstrated that Wnt11b-HA and Wnt5a-myc were able to form homodimers, but not heterodimers in *Xenopus* embryos. To investigate whether Wnt8a and Wnt11b could interact, the colocalisation Wnt8a-HA-GFP and Wnt11b-HA-Venus was examined in *Xenopus* animal caps. Embryos were microinjected bilaterally in the animal hemisphere with mRNA encoding *mRFP, Wnt8a-HA-GFP* and *Wnt11b-HA-Venus*. In addition embryos were microinjected with mRNA encoding *Sulf1* or *Sulf1 C-A.* Embryos were prepared for confocal microscopy as describe previously. Wnt8a-HA-GFP and Wnt11b-HA-Venus displayed a high degree of colocalisation in control conditions (Figure 5.23A-E). Over-expression of Sulf1 did not alter the colocalisation of Wnt8a-HA-GFP and Wnt11b-HA-Venus (compare Figure 5.23F-J to 5.23A-E). Sulf1 does not affect the colocalisation of Wnt8a-HA-GFP and Wnt11b-HA-Venus when all three are over-expressed together (compare Figure 5.23 to Figure 5.13). The data from Figure 5.23A-J was quantified in Figure 5.23K-L. The Coloc 2 function of Fiji Image J was used to generate the data, see methods 2.5.4 for details. M1 represents the colocalisation between Wnt8a-HA-GFP and

Figure 5.23; Sulf1 does not affect the colocalisation of Wnt8a-HA-GFP and Wnt11b-HA-Venus.
mRNA encoding *mRFP* (500pg), *Wnt8a-HA-GFP* (1ng) and *Wnt11b-HA-Venus* (1ng) was injected bilaterally into the animal hemisphere of embryos at the two cell stage. Embryos were also injected with mRNA encoding either *Sulf1 C-A* (4ng) or *Sulf1* (4ng). Embryos were cultured until NF stage 8 and then animal cap explants were taken and cultured for four hours at 21˚C prior to imaging by confocal microscopy. [A-E] Control animal caps over-expressing Sulf1 C-A and [F-J] animal caps over-expressing Sulf1. The white boxes in [D] and [I] mark the areas used to created [E] and [J] respectively. In both control and Sulf1 over-expressing conditions, Wnt8a-HA-GFP and Wnt11b-HA-Venus showed a high degree of colocalisation. [K-L] Graphs quantifying the colocalisation of Wnt8a-HA-GFP and Wnt11b-HA-Venus. [K] Over-expression of Sulf1 does not alter the colocalisation between Wnt8a-HA-GFP and Wnt11b-HA-Venus. [L] Sulf1 does not alter the colocalisation between Wnt11b-HA-Venus and Wnt8a-HA-GFP. mRFP (magenta), Wnt8a-HA-GFP (green), Wnt11b-HA-Venus (yellow), scale bars represent 20µm. (NS) marks non-significant differences, Mann-Whitney U, error bars represent s.e.m, N = Number of embryos.

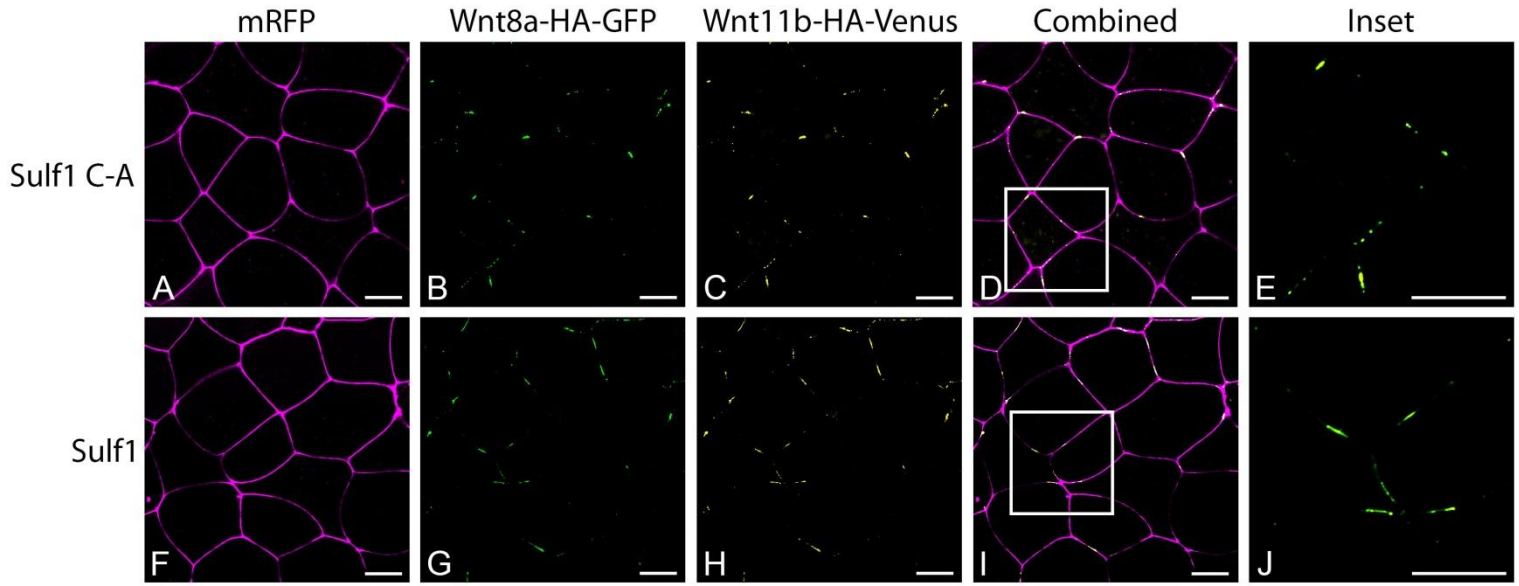
mRFP
Wnt8a-HA-GFP
Wnt11b-HA-Venus
Combined
Inset
Sulf1 C-A
Sulf1
A
B
C
D
E
F
G
H
I
J

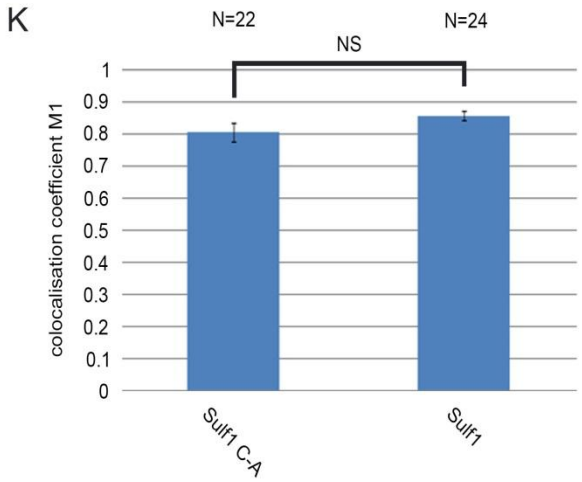
K
N=22
N=24
NS
colocalisation coefficient M1
1
0.9
0.8
0.7
0.6
0.5
0.4
0.3
0.2
0.1
0
Sulf1 C-A
Sulf1

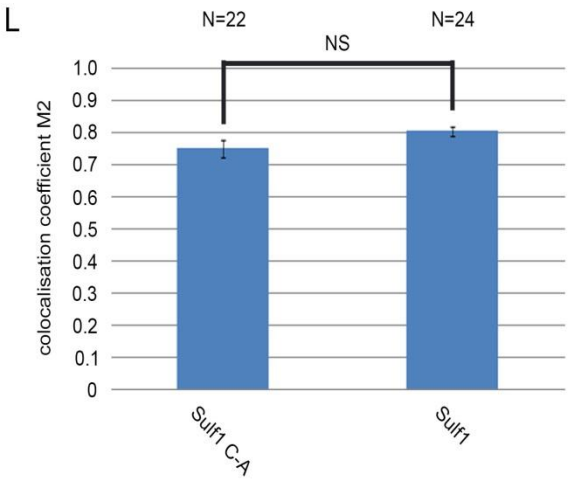
L
N=22
N=24
NS
colocalisation coefficient M2
1.0
0.9
0.8
0.7
0.6
0.5
0.4
0.3
0.2
0.1
0
Sulf1 C-A
Sulf1

Wnt11b-HA-Venus and M2 represents the colocalisation between Wnt11b-HA-Venus and Wnt8a-HA-GFP. Approximately 80% of Wnt8a-HA-GFP particles colocalised with Wnt11-HA-Venus in control (Sulf1 C-A) conditions (Figure 5.23K). Approximately 75% of Wnt11b-HA-Venus particles colocalised with Wnt8a-HA-GFP (Figure 5.23L). Over-expression of Sulf1 did not alter the colocalisation of Wnt8a-HA-GFP and Wnt11b-HA-Venus.

5.2.8 Sulf1 enhances the range of Wnt8a and Wnt11b-HA-GFP ligand diffusion

The data thus far has shown that Sulf1 enhances the levels of Wnt11b-HA-GFP on the cell membrane and causes a qualitative change in the shape of Wnt8a and Wnt11b-HA-GFP particles. In addition, Sulf1 enhanced the colocalisation between Wnt11b-HA-Venus and caveolin-GFP, but did not alter the colocalisation between Wnt8a-HA-GFP and Wnt11b-HA-Venus. To investigate a role for Sulf1 in Wnt ligand diffusion, an assay to measure diffusion was developed. Embryos were microinjected with mRNA encoding either *mCerulean* (a farnesylated version of cerulean) or *mRFP* together with *Wnt8a/Wnt11b-HA-GFP* into one blastomere of an embryo at the four cell stage. In addition, embryos were microinjected in the same cell with mRNA encoding either *LacZ, Sulf1 C-A,* or *Sulf1.* Embryos were prepared for confocal microscopy as described previously. The distance that Wnt8a/Wnt11b-HA-GFP could diffuse away from cells expressing it was then analysed (see Figure 5.24 for a diagram).

Wnt8a-HA-GFP is capable of diffusing 2-3 cell diameters away from cells expressing it, when over-expressed together with LacZ (Figure 5.24B). A high laser power was used to visualise Wnt8a/Wnt11b-HA-GFP diffusing away from cells expressing the ligands. Consequently, cells expressing Wnt8a/Wnt11b-HA-GFP appear bright green. Over-expression of either Sulf1 or Sulf1 C-A in the same cell as Wnt8a-HA-GFP enhanced the range of Wnt8a-HA-GFP diffusion (compare Figure 5.24C and 5.24D to 5.24B). In contrast to Wnt8a-HA-GFP, Wnt11b-HA-GFP shows little diffusion in control conditions (LacZ) (compare Figure 5.24E to 5.24B). Over-expression of either Sulf1 or Sulf1 C-A together with Wnt11b-HA-GFP dramatically

Figure 5.24; Sulf1 enhances the range of Wnt8a/Wnt11b-HA-GFP diffusion when expressed in the same cells.
[A] Diagram illustrating the assay used to investigate the effects of Sulf1 on the range of Wnt8a/Wnt11b-HA-GFP diffusion. mRNA encoding either *mCerulean* (600pg) or *mRFP* (600pg) was injected together with mRNA encoding *Wnt8a*/*Wnt11b-HA-GFP* (2ng) into the animal hemisphere of one blastomere of an embryo at the four cell stage. In addition mRNA encoding *LacZ* (4ng), *Sulf1 C-A* (4ng) or *Sulf1* (4ng) was injected into the same cell. Embryos were cultured until NF stage 8 and then animal cap explants were taken and cultured for four hours at 21˚C prior to imaging by confocal microscopy. The distance that Wnt8a/Wnt11b-HA-GFP could diffuse away from the cell expressing was then analysed. [B-C] Embryos injected with *mCerulean*, *Wnt8a-HA-GFP* and [B] *LacZ* or [C] *Sulf1C-A.* [D] Embryo injected with *mRFP*, *Wnt8a-HA-GFP* and *Sulf1.* [E-F] Embryos injected with *mCerulean*, *Wnt11b-HA-GFP* and [E] *LacZ* or [F] *Sulf1 C-A.* [G] Embryo injected with *mRFP*, *Wnt11b-HA-GFP* and *Sulf1.* Sulf1 enhances the range of diffusion of both Wnt8a-HA-GFP and Wnt11b-HA-GFP in animal caps. mCeurlean (blue), Wnt-HA-GFP (green) and mRFP (magenta), scale bars represent 20μm. A high laser power was used to visualise Wnt8a/Wnt11b-HA-GFP diffusing away from cells expressing the ligands, consequently the cells expressing Wnt8a/Wnt11b-HA-GFP appear bright green.

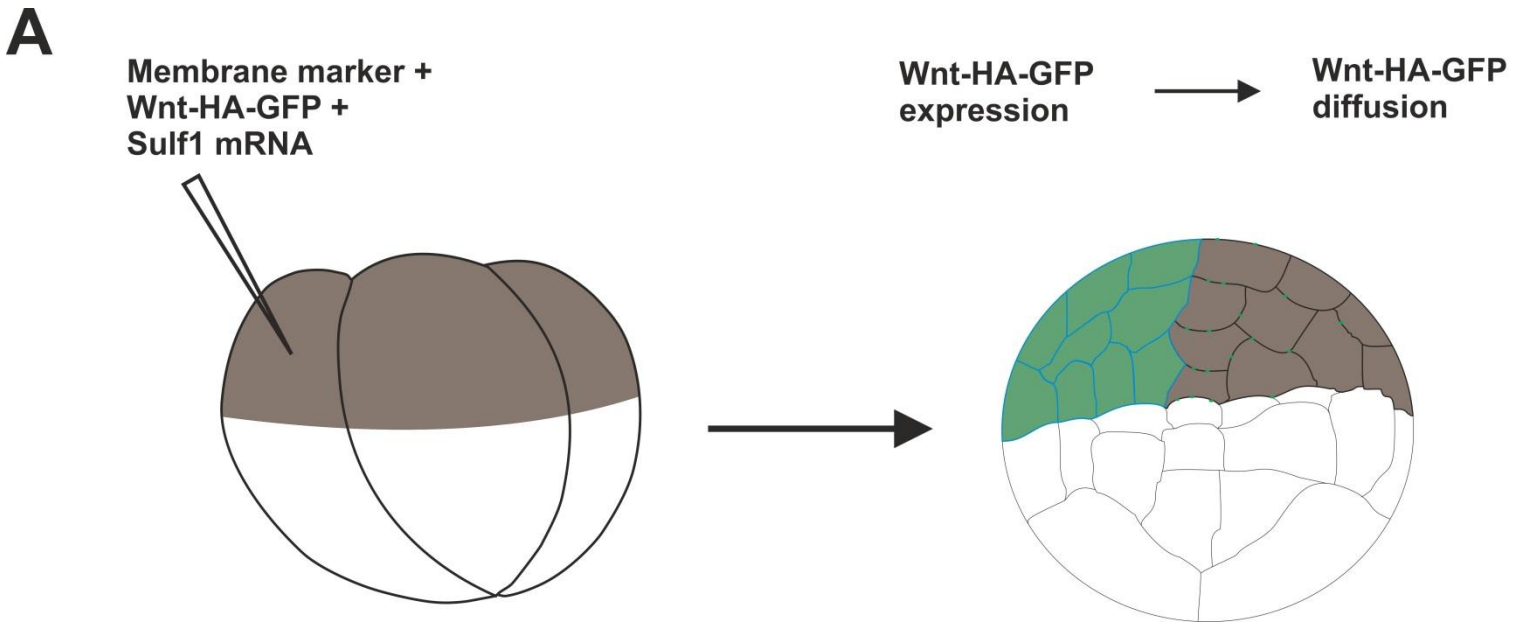

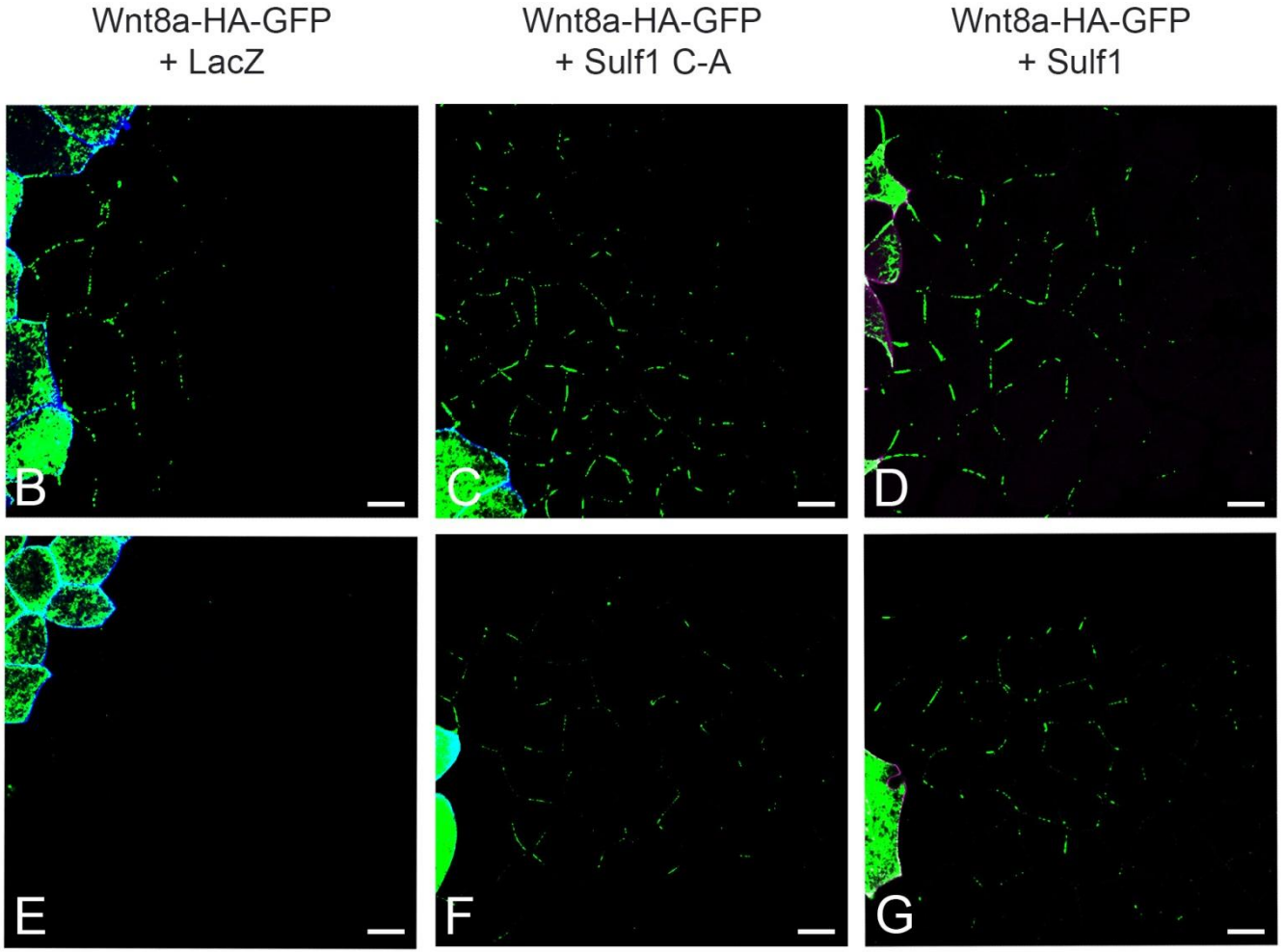
Wnt8a-HA-GFP
+ LacZ
Wnt8a-HA-GFP
+ Sulf1 C-A
Wnt8a-HA-GFP
+ Sulf1
B
C
D
E
F
G
Wnt11b-HA-GFP
+ LacZ
Wnt11b-HA-GFP
+ Sulf1 C-A
Wnt11b-HA-GFP
+ Sulf1

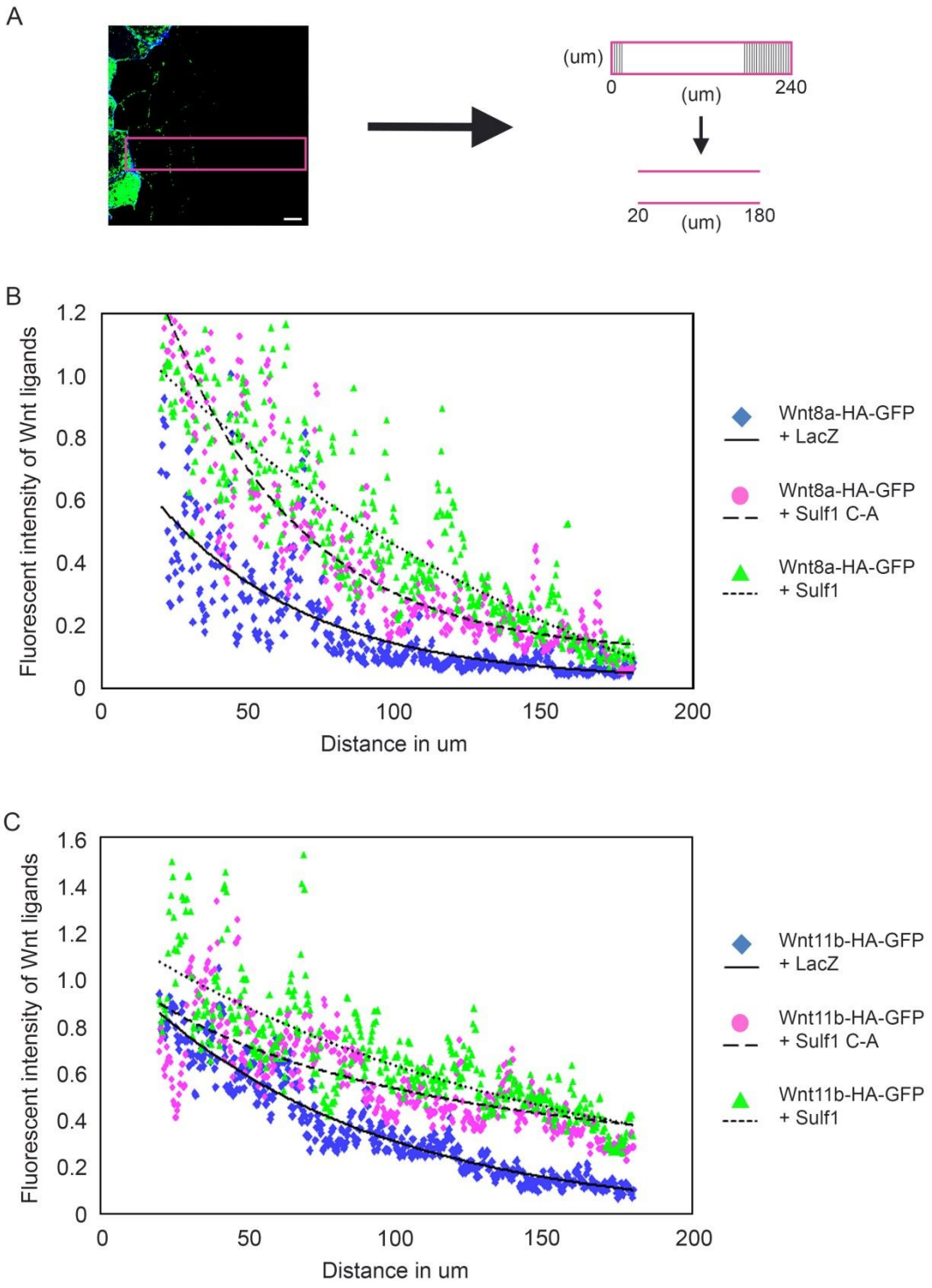

Figure 5.25; Graphs illustrating the effects of Sulf1 on Wnt8a/Wnt11b-HA-GFP diffusion

[A] Diagram of how each image was prepared for analysis using Fiji image J, see methods 2.5.5 for details. [B] Plots illustrating the effects of Sulf1 and Sulf1 C-A on the amount of Wnt8a-HA-GFP diffusing over the 160µm analysed. Plots were prepared using data from a minimum number of 23 embryos per condition. Curves were fit in Sigmaplot 12.5 using a single exponential decay model with three parameters. [C] Plots illustrating the effects of Sulf1 and Sulf1 C-A on the amount of Wnt11b-HA-GFP diffusing over the 160µm analysed. Plots were prepared using data from a minimum number of 20 embryos per condition. Curves were fit in Sigmaplot 12.5 using a single exponential decay model with three parameters for the LacZ and Sulf1 curves and a hyperbolic decay model with two parameters for the Sulf1 C-A curve.

Increased the range of diffusion of Wnt11b-HA-GFP (compare Figure 5.24F and 5.24G to 5.24E). Sulf1 and Sulf1 C-A enhanced the range of Wnt8a and Wnt11b-HA-GFP diffusion in this assay.

Fiji image J was used to quantify the range of diffusion of Wnt8a and Wnt11b-HA-GFP in animal caps (see methods 2.5.5 for details). Identical imaging conditions were used to collect the data for Figures 5.24-5.25 and the intensity of the green channel was not altered during the analysis. Briefly, each image was orientated so that the maximum distance of Wnt-HA-GFP diffusion could be measured. A box measuring 100pixels X 650pixels was placed on each image and the blue and red channels of each image were set to 0. The average fluorescent intensity of GFP per pixel inside the box was then obtained using the Multi plot function of Fiji image J. As illustrated in Figure 5.25A, the measurement of Wnt-HA-GFP diffusion could not always begin from a flat surface. Because of this the measuring box was deliberately drawn so that the start of the box overlapped with the high levels of GFP in Wnt-HA-GFP expressing cells. High levels of GFP in the expressing cells distorted the diffusion plots, so to address this the first 20µm of each box was not plotted. Pilot studies revealed that due to the curved nature of an animal cap 180µm was the maximum distance that could be reliably measured. This meant that the maximum distance of Wn8a and Wnt11b-HA-GFP diffusion could not be analysed. Instead, the levels of Wnt8a and Wnt11b-HA-GFP signal intensity were measured over a 160µm distance. A diagram of the parameters used to measure Wnt-HA-GFP diffusion can be seen (Figure 5.25A)

Scatter graphs were plotted to analyse the diffusion of Wnt-HA-GFP away from either control regions, or regions over-expressing Sulf1. The graphs were plotted using data obtained from a minimum of 20 embryos per condition, over 4 separate experiments. The average pixel intensity of GFP with increasing distance from the source was plotted for each condition. Curves were fitted to the scatter plots using the regression wizard in SigmaPlot 12.5 (see methods 2.5.5 for details). Five of the curves shown in Figure 5.25 were plotted using the exponential decay equation $F=Y0+A*EXP^{(-bX)}$. However, Wnt11b-HA-GFP diffusing away from a region

Table 5.2; Parameters of the curves shown in Figure 5.25

Condition	Equation of the curve	Predicted Y max (pixel intensity)	Predicted Y min (pixel intensity)	Predicted Y half-life (pixel intensity)	Predicted X half-life (μm)
Wnt8a-HA-GFP + LacZ	F=0.0213+0.8287*EXP(-0.0195*X)	0.582 (CI 0.531-0.627)	0.046 (CI 0.033-0.07)	0.314 (CI 0.282-0.349)	53.33 (CI 48.31-59.88)
Wnt8a-HA-GFP + Sulf1 C-A	F=0.1042+1.7894*EXP(-0.0222*X)	1.252 (CI 0.531-0.627)	0.137 (CI 0.165-0.115)	0.695 (CI 0.65-0.74)	49.95 (CI 47-53.6)
Wnt8a-HA-GFP + Sulf1	F=-0.05276+1.782*EXP(-0.0057*X)	1.014 (CI 0.317-1.684)	0.092 (CI 0.389--0.205)	1.036 (CI 0.056-1.036)	75.71 (CI 75.71-89.56)
Wnt11b-HA-GFP + LacZ	F=-0.0214+1.1182*EXP(-0.0124*X)	0.851 (CI 0.803-0.9)	0.099 (CI 0.087-0.121)	0.475 (CI 0.445-0.511)	65.51 (CI 62.28-69.27)
Wnt11b-HA-GFP + Sulf1 C-A	F=(1.0752*96.6022)/(96.6022*X)	0.89 (CI 0.81-0.97)	0.38 (0.31-0.44)	0.633 (CI 0.56-0.705)	67.45 (CI 64.79-69.73)
Wnt11b-HA-GFP + Sulf1	F=0.0523+1.1704*EXP(-0.0071*X)	1.068 (CI 0.633-1.479)	0.378 (CI 0.25-0.555)	0.723 (CI 0.442-1.017)	78.41 (CI 69.50-88.64)

Asterisks = multiplication terms

EXP = inverse natural Log

X = values on the X axis (distance in μm from the source)

CI = 95% confidence intervals

Red text marks the Wnt11b-HA-GFP + Sulf1 C-A curve, which was fit with a different type of model to all of the other data

expressing Sulf1 C-A was plotted using a hyperbolic decay model, F=(A*B)/(B*X) (Figure 5.25). Parameters for each of the curves can be seen in Table 5.2. The rate of decay for each of the exponential curves is predicted by the decay constant (¯b). The more negative the value of b, the faster the rate of decay. The decay constant for Wnt8a-HA-GFP diffusing away from a region expressing LacZ is ¯0.0195. In contrast over-expression of Sulf1 reduced the rate of Wnt8a-HA-GFP decay to ¯0.0057. Sulf1 is reducing the rate of Wnt8a-HA-GFP decay, allowing the ligand to diffuse further from the region over-expressing it. This is reflected in the predicted half-lives (T1/2), for control (LacZ) and Suf1 over-expressing conditions. In control conditions the predicted T1/2 for Wnt8a-HA-GFP is 53.33µm. Over-expressing Sulf1 resulted in an increase in the predicted T1/2 to 75.71µm. Wnt8a-HA-GFP diffusing away form an area expressing Sulf1 C-A had a similar rate of decay (¯0.022) and predicted T/2 (49.95µm) to that of Wnt8a-HA-GFP in control conditions. However, the predicted minimum Y value at 180µm, for Wnt8a-HA-GFP in Sulf1 C-A conditions, was over double that Wnt8a-HA-GFP in control conditions (0.137 compared to 0.046). One prediction from this is that Sulf1 C-A is extending the range of Wnt8a-HA-GFP diffusion without altering the rate of ligand decay. It was difficult to compare the Y minimum value for Sulf1, as the 95% confidence intervals predict that this value could be anywhere in the range of 0.389-¯0.205.

The decay rate of Wnt11b-HA-GFP in control (LacZ over-expressing) conditions was ¯0.0124. This was less negative than that of Wnt8a-HA-GFP in control conditions, suggesting that Wnt11b-HA-GFP decays at a slower rate than Wnt8a-HA-GFP (see Figure 5.25 and Table 5.2). However Wnt11b-HA-GFP, had a higher Y minimum at 180µm than Wnt8a-HA-GFP (compare 0.099-0.046), indicating that Wnt11b-HA-GFP is able to diffuse further than Wnt8a-HA-GFP in control conditions. Over-expression of Sulf1 reduced the rate of Wnt11b-HA-GFP decay and enhanced the T1/2 of Wnt11b-HA-GFP form 65.51-78.41µm. The data for Wnt11b-HA-GFP diffusing away from a region over-expressing Sulf1 C-A did not fit an exponential decay model well. Consequently it is difficult to compare this curve to the others plotted. One prediction from this though is that Sulf1 C-A is altering the diffusion of Wnt11b-HA-GFP, as it is no longer able to be fitted

using an exponential decay model. The Y minimum value of Wnt11b-HA-GFP in Sulf1 C-A conditions was higher than that of Wnt11b-HA-GFP in control conditions (compare 0.38-0.099), however the T1/2s were similar (compare 67.45-65.51). These findings are similar for those for Wnt8a-HA-GFP. The data suggests that Sulf1 decreases the rates of decay, but enhances the range of diffusion for both Wnt8a and Wnt11b-HA-GFP. In contrast, Sulf1 C-A enhanced the range of diffusion of both Wnt8a and Wnt11b-HA-GFP, without affecting the rate of decay of either ligand. One prediction from this is that Sulf1 has a catalytic domain independent role in regulating Wnt8a and Wnt11b-HA-GFP secretion/diffusion in *Xenopus*. This would agree with findings in chapter 4, which demonstrated Sulf1 C-A to be a hypomorphic mutant.

5.2.9 Sulf1 does not affect the dimerization of Wnt8a and Wnt11b-HA in non-reducing conditions.

Sulf1 enhances the diffusion of Wnt8a and Wnt11b-HA-GFP in *Xenopus* animal explants. Norrin is a Wnt agonist that regulates vascular development in the eye and ear through interactions with Fz4 (Xu et al., 2004). Norrin is a cysteine knot protein, which can assemble into dimers/oligomers using disulphide bridges (Perez-Vilar and Hill, 1997). Work by Cha et al., (2008) demonstrated that Wnt8a-HA and Wnt11b-HA were able to form dimers under non-reducing conditions in *Xenopus*. Western blotting was used to detect Wnt ligands of different molecular weights that might indicate oligomer formation. mRNA encoding *Wnt8a-HA, Wnt11b-HA, Sulf1* or a mixture of the three was injected bilaterally into the animal hemisphere of embryos at the two cell stage. Embryos were cultured until NF stage 8 and then animal caps were taken and cultured until NF stage 10.5. Animal caps were then snap frozen for western blot. Samples were prepared using either the standard or a non-reducing loading buffer (see methods 2.1.2 for details), and then run on a denaturing gel.

Under reducing conditions Wnt8a-HA was detected as a doublet with a major band between 55 and 40Kda and a minor band just below 40Kda (Figure 5.26A). Under non-reducing conditions the Wnt8a doublet is present, but

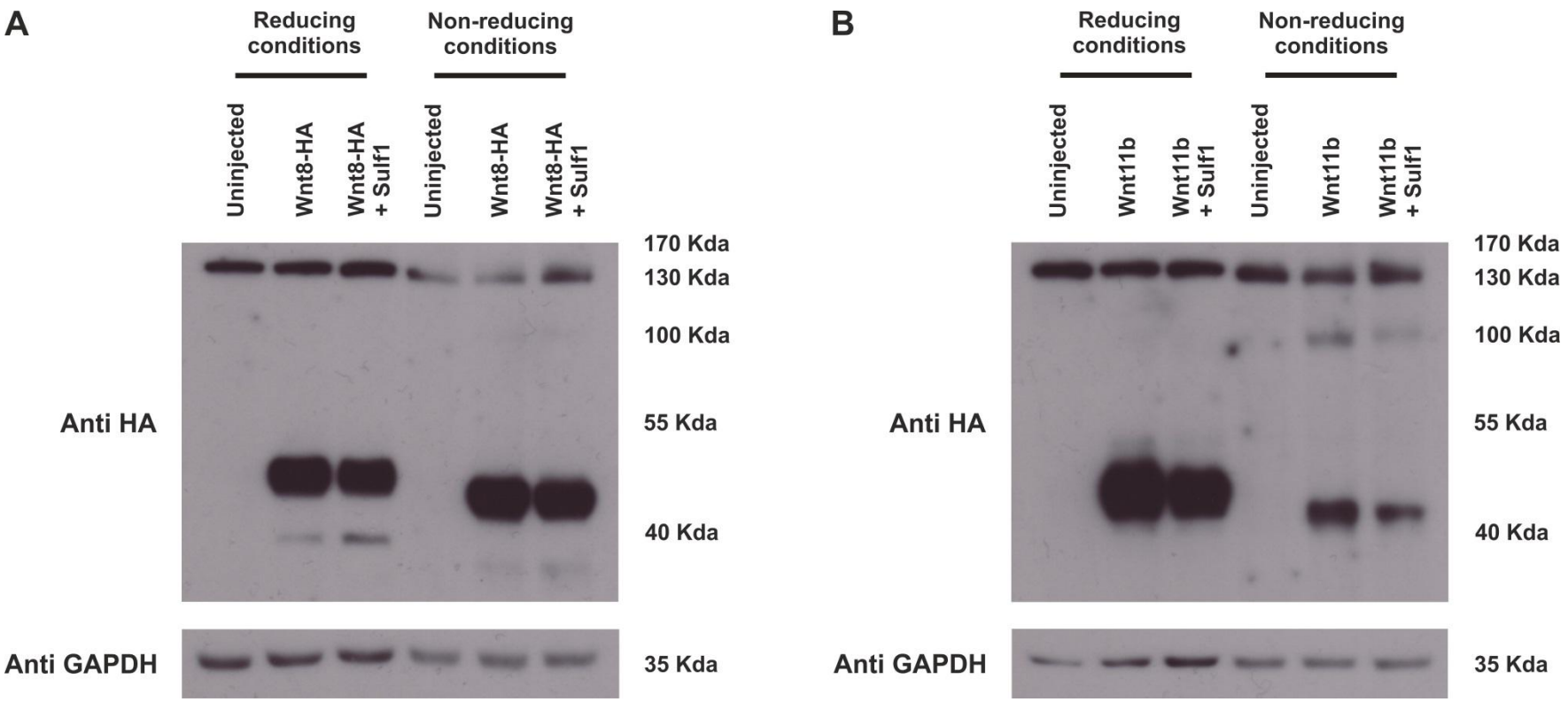

Figure 5.26; Sulf1 does not affect Wnt8a-HA or Wnt11b-HA complex formation under non-reducing conditions.
mRNA encoding *Wnt8a-HA* (500pg), *Wnt11b-HA* (500pg), *Sulf1* (4ng) or a mixture of the three were injected bilaterally into the animal hemisphere of embryos at the two cell stage. Embryos were cultured until NF stage 8 and then animal caps were taken and cultured until NF stage 10.5. Animal caps were then snap frozen for western blot. Samples were prepared using a standard or non-reducing loading buffer (see methods 2.3.15 for details), and then run on a denaturing gel. Animal caps over-expressing [A] Wnt8a-HA and Sulf1 and [B] Wnt11b-HA and Sulf1. Sulf1 does not affect the speed of migration or size of Wnt8a and Wnt11b-HA complexes.

Wnt8a-HA migrated faster on the gel. Sulf1 did not alter the oligomerization of Wnt8a-HA complexes. Under non-reducing conditions, Wnt11b-HA is present as a single band between 55 and 40Kda in size (Figure 5.26B). Under reducing conditions a second, high weight band can be seen for Wnt11b-HA between 130 and 100Kda. Sulf1 did not alter the migration speed of Wnt11b-HA or the size of Wnt11b-HA complexes. One prediction from this is that Sulf1 does not affect the oligomerization of Wnt8a/Wnt11b-HA by altering disulphide bridge formation.

5.2.10 Sulf1 regulates the stability/diffusion of Wnt8a and Wnt11b-HA-GFP in cells receiving the ligands

Thus far this thesis has examined the effects of Sulf1 on Wnt signalling when Wnt and Sulf1 are over-expressed together in the same cells. In contrast, work in cell culture has examined the effects of Sulf1 in cells receiving, but not producing Wnt ligands (Ai et al., 2003; Dhoot et al., 2001; Tang and Rosen, 2009). To investigate the effects of Sulf1 on Wnt ligand diffusion in cells receiving Wnt, the diffusion assay from Figure 5.24 was modified. mRNA encoding *mCerulean* (600pg) and *Wnt8a/Wnt11b-HA-GFP* (2ng) was injected into the animal hemisphere of one blastomere of an embryo at the four cell stage. mRNA encoding *mRFP* (600pg) and *LacZ* (4ng), *Sulf1 C-A* (4ng) or *Sulf1* (4ng) was injected into an adjacent blastomere at the four cell stage. Embryos were prepared for confocal microscopy as previously described. The distance that Wnt8a and Wnt11b-HA-GFP could diffuse into a region expressing Sulf1 was then analysed (see Figures 5.27A and 5.28A for diagrams).

Wnt8a-HA-GFP was able to diffuse 2-3 cell diameters through a region expressing LacZ (Figure 5.27B-E). This was similar to the diffusion of Wnt8a-HA-GFP in control conditions in the previous diffusion assay (Figure 5.24B). Wnt8a-HA-GFP was less stable in regions over-expressing Sulf1 C-A (compare Figure 5.27F-I to 5.27B-E). However, Wnt8a-HA-GFP was able to diffuse much further through a region expressing Sulf1 than an area expressing LacZ (compare Figure 5.27J-M to 5.27B-E). Importantly, there was no increase in the levels of Wnt8a-HA-GFP diffusing through a Sulf1

Figure 5.27; Sulf1 enhances the range of Wnt8a-HA-GFP diffusion when over-expressed in cells adjacent to those expressing Wnt8a-HA-GFP.
[A] Diagram illustrating the assay used to investigate the effects of Sulf1 on the range of Wnt8a-HA-GFP diffusion. mRNA encoding *mCerulean* (600pg) and *Wnt8a-HA-GFP* (2ng) was injected into the animal hemisphere of one blastomere of an embryo at the four cell stage. mRNA encoding *mRFP* (600pg) and *LacZ* (4ng), *Sulf1 C-A* (4ng) or *Sulf1* (4ng) was injected into an adjacent blastomere at the four cell stage. Embryos were cultured until NF stage 8 and then animal cap explants were taken and cultured for four hours at 21˚C prior to imaging by confocal microscopy. The distance that Wnt8a-HA-GFP could diffuse into a region expressing Sulf1 was analysed. [B-M] Embryos over-expressing [B-E] LacZ, [F-I] Sulf1 C-A and [J-M] Sulf1 in cells receiving Wnt8a-HA-GFP. Sulf1 enhanced the range of Wnt8a-HA-GFP diffusion, but did not affect the overall levels of Wnt8a-HA-GFP on the cell membrane. mCerulean (yellow), Wnt8a-HA-GFP (green), mRFP (magenta), scale bars represent 20μm.

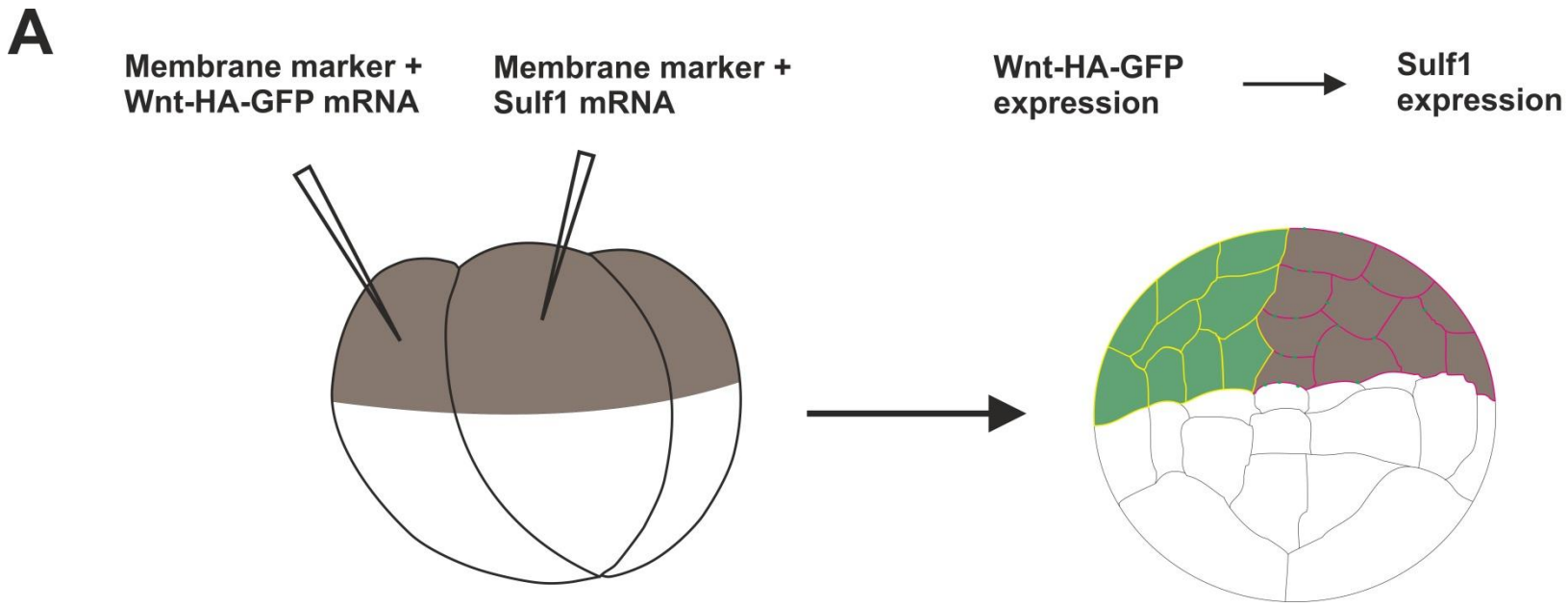

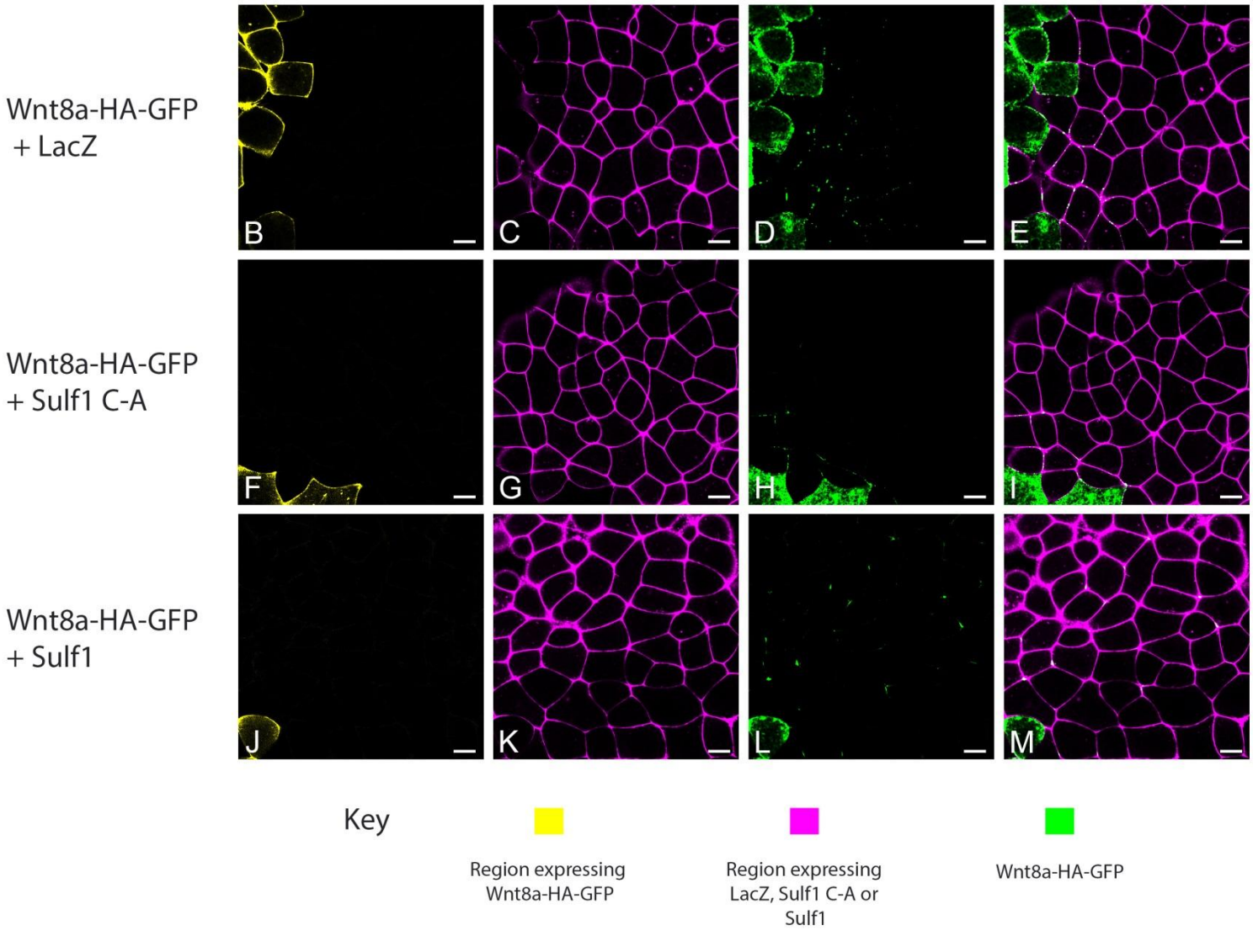
Wnt8a-HA-GFP
+ LacZ
Wnt8a-HA-GFP
+ Sulf1 C-A
Wnt8a-HA-GFP
+ Sulf1
B
C
D
E
F
G
H
I
J
K
L
M
Key
Region expressing
Wnt8a-HA-GFP
Region expressing
LacZ, Sulf1 C-A or
Sulf1
Wnt8a-HA-GFP

Figure 5.28; Sulf1 enhances both the range of diffusion and levels of Wnt11b-HA-GFP when over-expressed in cells adjacent to those expressing Wnt11b-HA-GFP.
[A] Diagram illustrating the assay used to investigate the effects of Sulf1 on the range of Wnt11b-HA-GFP diffusion. mRNA encoding *mCerulean* (600pg) and *Wnt11b-HA-GFP* (2ng) was injected into the animal hemisphere of one blastomere of an embryo at the four cell stage. mRNA encoding *mRFP* (600pg) and *LacZ* (4ng), *Sulf1 C-A* (4ng) or *Sulf1* (4ng) was injected into an adjacent blastomere at the four cell stage. Embryos were cultured until NF stage 8 and then animal cap explants were taken and cultured for four hours at 21˚C prior to imaging by confocal microscopy. The distance that Wnt11b-HA-GFP could diffuse into a region expressing Sulf1 was analysed. [B-M] Embryos over-expressing [B-E] LacZ, [F-I] Sulf1 C-A and [J-M] Sulf1 in cells receiving Wnt11b-HA-GFP. Sulf1 enhanced the range of Wnt11b-HA-GFP diffusion and increased the overall levels of Wnt11b-HA-GFP on the cell membrane. mCerulean (yellow), Wnt11b-HA-GFP (green), mRFP (magenta), scale bars represent 20µm.

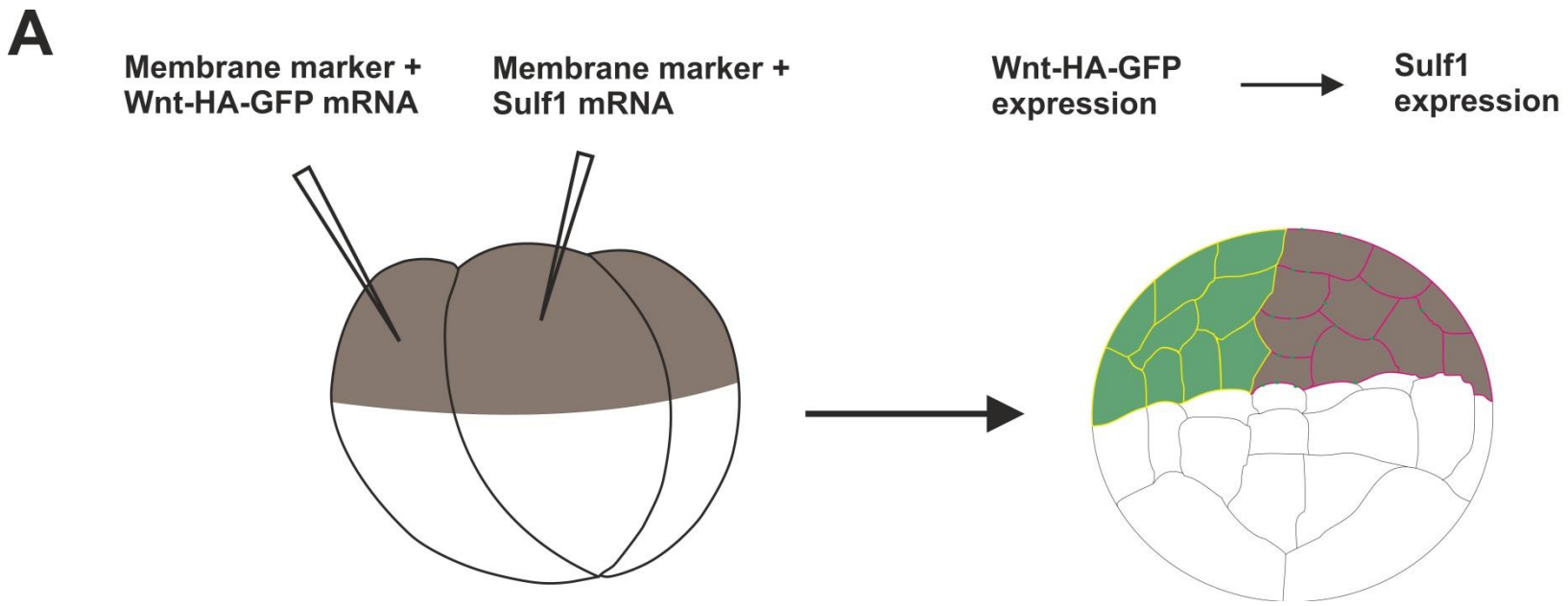

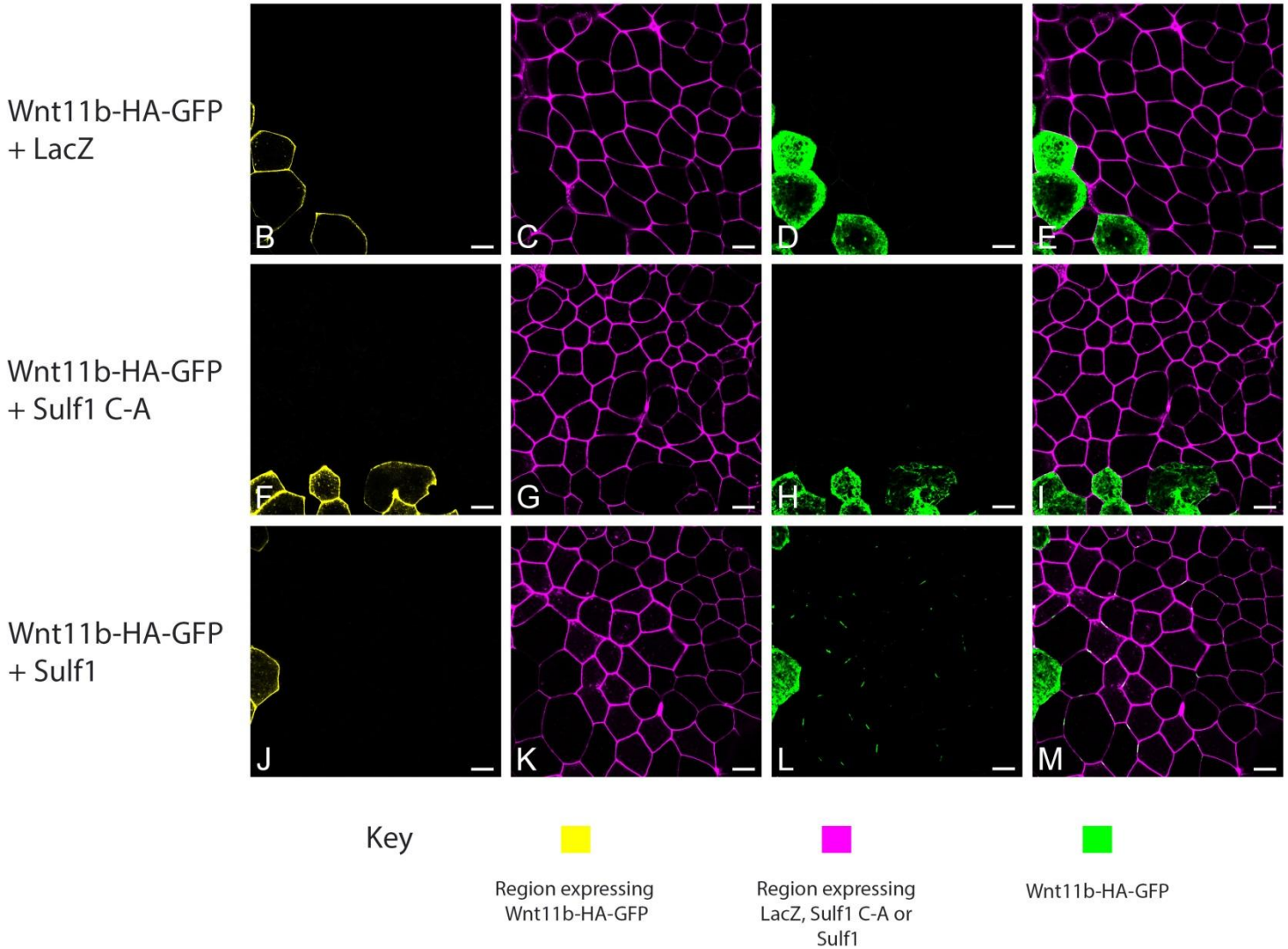
Wnt11b-HA-GFP
+ LacZ
Wnt11b-HA-GFP
+ Sulf1 C-A
Wnt11b-HA-GFP
+ Sulf1
B
C
D
E
F
G
H
I
J
K
L
M
Key
Region expressing
Wnt11b-HA-GFP
Region expressing
LacZ, Sulf1 C-A or
Sulf1
Wnt11b-HA-GFP

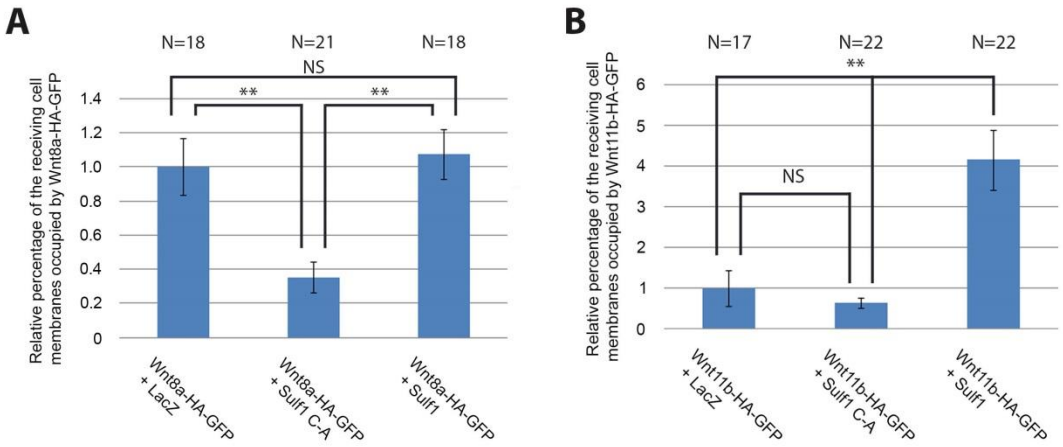

Figure 5.29; Sulf1 enhances the levels of Wnt11b-HA-GFP on the cell membrane. Graphs illustrating the data shown in [A] Figure 5.27 and [B] Figure 5.28. The data was quantified using the same programme as for Figure 5.13. Asterisks mark significant differences (**P<0.01), NS marks non-significant differences, Mann-Whitney U, N = number of embryos.

expressing region, instead the puncta appeared more diffuse. One prediction from this is that Sulf1 enhances the spreading of Wnt8a-HA-GFP, reducing its local concentration.

Wnt11b-HA-GFP was barley detected in regions expressing LacZ (Figure 5.28B-E). This was similar to the findings of the previous diffusion assay (Figure 5.24E). Over-expression of Sulf1 C-A in the region adjacent to Wnt11b-HA-GFP did not alter the range of Wnt11b-HA-GFP diffusion (Figure 5.28F-I). In contrast Wnt11b-HA-GFP was readily detectable on the surface of receiving cells expressing Sulf1 (compare Figure 5.28J-M). One interpretation of this data is that Sulf1 stabilises Wnt11b-HA-GFP on the cell membrane, allowing it to diffuse further.

The levels of Wnt8a and Wnt11b-HA-GFP associating with the plasma membrane of Wnt receiving cells are quantified in Figure 5.29. The data was quantified using the same Matlab program as for Figure 5.13. Only the Wnt8a and Wnt11b-HA-GFP associated with the cells marked in magenta were quantified (Figure 5.27 and 5.28). Over-expression of Sulf1 C-A caused a decrease in the relative levels of Wnt8a-HA-GFP associating with the plasma membrane compared to control (LacZ) conditions (Figure 5.29A).

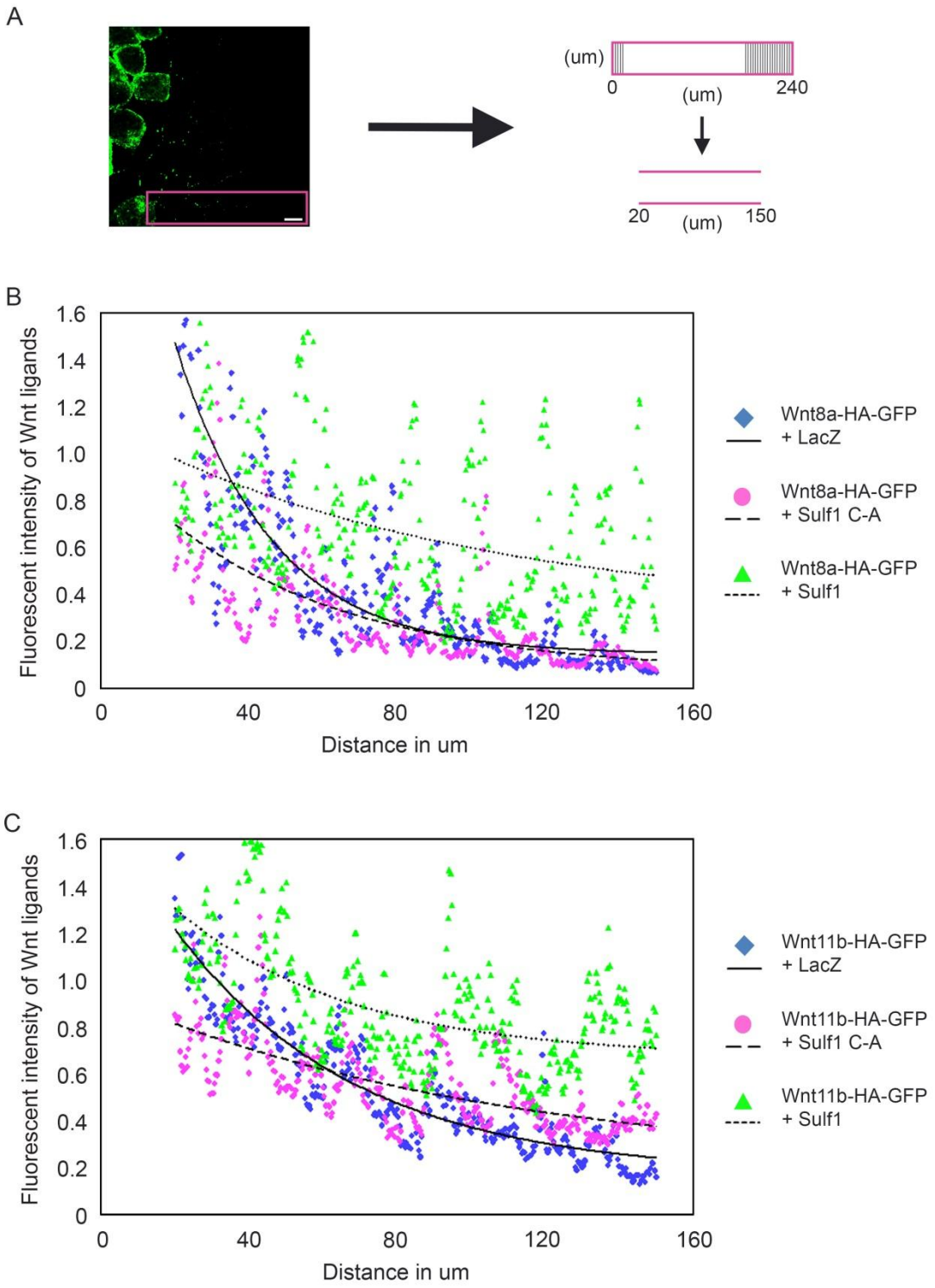

Figure 5.30; Graphs illustrating the effects of Sulf1 on Wnt8a/Wnt11b-HA-GFP diffusion.

[A] Diagram of how each image was prepared for analysis using Fiji image J, see methods 2.5.5 for details. [B] Plots illustrating the effects of Sulf1 and Sulf1 C-A on the amount of Wnt8a-HA-GFP diffusing over the 150µm analysed. Plots were prepared using data from a minimum number of 18 embryos per condition. Curves were fit in Sigmaplot 12.5 using a single exponential decay model with three parameters [C] Plots illustrating the effects of Sulf1 and Sulf1 C-A on the amount of Wnt11b-HA-GFP diffusing over the 150µm analysed. Plots were prepared using data from a minimum number of 17 embryos per condition. Curves were fit in Sigmaplot 12.5 using a single exponential decay model with three parameters.

Table 5.3; Parameters of the curves shown in Figure 5.30

Condition	Equation of the curve	Predicted Y max (pixel intensity)	Predicted Y min (pixel intensity)	Predicted Y half-life (pixel intensity)	Predicted X half-life (μm)
Wnt8a-HA-GFP + LacZ	F=0.1438+2.86*EXP(-0.0384*X)	1.47 (CI 1.367-1.547)	0.15 (CI 0.123-0.187)	0.81 (CI 0.75-0.87)	37.93 (CI 35.67-40.42)
Wnt8a-HA-GFP + Sulf1 C-A	F=0.0673+0.93*EXP(-0.0195*X)	0.697 (CI 0.617-0.767)	0.12 (CI 0.104-0.164)	0.41 (CI 0.37-0.47)	51.22 (CI 44.75-58.96)
Wnt8a-HA-GFP + Sulf1	F=0.308+0.8241*EXP(-0.0105*X)	0.976 (CI 0.387-1.477)	0.48 (CI 0.671-0.809)	0.73 (CI 0.53-1.15)	63.74 (CI 46.14-92.3)
Wnt11b-HA-GFP + LacZ	F=0.1676+1.5761*EXP(-0.0204*X)	1.216 (CI 1.159-1.216)	0.24 (CI 0.224-0.27)	0.726 (CI 0.629-0.769)	50.64 (CI 47.63-54.14)
Wnt11b-HA-GFP + Sulf1 C-A	F=0.1975+0.75*EXP(-0.0095*X)	0.814 (CI 0.49-1.109)	0.38 (CI 0.325-0.525)	0.595 (CI 0.408-0.817)	66.09 (CI 55.56-79.12)
Wnt11b-HA-GFP + Sulf1	F=0.6711+0.97*EXP(-0.0214*X)	1.304 (CI 1.187-1.394)	0.71 (CI 0.708-0.775)	1.007 (CI 0.948-1.084)	49.58 (CI 41.85-62.03)

Asterisks = multiplication terms

EXP = inverse natural Log

X = values on the X axis (distance in μm from the source)

CI = 95% confidence intervals

Over-expression of Sulf1 had no effect on the relative levels of Wnt8a-HA-GFP associating with the cell membrane compared to LacZ conditions. In contrast, over-expression of Sulf1 enhanced the levels of Wnt11b-HA-GFP associating with the membranes of receiving cells. Sulf1 increased the overall levels of Wnt11b-HA-GFP, but not Wnt8a-HA-GFP detected on receiving cells over-expressing Sulf1.

Fiji image J was used to quantify the range of Wnt8a and Wnt11b-HA-GFP diffusion through regions over-expressing Sulf1 (see method 2.5.5 for details). Identical imaging conditions were used to collect the data for Figures 5.27-5.28 and the intensity of the green channel was not altered during the analysis. The method of quantification was identical to that used to produce Figure 5.25, except that the maximum range of diffusion was reduced to 150µm. This was a reflection of the need to have two specific domains adjacent to each other, rather than one domain diffusing out into an unlabelled background (compare Figures 5.27 and 5.28 to 5.24). Scatter graphs comparing the rates of decay of Wnt8a and Wnt11b-HA-GFP diffusing through different regions can be seen (Figures 5.30B and C). All of the curves for this data were fitted in Sigmaplot 12.5 using the exponential decay equation $F=Y0+A*EXP^{(-bX)}$ (see Table 5.3 for parameters). Wnt8a-HA-GFP signal intensity decayed at a rate of ¯0.0384, when diffusing through control (LacZ) conditions. Over-expression of Sulf1 C-A, in receiving cells, reduced the rate of decay to ¯0.0195 and this rate was reduced further by the over-expression of Sulf1 (¯0.0105). The reduced rates of decay were coupled to an increase in the predicted T1/2s for Wnt8a-HA-GFP. In control conditions the T1/2 for Wnt8a-HA-GFP was 37.93µm. Over-expression of Sulf1 C-A in receiving cells increased this to 51.22µm with Sulf1 increasing this further to 63.74µm. In addition, over-expression of Sulf1 increased the minimum Y value at 150µm from 0.15 (control) and 0.12 (Sulf1 C-A) conditions to 0.48. Similar to Figure 5.25, over-expression of Sulf1 reduces the rate of decay of Wnt8a-HA-GFP, but enhances the range of ligand diffusion.

The rate of decay of Wnt11b-HA-GFP diffusing into control (LacZ) conditions was ¯0.0204. This is lower than the rate of decay for Wnt8a-HA-GFP

diffusing into control conditions. The predicted T1/2 of Wnt11b-HA-GFP in control conditions was 50.64μm compared to 37.93μm for Wnt8a-HA-GFP. One conclusion from this is that similar to Figures 5.24-5.25, Wnt11b-HA-GFP ligands are able to diffuse further and decay at a lower rate than Wnt8a-HA-GFP ligands in control conditions. Over-expression of Sulf1 C-A in receiving cells reduced the decay rate of Wnt11b-HA-GFP to ¯0.0095 and increased the predicted T1/2 to 66.09μm. Over-expression of Sulf1 in receiving cells did not dramatically alter either the decay rate (¯0.0214) or the T1/2 (49.58μm) of Wnt11b-HA-GFP compared to control conditions. However Sulf1 was able to increase the predicted Y minimum value at 150μm from 0.726 to 1.007.

Sulf1 C-A and Sulf1 reduce the rate of Wnt8a-HA-GFP signal decay, enhancing the range of Wnt8a-HA-GFP diffusion when over-expressed in receiving cells. In contrast, whereas Sulf1 C-A reduces the rate of Wnt11b-HA-GFP decay, Sulf1 does not. Sulf1 enhances the range of Wnt8a-HA-GFP diffusion by reducing the rate at which the ligand decays. In contrast, Sulf1 enhances the overall levels of Wnt11b-HA-GFP that can be detected on the cell membrane, increasing the range of Wnt11b-HA-GFP diffusion without altering the rate of ligand decay.

5.2.11 Sulf1 increases the levels of glypican4-cerulean associating with the cell membrane

Sulf1 is able to enhance the range of Wnt8a and Wnt11b-HA-GFP diffusion in *Xenopus* animal caps. The ability of Sulf1 to alter the range of Wnt diffusion is similar to manipulating the levels of dlp in *Drosophila* (Franch-Marro et al., 2005; Yan et al., 2009). In order to investigate the effects of Sulf1 on HSPG distribution, a fluorescently tagged version of glypican4 was developed (see methods 2.4.3 for details). Briefly glypican4 was tagged C terminally with cerulean. The cerulean tag was inserted upstream of the glypican4 GPI anchor region, in a sequence that is only conserved in *Xenopus tropicalis* and *Xenopus laevis*. This allowed the effects of Sulf1 on glypican4 distribution to be analysed.

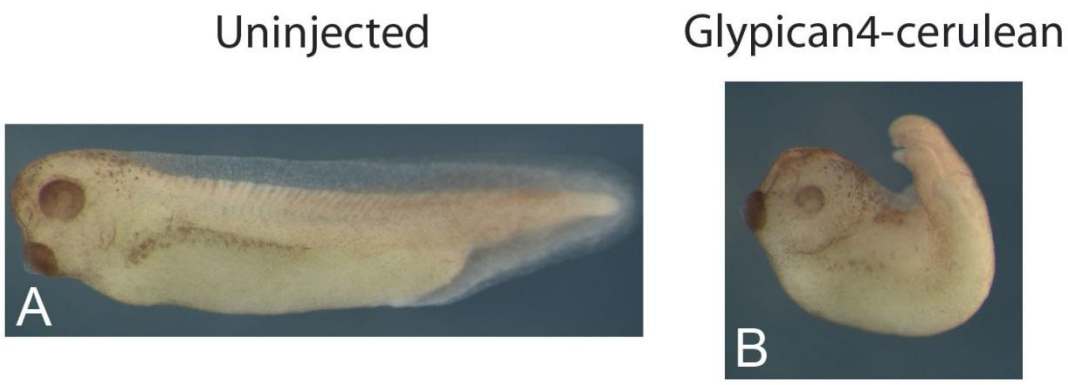

Figure 5.31; Glypican4-cerulean is biologically active.
mRNA encoding *glypican4-cerulean* (500pg) was injected into both dorsal blastomeres of an embryo at the four cell stage. Embryos were cultured until NF stage 37/38 and then examined for phenotype. [A] Lateral view of an uninjected embryo. [B] Lateral view of an embryo over-expressing glypican4-cerulean. Glypican4-cerulean caused gastrulation defects in whole embryos.

To determine whether glypican4-cerulean was biologically active, mRNA encoding *glypican4-cerulean* was injected into both dorsal blastomeres of a four cell stage embryo. Embryos were cultured until NF stage 36/37 and analysed for phenotype. Over-expression of glypican4-cerulean caused a shortening of the anterior/posterior axes of the embryo (Figure 5.31B). These defects were similar to those caused by glypican4 in *Xenopus* (Ohkawara et al., 2003). Glypican4-cerulean is biologically active in *Xenopus*.

To investigate whether Sulf1 could alter the distribution of HSPGs, glypican4-cerulean was visualised in animal caps. Embryos were microinjected bilaterally in the animal hemisphere with mRNA encoding *mRFP* and *glypican4-cerulean*. In addition, embryos were microinjected with mRNA encoding *LacZ, Sulf1 C-A* or *Sulf1*. Embryos were prepared for confocal microscopy as described previously. In the presence of LacZ, glypican4-cerulean can be detected at low levels on the plasma membrane (Figure 5.32A-D). Over-expression of Sulf1 C-A enhances the accumulation of glypican4-cerulean on the cell membrane, with glypican4-cerulean beginning to form aggregates (Figure 5.32E-H). Over-expression of Sulf1 enhances the accumulation of glypican4-cerulean further (compare Figure 5.32I-L to 5.32E-H). In addition, in the presence of Sulf1 glypican4-cerulean forms large aggregates. The data from Figure 5.32A-L is quantified in Figure 5.32M.

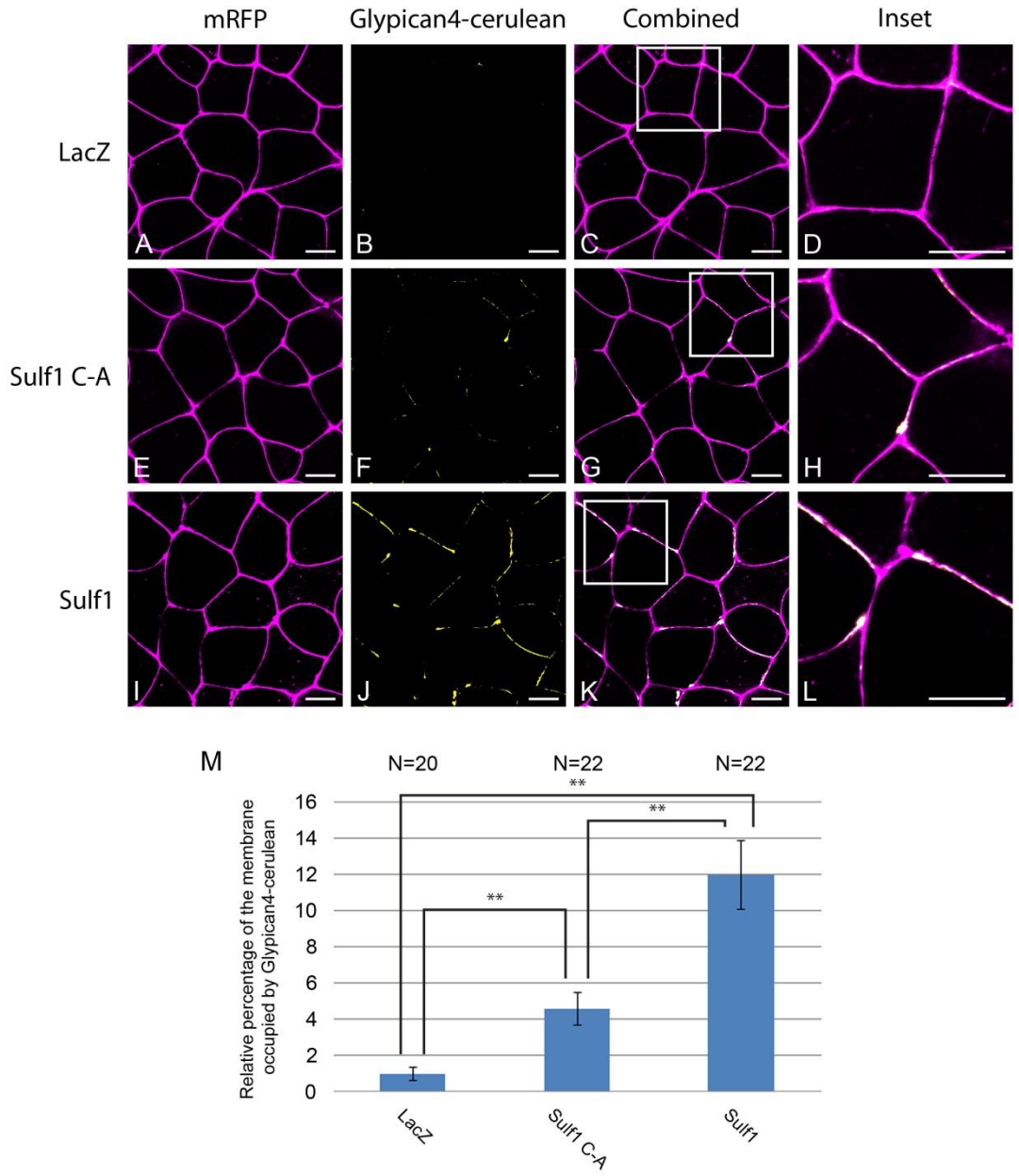

Figure 5.32; Sulf1 enhances the levels of glypican4-cerulean associating with the plasma membrane.
mRNA encoding *mRFP* (500pg) and *glypican4-cerulean* (250pg) was injected bilaterally into the animal hemisphere of embryos at the two cell stage. In addition embryos were injected with mRNA encoding *LacZ* (4ng), *Sulf1 C-A* (4ng) or *Sulf1* (4ng). Embryos were cultured until NF stage 8 and then animal cap explants were taken and cultured for four hours at 21˚C prior to imaging by confocal microscopy. [A-D] Control animal caps over-expressing LacZ. Animal caps over-expressing [E-H] Sulf1 C-A and [I-L] Sulf1. The white boxes in [C], [G] and [K] mark the areas used to create panels [D], [H] and [L] respectively. Over-expression of Sulf1 enhances the accumulation of glypican4-cerulean on the cell membrane. [M] Graph quantifying the relative levels of glypican4-cerulean on the cell membrane. Data obtained using a programme written in Matlab. Asterisks mark significant differences (**P<0.01) Mann-Whitney U, error bars represent s.e.m. mRFP (magenta), glypican4-cerulean (yellow), scale bars represent 20µm, N = number of embryos.

The data was quantified by a programme written in Matlab. Sulf1 enhances the accumulation of glypican4-cerulean on the cell membrane.

5.3.0 Discussion

The aim of this chapter was to investigate a mechanism of action for the distinct effects of Sulf1 on canonical and non-canonical Wnt signalling. It has been shown that Sulf1 alters the ability of Wnt8a and Wnt11b to bind LRP6. In addition, Sulf1 increases the association of the non-canonical Wnt signalling complex (Ror2 and Fz7) in the presence of Wnt11b (Pownall laboratory unpublished communication; Freeman et al., 2008). Work in *Drosophila* has shown that Sulf1 restricts the diffusion of Wg in the wing disc, inhibiting the activation of both low and high threshold Wg target genes (Kleinschmit et al., 2010; You et al., 2011). In this chapter data is presented, which demonstrates that Sulf1 affects the secretion/stability/diffusion of Wnt4, Wnt8a and Wnt11b. Sulf1 can alter the range of diffusion and rate of decay of both Wnt8a and Wnt11b-HA-GFP. These findings indicate that Sulf1 can regulate Wnt morphogen gradients in vertebrates, as has been described for Wg in *Drosophila* (Kleinschmit et al., 2010, 2013; You et al., 2011).

5.3.1 Wnt11b inhibits Wnt8a signalling, but not vice versa

Sulf1 inhibits the ability of Wnt8a to activate canonical Wnt signalling, but enhances the ability of Wnt11b to activate both canonical and non-canonical Wnt signalling. Components of the Wnt/Ca^{2+} signalling pathway inhibit canonical Wnt signalling *in vivo* (Kuhl, 2002; Kuhl et al., 2000). One prediction from this is that increased activation of non-canonical Wnt signalling by Sulf1 could indirectly inhibit canonical Wnt signalling. To investigate this, cross talk between Wnt8a and Wnt11b in axis duplication and animal cap assays was investigated. As shown previously by Torres et al., (1996) Wnt11b inhibits the ability of Wnt8a to induce axis duplication. In contrast, Wnt8a does not block the inhibitory effect of Wnt11b on convergent extension, or the ability of Wnt11b to induce Dvl-GFP translocation in animal cap assays. It is possible that Sulf1 enhancement of non-canonical Wnt signalling may underlie its inhibition of Wnt8a signalling, however not all evidence supports this idea. Sulf1 does not inhibit the ability of Wnt3a to activate canonical Wnt signalling (chapter 3),

which is inconsistent with the notion that Sulf1 indirectly inhibits canonical signalling by activating non-canonical Wnt signalling.

It is possible that non-canonical Wnt ligands, stabilised in response to Sulf1, may inhibit Wnt8a signalling extracellularly in a ligand dependent manner (Maye et al., 2004). In chapter 3, Sulf1 inhibits Wnt8a signalling inside the domain of *Sulf1* expression, but enhances the range of Wnt8a signalling, resulting in two ectopic domains of *chordin* expression (Figure 3.6). In this chapter, Sulf1 was shown to enhance the range of diffusion of both Wnt8a-HA-GFP and Wnt11b-HA-GFP in animal cap explants. One prediction from this is that Sulf1 would enhance the range of diffusion of Wnt8a as well as endogenous non-canonical Wnt ligands. If non-canonical Wnt ligands were the reason for the inhibition of Wnt8a signalling, this effect is likely to be maintained outside of the domain of Sulf1 expression. Non-canonical Wnt signalling antagonises canonical Wnt signalling, but this is unlikely to be a mechanism to explain the effects of Sulf1 on Wnt signalling.

5.3.2 Sulf1 enhances the colocalisation of caveolin-GFP with Wnt11b-HA-Venus, but not Wnt8a-HA-Venus

Work in cell culture has shown that components of the canonical Wnt signalling pathway colocalise with caveolin-GFP (Bilic et al., 2007; Yamamoto et al., 2006, 2008). Non-canonical Wnt signalling has been shown to depend on clathrin dependent endocytosis (Kim and Han, 2007; Kim et al., 2008). Interestingly, over-expression of Dkk1 redistributes active LRP6 from detergent insoluble lipid rafts to detergent soluble membranes. In addition, knockdown of *clathrin* blocks the ability of Dkk1 to inhibit canonical Wnt signalling (Yamamoto et al., 2008). One prediction from this is that the redistribution of canonical Wnt components away from caveolin would inhibit canonical Wnt signalling.

To determine whether Sulf1 could alter the colocalisation of Wnt ligands with caveolin, Wnt8a-HA-Venus and Wnt11b-HA-Venus were developed. Wnt8a and Wnt11b-HA-Venus were over-expressed at higher levels in this assay than are normally required for signalling. This is was so that the ligands could be visualised and is a limitation of over-expression work. Embryos were

microinjected with the same amount of mRNA encoding *Wnt8a and Wnt11-HA-Venus*. In addition, each of the ligands, as well as caveolin-GFP, occupied discrete domains on the plasma membrane, rather than being expressed on all parts of the membrane. One prediction from this is that the preferential colocalisation of Wnt8a-HA-Venus and caveolin-GFP is a reflection of Wnt8a having an intrinsic affinity for caveolin-GFP and not that the system is being over whelmed by the levels of fluorescent Wnts.

Wnt8a-HA-Venus showed a greater degree of colocalisation with caveolin-GFP than Wnt11b-HA-Venus in control conditions (Sulf1 C-A expressing). This is consistent with the requirement of caveolin dependent internalisation for canonical Wnt signalling (Bilic et al., 2007; Yamamoto et al., 2006).Over-expression of Sulf1 did not affect the colocalisation of Wnt8a-HA-Venus with caveolin-GFP, but did increase the colocalisation of caveolin-GFP with Wnt11b-HA-Venus. This is consistent with Sulf1 enhancing Wnt11b activation of canonical Wnt signalling. The catalytic activity of Sulf1 does not alter the caveolin-GFP dependent internalisation of Wnt8a-HA-Venus, but increases the association between caveolin-GFP and Wnt11b-HA-Venus.

5.3.3 Sulf1 regulates the stability and diffusion of Wnt8a and Wnt11b-HA-GFP in *Xenopus* animal caps

Work in *Drosophila* has shown that Sulf1 inhibits Wg signalling by reducing the extracellular concentration of Wg protein (Kleinschmit et al., 2010; You et al., 2011). Three separate assays were employed to investigate the role of Sulf1 in regulating Wnt ligand stability and diffusion in explant studies.

Sulf1 enhances the secretion/stability of Wnt8a and Wnt11b-HA-GFP

Over-expression of Sulf1 and Wnt8a/Wnt11b-HA-GFP in the same cells enhances the levels of Wnt11b, but not Wnt8a-HA-GFP, on the cell membrane. The increase in Wnt11b-HA-GFP on the membrane could be due to an increase in the secretion of Wnt11b-HA-GFP. Alternatively, the increase could be due to a greater stability of the ligand on the cell membrane. Evi acts as a chaperone

to traffic Wg from the golgi to the cell surface (Bänziger et al., 2006; Bartscherer et al., 2006). A Golgi targeted version of Sulf1, shows a similar activity to wildtype Sulf1 indicating that some aspects of Sulf1 function occur in the golgi (Ai et al., 2003). Over-expression of Evi in *Drosophila* enhances the secretion of Wg in the wing disc (Belenkaya et al., 2008). One prediction from this is that Sulf1 could enhance the ability of Evi to traffic Wnt11b to the cell membrane.

Sulf1 enhances the abilities of Wnt4 and Wnt11b to activate non-canonical Wnt signalling. Wnt11b-HA-Venus is able to induce the translocation of Dvl-GFP to the cell membrane. Over-expression of Sulf1 enhances the stability of Wnt11b-HA-Venus on the cell membrane and this is mirrored by an increase in the levels of Dvl-GFP at the cell membrane. One prediction from this is that Sulf1 enhances the ability of Wnt4 and Wnt11b to activate non-canonical Wnt signalling, by increasing the stability of both ligands. However Sulf1 is also able to induce qualitative changes in the shape of Wnt-HA-GFP puncta. Sulf1 increases the average size of Wnt11b-HA-GFP puncta colocalising with the cell membrane. Wnt11b interacts with Ror2, when both proteins are over-expressed in *Xenopus* (Hikasa et al., 2002). Over-expression of Sulf1 does not alter the interaction between Wnt11b and Ror2. However, if Wnt11b, Ror2 and Fz7 are all over-expressed, Sulf1 increases the ability of Ror2 to interact with Fz7 (Pownall laboratory unpublished communication). One prediction from this is that Sulf1 favours the formation of large Wnt11b-Ror2-Fz7 oligomers on the cell surface. This is consistent with Sulf1 inducing the formation of large aggregates of Wnt11b-HA-GFP on the cell membrane. Sulf1 increased the stability, but not the average size of Wnt4-HA-GFP puncta on the cell membrane. Activation of non-canonical Wnt signalling likely depends on both the overall amount of Wnt ligands on the cell surface and the formation of large Wnt ligand-receptor complexes.

Sulf1 causes a reduction in the average circularity of Wnt8a and Wnt11b-HA-GFP puncta. Sulf1 does cause a small increase in Wnt4-HA-GFP circularity, however this may be an artefact of where Wnt4-HA-GFP naturally accumulates in animal cap cells. Why these less spherical aggregates of Wnt11b are important for non-canonical Wnt signalling is unclear. It is possible that less spherical aggregates favour the formation of larger receptor complexes as

described for Fz7 and Ror2, but not binding to LRP6. Alternatively the reduction in circularity may actively inhibit the binding of Wnt ligands to LRP6, as is seen for Wnt8a (Pownall laboratory unpublished data). Another possibility is that the reduction in circularity of Wnt8a-HA-GFP particles could result in the masking of key residues required for its activity, for example, the palmitoleic acid modification. This would explain how Sulf1 could specifically inhibit the binding of Wnt8a, but not Wnt11b, to LRP6. Together these data suggest that the qualitative shape of Wnt particles may alter their ability to bind Wnt receptors *in vivo.*

Sulf1 enhances the levels of Wnt8a and Wnt11b-HA-GFP diffusing away from a region expressing Sulf1

Sulf1 caused a decrease in the rate of decay, but an increase in the range of diffusion of Wnt8a and Wnt11b-HA-GFP in animal caps. Wnt ligands are highly hydrophobic and are not freely diffusible in the extracellular space. A similar problem is faced by Hh proteins, which are modified by the addition of cholesterol and palmitic acid during ligand synthesis (Pepinsky et al., 1998; Porter et al., 1996). Hh ligands use HSPGs as a scaffold to from multimers for long range diffusion *in vivo* (Goetz et al., 2006; Vyas et al., 2008). To investigate whether Sulf1 altered the ability of Wnt8a/Wnt11b-HA to form multimers, Wnt8a and Wnt11b-HA proteins were visualised using non-reducing western blots (Figure 5.26). The Wnt agonist Norrin has previously been shown to assemble into dimers/oligomers by disulphide bridge formation (Perez-Vilar and Hill, 1997). No change in the oligomerization of Wnt8a/Wnt11b-HA in response to Sulf1 was detected. However, in order to make firm conclusions about Wnt oligomerization, native blots should be performed.

Secretion on exosomes/lipoprotein particles and secretion from reggie/flotillin lipid raft domains have all been proposed as mechanisms for regulating Wnt/Wg ligand diffusion *in vivo* (Greco et al., 2001; Gross et al., 2012; Katanaev et al., 2008; Neumann et al., 2009; Panáková et al., 2005). Lipophorin particles bind to the HS chains of dally and dlp on the surface of the *Drosophila* wing disc (Eugster et al., 2007). One prediction from this is that dally and/or dlp may recruit lipophorin particles to package Wg for secretion in the wing disc.

Reggie/flotillin microdomains have also been suggested as specific domains to recruit lipophorin particles, reviewed by (Solis et al., 2013). Sulf1 may promote the formation of specific domains to package Wnt/Wg for secretion.

Secreted inhibitors of Wg signalling also have a role in regulating Wg diffusion. Members of the Sfrp family and the lipocalin Swim promote long range Wnt/Wg signalling in embryos (Esteve et al., 2011; Mii and Taira, 2009; Mulligan et al., 2012). Sfrp1 is a biphasic activator of Wg signalling in S2 cells, potentiating Wg signalling at low concentration, but inhibiting it at high concentrations. Sfrp1 binds to Wg in vitro and the binding is enhanced by the presence of exogenous heparin (Uren et al., 2000). It is possible that Sulf1 may regulate the release of secreted inhibitors of Wnt signalling from the cell surface. Sulf1 induces the release of the BMP inhibitor noggin, Zimmerman et al., (1996) from the surface of cells and this results in the activation of BMP signalling (Viviano et al., 2004). Sulf1 may enhance the diffusion of Wnt8a and Wnt11b-HA-GFP by altering their association with secreted inhibitors of Wnt/Wg signalling.

Wnt8a and Wnt11b-HA-GFP diffuse further though regions expressing Sulf1

This thesis has focused on examining the effects of Sulf1 on Wnt signalling, when Sulf1 and Wnt are over-expressed in the same cells. These assays are fundamentally different to those performed by (Ai et al., 2003; Dhoot et al., 2001; Tang and Rosen, 2009). Over-expression of Sulf1 in Wnt11b-HA-GFP receiving cells enhanced the stability of Wnt11b-HA-GFP on the cell membrane. In addition, over-expression of Sulf1 increased the range of Wnt11b-HA-GFP diffusion, without altering the rate of Wnt11b-HA-GFP signal decay. The increased stability of Wnt11b-HA-GFP on Sulf1 expressing cells means that the ligands diffuse further, without affecting the overall shape of the gradient. Over-expression of Sulf1 in Wnt8a-HA-GFP receiving cells expands the range Wnt8a-HA-GFP diffusion. However, Sulf1 did not increase the overall levels of Wnt8a-HA-GFP associating with the membranes of receiving cells, this results in a reduction in the concentration of Wnt8a-HA-GFP close to the source.

Whether or not a change in the diffusivity of a ligand increases or decreases the amount of detectable signal will depend on other parameters in the

environment. The data in Figures 5.25 and 5.30 are fitted with exponential decay curves. One prediction from this is that Wnt8a and Wnt11b-HA-GFP are being degraded with a constant probability in the environment (Eldar et al., 2003). In this scenario, increasing the diffusivity of Wnt8a/Wnt11b-HA-GFP alone would be predicted to decrease the amount of ligand detected. The Wnt8a and Wnt11b-HA-GFP puncta detected in Figures 5.24, 5.27 and 5.28 are likely to represent protein oligomers and the further these migrate away from a region expressing Wnt, the smaller they appear, until they can no longer be detected (see Figure 5.24). However by enhancing the stability of Wnt11b-HA-GFP in receiving cells, Sulf1 is able to increase both the range of diffusion and amount of ligand detected (see Figure 5.29). Dlp has a similar effect on the Wg morphogen gradient in *Drosophila* (Han et al., 2005). Sulf1 increases the range of diffusion of Wnt8a-HA-GFP without altering the overall levels of the ligand on the plasma membrane (Figure 5.29). As mentioned above, Hh proteins form multimeric complexes *in-vivo* (Goetz et al., 2006). A mutant version of Hh that cannot form multimers retains its signalling activity, but is unable to activate long range Hh signalling (Lewis et al., 2001). One conclusion from this is that Hh multimers are required for long range Hh signalling (Goetz et al., 2006; Lewis et al., 2001). Sulf1 may increase the diffusivity of Wnt8a-HA-GFP by reducing the binding of large, long range, Wnt8a-HA-GFP oligomers to receiving cells. In this scenario, the Wnt8a-HA-GFP puncta would continue to be detected even at a long distance from the source (see Figure 5.27).

In *Drosophila*, dlp promotes the long range diffusion of Wg, increasing the activation of low threshold Wg target genes at the expense of high threshold genes (Han et al., 2005; Yan et al., 2009). The lipocalin Swim and Reggie1/flotillin microdomains perform similar functions (Katanaev et al., 2008; Mulligan et al., 2012). Sulf1 enhances the range of diffusion of Wnt8a-HA-GFP reducing the local concentration of the ligand. An increased range of diffusion of a ligand does not necessarily indicate an increased range of signalling. Increasing the diffusivity of a ligand can actually decrease its concentration close to the source. If the concentration of the ligand is now below the level required to activate gene transcription, then the increase in diffusion actually decreases the range of signalling, reviewed by (Lander, 2007; Müller and Schier, 2011). The fitted curves in Figure 5.30B predict a higher concentration

of Wnt8a-HA-GFP in control (LacZ) conditions over the first 20μm of the graph, compared to Sulf1 conditions. A reduction in the concentration of Wnt8a close to the source could inhibit the ability of Wnt8a to activate high threshold target genes such as *chordin* in *Xenopus*. Work modelling the SHh gradient has shown that reducing the diffusion of SHh could actually increase the range of SHh signalling in the ventral neural tube (Saha and Schaffer, 2006). Together these data suggest that Sulf1 may have a role in promoting the long range signalling of Wnt8a at the expense of short range targets.

One limitation of the diffusion experiments shown in Figures 5.24, 5.27 and 5.28 is that the images were taken at the same time points. Consequently, it is unclear whether or not the images depict a steady state gradient. This is important, because if the curves do not reflect the steady state gradients for Wnt8a and Wnt11b-HA-GFP then information regarding the ranges of ligand diffusion and rates of ligand decay could be misleading. For example, if either Wnt8a or Wnt11b-HA-GFP are reversibly binding to non-specific sites then this would increase the amount of time the gradient takes to reach a steady state. If the gradient was analysed before reaching a steady state then the effects of non-specific binding would make it look like there was a higher concentration of ligand close to the source, with a shorter range of diffusion (Lander, 2007). However, whether or not a morphogen requires a steady state gradient in order to pattern tissue has been disputed (Dorfman and Shilo, 2001; Strigini and Cohen, 1999). Future work should involve imaging Wnt-HA-GFP diffusion at different time points.

The data in this chapter suggests that Sulf1 can regulate Wnt ligand secretion/stability in Wnt expressing cells and stability/diffusion in Wnt receiving cells. Sulf1 has been shown to have multiple roles in regulating Hh signalling in the *Drosophila* wing disc. Over-expression of Sulf1 in the posterior compartment of the wing disc potentiates Hh signalling. However, over-expression of Sulf1 in the anterior compartment inhibits Hh signalling (Wojcinski et al., 2011). Sulf1 potentiates Hh signalling when over-expressed in Hh producing cells, but inhibits Hh signalling in Hh receiving cells. The opposite effects of Sulf1 on Hh signalling are likely due to the HSPG/receptor context in each compartment. Sulf1 preferentially removes 6-O sulphate groups from HS,

but has not been shown to have a preference for particular types of HSPG (Morimoto-Tomita et al., 2002; Viviano et al., 2004). One prediction from this is that the desulphation of different HSPGs will have opposite effects on Hh signalling in *Drosophila.* In addition, the presence of patched in the anterior compartment may be responsible for the inhibitory effects of Sulf1 on Hh signalling. Sulf1 has multiple effects on Wnt ligand diffusion and this makes it interpreting the effects of Suf1 on Wnt signalling challenging.

5.3.4 The effects of Sulf1 on Wg signalling in *Drosophila*

In *Drosophila,* Sulf1 inhibits Wg signalling by reducing the levels of extracellular Wg protein in the wing disc (Kleinschmit et al., 2010, 2013; You et al., 2011). It has been proposed that removal of the 6-O sulphate group by Sulf1 destabilise Wg protein on the cell surface, leading to its degradation via the lysosomal pathway (Kleinschmit et al., 2013). The effects of Sulf1 on Wnt8a signalling mirror the effects on Wg signalling, however the mechanism of action of Sulf1 is different. Rather than reducing the overall levels of Wnt8a-HA-GFP, Sulf1 enhances the diffusion of Wnt8a-HA-GFP, reducing its local concentration. The reason for the different actions of Sulf1 in *Drosophila* and *Xenopus* is unclear. Human Sulf1 has been shown to enhance the ability of Wnt1 and Wnt3a to activate Topflash in HEK 293 cells (Tang and Rosen, 2009). Importantly, over-expression of Human Sulf1 in *Drosophila* reduces the levels of extracellular Wg in the wing disc (Kleinschmit et al., 2013). One conclusion from this is that it is the ligand/environment that dictates the effects of Sulf1, rather than differences in the enzyme itself. Given the ligand specific effects exhibited by Sulf1 during axis duplication, it would be interesting to analyse the effects of Sulf1 on Wg in this assay. The effects of Sulf1 on Wnt/Wg signalling are specific to the system being analysed. This has important implications for predicting the role of Sulf1 in regulating Wnt signalling in Humans.

5.3.5 Sulf1 does not require the catalytic domain to enhance Wnt secretion

Data presented in chapter 4 showed that Sulf1 C-A was a hypomorphic mutant. Sulf1 C-A is able to enhance the range of diffusion of Wnt8a and Wnt11b-HA-GFP when over-expressed in both Wnt producing and Wnt receiving cells. Sulf1 C-A-GFP and Sulf1-GFP display similar protein localisation when over-expressed in *Xenopus* animal caps, localising to discrete microdomains on the cell surface (Pownall laboratory unpublished data). One prediction from this is that the catalytic independent role of Sulf1 may involve organising microdomains involved in the secretion of Wnt ligands. Reggie1/flotillin microdomains form a molecular scaffold inside the cell and are required for the long range diffusion of Wg in *Drosophila* (Katanaev et al., 2008; Neumann-Giesen et al., 2004; Stuermer and Plattner, 2005). Sulf1 is found localised to the same lipid raft fractions as flotillin in HEK293 cells (Tang and Rosen, 2009). Sulf1 may have a catalytic domain independent role in organising microdomains that promote Wnt secretion *in vivo.*

5.3.6 Sulf1 regulates the accumulation of glypican4-cerulean on the cell membrane

Both Sulf1 and Sulf1 C-A were able to enhance the accumulation of glypican4-cerulean on the cell membrane. One prediction from this is that Sulf1 may play a direct role in microdomain assembly on the cell membrane. Sulf1 has previously been shown together with dally and dlp to regulate Wg and Hh signalling in *Drosophila*, however no change in the levels of dally or dlp in response to Sulf1 have been reported (Kleinschmit et al., 2010; Wojcinski et al., 2011; You et al., 2011). Glypican4 localises to both detergent soluble and detergent insoluble microdomains in HEK 293 cells and enhances the abilities of both Wnt3a and Wnt5a to activate Wnt signalling (Sakane et al., 2012). A chimeric form of glypican4 that preferentially localises to detergent soluble membranes, enhances Wnt5a activation of non-canonical Wnt signalling, but inhibits Wnt3a activation of canonical Wnt signalling (Sakane et al., 2012). The microdomain localisation of glypican4 is important for its role in Wnt signalling.

Sulf1 may enhance the formation of glypican4 microdomians that favour the secretion/reception of specific Wnt ligands.

5.3.7 Summary

Taken together the results in this chapter point to a role for Sulf1 in regulating the secretion/diffusion of Wnt ligands. Sulf1 is able to influence the formation of Wnt8a and Wnt11b-HA-GFP gradients in animal caps and this sugests a mechanism for the effects seen in whole embryos. The effects of Sulf1 on Wnt diffusion are ligand specific and can differ depending on whether Sulf1 is expressed in Wnt secreting or Wnt receiving cells. It is possible that Sulf1 has roles in regulating microdomain formation *in vivo* and this would likely influence Wnt secretion/Wnt signal reception in different cell types. It is clear from the data presented here that although aspects of the 'catch and present' model are consistent between cell culture and *Xenopus,* the model alone is insufficient (Ai et al., 2003). This thesis proposes a ligand specific model for interpreting the effects of Sulf1 on Wnt signalling. Due to the ligand/environment specific role for Sulf1 in regulating Wnt signalling, the findings here are not necessarily directly transferable to Human development and disease. It will be important to profile the role that different HSPGs play in Wnt signalling and analyse the importance of Sulf1 in regulating microdomain formation in future.

6.0 Discussion

This thesis demonstrates that Sulf1 can differentially affect canonical and non-canonical Wnt signalling. The findings in *Xenopus* do not support the accepted model based on cell culture studies, where Sulf1 potentiates canonical Wnt signalling (Ai et al., 2003; Dhoot et al., 2001; Tang and Rosen, 2009; Tran et al., 2012). In addition, the data in this thesis differs from some of the findings describing the role of Sulf1 in *Drosophila,* which is itself different from the established model (Ai et al., 2003; Kleinschmit et al., 2010, 2013; You et al., 2011). The differences between these findings could be due to the ligands tested or complement of HSPGs/Wnt receptors present in each system. Also, the differences may be due to whether Sulf1 is expressed in cells secreting or receiving Wnt ligands. Sulf1 enhanced the ability of Wnt4 and Wnt11b to activate non-canonical Wnt signalling. This disagrees with some of the findings by Tran et al., (2012), but does support a common mechanism for the effects of Sulf1 on non-canonical Wnt signalling in *Xenopus*.

6.1 The effects of Sulf1 on Wnt signalling in *Xenopus*

Tables are presented to summarise the effects of Sulf1 on Wnt signalling (Tables 6.1 and 6.2). The following sections will discuss possible models to explain how Sulf1 regulates Wnt signalling in *Xenopus.*

Wnt3a

Wnt3a was selected to investigate the effects of Sulf1 on canonical Wnt signalling, as previous work has shown that Sulf1 potentiates the ability of Wnt3a to activate Topflash in cell culture (Tang and Rosen, 2009). In contrast to this, Sulf1 did not alter the ability of Wnt3a to induce ectopic *chordin* expression in *Xenopus*. However, Sulf1 did increase the width of the ectopic domain of *chordin* expression induced. One prediction from this is that Sulf1 enhances the stability/long range diffusion of Wnt3a. Unfortunately a Wnt3a-HA-GFP construct was never developed, so the experiments undertaken with other tagged Wnt ligands were not possible. Sulf1 does not alter the ability of Wnt3a to bind LRP6, which is consistent with the data in this thesis (Pownall laboratory unpublished data). One conclusion from this is that the increase in

Table 6.1; The effects of Sulf1 on Wnt signalling in *Xenopus*

Ligand	Canonical Wnt signalling	Non-canonical Wnt signalling
Wnt3a	Sulf1 does not enhance or inhibit the ability of Wnt3a to induce ectopic *chordin* expression, but does increase the width of the ectopic *chordin* domain induced.	Not tested
Wnt4	Not tested	Sulf1 enhances the ability of Wnt4 to induce Dvl-GFP translocation to the cell membrane in animal caps.
Wnt8a	Sulf1 inhibits the ability of Wnt8a to stabilise β-catenin in animal caps. Sulf1 inhibits the ability of Wnt8a to induce axis duplication and ectopic *Xnr3/chordin* expression. However, Wnt8a that can diffuse away from an area expressing Sulf1 does activate *chordin* expression.	Sulf1 does not alter the ability of Wnt8a to affect convergent extension, or induce Dvl-GFP translocation to the cell membrane in animal caps.
Wnt11b	Sulf1 enhances the ability of Wnt11b to induce ectopic *chordin* expression.	Sulf1 enhances the ability of Wnt11b to inhibit convergent extension and induce Dvl-GFP translocation to the cell membrane in animal caps.

range of Wnt3a signalling is not due to a decrease in its ability to bind LRP6. Wnt3a has previously been shown to bind heparin and this is inhibited by pre-treating heparin with Sulf2 (Tran et al., 2012). Wnt ligand diffusion is restricted by binding to Wnt receptors and HSPGs in the ECM (Eldar et al., 2003). Over-expression of Sulf1 in *Xenopus* may reduce the binding of Wnt3a to HS as it diffuses away from the region expressing it. One prediction from this is that Sulf1 could increase the range of Wnt3a diffusion, without inhibiting the ability of Wnt3a to activate canonical Wnt signalling. Further investigation is required in order to explain how Sulf1 regulates Wnt3a signalling.

Wnt4

Wnt4 was selected to investigate the effects of Sulf1 on non-canonical Wnt signalling, because of its possible interaction with Sulf1 during kidney formation in *Mouse* and *Xenopus* (Freeman et al., 2008; Holst et al., 2007; McGrew et al., 1992; Stark et al., 1994). Sulf1 enhances the ability of Wnt4 to activate non-

Table 6.2; The effects of Sulf1 on Wnt-HA-GFP ligands in animal caps

Ligand	Effects of Sulf1 on Wnt ligands in the same cells	Effects of Sulf1 on Wnt ligands diffusing away from a source	Effects of Sulf1 on Wnt ligands diffusing into a region expressing Sulf1
Wnt4-HA-GFP	• Sulf1 increases the amount of Wnt4 colocalising with the cell membrane • Sulf1 increases the average number of particles • Sulf1 does not alter the average size of particles • Sulf1 increases the average circularity of particles	• Not tested	• Not tested
Wnt8a-HA-GFP	• Sulf1 does not alter the amount of Wnt8a colocalising with the cell membrane • Sulf1 causes a decrease in the average number of particles • Sulf1 has no effect on average particle size • Sulf1 decreases the average circularity of particles	• Sulf1 decreases the rate of decay of fluorescently tagged Wnt8a, increasing its range of diffusion	• Sulf1 does not alter the amount of Wnt8a colocalising with the cell membrane of receiving cells • Sulf1 enhances the range of Wnt8a diffusion, reducing the concentration of Wnt8a close to the source
Wnt11b-HA-GFP	• Sulf1 increases the amount of Wnt11b colocalising with the cell membrane • Sulf1 increases the average number and size of particles • Sulf1 decreases the average circularity of particles	• Sulf1 decreases the rate of decay of fluorescently tagged Wnt11b, increasing its range of diffusion	• Sulf1 increases the amount of Wnt11b colocalising with the cell membrane of receiving cells • Sulf1 enhances the range of Wnt11b diffusion, without altering the rate of decay (the shape of the Wnt11b gradient is maintained)

canonical Wnt signalling. In addition, Sulf1 increases both the number of Wnt4-HA-GFP particles and the overall amount of Wnt4-HA-GFP colocalising with the cell membrane. Microinjection of increasing amounts of *Wnt4* mRNA increases the translocation of Dvl-GFP to the cell membrane (Pownall laboratory unpublished data). One prediction from this is that increasing the stability of Wnt4 on the cell membrane would lead to an increase in Dvl-GFP translocation. Similar to Wnt11b, Wnt4 binds to Ror2 when over-expressed in *Xenopus*. Sulf1 does not alter the interaction between Wnt4 and Ror2, although this was investigated in the absence of Fz7 (Pownall laboratory unpublished data). Importantly, Sulf1 did not increase the average size of Wnt4-HA-GFP puncta, or cause a decrease in the average circularity of particles. One prediction from this is that Sulf1 is not causing a qualitative change in Wnt4-HA-GFP puncta that would favour the formation of large ligand receptor complexes. Together the data suggests that Sulf1 enhances the ability of Wnt4 to activate non-canonical Wnt signalling by increasing the amount of Wnt4 present on the plasma membrane.

Wnt8a

Wnt8a was selected to investigate the effects of Sulf1 on canonical Wnt signalling because it was previously used in the development of the 'catch and present model'. Specifically, Sulf1 reduced the binding of tagged Wnt8a to heparin and glypican1. This was proposed to liberate Wnt8a from the cell surface allowing it to activate canonical Wnt signalling (Ai et al., 2003). Interestingly, a reduction in the binding of Wnt/Wg to HS may be the one consistent effect of Sulf1 in *Xenopus, Drosophila* and cell culture. Over-expression of Sulf1 in *Drosophila* results in a reduction in the detectable levels of extracellular Wg (Kleinschmit et al., 2010; You et al., 2011). This has been proposed to be due to an increase in Wg degradation by the endosomal pathway (Kleinschmit et al., 2013). However, it is possible that over-expressing Sulf1 reduces the ability of Wg to bind HS, causing Wg to diffuse throughout the wing disc, leading to a reduction in the detectable levels of extracellular Wg. In *Xenopus,* over-expression of Sulf1 in Wnt receiving cells reduces the ability of Wnt8a-HA-GFP to bind to the cell surface, extending its range of diffusion. In addition, over-expression of Sulf1 in Wnt expressing cells extended the range of

Wnt8a-HA-GFP diffusion suggesting that Sulf1 may be able to alter the packaging of Wnt ligands during their secretion.

A model for how Sulf1 inhibits the ability of Wnt8a to activate canonical Wnt signalling is presented (Figure 6.0). Data from chapter 3 shows that Sulf1 inhibits the ability of Wnt8a to stabilise β-catenin and induce the expression of ectopic *chordin* and *Xnr3* in whole embryos. However, the key assay for discerning the effects of Sulf1 on Wnt8a signalling is the *chordin* induction assay. Sulf1 inhibits the ability of Wnt8a to induce ectopic *chordin* expression inside the region over-expressing Sulf1. However, Wnt8a that could diffuse out of the domain expressing Sulf1 was able to induce *chordin* expression. One prediction from this is that the effects of Sulf1 in Wnt receiving cells are more important than those in producing cells for inhibiting Wnt8a signalling. In chapter 5, in control conditions, Wnt8a-HA-GFP has a limited range of diffusion, accumulating close to the source of the Wnt secreting cells (Figure 6.0A). Over-expression of Sulf1 in Wnt receiving cells, decreased the concentration of Wnt8a-HA-GFP close to the source. This brings the concentration of Wnt8a below that required to activate the expression of high threshold Wnt target genes. However, Wnt8a is able to freely diffuse through the region expressing Sulf1, until it reaches the edge of the Sulf1 domain. As Wnt8a passes out of the area expressing Sulf1 it can then accumulate at high concentrations on wildtype cells. This results in the activation of high threshold Wnt target genes at a distance from the source (Figure 6.0B).

The data in this thesis can be used to predict how Sulf1 is affecting Wnt8a signalling, but not exactly what the mechanism of action for Sulf1 is. Over-expression of Sulf1 in Wnt secreting cells causes a qualitative change in Wnt8a-HA-GFP puncta, leading to them becoming less spherical. It is possible that this allows them to form oligomers that favour long range diffusion, as predicted for HSPGs and Hh signalling proteins (Goetz et al., 2006; Vyas et al., 2008). Alternatively the change in shape could result in key residues required for Wnt8a signalling becoming buried in Wnt8a oligomers, inhibiting signalling. However, whether or not either of these occurs, the key mechanism for Sulf1 inhibiting Wnt8a signalling lies in the receiving cells.

Figure 6.0; Sulf1 inhibits Wnt8a signalling by increasing the range of Wnt8a diffusion.
Diagram depicting a model for the effects of Sulf1 on Wnt8a signalling in *Xenopus.* [A] In control conditions Wnt8a is only able to diffuse a short distance from source cells. Cells close to the source are exposed to high levels of Wnt8a, with a sharp decline in the concentration of Wnt8a with increasing distance from the source. [B] In the presence of Sulf1, Wnt8a particles undergo a qualitative change in shape. Sulf1 inhibits the binding of Wnt8a to the cell surface and enhances the range of Wnt8a diffusion. This results in a reduction in the local concentration of Wnt8a, which is then able to activate high threshold Wnt8a target genes at a distance from the source.

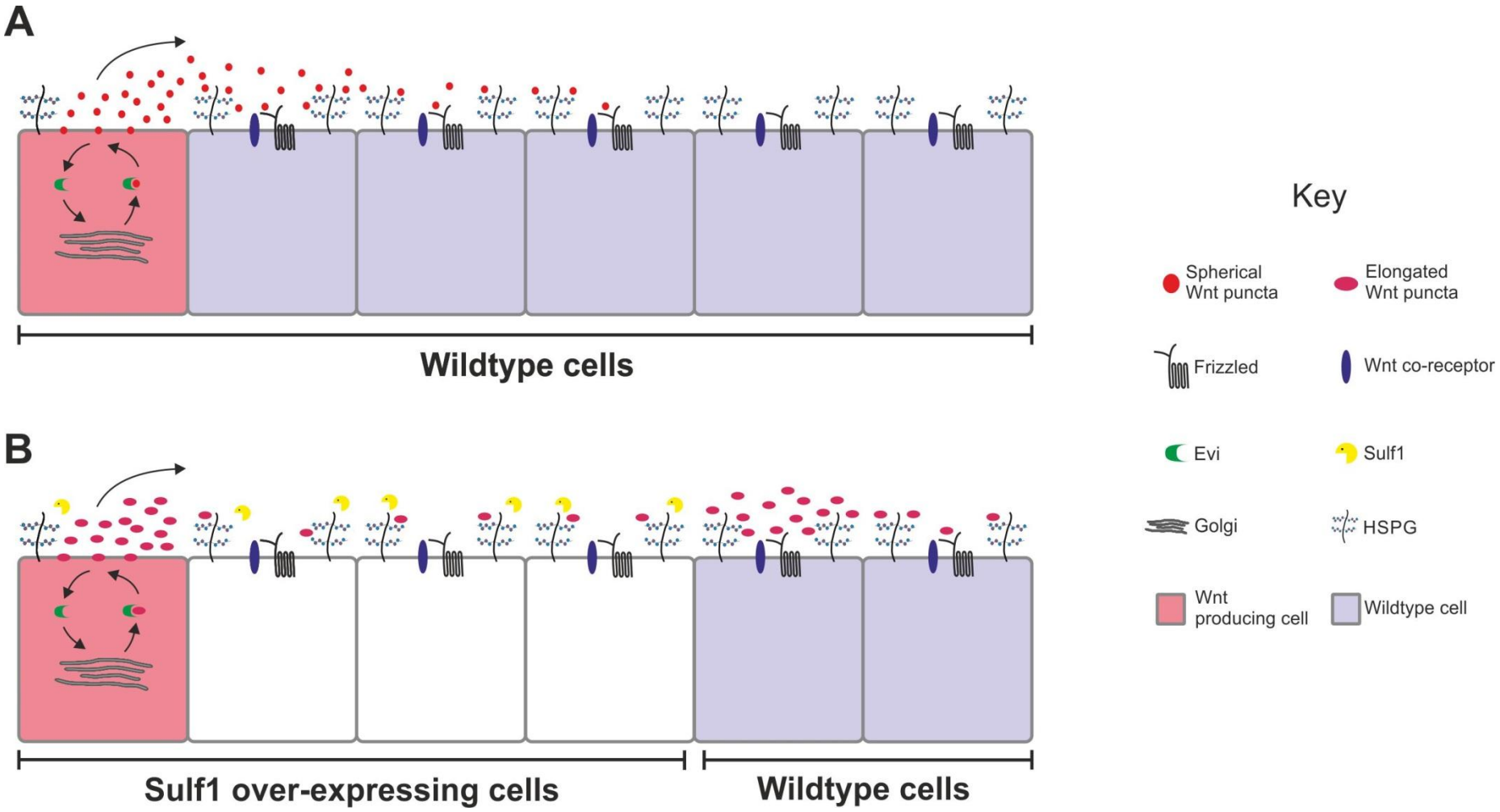
A
Wildtype cells
B
Sulf1 over-expressing cells
Wildtype cells
Key
Spherical Wnt puncta
Elongated Wnt puncta
Frizzled
Wnt co-receptor
Evi
Sulf1
Golgi
HSPG
Wnt producing cell
Wildtype cell

The graph in Figure 5.30 demonstrates that Wnt8a-HA-GFP diffuses further through a region over-expressing Sulf1. One prediction from this is that Sulf1 reduces the ability of Wnt8a-HA-GFP to bind to cells. Work by Ai et al., (2003) demonstrated that Sulf1 inhibits the ability of Wnt8a to bind heparin. In addition unpublished work from the Pownall laboratory has shown that Sulf1 inhibits the ability of Wnt8a to bind LRP6. Whether or not the decreased ability of Wnt8a to bind HS is directly responsible for the loss of LRP6 binding is unclear. The 6-O sulphate group of heparan is required to stabilise FGF ligand receptor complexes (Ornitz, 2000; Pellegrini et al., 2000; Schlessinger et al., 2000). Removal of the 6-O sulphate group from HS inhibits the ability of FGF2 to bind FGFr1, but not to heparin (Wang et al., 2004). It is possible that 6-O sulphated HSPGs are directly required for the formation of Wnt8a-LRP6 complexes. Alternatively, Wnt8a binding to HS chains could simply concentrate it on the cell membrane, increasing the probability of it associating with LRP6.

The qualitative change in the shape of Wnt8a-HA-GFP puncta could also be due to changes in Wnt receiving cells. Sulf1 C-A is able to increase the range of Wnt8a-HA-GFP diffusion when over-expressed in Wnt receiving cells. One prediction from this is that Sulf1 has a non-catalytic role in regulating Wnt ligand diffusion. Sulf1 is found to localise to lipid raft fractions in HEK293 cells (Tang and Rosen, 2009). In addition, Sulf1 and Sulf1 C-A are able to induce the clustering of glypican4-cerulean into discrete domains of the cell membranes of animal caps. The qualitative change in shape of Wnt8a-HA-GFP puncta in chapter 5 could be in response to the re-organisation of microdomains on the surface of Wnt receiving cells.

To summarise, Sulf1 reduces the ability of Wnt8a to bind to cells receiving Wnt8a, in a similar manner to that seen in Ai et al., (2003) and possibly (Kleinschmit et al., 2010; You et al., 2011). This prevents the accumulation of Wnt8a protein and inhibits the activation of high threshold Wnt target genes. However, Sulf1 encourages Wnt8a to diffuse away from the region expressing Sulf1, allowing activation of canonical Wnt signalling at a distant site. Reggie1/flotillin and dlp in *Drosophila*, and members of the sFRP family in vertebrates have been shown to enhance long range diffusion by inhibiting Wnt/Wg binding to the cell surface (Esteve et al., 2011; Katanaev et al., 2008;

Mii and Taira, 2009; Mulligan et al., 2012). Sulf1 has a similar role enhancing the long range signalling of Wnt8a in *Xenopus.*

Wnt11b

Wnt11b was selected to investigate the effects of Sulf1 on Wnt signalling because of its possible interaction with Sulf1 during organiser formation, somitogenesis and neural crest migration in *Xenopus* (Freeman et al., 2008; Guiral et al., 2010; Ku and Melton, 1993). Sulf1 enhances the ability of Wnt11b to activate non-canonical Wnt signalling, which is opposite to what would have been predicted based on work by (Tran et al., 2012). Interestingly, Sulf1 also enhanced the ability of Wnt11b to induce ectopic *chordin* expression. The ectopic domains of *chordin* induced were much broader than those induced by Wnt3a or Wnt8a alone. Sulf1 is able to enhance the ability of Wnt11b to activate both canonical and non-canonical Wnt signalling, in addition to increasing the range of Wnt11b signalling.

A model for how Sulf1 enhances Wnt11b signalling is presented (Figure 6.1). Sulf1 enhances the range of Wnt11b diffusion when over-expressed in Wnt secreting or Wnt receiving cells. However, unlike the data for Wnt8a, it is difficult to predict whether the presence of Sulf1 in secreting cells, or receiving cells is more important for its effects on non-canonical Wnt signalling. This question could be answered by using a modified version of the assay shown in Figures 5.27 and 5.28, where Wnt11b and Dvl-GFP could be over-expressed in adjacent cells. Sulf1 could then be over-expressed in Wnt secreting, or Wnt receiving cells and the effects on signalling could be analysed.

Sulf1 increases the overall levels of Wnt11b-HA-GFP that are detected on the surface of cells, despite reducing the total levels of Wnt11b-HA-GFP in animal caps (see Figure 5.12). In addition Sulf1 causes an increase in the average size and a reduction in circularity of Wnt11b-HA-GFP puncta. One prediction from this is that the increased stability of Wnt11b on the cell membrane enhances the activation of non-canonical Wnt signalling (Figure 6.1B). Interestingly this is exactly opposite to the effects of Sulf1 on Wg stability and signalling in *Drosophila* (Kleinschmit et al., 2010; You et al., 2011). The qualitative change in size and shape of Wnt11b particles may also reflect the

Figure 6.1; Sulf1 increases the overall levels of Wnt11b on the cell membrane and enhances the range of Wnt11b diffusion.
Diagram depicting a model for the effects of Sulf1 on Wnt11b signalling in *Xenopus.* [A] In control conditions hardly any Wnt11b can be detected on the cell surface. Wnt11b that is present on the cell surface is able to diffuse two or three cell diameters and activate non-canonical Wnt signalling in receiving cells. [B] Sulf1 dramatically enhances the secretion of Wnt11b and its stability in the ECM. In addition Sulf1 causes a qualitative change in shape of Wnt11b puncta resulting in the formation of large non-canonical signalling complexes. The increased stability and diffusion of Wnt11b allows the activation of Wnt signalling over a broader range of cells. In addition the increased amount of Wnt11b present on the cell surface results in the cross activation of canonical Wnt signalling.

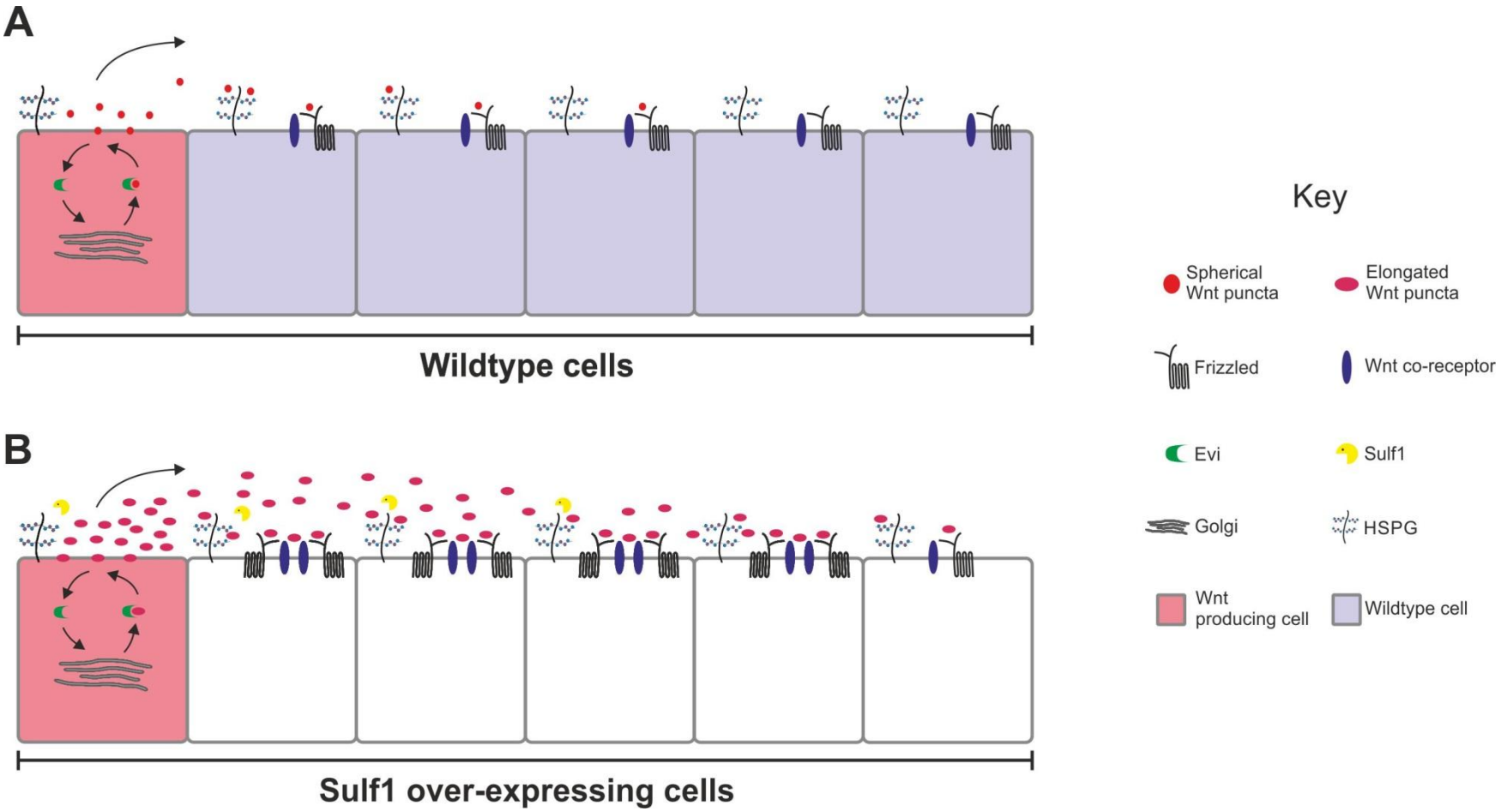
A
Wildtype cells
B
Sulf1 over-expressing cells
Key
Spherical Wnt puncta
Elongated Wnt puncta
Frizzled
Wnt co-receptor
Evi
Sulf1
Golgi
HSPG
Wnt producing cell
Wildtype cell

enhancement of non-canonical Wnt signalling. In Figure 5.18, Sulf1 increases the levels of Wnt11b-HA-Venus accumulation on the cell membrane. This is coupled to an increase in the aggregation of Dvl-GFP on the inside of the plasma membrane. In addition, unpublished data from the Pownall laboratory has shown that Sulf1 enhances the formation of Fz7-Ror2 oligomers in the presence of Wnt11b. One conclusion form this is that Sulf1 enhances the formation or stability of non-canonical receptor complexes (Figure 6.1B). Sulphated HSPGs are required for the formation of stable FGF and BMP signalling complexes (Freeman et al., 2008; Wang et al., 2004).

How exactly a reduction in the circularity of Wnt11b favours the activation of non-canonical Wnt signalling is unclear, although it is possible that more elongated Wnt11b particles favour the formation of large ligand receptor complexes. However one possibility is that a reduction in Wnt8a circularity would enhances its ability to activate non-canonical Wnt signalling, which was not the case in this thesis. Sulf1 enhanced the range of diffusion of both Wnt8a and Wnt11b-HA-GFP when over-expressed in Wnt secreting cells. It is possible that the change in circularity of both ligands reflects a related change in how the ligands are packaged for secretion.

Sulf1 enhances both the secretion of Wnt11b-HA-GFP and its stability on receiving cells. The over-all effect of this is to enhance the range of Wnt11b diffusion, without reducing the concentration of Wnt11b close to the source. This means that the overall shape of the Wnt11b diffusion gradient is maintained (see Figure 5.30C). The net result of this is an increase in the level and range of Wnt11b signalling across the range of cells expressing Sulf1 (Figure 6.1B).

Sulf1 enhances the ability of Wnt11b to induce ectopic *chordin* expression. In addition, Sulf1 enhances the colocalisation of caveolin-GFP with Wnt11b-HA-Venus. Work by Freeman et al., (2008) has shown that Sulf1 increases the ability of Wnt11b to bind LRP6. The effects of Sulf1 are ligand specific, as Sulf1 does not alter the binding of Wnt3a and inhibits the binding of Wnt8a to LRP6 (Pownall laboratory unpublished data). One possibility is that the increased stabilisation of Wnt11b on the cell surface results in the non-specific binding of

Wnt11b to LRP6. An increase in the binding of Wnt11b to LRP6 would then result in the clustering of activated LRP6 receptors, which have been shown to colocalise with caveolin (Bilic et al., 2007).

The ability of Sulf1 to increase Wnt11b activation of canonical Wnt signalling is interesting, given that Wnt11b and HSPGs are required for endogenous organiser formation in *Xenopus* (Tao et al., 2005). In addition, *Wnt11b* and *Sulf1* mRNA colocalise in the dorsal-vegetal cells of the early cleavage embryo (Freeman et al., 2008). Tao et al., (2005) demonstrated that maternal depletion of *Wnt11b* inhibited the induction of β-catenin, but not VegT dependent genes. This points towards Wnt11b functioning specifically in the activation of the canonical Wnt signalling pathway. One conclusion from this is that in the dorso-vegetal environment of the early embryo Wnt11b is specifically required to activate canonical Wnt signalling. In this scenario, Sulf1 enhancing the stability of Wnt11b, would potentiate the organiser inducing activity of Wnt11b. This prediction is backed up by data from Figure 3.7, in which Sulf1 enhances the size and the breadth of the endogenous organiser when over-expressed in *Xenopus*.

The models shown above depict how Sulf1 is predicted to have different effects on the signalling activities of Wnt3a, Wnt4, Wnt8a and Wnt11b. However, one important consideration for interpreting these effects is that cell signalling pathways do not function in isolation. For example, BMP2 potentiates the ability of Wnt3a to activate Topflash in cell culture (Nakashima et al., 2005). In addition, inhibiting either non-canonical Wnt or FGF signalling inhibits activin induced convergent extension in animal caps (Cornell and Kimelman, 1994; Tada and Smith, 2000). Sulf1 has been shown to regulate Wnt/Wg, Hh, FGF and BMP signalling in *Drosophila* and vertebrates (Freeman et al., 2008; Kleinschmit et al., 2010; Meyers et al., 2013; Wang et al., 2004; Wojcinski et al., 2011). Understanding how alterations in one signalling pathway affects others is an important consideration when studying the role of Sulf1 in cells. When Sulf1 and Wnt are over-expressed together, the effects of Sulf1 on Wnt signalling are effectively being assayed in a background in which BMP and FGF signalling are supressed. This adds an extra layer of complexity to interpreting the effects of Sulf1 on Wnt signalling. One prediction from this is that Sulf1 may

have different effects on Wnt signalling, depending on which other signalling pathways are active in the system. The types of signalling pathway present in a system will likely feed into the environment specific role of Sulf1 in regulating Wnt signalling.

6.2 The effects of Sulf1 on BMP signalling in different systems

The effects of Sulf1 on Wnt signalling in *Xenopus* are different to those in cell culture. A similar situation is found for the role of Sulf1 in regulating BMP signalling. The BMP inhibitor noggin, Zimmerman et al., (1996) binds to HSPGs on the cell surface inhibiting BMP signalling in CHO cells (Paine-Saunders et al., 2002). Transfection of these cells with Sulf1 results in the release of noggin from the cell surface and the activation of BMP signalling (Viviano et al., 2004). *Sulf1* knockout mice show a reduction in BMP signalling in the knee joints, associated with cartilage degeneration and early onset arthritis. In addition, knockdown of *Sulf1* in Human chondrocytes inhibits the ability of BMP7 to activate BMP signalling (Otsuki et al., 2010). Together these data suggest that Sulf1 potentiates the ability of BMP ligands to activate cell signalling.

In contrast Sulf1 inhibits BMP signalling in both *Xenopus,* Freeman et al., (2008) and *Zebrafish,* Meyers et al., (2013) during development. Over-expression of Sulf1 inhibits the ability of BMP4 to activate BMP signalling in *Xenopus* animal caps (Freeman et al., 2008). In addition, microinjection of morpholinos targeting Sulf1 results in a reduction in Pax6 expression during neurulation, Freeman et al., (2008), consistent with increased BMP signalling (Hartley et al., 2001). In *Zebrafish,* injection of morpholinos targeting *Sulf1,* causes an increase in BMP signalling in the somites and disrupts the migration of the horizontal myoseptum. Both of these phenotypes are rescued by treating embryos with the BMP inhibitor LDN (Meyers et al., 2013). These findings suggest that Sulf1 negatively regulates BMP signalling during development and are opposite to those from *Mouse* and cell culture (Otsuki et al., 2010; Viviano et al., 2004). Together these data suggest that the effects of Sulf1 on BMP signalling depend on the environment in which BMP is expressed, similar to the effects of Sulf1 on Wnt signalling.

6.3 A role for exosomes in Wnt ligand diffusion

Over-expression of Sulf1 results in a qualitative change in shape of Wnt8a and Wnt11b-HA-GFP puncta on the cell membrane. This could be due to alterations in the way in which the Wnt ligands are being packaged for secretion. Recent work by Beckett et al., (2013) has cast doubt on the role of exosomes during Wg signalling in *Drosophila*. Wnt8a and Wnt11b-HA-GFP were found associated with cell membranes while diffusing through *Xenopus* animal caps and no transcytosis was detected in this system. The long range diffusion of Xnr2-EGFP, Williams et al., (2004) and activin-Alexa488, Hagemann et al., (2009) have also previously been investigated in *Xenopus* animal caps. Both ligands were found to form morphogen gradients by long range diffusion. Xnr2-EGFP was not found to associate with exosome like vesicles during morphogen gradient formation (Williams et al., 2004). In addition, activin-Alexa488 was able to form long range signalling gradients in the presence of DN*Rab5 (Hagemann et al., 2009). Together these data suggest that exosomes and transcytosis are not be required for long range Wnt/Xnr2/activin diffusion in *Xenopus.*

6.4 Importance of apical/basal polarity during Wnt/Wg secretion

Data in this thesis has revealed that Sulf1 can alter the membrane localisation of glypican4-cerulean. In *Drosophila,* Wg is secreted apically and then redistributed to the basolateral membrane via transcytosis (Simmonds et al., 2001; Strigini and Cohen, 2000). This has been shown to require dlp and the *Drosophila* homologue of dynamin, shibire (van der Bliek and Meyerowrtz, 1991; Chen et al., 1991; Gallet et al., 2008). Disrupting the basolateral localisation of Wg inhibits Wg signalling (Simmonds et al., 2001). Recently the polarised secretion of Wnt3a and Wnt11 has been identified in MDCK cells (Yamamoto et al., 2013). Wnt11 was found to be secreted apically, with Wnt3a secreted basolaterally and biochemical analysis of the Wnt ligands revealed that glycosylation at amino acid 40 was required for the apical targeting of Wnt11. In addition, the clathrin subunits AP1 and 2 were required for Wnt3a,

but not Wnt11 secretion (Yamamoto et al., 2013). The targeted secretion of Wnt/Wg is important for its signalling activity and different Wnt ligands rely on distinct trafficking mechanisms for secretion. One prediction from this is that Sulf1 may alter the targeted secretion of different Wnt ligands.

During the project it was difficult to investigate the apical/basal polarity of Wnt8a and Wnt11b-HA-GFP in animal caps. This was due in part to a lack of available markers of apical/basal compartments in live tissue. In addition, the large amount of yolk protein in the animal cap cells made it difficult to penetrate deep into the tissue using confocal microscopy. The analysis of GFP tagged Wnt ligands used confocal microscopy on a single (lateral) plain of cells. Based on the Z stacks that were taken, animal cap cells were imaged at a depth of approximately 5μm from the apical pole of the cells. Future studies using multiphoton microscopy should help to increase the depth at which animal explants can be imaged. Given the role of dlp in Wg trafficking, Gallet et al., (2008), it is important to determine whether Sulf1 increases the total levels of glypican4-cerulean, or alters the cell membrane on which it accumulates (Figure 5.32). The 6-O sulphate group on the GAG chains of glypican-4/dlp may be important for its apical/basal polarity and could provide a mechanism to explain the effects of Sulf1 on Wnt signalling.

6.5 A role for Sulf1 in regulating Wnt signalling during development.

This thesis has been concerned with how Sulf1 is able to affect Wnt signalling using *Xenopus*, but not how Sulf1 regulates Wnt signalling during development. Sulf1 displays a dynamic expression pattern during development and is found in regions involved in inductive interactions, cell proliferation and cell migration. These regions include the posterior paraxial mesoderm during somite formation, the floor plate of the neural tube, the neural crest and the developing pronephros (Freeman et al., 2008; Gorsi et al., 2010; Ratzka et al., 2010). The dynamic expression of Sulf1 reflects its role in regulating multiple signalling pathways during development. For example, microinjection of morpholinos targeted against Sulf1 into *Xenopus* results in elevated pSmad1 and dpERK, indicating Sulf1 normally inhibits BMP and FGF signalling during development

(Freeman et al., 2008). In addition, Sulf1 is required to restrict the action of SHh during the dorsal/ventral patterning of the neural tube (Pownall laboratory unpublished data). Sulf1 has multiple roles in regulating cell signalling during development.

Analysing the function of Sulf1 during *Mouse* development is hampered by the functional redundancy it shares with Sulf2. *Sulf1* single knockout mice are viable and healthy, with no obvious defects (Holst et al., 2007; Lamanna et al., 2006; Ratzka et al., 2010). *Sulf2* knockout mice are viable, but show a small reduction in size compared to wildtype mice (Lamanna et al., 2006; Lum et al., 2007). In contrast *Sulf1/2* double knockout mice die perinatally with defects in the formation of the sternum, radial bones, vertebrae and a significant reduction in the size of the kidneys (Holst et al., 2007; Ratzka et al., 2008). In addition, *Sulf1/2* knockout mice have an enlarged oesophagus accompanied with breathing difficulties (Ai et al., 2007). Analysis of the oesophagus in these mice revealed a reduction in the innervation of the oesophageal smooth muscle leading to defects in peristalsis. This may account for some of the difference in weight between wildtype and *Sulf1/2* double knockout pups.

One interesting role for Sulf1/2 during *Mouse* development is in regulating the size of the adult kidney. *Sulf1/2* knockout mice show a reduction in kidney weight and size compared to control mice. A reduction in kidney size is also seen in *Wnt4,* Stark et al., (1994) and *Wnt11,* Majumdar et al., (2003) knockout mice. Wnt11 is required for uteric bud branching, Kispert et al., (1996) and Wnt4 for tubulogenesis, Kispert et al., (1998) during kidney formation and both of these processes will require cell polarisation and migration. In addition, HSPGs are required for Wnt4 induced metanephric kidney tubulogenesis *in vitro* (Kispert et al., 1998). This thesis demonstrates that Sulf1 potentiates the ability of Wnt4/Wnt11b to activate non-canonical Wnt signalling. One prediction from this, is that Sulf1 may regulate cell polarisation and migration via non-canonical Wnt signalling *in vivo*. In *Xenopus,* Wnt4 and Sulf1 are both expressed in the pronephros during early/mid tailbud stages, suggesting a possible interaction (Pownall laboratory unpublished data). Future investigations into the effects of Sulf1 on non-canonical Wnt signalling during *Xenopus* development should focus on morphogenesis in the pronephros.

Sulf1 may also regulate non-canonical Wnt signalling during neural crest migration. The neural crest is a transient population of cells that are induced at the border between the neural and non-neural ectoderm. Once induced, neural crest cells undergo an epithelial to mesenchymal transition and delaminate from the neighbouring epithelial cells. The neural crest then migrates throughout the developing embryo contributing to a variety of tissues including the peripheral nervous system, pigmented cells, craniofacial structures and the outflow tract of the heart, reviewed by (Basch et al., 2004; Theveneau and Mayor, 2012). The extracellular environment provides a permissive substrate for neural crest cells and the HSPG syndecan4 is required both autonomously and non-autonomously for neural crest cell migration (Matthews et al., 2008). Directed migration of the neural crest requires a process known as contact inhibition, where migrating populations of cells retract their protrusions and change direction on contact with each other (Abercrombie and Heaysman, 1953, 1954). Contact inhibition requires cell-cell contacts and components of the non-canonical Wnt signalling pathway including Wnt11, Dvl, Rac and RhoA (Carmona-Fontaine et al., 2008; Theveneau et al., 2010).

Wnt11b is expressed adjacent to the migrating neural crest in *Xenopus* embryos (De Calisto et al., 2005). Microinjection of mRNA encoding *Wnt11b* or *DN*Wnt11b,* disrupts the migration of the cranial neural crest. In addition, grafts from donor embryos over-expressing Wnt11b, were able to inhibit neural crest migration non-autonomously in host embryos in the region in which they were transplanted (De Calisto et al., 2005). *Sulf1* and *Sulf2* are both expressed in the cranial neural crest in *Xenopus* (Freeman et al., 2008; Guiral et al., 2010). Knockdown of *Sulf1* or *Sulf2* in either the neural crest cells, or the extracellular environment, disrupts neural crest cell migration (Guiral et al., 2010). Explant studies have shown that Wnt11b and Dvl accumulate in microdomains on the membrane of neural crest cells that collide (Carmona-Fontaine et al., 2008). This is similar to the accumulation of Wnt11b and Dvl on the plasma membrane of animal cap explants over-expressing Sulf1, shown in chapters 4 and 5. Sulf1 enhances non-canonical Wnt signalling and Sulf1, Sulf2 and Wnt11b all have roles during neural crest migration.

6.6 Sulf1 and cancer

Sulf1 regulates a diverse array of signalling pathways during development, making it a prime candidate for misregulation in disease. Changes in Sulf1 expression are correlated with a variety of cancers including lung, pancreatic, gastric, liver, breast and ovarian cancer (Bret et al., 2011; Hur et al., 2012; Lai et al., 2003; Nawroth et al., 2007). Originally, Sulf1 was identified as a tumour suppressor gene in cancer formation. Lai et al., (2004) found *Sulf1* to be down regulated in primary hepatocellular carcinomas. Analysis of the hepatocellular carcinoma cell line SNU449, showed that this was due to hypermethylation of the Sulf1 promoter. Transfection of SNU449 cells with *Sulf1* inhibited cell proliferation in response to bFGF and cell survival in response to staurosporine. In addition, Narita et al., (2007) demonstrated that *Sulf1* was down regulated in 60% of primary breast cancers isolated from patients. However, *Sulf1* has also been found to be up regulated in lung, breast and gastric cancers, Bret et al., (2011) indicating that in some cases Sulf1 acts as an oncogene. Sulf1 expression was found to be associated with aggressive gastric cancers and gastric cancer patients that showed Sulf1 expression were found to have a significant reduction in five year survival rates (Hur et al., 2012). Transfection of the gastric cancer cell line AGS with *Sulf1* enhanced tumour formation in nude mice (Hur et al., 2012).

The role of Sulf1 in cancer is a good example of what has been discussed in this thesis. Whether Sulf1 acts as a tumour suppressor, or an oncogene, is dependent on the cellular environment in which it is found. FGF signalling has been heavily linked to tumorigenesis for hepatocellular carcinoma, reviewed by (Cheng et al., 2011). One prediction from this is that Sulf1 will act as a tumour suppressor during hepatocellular carcinoma and that expression of Sulf1 in these tumours will be correlated with an increased rate of survival. In gastric cancer, Sulf1 is correlated with more aggressive tumours, and may potentiate canonical Wnt signalling in order to promote cell survival. This would be similar to the effects observed by Ai et al., (2003); Dhoot et al., (2001); Tang and Rosen, (2009) on Wnt signalling in cell culture. Yang et al., (2011) found that high or low levels of *Sulf1* correlated with a poor prognosis in patients with hepatocellular carcinoma. Patients expressing ‘medium’ levels of *Sulf1* were

found to have a higher rate of survival (Yang et al., 2011). This suggests that any misregulation of Sulf1 can promote tumorigenesis. In addition, (Li et al., 2011) found that the gastric cancer cell lines MKN28 and AGS respond differently to Sulf1 in culture. Transfection of MKN28 cells, but not AGS cells with Sulf1 inhibits cell proliferation and migration in cell culture assays. In addition, Sulf1 inhibited β-catenin stabilisation in MKN28 cells, but not AGS cells (Li et al., 2011). The role of Sulf1 in tumorigenesis seems to depend on the types of signalling molecules misregulated and the environment in which the tumour develops.

One area of cancer biology in which Sulf1 is likely to be important is the transition from growth to metastasis. Sulf1 is a negative regulator of FGF and VEGF signalling during development and tumorigenesis (Freeman et al., 2008; Fujita et al., 2009; Lai et al., 2003; Narita et al., 2006). One prediction from this is that Sulf1 will act as a negative regulator of cell proliferation and survival during tumour growth. Data in this thesis has shown that Sulf1 potentiates the ability of Wnt4 and Wnt11b to activate non-canonical signalling. It is possible that Sulf1 may be required to potentiate non-canonical Wnt signalling during tumour metastasis. The effects of Sulf1 during tumorigenesis may not only relate to the cellular environment in which Sulf1 is expressed, but also the stage of cancer development. The extracellular nature of Sulf1, and the fact that it is an enzyme, makes it a good potential target for drug development for cancers known to have elevated Sulf1 activity.

6.7 Summary

Sulf1 regulates multiple cell signalling pathways during development. Since its discovery in 2001, Sulf1 has been shown to potentiate canonical Wnt signalling in cell culture (Ai et al., 2003; Dhoot et al., 2001; Tang and Rosen, 2009). In contrast Sulf1 has been found to negatively regulate Wg signalling in *Drosophila* (Kleinschmit et al., 2010, 2013; You et al., 2011). The aim of this thesis was to investigate the effects of Sulf1 on canonical and non-canonical Wnt signalling in *Xenopus*. In addition, it was important to establish a possible mechanism for these effects. This thesis has shown that the effects of Sulf1 on Wnt signalling in *Xenopus* are ligand specific and likely to depend on the complement of HSPGs and Wnt receptors present in the environment. In addition, Sulf1 is able to regulate the formation of gradients of GFP tagged Wnt ligands in *Xenopus* animal cap explants. Understanding how Sulf1 modulates cell signalling in different contexts will be important for understanding how embryos develop and may inform more applied research to develop novel treatments of Human disease.

Appendices

Plasmid maps

CS2+ Vector

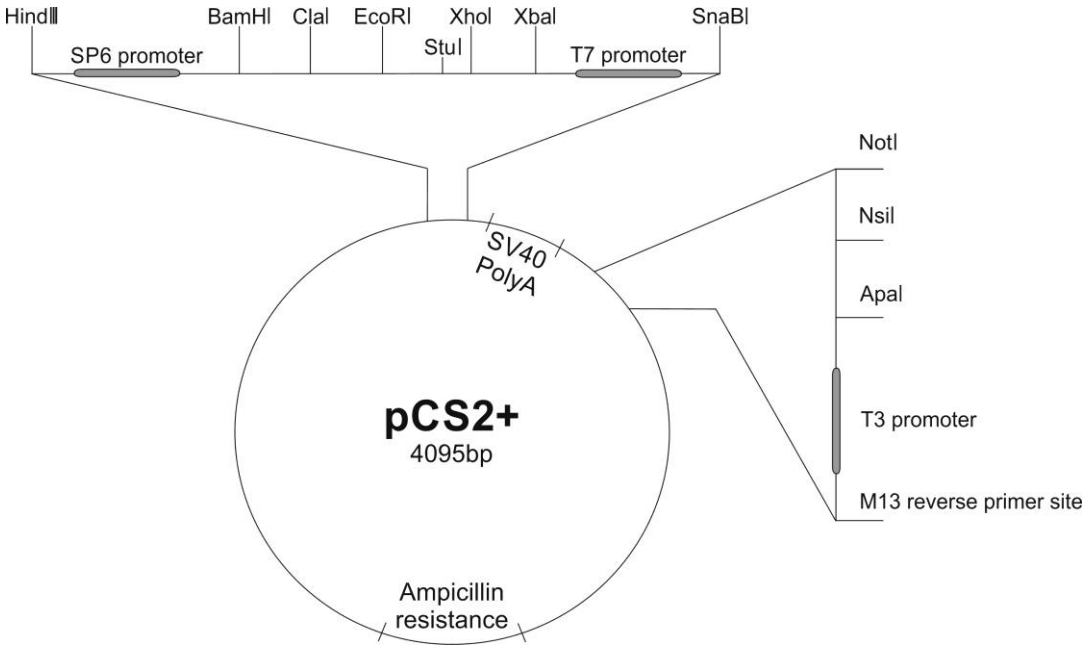

Glypican4-Cerulean in CS2+

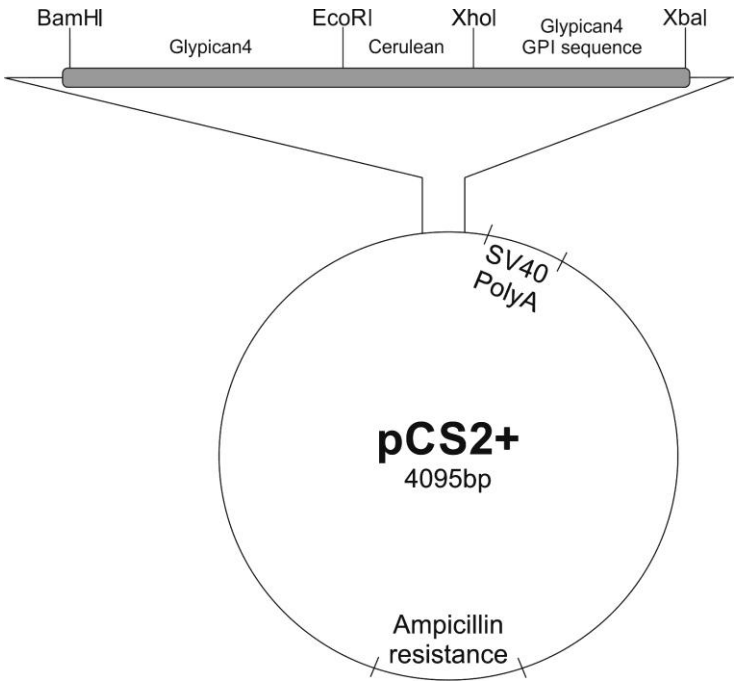

mCerulean in CS2+

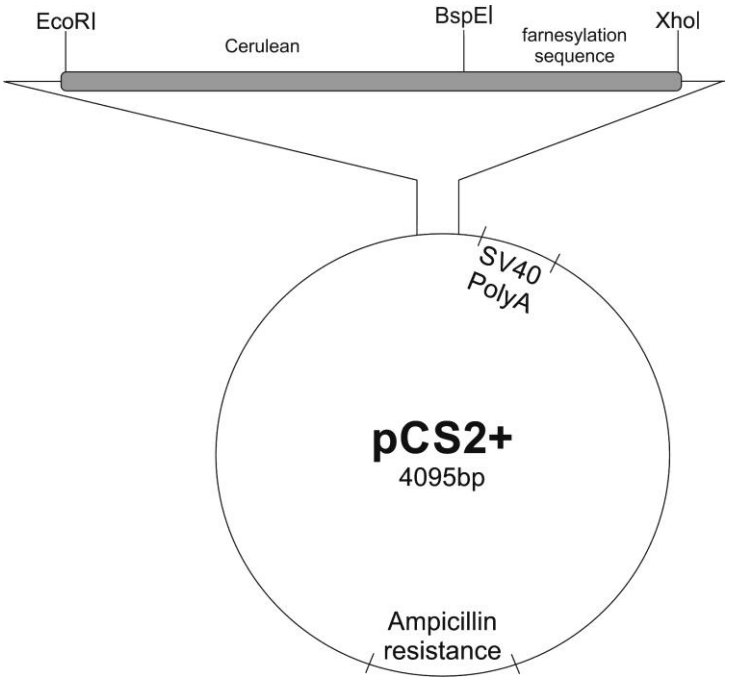

Wnt8a-HA-GFP/Venus

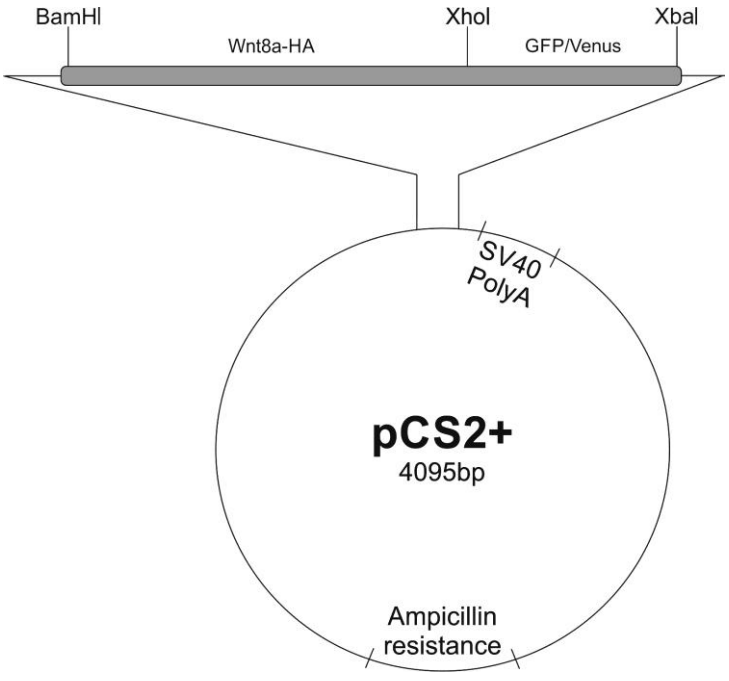

Wnt11b-HA-GFP/Venus

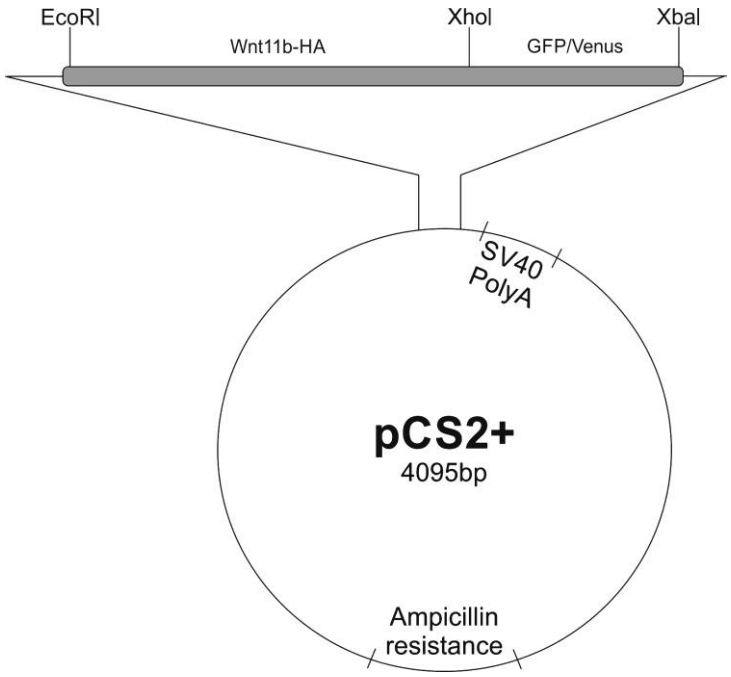

Abbreviations

2-OST = 2-O-sulfotransferase
3-OST = 3-O-sulfotransferase
6-OST = 6-O-sulfotransferase
APC = Adenomatous polyposis coli
AP buffer = Alkaline phosphatase buffer
APS = Ammonium persulfate
Bcl9 = B-Cell CLL/Lymphoma9
bFGF = Basic FGF
BMB = Boehringer Mannheim blocking reagent
BMP = Bone morphogenetic proteins
Botv = Brother of tout velu
BSA = Bovine serum albumin
Buffer H = Homogenisation buffer
C1-6 = Carbon atom 1-6
C5-epimerase = Heparosan-N-sulfate d-glucuronosyl5-epimerase
C.elegans = Caenorhabditis elegans
CamKII = Calcium/calmodulin kinaseII
CE = Convergent extension
CI = Confidence interval
Ck1 = Casein kinase 1
CRD = Cysteine rich domain
Cthrc1 = Collagen triple helix repeat containing protein1
Daam1 = Dishevelled associated activator of morphogenesis
Dally = Division abnormally delayed
DAI = Dorso-anterior index
Dbt = Double time
DEP = Dishevelled, Egl-10 and Pleckstrin
DFz = *Drosophila* frizzled
DIG NTP = Digoxygenin nucleotide triphosphate
Dint1 = *Drosophila* int1
DIX = Dvl and axin
Dkk1 = Dickkopf1
Dlp = Dally like protein
DMZ = Dorsal marginal Zone
DN* = Dominant negative
DPar1 = *Drosophila* Par1

dpERK = Diphospho-ERK
Dpp = Decapentaplegic
Dsh = Dishevelled (*Drosophila)*
DTT = Dithiothreitol
Dvl = Dishevelled (Vertebrate)
Dvl-GFP = Dishevelled fused to green fluorescent protein
ECM = Extracellular matrix
EDTA = Ethylenediaminetetraacetic acid
EGTA = Ethylene glycol tetraacetic acid
Ejcs = Excitatory junctional currents
EMS = Ethyl methanesulfonate
Evi = Evenness interrupted
EXTL = EXT like gene
FGF = Fibroblast growth factor
FGFr = Fibroblast growth factor receptor
Frat1 = Frequently rearranged in advanced T-cell lymphomas1
Fz = Frizzled
GAG = Glycosaminoglycan
GAPs = GTPase activating proteins
Gbb = Glass bottom boat
GEFs = Guanine nucleotide exchange factors
GFP = Green fluorescent protein
GlcA = Glucuronic acid
GlcNAc = N-acetylglucosamine
GlcNS = N-sulfoglucosamine
GOF = Gain of function mutation
GPCr = G protein coupled receptor
GPI = Glycophosphatidylinositol
Grg = Gro-related gene
GSK3β = Glycogen synthase kinase-3β
GEFs = Guanine nucleotide exchange factors
HCG = Human chronic gonadotropin
Hh = Hedgehog
HS = Heparan sulphate
HSPG = Heparan sulphate proteoglycans
IdoA = Iduronic acid
Irp = Int related protein
JNK = Jun N terminal kinase

Lb media = Luria-Bertani media
L15 = Leibovitz L15 media with L-glutamine
Lef/Tcf = Lymphoid enhancing factor/T cell factor
LiCl = Lithium chloride
LOF = Loss of function
MAB = Maleic acid Buffer
Mad = Mothers against decapentaplegic
MAPK = Mitogen activated protein kinase
mCerulean = Farnesylated cerulean
Mmtv = Mouse mammary tumour virus
MOPs = Morpholinepropanesulfonic acid
mRFP = Farnesylated red fluorescent protein
MRS = Modified Ringer's saline
NAM = Normal amphibian medium
NF = Nieuwkoop and Faber
NLK = NEMO-like kinase
NDST = N-deacetylation/N-sulphation
Pan = Pangolin
PAPS = 3'-phosphoadenosine 5'-phosphosulfate
PBS = Phosphate buffered saline
PCP = Planar cell polarity
PKC = Protein kinase C
pSmad1 = Phosphorylated Smad1
pSmad2 = Phosphorylated Smad2
Ptl = Pipetail
RGS = Regulator of G protein synthesis
Rock = Rho associated kinase
RNAi = RNA interference
Running buffer = Tris-glycine running buffer
SDS = Sodium dodecyl sulphate
Ser/thr = Serine/threonine
Sfrp = Secreted frizzled related protein
Shh = Sonic Hedgehog
shRNA = Small hairpin RNA
siRNA = Small interfering RNA
Slb = Silberblick
Sotv = Sister of tout velu
Sqv = Squashed vulva

S.e.m = Standard error of the mean
Stbm = Van gogh/strabismus
T1/2 = Half-life
TAB1 = TAK1 binding protein1
TAK1 = TGF-β activated kinase1
TBS = Tris buffered saline
TGF-β = Transforming growth factor-β
TAE buffer = Tri-acetate-EDTA buffer
Transfer buffer = Tris-glycine transfer buffer
Ttv = Tout velu
Ub = Ubiquitin
UV = Ultra violet
Venus = Yellow fluorescent protein
VMZ = Ventral marginal zone
wGEF = Weak activating GEF
Wg = Wingless
Wnt = Wingless related integration site
Wnt3aC77A = Wnt3a cysteine 77 to alanine
Wnt3aS209A = Wnt3a serine 209 to alanine
Wnt11r = Wnt11 related
XlWnt11b = Wnt11b
XtWnt11b2 = Wnt11b2
Xnr = Xenopus nodal related
Xl = *Xenopus laevis*
Xt = *Xenopus tropicalis*
Yeast RNA = Yeast sodium salt ribonucleic acid
YFP = Yellow fluorescent protein
ZW3 = Zeste-white 3

References

Abercrombie, M., and Heaysman, J.E.M. (1953). Observations on the social behaviour of cells in tissue culture: I. Speed of movement of chick heart fibroblasts in relation to their mutual contacts. Experimental Cell Research *5*, 111–131.

Abercrombie, M., and Heaysman, J.E.M. (1954). Observations on the social behaviour of cells in tissue culture: II. “Monolayering” of fibroblasts. Experimental Cell Research *6*, 293–306.

Aberle, H., Bauer, A., Stappert, J., Kispert, A., and Kemler, R. (1997). beta-catenin is a target for the ubiquitin-proteasome pathway. EMBO J. *16*, 3797–3804.

Adler, P.N. (2002). Planar Signaling and Morphogenesis in Drosophila. Developmental Cell *2*, 525–535.

Adler, P.N., Charlton, J., and Vinson, C. (1987). Allelic variation at the frizzled locus of Drosophila. Developmental Genetics *8*, 99–119.

Agius, E., Oelgeschlager, M., Wessely, O., Kemp, C., and De Robertis, E.M. (2000). Endodermal Nodal-related signals and mesoderm induction in Xenopus. Development *127*, 1173–1183.

Ahn, J., Ludecke, H.J., Lindow, S., Horton, W.A., Lee, B., Wagner, M.J., Horsthemke, B., and Wells, D.E. (1995). Cloning of the putative tumour suppressor gene for hereditary multiple exostoses (EXT1). Nat Genet *11*, 137–143.

Ai, X., Do, A.T., Lozynska, O., Kusche-Gullberg, M., Lindahl, U., and Emerson, C.P. (2003). QSulf1 remodels the 6-O sulfation states of cell surface heparan sulfate proteoglycans to promote Wnt signaling. J Cell Biol *162*, 341–351.

Ai, X., Do, A.T., Kusche-Gullberg, M., Lindahl, U., Lu, K., and Emerson, C.P. (2006). Substrate specificity and domain functions of extracellular heparan sulfate 6-O-endosulfatases, QSulf1 and QSulf2. J Biol Chem *281*, 4969–4976.

Ai, X., Kitazawa, T., Do, A.-T., Kusche-Gullberg, M., Labosky, P.A., and Emerson, C.P., Jr (2007). SULF1 and SULF2 regulate heparan sulfate-mediated GDNF signaling for esophageal innervation. Development *134*, 3327–3338.

Aikawa, J., and Esko, J.D. (1999). Molecular Cloning and Expression of a Third Member of the Heparan Sulfate/Heparin GlcNAcN-Deacetylase/ N-Sulfotransferase Family. J. Biol. Chem. *274*, 2690–2695.

Aikawa, J., Grobe, K., Tsujimoto, M., and Esko, J.D. (2001). Multiple isozymes of heparan sulfate/heparin GlcNAc N-deacetylase/GlcN N-sulfotransferase. Structure and activity of the fourth member, NDST4. J. Biol. Chem. *276*, 5876–5882.

Almeida, R., Levery, S.B., Mandel, U., Kresse, H., Schwientek, T., Bennett, E.P., and Clausen, H. (1999). Cloning and expression of a proteoglycan UDP-galactose:beta-xylose beta1,4-galactosyltransferase I. A seventh member of the human beta4-galactosyltransferase gene family. J Biol Chem *274*, 26165–26171.

Amaya, E., Musci, T.J., and Kirschner, M.W. (1991). Expression of a dominant negative mutant of the FGF receptor disrupts mesoderm formation in Xenopus embryos. Cell *66*, 257–270.

Amaya, E., Stein, P.A., Musci, T.J., and Kirschner, M.W. (1993). FGF signalling in the early specification of mesoderm in Xenopus. Development *118*, 477–487.

Arikawa-Hirasawa, E., Watanabe, H., Takami, H., Hassell, J.R., and Yamada, Y. (1999). Perlecan is essential for cartilage and cephalic development. Nat. Genet. *23*, 354–358.

Asashima, M. (1990). Mesodermal induction in early amphibian embryos by activin A (erythroid differentiation factor). Development Genes and Evolution *198*, 330–335.

Attar, N., and Cullen, P.J. (2010). The retromer complex. Adv. Enzyme Regul. *50*, 216–236.

Axelrod, J.D. (2001). Unipolar membrane association of Dishevelled mediates Frizzled planar cell polarity signaling. Genes Dev. *15*, 1182–1187.

Axelrod, J.D., Miller, J.R., Shulman, J.M., Moon, R.T., and Perrimon, N. (1998). Differential recruitment of Dishevelled provides signaling specificity in the planar cell polarity and Wingless signaling pathways. Genes Dev *12*, 2610–2622.

Babu, P. (1977). Early developmental subdivisions of the wing disk in Drosophila. Mol. Gen. Genet. *151*, 289–294.

Bäckström, G., Höök, M., Lindahl, U., Feingold, D.S., Malmström, A., Rodén, L., and Jacobsson, I. (1979). Biosynthesis of heparin. Assay and properties of the microsomal uronosyl C-5 epimerase. J. Biol. Chem. *254*, 2975–2982.

Baeg, G.H., Lin, X., Khare, N., Baumgartner, S., and Perrimon, N. (2001). Heparan sulfate proteoglycans are critical for the organization of the extracellular distribution of Wingless. Development *128*, 87–94.

Baeuerle, P.A., and Huttner, W.B. (1986). Chlorate — a potent inhibitor of protein sulfation in intact cells. Biochemical and Biophysical Research Communications *141*, 870–877.

Bai, X., Zhou, D., Brown, J.R., Crawford, B.E., Hennet, T., and Esko, J.D. (2001). Biosynthesis of the linkage region of glycosaminoglycans: cloning and activity of galactosyltransferase II, the sixth member of the beta 1,3-galactosyltransferase family (beta 3GalT6). J Biol Chem *276*, 48189–48195.

Baker, J.R., Roden, L., and Stoolmiller, A.C. (1972). Biosynthesis of chondroitin sulfate proteoglycan. Xylosyl transfer to Smith-degraded cartilage proteoglycan and other exogenous acceptors. J Biol Chem *247*, 3838–3847.

Bänziger, C., Soldini, D., Schütt, C., Zipperlen, P., Hausmann, G., and Basler, K. (2006). Wntless, a conserved membrane protein dedicated to the secretion of Wnt proteins from signaling cells. Cell *125*, 509–522.

Bartscherer, K., Pelte, N., Ingelfinger, D., and Boutros, M. (2006). Secretion of Wnt ligands requires Evi, a conserved transmembrane protein. Cell *125*, 523–533.

Basch, M.L., García-Castro, M.I., and Bronner-Fraser, M. (2004). Molecular mechanisms of neural crest induction. Birth Defects Research Part C: Embryo Today: Reviews *72*, 109–123.

Beckett, K., Monier, S., Palmer, L., Alexandre, C., Green, H., Bonneil, E., Raposo, G., Thibault, P., Le Borgne, R., and Vincent, J.-P. (2013). Drosophila S2 cells secrete wingless on exosome-like vesicles but the wingless gradient forms independently of exosomes. Traffic *14*, 82–96.

Behrens, J., von Kries, J.P., Kühl, M., Bruhn, L., Wedlich, D., Grosschedl, R., and Birchmeier, W. (1996). Functional interaction of beta-catenin with the transcription factor LEF-1. Nature *382*, 638–642.

Beiman, M., Shilo, B.Z., and Volk, T. (1996). Heartless, a Drosophila FGF receptor homolog, is essential for cell migration and establishment of several mesodermal lineages. Genes Dev. *10*, 2993–3002.

Belenkaya, T.Y., Han, C., Standley, H.J., Lin, X., Houston, D.W., Heasman, J., and Lin, X. (2002). pygopus encodes a nuclear protein essential for Wingless/Wnt signaling. Development *129*, 4089–4101.

Belenkaya, T.Y., Wu, Y., Tang, X., Zhou, B., Cheng, L., Sharma, Y.V., Yan, D., Selva, E.M., and Lin, X. (2008). The retromer complex influences Wnt secretion by recycling wntless from endosomes to the trans-Golgi network. Dev. Cell *14*, 120–131.

Bellaiche, Y., The, I., and Perrimon, N. (1998). Tout-velu is a Drosophila homologue of the putative tumour suppressor EXT-1 and is needed for Hh diffusion. Nature *394*, 85–88.

Bernfield, M., Gotte, M., Park, P.W., Reizes, O., Fitzgerald, M.L., Lincecum, J., and Zako, M. (1999). Functions of cell surface heparan sulfate proteoglycans. Annu Rev Biochem *68*, 729–777.

Bethani, I., Skanland, S.S., Dikic, I., and Acker-Palmer, A. (2010). Spatial organization of transmembrane receptor signalling. EMBO J *29*, 2677–2688.

Bhanot, P., Brink, M., Samos, C.H., Hsieh, J.C., Wang, Y., Macke, J.P., Andrew, D., Nathans, J., and Nusse, R. (1996). A new member of the frizzled family from Drosophila functions as a Wingless receptor. Nature *382*, 225–230.

Bilic, J., Huang, Y.L., Davidson, G., Zimmermann, T., Cruciat, C.M., Bienz, M., and Niehrs, C. (2007). Wnt induces LRP6 signalosomes and promotes dishevelled-dependent LRP6 phosphorylation. Science *316*, 1619–1622.

Binari, R.C., Staveley, B.E., Johnson, W.A., Godavarti, R., Sasisekharan, R., and Manoukian, A.S. (1997). Genetic evidence that heparin-like glycosaminoglycans are involved in wingless signaling. Development *124*, 2623–2632.

Van der Bliek, A.M., and Meyerowrtz, E.M. (1991). Dynamin-like protein encoded by the Drosophila shibire gene associated with vesicular traffic. Nature *351*, 411–414.

Bornemann, D.J., Duncan, J.E., Staatz, W., Selleck, S., and Warrior, R. (2004). Abrogation of heparan sulfate synthesis in Drosophila disrupts the Wingless, Hedgehog and Decapentaplegic signaling pathways. Development *131*, 1927–1938.

Bourouis, M., Moore, P., Ruel, L., Grau, Y., Heitzler, P., and Simpson, P. (1990). An early embryonic product of the gene shaggy encodes a serine/threonine protein kinase related to the CDC28/cdc2+ subfamily. EMBO J *9*, 2877–2884.

Boutin, C., Goffinet, A.M., and Tissir, F. (2012). Celsr1-3 cadherins in PCP and brain development. Curr. Top. Dev. Biol. *101*, 161–183.

Boutros, M., Paricio, N., Strutt, D.I., and Mlodzik, M. (1998). Dishevelled activates JNK and discriminates between JNK pathways in planar polarity and wingless signaling. Cell *94*, 109–118.

Bouwmeester, T., Kim, S.-H., Sasai, Y., Lu, B., and Robertis, E.M.D. (1996). Cerberus is a head-inducing secreted factor expressed in the anterior endoderm of Spemann's organizer. Nature *382*, 595–601.

Brandan, E., and Hirschberg, C.B. (1988). Purification of rat liver N-heparan-sulfate sulfotransferase. J. Biol. Chem. *263*, 2417–2422.

Branney, P.A., Faas, L., Steane, S.E., Pownall, M.E., and Isaacs, H.V. (2009). Characterisation of the fibroblast growth factor dependent transcriptome in early development. PLoS One *4*, e4951.

Brannon, M., Gomperts, M., Sumoy, L., Moon, R.T., and Kimelman, D. (1997). A beta-catenin/XTcf-3 complex binds to the siamois promoter to regulate dorsal axis specification in Xenopus. Genes Dev. *11*, 2359–2370.

Bret, C., Moreaux, J., Schved, J.-F., Hose, D., and Klein, B. (2011). SULFs in human neoplasia: implication as progression and prognosis factors. J Transl Med *9*, 72.

Brown, J.C., Sasaki, T., Göhring, W., Yamada, Y., and Timpl, R. (1997). The C-terminal domain V of perlecan promotes beta1 integrin-mediated cell adhesion, binds heparin, nidogen and fibulin-2 and can be modified by glycosaminoglycans. Eur. J. Biochem. *250*, 39–46.

Brown, S.D., Twells, R.C.J., Hey, P.J., Cox, R.D., Levy, E.R., Soderman, A.R., Metzker, M.L., Caskey, C.T., Todd, J.A., and Hess, J.F. (1998). Isolation and Characterization ofLRP6,a Novel Member of the Low Density Lipoprotein Receptor Gene Family. Biochemical and Biophysical Research Communications *248*, 879–888.

Brunner, E., Peter, O., Schweizer, L., and Basler, K. (1997). pangolin encodes a Lef-1 homologue that acts downstream of Armadillo to transduce the Wingless signal in Drosophila. Nature *385*, 829–833.

Budhidarmo, R., Nakatani, Y., and Day, C.L. (2012). RINGs hold the key to ubiquitin transfer. Trends in Biochemical Sciences *37*, 58–65.

Bullock, S.L., Fletcher, J.M., Beddington, R.S.P., and Wilson, V.A. (1998). Renal agenesis in mice homozygous for a gene trap mutation in the gene encoding heparan sulfate 2-sulfotransferase. Genes Dev. *12*, 1894–1906.

Cadigan, K.M., Fish, M.P., Rulifson, E.J., and Nusse, R. (1998). Wingless repression of Drosophila frizzled 2 expression shapes the Wingless morphogen gradient in the wing. Cell *93*, 767–777.

De Calisto, J., Araya, C., Marchant, L., Riaz, C.F., and Mayor, R. (2005). Essential role of non-canonical Wnt signalling in neural crest migration. Development *132*, 2587–2597.

Cano-Gauci, D.F., Song, H.H., Yang, H., McKerlie, C., Choo, B., Shi, W., Pullano, R., Piscione, T.D., Grisaru, S., Soon, S., et al. (1999). Glypican-3-deficient mice exhibit developmental overgrowth and some of the abnormalities typical of Simpson-Golabi-Behmel syndrome. J. Cell Biol. *146*, 255–264.

Carey, D.J., Evans, D.M., Stahl, R.C., Asundi, V.K., Conner, K.J., Garbes, P., and Cizmeci-Smith, G. (1992). Molecular cloning and characterization of N-syndecan, a novel transmembrane heparan sulfate proteoglycan. J. Cell Biol. *117*, 191–201.

Carmona-Fontaine, C., Matthews, H.K., Kuriyama, S., Moreno, M., Dunn, G.A., Parsons, M., Stern, C.D., and Mayor, R. (2008). Contact inhibition of locomotion in vivo controls neural crest directional migration. Nature *456*, 957–961.

Cavallo, R.A., Cox, R.T., Moline, M.M., Roose, J., Polevoy, G.A., Clevers, H., Peifer, M., and Bejsovec, A. (1998). Drosophila Tcf and Groucho interact to repress Wingless signalling activity. Nature *395*, 604–608.

Cha, S.W., Tadjuidje, E., Tao, Q., Wylie, C., and Heasman, J. (2008). Wnt5a and Wnt11 interact in a maternal Dkk1-regulated fashion to activate both canonical and non-canonical signaling in Xenopus axis formation. Development *135*, 3719–3729.

Chae, J., Kim, M.J., Goo, J.H., Collier, S., Gubb, D., Charlton, J., Adler, P.N., and Park, W.J. (1999). The Drosophila tissue polarity gene starry night encodes a member of the protocadherin family. Development *126*, 5421–5429.

Chakrabarti, A., Matthews, G., Colman, A., and Dale, L. (1992). Secretory and inductive properties of Drosophila wingless protein in Xenopus oocytes and embryos. Development *115*, 355–369.

Chen, M.S., Obar, R.A., Schroeder, C.C., Austin, T.W., Poodry, C.A., Wadsworth, S.C., and Vallee, R.B. (1991). Multiple forms of dynamin are encoded by shibire, a Drosophila gene involved in endocytosis. Nature *351*, 583–586.

Chen, W., ten Berge, D., Brown, J., Ahn, S., Hu, L.A., Miller, W.E., Caron, M.G., Barak, L.S., Nusse, R., and Lefkowitz, R.J. (2003). Dishevelled 2 recruits beta-arrestin 2 to mediate Wnt5A-stimulated endocytosis of Frizzled 4. Science *301*, 1391–1394.

Cheng, A.-L., Shen, Y.-C., and Zhu, A.X. (2011). Targeting fibroblast growth factor receptor signaling in hepatocellular carcinoma. Oncology *81*, 372–380.

Cho, K.W.Y., Blumberg, B., Steinbeisser, H., and De Robertis, E.M. (1991). Molecular nature of Spemann's organizer: the role of the Xenopus homeobox gene goosecoid. Cell *67*, 1111–1120.

Choi, S.-C., and Han, J.-K. (2002). Xenopus Cdc42 regulates convergent extension movements during gastrulation through Wnt/Ca2+ signaling pathway. Dev. Biol. *244*, 342–357.

Christian, J.L., McMahon, J.A., McMahon, A.P., and Moon, R.T. (1991). Xwnt-8, a Xenopus Wnt-1/int-1-related gene responsive to mesoderm-inducing growth factors, may play a role in ventral mesodermal patterning during embryogenesis. Development *111*, 1045–1055.

Clevers, H., and van de Wetering, M. (1997). TCF/LEF factor earn their wings. Trends Genet. *13*, 485–489.

Cornell, R.A., and Kimelman, D. (1994). Activin-mediated mesoderm induction requires FGF. Development *120*, 453–462.

Crawford, B.E., Olson, S.K., Esko, J.D., and Pinhal, M.A.S. (2001). Cloning, Golgi Localization, and Enzyme Activity of the Full-length Heparin/Heparan Sulfate-Glucuronic Acid C5-epimerase. J. Biol. Chem. *276*, 21538–21543.

Datta, S., and Kankel, D.R. (1992). l(1)trol and l(1)devl, loci affecting the development of the adult central nervous system in Drosophila melanogaster. Genetics *130*, 523–537.

David, G., Lories, V., Decock, B., Marynen, P., Cassiman, J.J., and Berghe, H.V. den (1990). Molecular cloning of a phosphatidylinositol-anchored membrane heparan sulfate proteoglycan from human lung fibroblasts. J Cell Biol *111*, 3165–3176.

David, G., Schueren, B. van der, Marynen, P., Cassiman, J.J., and Berghe, H. van den (1992). Molecular cloning of amphiglycan, a novel integral membrane heparan sulfate proteoglycan expressed by epithelial and fibroblastic cells. J Cell Biol *118*, 961–969.

Davidson, G., Wu, W., Shen, J., Bilic, J., Fenger, U., Stannek, P., Glinka, A., and Niehrs, C. (2005). Casein kinase 1 gamma couples Wnt receptor activation to cytoplasmic signal transduction. Nature *438*, 867–872.

Deardorff, M.A., Tan, C., Conrad, L.J., and Klein, P.S. (1998). Frizzled-8 is expressed in the Spemann organizer and plays a role in early morphogenesis. Development *125*, 2687–2700.

Dhoot, G.K., Gustafsson, M.K., Ai, X.B., Sun, W.T., Standiford, D.M., and Emerson, C.P. (2001). Regulation of Wnt signaling and embryo patterning by an extracellular sulfatase. Science *293*, 1663–1666.

Dickinson, J., and Fowler, S.J. (2002). Quantification of Proteins on Western Blots Using ECL. In The Protein Protocols Handbook, J.M. Walker, ed. (Humana Press), pp. 429–437.

Diez-Roux, G., and Ballabio, A. (2005). Sulfatases and human disease. Annu Rev Genomics Hum Genet *6*, 355–379.

Djiane, A., Riou, J., Umbhauer, M., Boucaut, J., and Shi, D. (2000). Role of frizzled 7 in the regulation of convergent extension movements during gastrulation in Xenopus laevis. Development *127*, 3091–3100.

Dolan, M., Horchar, T., Rigatti, B., and Hassell, J.R. (1997). Identification of sites in domain I of perlecan that regulate heparan sulfate synthesis. J. Biol. Chem. *272*, 4316–4322.

Dorey, K., and Amaya, E. (2010). FGF signalling: diverse roles during early vertebrate embryogenesis. Development *137*, 3731–3742.

Dorfman, R., and Shilo, B.Z. (2001). Biphasic activation of the BMP pathway patterns the Drosophila embryonic dorsal region. Development *128*, 965–972.

Du, S.J., Purcell, S.M., Christian, J.L., McGrew, L.L., and Moon, R.T. (1995). Identification of distinct classes and functional domains of Wnts through expression of wild-type and chimeric proteins in Xenopus embryos. Mol Cell Biol *15*, 2625–2634.

Durbin, J., and Watson, G.S. (1950). Testing for serial correlation in least squares regression. I. Biometrika *37*, 409–428.

Durbin, J., and Watson, G.S. (1951). Testing for serial correlation in least squares regression. II. Biometrika *38*, 159–178.

Dytham, C. (2005). Choosing and Using Statistics; A Biologist's Guide (Blackwell Publishing).

Eldar, A., Rosin, D., Shilo, B.-Z., and Barkai, N. (2003). Self-enhanced ligand degradation underlies robustness of morphogen gradients. Dev. Cell *5*, 635–646.

Elinson, R.P. (1985). Changes in levels of polymeric tubulin associated with activation and dorsoventral polarization of the frog egg. Dev. Biol. *109*, 224–233.

Elinson, R.P., and Rowning, B. (1988). A transient array of parallel microtubules in frog eggs: Potential tracks for a cytoplasmic rotation that specifies the dorso-ventral axis. Developmental Biology *128*, 185–197.

Esko, J.D., and Selleck, S.B. (2002). Order out of chaos: assembly of ligand binding sites in heparan sulfate. Annu Rev Biochem *71*, 435–471.

Esko, J.D., Stewart, T.E., and Taylor, W.H. (1985). Animal cell mutants defective in glycosaminoglycan biosynthesis. PNAS *82*, 3197–3201.

Esteve, P., Sandonìs, A., Ibañez, C., Shimono, A., Guerrero, I., and Bovolenta, P. (2011). Secreted frizzled-related proteins are required for Wnt/β-catenin signalling activation in the vertebrate optic cup. Development *138*, 4179–4184.

Eugster, C., Panáková, D., Mahmoud, A., and Eaton, S. (2007). Lipoprotein-heparan sulfate interactions in the Hh pathway. Dev. Cell *13*, 57–71.

Fagotto, F., Jho, E. h, Zeng, L., Kurth, T., Joos, T., Kaufmann, C., and Costantini, F. (1999). Domains of axin involved in protein-protein interactions, Wnt pathway inhibition, and intracellular localization. J. Cell Biol. *145*, 741–756.

Fainsod, A., Steinbeisser, H., and De Robertis, E.M. (1994). On the function of BMP-4 in patterning the marginal zone of the Xenopus embryo. EMBO J *13*, 5015–5025.

Fainsod, A., Deissler, K., Yelin, R., Marom, K., Epstein, M., Pillemer, G., Steinbeisser, H., and Blum, M. (1997). The dorsalizing and neural inducing gene follistatin is an antagonist of BMP-4. Mech. Dev. *63*, 39–50.

Fan, G., Xiao, L., Cheng, L., Wang, X., Sun, B., and Hu, G. (2000). Targeted disruption of NDST-1 gene leads to pulmonary hypoplasia and neonatal respiratory distress in mice. FEBS Letters *467*, 7–11.

Fay, M.P., and Proschan, M.A. (2010). Wilcoxon-Mann-Whitney or t-test? On assumptions for hypothesis tests and multiple interpretations of decision rules. Stat Surv *4*, 1–39.

Feiguin, F., Hannus, M., Mlodzik, M., and Eaton, S. (2001). The ankyrin repeat protein Diego mediates Frizzled-dependent planar polarization. Dev. Cell *1*, 93–101.

Filmus, J., Capurro, M., and Rast, J. (2008). Glypicans. Genome Biology *9*, 224.

Fisher, A.L., and Caudy, M. (1998). Groucho proteins: transcriptional corepressors for specific subsets of DNA-binding transcription factors in vertebrates and invertebrates. Genes Dev. *12*, 1931–1940.

Franch-Marro, X., Marchand, O., Piddini, E., Ricardo, S., Alexandre, C., and Vincent, J.-P. (2005). Glypicans shunt the Wingless signal between local signalling and further transport. Development *132*, 659–666.

Franch-Marro, X., Wendler, F., Griffith, J., Maurice, M.M., and Vincent, J.-P. (2008a). In vivo role of lipid adducts on Wingless. J. Cell. Sci. *121*, 1587–1592.

Franch-Marro, X., Wendler, F., Guidato, S., Griffith, J., Baena-Lopez, A., Itasaki, N., Maurice, M.M., and Vincent, J.-P. (2008b). Wingless secretion requires endosome-to-Golgi retrieval of Wntless/Evi/Sprinter by the retromer complex. Nat. Cell Biol. *10*, 170–177.

Freeman, S.D., Moore, W.M., Guiral, E.C., Holme, A.D., Turnbull, J.E., and Pownall, M.E. (2008). Extracellular regulation of developmental cell signaling by XtSulf1. Dev Biol *320*, 436–445.

Frese, M.A., Milz, F., Dick, M., Lamanna, W.C., and Dierks, T. (2009). Characterization of the human sulfatase Sulf1 and its high affinity heparin/heparan sulfate interaction domain. J Biol Chem *284*, 28033–28044.

Fujita, K., Takechi, E., Sakamoto, N., Sumiyoshi, N., Izumi, S., Miyamoto, T., Matsuura, S., Tsurugaya, T., Akasaka, K., and Yamamoto, T. (2009). HpSulf, a heparan sulfate 6-O-endosulfatase, is involved in the regulation of VEGF signaling during sea urchin development. Mech Dev *127*, 235–245.

Gallet, A., Staccini-Lavenant, L., and Thérond, P.P. (2008). Cellular Trafficking of the Glypican Dally-like Is Required for Full-Strength Hedgehog Signaling and Wingless Transcytosis. Developmental Cell *14*, 712–725.

Garriock, R.J., D'Agostino, S.L., Pilcher, K.C., and Krieg, P.A. (2005). Wnt11-R, a protein closely related to mammalian Wnt11, is required for heart morphogenesis in Xenopus. Dev Biol *279*, 179–192.

Garriock, R.J., Warkman, A.S., Meadows, S.M., D'Agostino, S., and Krieg, P.A. (2007). Census of vertebrate Wnt genes: isolation and developmental expression of Xenopus Wnt2, Wnt3, Wnt9a, Wnt9b, Wnt10a, and Wnt16. Dev Dyn *236*, 1249–1258.

Gerlitz, O., and Basler, K. (2002). Wingful, an extracellular feedback inhibitor of Wingless. Genes Dev. *16*, 1055–1059.

Giráldez, A.J., Copley, R.R., and Cohen, S.M. (2002). HSPG modification by the secreted enzyme Notum shapes the Wingless morphogen gradient. Dev. Cell *2*, 667–676.

Gisselbrecht, S., Skeath, J.B., Doe, C.Q., and Michelson, A.M. (1996). heartless encodes a fibroblast growth factor receptor (DFR1/DFGF-R2) involved in the directional migration of early mesodermal cells in the Drosophila embryo. Genes Dev. *10*, 3003–3017.

Glinka, A., Wu, W., Delius, H., Monaghan, A.P., Blumenstock, C., and Niehrs, C. (1998). Dickkopf-1 is a member of a new family of secreted proteins and functions in head induction. Nature *391*, 357–362.

Goetz, J.A., Singh, S., Suber, L.M., Kull, F.J., and Robbins, D.J. (2006). A highly conserved amino-terminal region of sonic hedgehog is required for the formation of its freely diffusible multimeric form. J. Biol. Chem. *281*, 4087–4093.

González, F., Swales, L., Bejsovec, A., Skaer, H., and Martinez Arias, A. (1991). Secretion and movement of wingless protein in the epidermis of the Drosophila embryo. Mech. Dev. *35*, 43–54.

Goodman, R.M., Thombre, S., Firtina, Z., Gray, D., Betts, D., Roebuck, J., Spana, E.P., and Selva, E.M. (2006). Sprinter: a novel transmembrane protein required for Wg secretion and signaling. Development *133*, 4901–4911.

Gorsi, B., Whelan, S., and Stringer, S.E. (2010). Dynamic expression patterns of 6-O endosulfatases during zebrafish development suggest a subfunctionalisation event for sulf2. Dev. Dyn. *239*, 3312–3323.

Gould, S.E., Upholt, W.B., and Kosher, R.A. (1992). Syndecan 3: a member of the syndecan family of membrane-intercalated proteoglycans that is expressed in high amounts at the onset of chicken limb cartilage differentiation. PNAS *89*, 3271–3275.

Gray, R.S., Roszko, I., and Solnica-Krezel, L. (2011). Planar Cell Polarity: Coordinating Morphogenetic Cell Behaviors with Embryonic Polarity. Developmental Cell *21*, 120–133.

Greco, V., Hannus, M., and Eaton, S. (2001). Argosomes: a potential vehicle for the spread of morphogens through epithelia. Cell *106*, 633–645.

Gross, J.C., Chaudhary, V., Bartscherer, K., and Boutros, M. (2012). Active Wnt proteins are secreted on exosomes. Nat Cell Biol *14*, 1036–1045.

Gubb, D., and García-Bellido, A. (1982). A genetic analysis of the determination of cuticular polarity during development in Drosophila melanogaster. J Embryol Exp Morphol *68*, 37–57.

Gubb, D., Green, C., Huen, D., Coulson, D., Johnson, G., Tree, D., Collier, S., and Roote, J. (1999). The balance between isoforms of the prickle LIM domain protein is critical for planar polarity in Drosophila imaginal discs. Genes Dev. *13*, 2315–2327.

Guimond, S., Maccarana, M., Olwin, B.B., Lindahl, U., and Rapraeger, A.C. (1993). Activating and inhibitory heparin sequences for FGF-2 (basic FGF). Distinct requirements for FGF-1, FGF-2, and FGF-4. J. Biol. Chem. *268*, 23906–23914.

Guiral, E.C., Faas, L., and Pownall, M.E. (2010). Neural crest migration requires the activity of the extracellular sulphatases XtSulf1 and XtSulf2. Dev. Biol. *341*, 375–388.

Gurdon, J.B., and Bourillot, P.Y. (2001). Morphogen gradient interpretation. Nature *413*, 797–803.

Habas, R., Kato, Y., and He, X. (2001). Wnt/Frizzled activation of Rho regulates vertebrate gastrulation and requires a novel Formin homology protein Daam1. Cell *107*, 843–854.

Habas, R., Dawid, I.B., and He, X. (2003). Coactivation of Rac and Rho by Wnt/Frizzled signaling is required for vertebrate gastrulation. Genes Dev *17*, 295–309.

Habuchi, H., Nagai, N., Sugaya, N., Atsumi, F., Stevens, R.L., and Kimata, K. (2007). Mice deficient in heparan sulfate 6-O-sulfotransferase-1 exhibit defective heparan sulfate biosynthesis, abnormal placentation, and late embryonic lethality. J. Biol. Chem. *282*, 15578–15588.

Hacker, U., Nybakken, K., and Perrimon, N. (2005). Heparan sulphate proteoglycans: the sweet side of development. Nat Rev Mol Cell Biol *6*, 530–541.

Häcker, U., Lin, X., and Perrimon, N. (1997). The Drosophila sugarless gene modulates Wingless signaling and encodes an enzyme involved in polysaccharide biosynthesis. Development *124*, 3565–3573.

Haerry, T.E., Heslip, T.R., Marsh, J.L., and O'Connor, M.B. (1997). Defects in glucuronate biosynthesis disrupt Wingless signaling in Drosophila. Development *124*, 3055–3064.

Hagemann, A.I., Xu, X., Nentwich, O., Hyvonen, M., and Smith, J.C. (2009). Rab5-mediated endocytosis of activin is not required for gene activation or long-range signalling in Xenopus. Development *136*, 2803–2813.

Hamada, F., Tomoyasu, Y., Takatsu, Y., Nakamura, M., Nagai, S., Suzuki, A., Fujita, F., Shibuya, H., Toyoshima, K., Ueno, N., et al. (1999a). Negative regulation of Wingless signaling by D-axin, a Drosophila homolog of axin. Science *283*, 1739–1742.

Hamada, F., Murata, Y., Nishida, A., Fujita, F., Tomoyasu, Y., Nakamura, M., Toyoshima, K., Tabata, T., Ueno, N., and Akiyama, T. (1999b). Identification and characterization of E-APC, a novel Drosophila homologue of the tumour suppressor APC. Genes to Cells *4*, 465–474.

Hammerschmidt, M., Pelegri, F., Mullins, M.C., Kane, D.A., Brand, M., van Eeden, F.J., Furutani-Seiki, M., Granato, M., Haffter, P., Heisenberg, C.P., et al. (1996). Mutations affecting morphogenesis during gastrulation and tail formation in the zebrafish, Danio rerio. Development *123*, 143–151.

Han, C., Belenkaya, T.Y., Khodoun, M., Tauchi, M., and Lin, X. (2004). Distinct and collaborative roles of Drosophila EXT family proteins in morphogen signalling and gradient formation. Development *131*, 1563–1575.

Han, C., Yan, D., Belenkaya, T.Y., and Lin, X. (2005). Drosophila glypicans Dally and Dally-like shape the extracellular Wingless morphogen gradient in the wing disc. Development *132*, 667–679.

Hanzal-Bayer, M.F., and Hancock, J.F. (2007). Lipid rafts and membrane traffic. FEBS Lett *581*, 2098–2104.

Harland, R.M. (1991). In situ hybridization: an improved whole-mount method for Xenopus embryos. Methods Cell Biol *36*, 685–695.

Hart, M.J., de los Santos, R., Albert, I.N., Rubinfeld, B., and Polakis, P. (1998). Downregulation of beta-catenin by human Axin and its association with the APC tumor suppressor, beta-catenin and GSK3 beta. Curr. Biol. *8*, 573–581.

Hartley, K.O., Hardcastle, Z., Friday, R.V., Amaya, E., and Papalopulu, N. (2001). Transgenic Xenopus Embryos Reveal That Anterior Neural Development Requires Continued Suppression of BMP Signaling after Gastrulation. Developmental Biology *238*, 168–184.

Hassell, J.R., Robey, P.G., Barrach, H.J., Wilczek, J., Rennard, S.I., and Martin, G.R. (1980). Isolation of a heparan sulfate-containing proteoglycan from basement membrane. Proc. Natl. Acad. Sci. U.S.A. *77*, 4494–4498.

Hayano, S., Kurosaka, H., Yanagita, T., Kalus, I., Milz, F., Ishihara, Y., Islam, M.N., Kawanabe, N., Saito, M., Kamioka, H., et al. (2012). Roles of heparan sulfate sulfation in dentinogenesis. J. Biol. Chem. *287*, 12217–12229.

He, X., Saint-Jeannet, J.P., Wang, Y., Nathans, J., Dawid, I., and Varmus, H. (1997). A member of the Frizzled protein family mediating axis induction by Wnt-5A. Science *275*, 1652–1654.

Heasman, S.J., and Ridley, A.J. (2008). Mammalian Rho GTPases: new insights into their functions from in vivo studies. Nat Rev Mol Cell Biol *9*, 690–701.

Heasman, J., Crawford, A., Goldstone, K., Garner-Hamrick, P., Gumbiner, B., McCrea, P., Kintner, C., Noro, C.Y., and Wylie, C. (1994). Overexpression of cadherins and underexpression of β-catenin inhibit dorsal mesoderm induction in early Xenopus embryos. Cell *79*, 791–803.

Heasman, J., Kofron, M., and Wylie, C. (2000). βCatenin Signaling Activity Dissected in the Early Xenopus Embryo: A Novel Antisense Approach. Developmental Biology *222*, 124–134.

Heisenberg, C.P., Tada, M., Rauch, G.J., Saude, L., Concha, M.L., Geisler, R., Stemple, D.L., Smith, J.C., and Wilson, S.W. (2000). Silberblick/Wnt11 mediates convergent extension movements during zebrafish gastrulation. Nature *405*, 76–81.

Hemmati-Brivanlou, A., and Melton, D.A. (1992). A truncated activin receptor inhibits mesoderm induction and formation of axial structures in Xenopus embryos. Nature *359*, 609–614.

Hempel, J., Perozich, J., Romovacek, H., Hinich, A., Kuo, I., and Feingold, D.S. (1994). UDP-glucose dehydrogenase from bovine liver: primary structure and relationship to other dehydrogenases. Protein Sci. *3*, 1074–1080.

Hennekam, R.C. (1991). Hereditary multiple exostoses. J Med Genet *28*, 262–266.

Van den Heuvel, M., Nusse, R., Johnston, P., and Lawrence, P.A. (1989). Distribution of the wingless gene product in Drosophila embryos: a protein involved in cell-cell communication. Cell *59*, 739–749.

Van den Heuvel, M., Harryman-Samos, C., Klingensmith, J., Perrimon, N., and Nusse, R. (1993). Mutations in the segment polarity genes wingless and porcupine impair secretion of the wingless protein. EMBO J. *12*, 5293–5302.

Hey, P.J., Twells, R.C.J., Phillips, M.S., Yusuke Nakagawa, Brown, S.D., Kawaguchi, Y., Cox, R., Guochun Xie, Dugan, V., Hammond, H., et al. (1998). Cloning of a novel member of the low-density lipoprotein receptor family. Gene *216*, 103–111.

Hikasa, H., Shibata, M., Hiratani, I., and Taira, M. (2002). The Xenopus receptor tyrosine kinase Xror2 modulates morphogenetic movements of the axial mesoderm and neuroectoderm via Wnt signaling. Development *129*, 5227–5239.

Hild, M., Dick, A., Rauch, G.J., Meier, A., Bouwmeester, T., Haffter, P., and Hammerschmidt, M. (1999). The smad5 mutation somitabun blocks Bmp2b signaling during early dorsoventral patterning of the zebrafish embryo. Development *126*, 2149–2159.

Hofmann, K. (2000). A superfamily of membrane-bound O-acyltransferases with implications for Wnt signaling. Trends in Biochemical Sciences *25*, 111–112.

Holst, C.R., Bou-Reslan, H., Gore, B.B., Wong, K., Grant, D., Chalasani, S., Carano, R.A., Frantz, G.D., Tessier-Lavigne, M., Bolon, B., et al. (2007). Secreted sulfatases Sulf1 and Sulf2 have overlapping yet essential roles in mouse neonatal survival. PLoS ONE *2*, e575.

Hopf, M., Göhring, W., Kohfeldt, E., Yamada, Y., and Timpl, R. (1999). Recombinant domain IV of perlecan binds to nidogens, laminin-nidogen complex, fibronectin, fibulin-2 and heparin. Eur. J. Biochem. *259*, 917–925.

Hsieh, J.C., Kodjabachian, L., Rebbert, M.L., Rattner, A., Smallwood, P.M., Samos, C.H., Nusse, R., Dawid, I.B., and Nathans, J. (1999a). A new secreted protein that binds to Wnt proteins and inhibits their activities. Nature *398*, 431–436.

Hsieh, J.-C., Rattner, A., Smallwood, P.M., and Nathans, J. (1999b). Biochemical characterization of Wnt-Frizzled interactions using a soluble, biologically active vertebrate Wnt protein. PNAS *96*, 3546–3551.

Hu, G., Chung, Y.L., Glover, T., Valentine, V., Look, A.T., and Fearon, E.R. (1997). Characterization of human homologs of the Drosophila seven in absentia (sina) gene. Genomics *46*, 103–111.

Huber, O., Korn, R., McLaughlin, J., Ohsugi, M., Herrmann, B.G., and Kemler, R. (1996). Nuclear localization of beta-catenin by interaction with transcription factor LEF-1. Mech. Dev. *59*, 3–10.

Hur, K., Han, T.-S., Jung, E.-J., Yu, J., Lee, H.-J., Kim, W.H., Goel, A., and Yang, H.-K. (2012). Up-regulated expression of sulfatases (SULF1 and SULF2) as prognostic and metastasis predictive markers in human gastric cancer. J. Pathol. *228*, 88–98.

Ikeda, S., Kishida, S., Yamamoto, H., Murai, H., Koyama, S., and Kikuchi, A. (1998). Axin, a negative regulator of the Wnt signaling pathway, forms a complex with GSK-3beta and beta-catenin and promotes GSK-3beta-dependent phosphorylation of beta-catenin. EMBO J. *17*, 1371–1384.

Illes, J.C., Winterbottom, E., and Isaacs, H.V. (2009). Cloning and expression analysis of the anterior parahox genes, Gsh1 and Gsh2 from Xenopus tropicalis. Dev Dyn *238*, 194–203.

In der Rieden, P.M.J., Vilaspasa, F.L., and Durston, A.J. (2010). Xwnt8 directly initiates expression of labial Hox genes. Developmental Dynamics *239*, 126–139.

Isaacs, H.V., Pownall, M.E., and Slack, J.M. (1994a). eFGF regulates Xbra expression during Xenopus gastrulation. EMBO J *13*, 4469–4481.

Isaacs, H.V., Pownall, M.E., and Slack, J.M. (1994b). eFGF regulates Xbra expression during Xenopus gastrulation. EMBO J *13*, 4469–4481.

Ishikawa, T., Tamai, Y., Zorn, A.M., Yoshida, H., Seldin, M.F., Nishikawa, S., and Taketo, M.M. (2001). Mouse Wnt receptor gene Fzd5 is essential for yolk sac and placental angiogenesis. Development *128*, 25–33.

Ishitani, T., Ninomiya-Tsuji, J., Nagai, S., Nishita, M., Meneghini, M., Barker, N., Waterman, M., Bowerman, B., Clevers, H., Shibuya, H., et al. (1999). The TAK1–NLK–MAPK-related pathway antagonizes signalling between β-catenin and transcription factor TCF. Nature *399*, 798–802.

Ishitani, T., Kishida, S., Hyodo-Miura, J., Ueno, N., Yasuda, J., Waterman, M., Shibuya, H., Moon, R.T., Ninomiya-Tsuji, J., and Matsumoto, K. (2003). The TAK1-NLK mitogen-activated protein kinase

cascade functions in the Wnt-5a/Ca(2+) pathway to antagonize Wnt/beta-catenin signaling. Mol Cell Biol *23*, 131–139.

Itoh, K., Krupnik, V.E., and Sokol, S.Y. (1998). Axis determination in Xenopus involves biochemical interactions of axin, glycogen synthase kinase 3 and beta-catenin. Curr. Biol. *8*, 591–594.

Jacobsson, I., Lindahl, U., Jensen, J.W., Rodén, L., Prihar, H., and Feingold, D.S. (1984). Biosynthesis of heparin. Substrate specificity of heparosan N-sulfate D-glucuronosyl 5-epimerase. J. Biol. Chem. *259*, 1056–1063.

Janda, C.Y., Waghray, D., Levin, A.M., Thomas, C., and Garcia, K.C. (2012). Structural basis of Wnt recognition by Frizzled. Science *337*, 59–64.

Jemth, P., Smeds, E., Do, A.-T., Habuchi, H., Kimata, K., Lindahl, U., and Kusche-Gullberg, M. (2003). Oligosaccharide library-based assessment of heparan sulfate 6-O-sulfotransferase substrate specificity. J. Biol. Chem. *278*, 24371–24376.

Jessen, J.R., and Solnica-Krezel, L. (2004). Identification and developmental expression pattern of van gogh-like 1, a second zebrafish strabismus homologue. Gene Expr. Patterns *4*, 339–344.

Jessen, J.R., Topczewski, J., Bingham, S., Sepich, D.S., Marlow, F., Chandrasekhar, A., and Solnica-Krezel, L. (2002). Zebrafish trilobite identifies new roles for Strabismus in gastrulation and neuronal movements. Nat. Cell Biol. *4*, 610–615.

Jho, E., Zhang, T., Domon, C., Joo, C.-K., Freund, J.-N., and Costantini, F. (2002). Wnt/beta-catenin/Tcf signaling induces the transcription of Axin2, a negative regulator of the signaling pathway. Mol. Cell. Biol. *22*, 1172–1183.

Jho, E. h, Lomvardas, S., and Costantini, F. (1999). A GSK3beta phosphorylation site in axin modulates interaction with beta-catenin and Tcf-mediated gene expression. Biochem. Biophys. Res. Commun. *266*, 28–35.

Jones, C.M., Dale, L., Hogan, B.L., Wright, C.V., and Smith, J.C. (1996). Bone morphogenetic protein-4 (BMP-4) acts during gastrula stages to cause ventralization of Xenopus embryos. Development *122*, 1545–1554.

Kadowaki, T., Wilder, E., Klingensmith, J., Zachary, K., and Perrimon, N. (1996). The segment polarity gene porcupine encodes a putative multitransmembrane protein involved in Wingless processing. Genes Dev. *10*, 3116–3128.

Kamimura, K., Fujise, M., Villa, F., Izumi, S., Habuchi, H., Kimata, K., and Nakato, H. (2001). Drosophila heparan sulfate 6-O-sulfotransferase (dHS6ST) gene. Structure, expression, and function in the formation of the tracheal system. J. Biol. Chem. *276*, 17014–17021.

Kao, K.R., and Elinson, R.P. (1988). The entire mesodermal mantle behaves as Spemann's organizer in dorsoanterior enhanced Xenopus laevis embryos. Dev. Biol. *127*, 64–77.

Katanaev, V.L., Solis, G.P., Hausmann, G., Buestorf, S., Katanayeva, N., Schrock, Y., Stuermer, C.A., and Basler, K. (2008). Reggie-1/flotillin-2 promotes secretion of the long-range signalling forms of Wingless and Hedgehog in Drosophila. EMBO J *27*, 509–521.

Kawano, Y., and Kypta, R. (2003). Secreted antagonists of the Wnt signalling pathway. J. Cell. Sci. *116*, 2627–2634.

Kearns, A.E., Vertel, B.M., and Schwartz, N.B. (1993a). Topography of glycosylation and UDP-xylose production. J Biol Chem *268*, 11097–11104.

Kearns, A.E., Vertel, B.M., Walters, L.M., Flay, N., and Schwartz, N.B. (1993b). Xylosylation is an endoplasmic reticulum to Golgi event. J Biol Chem *268*, 11105–11112.

Keller, R.E. (1980). The cellular basis of epiboly: an SEM study of deep-cell rearrangement during gastrulation in Xenopus laevis. J Embryol Exp Morphol *60*, 201–234.

Keller, R.E. (1981). An experimental analysis of the role of bottle cells and the deep marginal zone in gastrulation of Xenopus laevis. J. Exp. Zool. *216*, 81–101.

Keller, R., and Danilchik, M. (1988). Regional expression, pattern and timing of convergence and extension during gastrulation of Xenopus laevis. Development *103*, 193–209.

Keller, R.E., and Schoenwolf, G.C. (1977). An SEM study of cellular morphology, contact, and arrangement, as related to gastrulation inXenopus laevis. Wilhelm Roux' Archiv *182*, 165–186.

Keller, R.E., Danilchik, M., Gimlich, R., and Shih, J. (1985). The function and mechanism of convergent extension during gastrulation of Xenopus laevis. J Embryol Exp Morphol *89 Suppl*, 185–209.

Khare, N., and Baumgartner, S. (2000). Dally-like protein, a new Drosophila glypican with expression overlapping with wingless. Mech. Dev. *99*, 199–202.

Khokha, M.K., Yeh, J., Grammer, T.C., and Harland, R.M. (2005). Depletion of three BMP antagonists from Spemann's organizer leads to a catastrophic loss of dorsal structures. Dev. Cell *8*, 401–411.

Kikuchi, A., Yamamoto, H., and Sato, A. (2009). Selective activation mechanisms of Wnt signaling pathways. Trends Cell Biol *19*, 119–129.

Kilian, B., Mansukoski, H., Barbosa, F.C., Ulrich, F., Tada, M., and Heisenberg, C.P. (2003). The role of Ppt/Wnt5 in regulating cell shape and movement during zebrafish gastrulation. Mech Dev *120*, 467–476.

Kim, G.H., and Han, J.K. (2007). Essential role for beta-arrestin 2 in the regulation of Xenopus convergent extension movements. EMBO J *26*, 2513–2526.

Kim, G.-H., and Han, J.-K. (2005). JNK and ROKalpha function in the noncanonical Wnt/RhoA signaling pathway to regulate Xenopus convergent extension movements. Dev. Dyn. *232*, 958–968.

Kim, B.T., Kitagawa, H., Tamura, J., Saito, T., Kusche-Gullberg, M., Lindahl, U., and Sugahara, K. (2001). Human tumor suppressor EXT gene family members EXTL1 and EXTL3 encode alpha 1,4-N-acetylglucosaminyltransferases that likely are involved in heparan sulfate/ heparin biosynthesis. Proc Natl Acad Sci U S A *98*, 7176–7181.

Kim, G.H., Her, J.H., and Han, J.K. (2008). Ryk cooperates with Frizzled 7 to promote Wnt11-mediated endocytosis and is essential for Xenopus laevis convergent extension movements. J Cell Biol *182*, 1073–1082.

Kim, H., Cheong, S.-M., Ryu, J., Jung, H.-J., Jho, E., and Han, J.-K. (2009). Xenopus Wntless and the retromer complex cooperate to regulate XWnt4 secretion. Mol. Cell. Biol. *29*, 2118–2128.

Kimelman, D., and Kirschner, M. (1987). Synergistic induction of mesoderm by FGF and TGF-beta and the identification of an mRNA coding for FGF in the early Xenopus embryo. Cell *51*, 869–877.

Kinoshita, N., Iioka, H., Miyakoshi, A., and Ueno, N. (2003). PKC delta is essential for Dishevelled function in a noncanonical Wnt pathway that regulates Xenopus convergent extension movements. Genes Dev *17*, 1663–1676.

Kishida, M., Hino Si, Michiue, T., Yamamoto, H., Kishida, S., Fukui, A., Asashima, M., and Kikuchi, A. (2001). Synergistic activation of the Wnt signaling pathway by Dvl and casein kinase Iepsilon. J. Biol. Chem. *276*, 33147–33155.

Kispert, A., Vainio, S., Shen, L., Rowitch, D.H., and McMahon, A.P. (1996). Proteoglycans are required for maintenance of Wnt-11 expression in the ureter tips. Development *122*, 3627–3637.

Kispert, A., Vainio, S., and McMahon, A.P. (1998). Wnt-4 is a mesenchymal signal for epithelial transformation of metanephric mesenchyme in the developing kidney. Development *125*, 4225–4234.

Kitagawa, H., Tone, Y., Tamura, J., Neumann, K.W., Ogawa, T., Oka, S., Kawasaki, T., and Sugahara, K. (1998). Molecular cloning and expression of glucuronyltransferase I involved in the biosynthesis of the glycosaminoglycan-protein linkage region of proteoglycans. J Biol Chem *273*, 6615–6618.

Klämbt, C., Glazer, L., and Shilo, B.Z. (1992). breathless, a Drosophila FGF receptor homolog, is essential for migration of tracheal and specific midline glial cells. Genes Dev. *6*, 1668–1678.

Klein, P.S., and Melton, D.A. (1996). A molecular mechanism for the effect of lithium on development. PNAS *93*, 8455–8459.

Kleinschmit, A., Koyama, T., Dejima, K., Hayashi, Y., Kamimura, K., and Nakato, H. (2010). Drosophila heparan sulfate 6-O endosulfatase regulates Wingless morphogen gradient formation. Dev Biol *345*, 204–214.

Kleinschmit, A., Takemura, M., Dejima, K., Choi, P.Y., and Nakato, H. (2013). Drosophila heparan sulfate 6-O endosulfatase Sulf1 facilitates Wg degradation. J Biol Chem.

Knippschild, U., Gocht, A., Wolff, S., Huber, N., Löhler, J., and Stöter, M. (2005). The casein kinase 1 family: participation in multiple cellular processes in eukaryotes. Cellular Signalling *17*, 675–689.

Kobayashi, T., Habuchi, H., Nogami, K., Ashikari-Hada, S., Tamura, K., Ide, H., and Kimata, K. (2010). Functional analysis of chick heparan sulfate 6-O-sulfotransferases in limb bud development. Dev. Growth Differ. *52*, 146–156.

Kojima, T., Shworak, N.W., and Rosenberg, R.D. (1992). Molecular cloning and expression of two distinct cDNA-encoding heparan sulfate proteoglycan core proteins from a rat endothelial cell line. J. Biol. Chem. *267*, 4870–4877.

Kozak, M. (1994). Determinants of translational fidelity and efficiency in vertebrate mRNAs. Biochimie *76*, 815–821.

Kramps, T., Peter, O., Brunner, E., Nellen, D., Froesch, B., Chatterjee, S., Murone, M., Züllig, S., and Basler, K. (2002). Wnt/Wingless Signaling Requires BCL9/Legless-Mediated Recruitment of Pygopus to the Nuclear β-Catenin-TCF Complex. Cell *109*, 47–60.

Krasnow, R.E., Wong, L.L., and Adler, P.N. (1995). Dishevelled is a component of the frizzled signaling pathway in Drosophila. Development *121*, 4095–4102.

Kresse, H., Paschke, E., von Figura, K., Gilberg, W., and Fuchs, W. (1980). Sanfilippo disease type D: deficiency of N-acetylglucosamine-6-sulfate sulfatase required for heparan sulfate degradation. Proc Natl Acad Sci U S A *77*, 6822–6826.

Kreuger, J., Perez, L., Giraldez, A.J., and Cohen, S.M. (2004). Opposing Activities of Dally-like Glypican at High and Low Levels of Wingless Morphogen Activity. Developmental Cell *7*, 503–512.

Ku, M., and Melton, D.A. (1993). Xwnt-11: a maternally expressed Xenopus wnt gene. Development *119*, 1161–1173.

Kuhl, M. (2002). Non-canonical Wnt signaling in Xenopus: regulation of axis formation and gastrulation. Semin Cell Dev Biol *13*, 243–249.

Kuhl, M., Sheldahl, L.C., Malbon, C.C., and Moon, R.T. (2000). Ca(2+)/calmodulin-dependent protein kinase II is stimulated by Wnt and Frizzled homologs and promotes ventral cell fates in Xenopus. J Biol Chem *275*, 12701–12711.

Kuhl, M., Geis, K., Sheldahl, L.C., Pukrop, T., Moon, R.T., and Wedlich, D. (2001). Antagonistic regulation of convergent extension movements in Xenopus by Wnt/beta-catenin and Wnt/Ca2+ signaling. Mech Dev *106*, 61–76.

Kusakabe, M., and Nishida, E. (2004). The polarity-inducing kinase Par-1 controls Xenopus gastrulation in cooperation with 14-3-3 and aPKC. EMBO J. *23*, 4190–4201.

Kusche-Gullberg, M., Eriksson, I., Pikas, D.S., and Kjellén, L. (1998). Identification and Expression in Mouse of Two Heparan Sulfate Glucosaminyl N-Deacetylase/N-Sulfotransferase Genes. J. Biol. Chem. *273*, 11902–11907.

Lai, J., Chien, J., Staub, J., Avula, R., Greene, E.L., Matthews, T.A., Smith, D.I., Kaufmann, S.H., Roberts, L.R., and Shridhar, V. (2003). Loss of HSulf-1 up-regulates heparin-binding growth factor signaling in cancer. J. Biol. Chem. *278*, 23107–23117.

Lai, J.-P., Chien, J.R., Moser, D.R., Staub, J.K., Aderca, I., Montoya, D.P., Matthews, T.A., Nagorney, D.M., Cunningham, J.M., Smith, D.I., et al. (2004). hSulf1 Sulfatase promotes apoptosis of hepatocellular cancer cells by decreasing heparin-binding growth factor signaling. Gastroenterology *126*, 231–248.

Lamanna, W.C., Baldwin, R.J., Padva, M., Kalus, I., Ten Dam, G., van Kuppevelt, T.H., Gallagher, J.T., von Figura, K., Dierks, T., and Merry, C.L.R. (2006). Heparan sulfate 6-O-endosulfatases: discrete in vivo activities and functional co-operativity. Biochem. J. *400*, 63–73.

Lamanna, W.C., Frese, M.A., Balleininger, M., and Dierks, T. (2008). Sulf loss influences N-, 2-O-, and 6-O-sulfation of multiple heparan sulfate proteoglycans and modulates fibroblast growth factor signaling. J Biol Chem *283*, 27724–27735.

Lander, A.D. (2007). Morpheus unbound: reimagining the morphogen gradient. Cell *128*, 245–256.

Lee, E., Salic, A., Krüger, R., Heinrich, R., and Kirschner, M.W. (2003). The Roles of APC and Axin Derived from Experimental and Theoretical Analysis of the Wnt Pathway. PLoS Biol *1*, e10.

Lee, P.H.A., Trowbridge, J.M., Taylor, K.R., Morhenn, V.B., and Gallo, R.L. (2004). Dermatan Sulfate Proteoglycan and Glycosaminoglycan Synthesis Is Induced in Fibroblasts by Transfer to a Three-dimensional Extracellular Environment. J. Biol. Chem. *279*, 48640–48646.

Lemaire, P., Garrett, N., and Gurdon, J.B. (1995). Expression cloning of Siamois, a Xenopus homeobox gene expressed in dorsal-vegetal cells of blastulae and able to induce a complete secondary axis. Cell *81*, 85–94.

Lewis, P.M., Dunn, M.P., McMahon, J.A., Logan, M., Martin, J.F., St-Jacques, B., and McMahon, A.P. (2001). Cholesterol modification of sonic hedgehog is required for long-range signaling activity and effective modulation of signaling by Ptc1. Cell *105*, 599–612.

Li, J., Mo, M.-L., Chen, Z., Yang, J., Li, Q.-S., Wang, D.-J., Zhang, H., Ye, Y.-J., Xu, J.-P., Li, H.-L., et al. (2011). HSulf-1 inhibits cell proliferation and invasion in human gastric cancer. Cancer Science *102*, 1815–1821.

Li, J.-P., Gong, F., Darwish, K.E., Jalkanen, M., and Lindahl, U. (2001). Characterization of the d-Glucuronyl C5-epimerase Involved in the Biosynthesis of Heparin and Heparan Sulfate. J. Biol. Chem. *276*, 20069–20077.

Li, L., Yuan, H., Weaver, C.D., Mao, J., Farr, G.H., 3rd, Sussman, D.J., Jonkers, J., Kimelman, D., and Wu, D. (1999). Axin and Frat1 interact with dvl and GSK, bridging Dvl to GSK in Wnt-mediated regulation of LEF-1. EMBO J. *18*, 4233–4240.

Lienkamp, S., Ganner, A., and Walz, G. (2012). Inversin, Wnt signaling and primary cilia. Differentiation *83*, S49–S55.

Lin, X., and Perrimon, N. (1999). Dally cooperates with Drosophila Frizzled 2 to transduce Wingless signalling. Nature *400*, 281–284.

Lin, X., Buff, E.M., Perrimon, N., and Michelson, A.M. (1999). Heparan sulfate proteoglycans are essential for FGF receptor signaling during Drosophila embryonic development. Development *126*, 3715–3723.

Lin, X., Wei, G., Shi, Z., Dryer, L., Esko, J.D., Wells, D.E., and Matzuk, M.M. (2000). Disruption of Gastrulation and Heparan Sulfate Biosynthesis in EXT1-Deficient Mice. Developmental Biology *224*, 299–311.

Lind, T., Tufaro, F., McCormick, C., Lindahl, U., and Lidholt, K. (1998). The putative tumor suppressors EXT1 and EXT2 are glycosyltransferases required for the biosynthesis of heparan sulfate. J Biol Chem *273*, 26265–26268.

Lindahl, U., and Roden, L. (1965). The Role of Galactose and Xylose in the Linkage of Heparin to Protein. J Biol Chem *240*, 2821–2826.

Liu, C., Kato, Y., Zhang, Z., Do, V.M., Yankner, B.A., and He, X. (1999a). β-Trcp couples β-catenin phosphorylation-degradation and regulates Xenopus axis formation. PNAS *96*, 6273–6278.

Liu, J., Shworak, N.W., Sinay, P., Schwartz, J.J., Zhang, L., Fritze, L.M.S., and Rosenberg, R.D. (1999b). Expression of Heparan Sulfate d-Glucosaminyl 3-O-Sulfotransferase Isoforms Reveals Novel Substrate Specificities. J. Biol. Chem. *274*, 5185–5192.

Lum, D.H., Tan, J., Rosen, S.D., and Werb, Z. (2007). Gene trap disruption of the mouse heparan sulfate 6-O-endosulfatase gene, Sulf2. Mol. Cell. Biol. *27*, 678–688.

Lyons, J.P., Mueller, U.W., Ji, H., Everett, C., Fang, X., Hsieh, J.-C., Barth, A.M., and McCrea, P.D. (2004). Wnt-4 activates the canonical beta-catenin-mediated Wnt pathway and binds Frizzled-6 CRD: functional implications of Wnt/beta-catenin activity in kidney epithelial cells. Exp. Cell Res. *298*, 369–387.

Maccarana, M., Casu, B., and Lindahl, U. (1993). Minimal sequence in heparin/heparan sulfate required for binding of basic fibroblast growth factor. J. Biol. Chem. *268*, 23898–23905.

Maccarana, M., Sakura, Y., Tawada, A., Yoshida, K., and Lindahl, U. (1996). Domain Structure of Heparan Sulfates from Bovine Organs. J. Biol. Chem. *271*, 17804–17810.

Majumdar, A., Vainio, S., Kispert, A., McMahon, J., and McMahon, A.P. (2003). Wnt11 and Ret/Gdnf pathways cooperate in regulating ureteric branching during metanephric kidney development. Development *130*, 3175–3185.

Malacinski, G.M., Brothers, A.J., and Chung, H.-M. (1977). Destruction of components of the neural induction system of the amphibian egg with ultraviolet irradiation. Developmental Biology *56*, 24–39.

Manders, E.M.M., Verbeek, F.J., and Aten, J.A. (1993). Measurement of co-localization of objects in dual-colour confocal images. Journal of Microscopy *169*, 375–382.

Marynen, P., Zhang, J., Cassiman, J.J., Van den Berghe, H., and David, G. (1989). Partial primary structure of the 48- and 90-kilodalton core proteins of cell surface-associated heparan sulfate proteoglycans of lung fibroblasts. Prediction of an integral membrane domain and evidence for multiple distinct core proteins at the cell surface of human lung fibroblasts. J. Biol. Chem. *264*, 7017–7024.

Massague, J., and Gomis, R.R. (2006). The logic of TGFbeta signaling. FEBS Lett *580*, 2811–2820.

Mathieu, J., Griffin, K., Herbomel, P., Dickmeis, T., Strähle, U., Kimelman, D., Rosa, F.M., and Peyriéras, N. (2004). Nodal and Fgf pathways interact through a positive regulatory loop and synergize to maintain mesodermal cell populations. Development *131*, 629–641.

Matthews, H.K., Marchant, L., Carmona-Fontaine, C., Kuriyama, S., Larraín, J., Holt, M.R., Parsons, M., and Mayor, R. (2008). Directional migration of neural crest cells in vivo is regulated by Syndecan-4/Rac1 and non-canonical Wnt signaling/RhoA. Development *135*, 1771–1780.

Maye, P., Zheng, J., Li, L., and Wu, D. (2004). Multiple mechanisms for Wnt11-mediated repression of the canonical Wnt signaling pathway. J Biol Chem *279*, 24659–24665.

McCormick, C., Leduc, Y., Martindale, D., Mattison, K., Esford, L.E., Dyer, A.P., and Tufaro, F. (1998). The putative tumour suppressor EXT1 alters the expression of cell-surface heparan sulfate. Nat Genet *19*, 158–161.

McCormick, C., Duncan, G., Goutsos, K.T., and Tufaro, F. (2000). The putative tumor suppressors EXT1 and EXT2 form a stable complex that accumulates in the Golgi apparatus and catalyzes the synthesis of heparan sulfate. Proc Natl Acad Sci U S A *97*, 668–673.

McCrea, P.D., Turck, C.W., and Gumbiner, B. (1991). A homolog of the armadillo protein in Drosophila (plakoglobin) associated with E-cadherin. Science *254*, 1359–1361.

McGrew, L.L., Otte, A.P., and Moon, R.T. (1992). Analysis of Xwnt-4 in embryos of Xenopus laevis: a Wnt family member expressed in the brain and floor plate. Development *115*, 463–473.

McMahon, A.P., and Moon, R.T. (1989). Ectopic expression of the proto-oncogene int-1 in Xenopus embryos leads to duplication of the embryonic axis. Cell *58*, 1075–1084.

Medina, A., Wendler, S.R., and Steinbeisser, H. (1997). Cortical rotation is required for the correct spatial expression of nr3, sia and gsc in Xenopus embryos. Int. J. Dev. Biol. *41*, 741–745.

Meyers, J., Planamento, J., Ebrom, P., Krulewitz, N., Wade, E., and Pownall, M.E. (2013). Sulf1 modulates BMP signaling and is required for somite morphogenesis and development of the horizontal myoseptum. Dev. Biol.

Mii, Y., and Taira, M. (2009). Secreted Frizzled-related proteins enhance the diffusion of Wnt ligands and expand their signalling range. Development *136*, 4083–4088.

Mikels, A.J., and Nusse, R. (2006). Purified Wnt5a protein activates or inhibits beta-catenin-TCF signaling depending on receptor context. PLoS Biol *4*, e115.

Miller, J.R. (2002). The Wnts. Genome Biol. *3*, REVIEWS3001.

Miller, J.R., Rowning, B.A., Larabell, C.A., Yang-Snyder, J.A., Bates, R.L., and Moon, R.T. (1999). Establishment of the dorsal-ventral axis in Xenopus embryos coincides with the dorsal enrichment of dishevelled that is dependent on cortical rotation. J. Cell Biol. *146*, 427–437.

Miyazono, K., Kamiya, Y., and Morikawa, M. (2010). Bone morphogenetic protein receptors and signal transduction. J. Biochem. *147*, 35–51.

Moeller, H., Jenny, A., Schaeffer, H.-J., Schwarz-Romond, T., Mlodzik, M., Hammerschmidt, M., and Birchmeier, W. (2006). Diversin regulates heart formation and gastrulation movements in development. Proc. Natl. Acad. Sci. U.S.A. *103*, 15900–15905.

Mohammadi, M., McMahon, G., Sun, L., Tang, C., Hirth, P., Yeh, B.K., Hubbard, S.R., and Schlessinger, J. (1997). Structures of the Tyrosine Kinase Domain of Fibroblast Growth Factor Receptor in Complex with Inhibitors. Science *276*, 955–960.

Molenaar, M., van de Wetering, M., Oosterwegel, M., Peterson-Maduro, J., Godsave, S., Korinek, V., Roose, J., Destrée, O., and Clevers, H. (1996). XTcf-3 Transcription Factor Mediates β-Catenin-Induced Axis Formation in Xenopus Embryos. Cell *86*, 391–399.

Mongiat, M., Fu, J., Oldershaw, R., Greenhalgh, R., Gown, A.M., and Iozzo, R.V. (2003). Perlecan protein core interacts with extracellular matrix protein 1 (ECM1), a glycoprotein involved in bone formation and angiogenesis. J. Biol. Chem. *278*, 17491–17499.

Moon, R.T., Campbell, R.M., Christian, J.L., McGrew, L.L., Shih, J., and Fraser, S. (1993). Xwnt-5A: a maternal Wnt that affects morphogenetic movements after overexpression in embryos of Xenopus laevis. Development *119*, 97–111.

Morimoto-Tomita, M., Uchimura, K., Werb, Z., Hemmerich, S., and Rosen, S.D. (2002). Cloning and characterization of two extracellular heparin-degrading endosulfatases in mice and humans. J Biol Chem *277*, 49175–49185.

Morin, P.J., Sparks, A.B., Korinek, V., Barker, N., Clevers, H., Vogelstein, B., and Kinzler, K.W. (1997). Activation of β-Catenin-Tcf Signaling in Colon Cancer by Mutations in β-Catenin or APC. Science *275*, 1787–1790.

Müller, P., and Schier, A.F. (2011). Extracellular Movement of Signaling Molecules. Developmental Cell *21*, 145–158.

Mulligan, K.A., Fuerer, C., Ching, W., Fish, M., Willert, K., and Nusse, R. (2012). Secreted Wingless-interacting molecule (Swim) promotes long-range signaling by maintaining Wingless solubility. Proc. Natl. Acad. Sci. U.S.A. *109*, 370–377.

Munemitsu, S., Albert, I., Souza, B., Rubinfeld, B., and Polakis, P. (1995). Regulation of intracellular beta-catenin levels by the adenomatous polyposis coli (APC) tumor-suppressor protein. Proc Natl Acad Sci U S A *92*, 3046–3050.

Myers, D.C., Sepich, D.S., and Solnica-Krezel, L. (2002). Bmp Activity Gradient Regulates Convergent Extension during Zebrafish Gastrulation. Developmental Biology *243*, 81–98.

Nagafuchi, A., and Takeichi, M. (1988). Cell binding function of E-cadherin is regulated by the cytoplasmic domain. EMBO J *7*, 3679–3684.

Nakashima, A., Katagiri, T., and Tamura, M. (2005). Cross-talk between Wnt and Bone Morphogenetic Protein 2 (BMP-2) Signaling in Differentiation Pathway of C2C12 Myoblasts. J. Biol. Chem. *280*, 37660–37668.

Nakato, H., Futch, T.A., and Selleck, S.B. (1995). The division abnormally delayed (dally) gene: a putative integral membrane proteoglycan required for cell division patterning during postembryonic development of the nervous system in Drosophila. Development *121*, 3687–3702.

Narita, K., Staub, J., Chien, J., Meyer, K., Bauer, M., Friedl, A., Ramakrishnan, S., and Shridhar, V. (2006). HSulf-1 inhibits angiogenesis and tumorigenesis in vivo. Cancer Res *66*, 6025–6032.

Narita, K., Chien, J., Mullany, S.A., Staub, J., Qian, X., Lingle, W.L., and Shridhar, V. (2007). Loss of HSulf-1 expression enhances autocrine signaling mediated by amphiregulin in breast cancer. J. Biol. Chem. *282*, 14413–14420.

Nawroth, R., van Zante, A., Cervantes, S., McManus, M., Hebrok, M., and Rosen, S.D. (2007). Extracellular Sulfatases, Elements of the Wnt Signaling Pathway, Positively Regulate Growth and Tumorigenicity of Human Pancreatic Cancer Cells. PLoS ONE *2*, e392.

Neumann, C., and Cohen, S. (1997a). Problems and paradigms: Morphogens and pattern formation. BioEssays *19*, 721–729.

Neumann, C.J., and Cohen, S.M. (1997b). Long-range action of Wingless organizes the dorsal-ventral axis of the Drosophila wing. Development *124*, 871–880.

Neumann, S., Coudreuse, D.Y.M., van der Westhuyzen, D.R., Eckhardt, E.R.M., Korswagen, H.C., Schmitz, G., and Sprong, H. (2009). Mammalian Wnt3a is released on lipoprotein particles. Traffic *10*, 334–343.

Neumann-Giesen, C., Falkenbach, B., Beicht, P., Claasen, S., LüErs, G., Stuermer, C.A.O., Herzog, V., and Tikkanen, R. (2004). Membrane and raft association of reggie-1/flotillin-2: role of myristoylation, palmitoylation and oligomerization and induction of filopodia by overexpression. Biochemical Journal *378*, 509.

Nguyen, V.H., Schmid, B., Trout, J., Connors, S.A., Ekker, M., and Mullins, M.C. (1998). Ventral and lateral regions of the zebrafish gastrula, including the neural crest progenitors, are established by a bmp2b/swirl pathway of genes. Dev. Biol. *199*, 93–110.

Niehrs, C. (2012). The complex world of WNT receptor signalling. Nat. Rev. Mol. Cell Biol. *13*, 767–779.

Nieuwkoop, P.D., and Faber, J. (1994). Normal table of Xenopus laevis. Garland Publishing, New York.

Nikaido, M., Tada, M., Saji, T., and Ueno, N. (1997). Conservation of BMP signaling in zebrafish mesoderm patterning. Mech. Dev. *61*, 75–88.

Nolo, R., Abbott, L.A., and Bellen, H.J. (2000). Senseless, a Zn finger transcription factor, is necessary and sufficient for sensory organ development in Drosophila. Cell *102*, 349–362.

Nusse, R., and Varmus, H. (2012). Three decades of Wnts: a personal perspective on how a scientific field developed. EMBO J. *31*, 2670–2684.

Nusse, R., and Varmus, H.E. (1982). Many tumors induced by the mouse mammary tumor virus contain a provirus integrated in the same region of the host genome. Cell *31*, 99–109.

Nüsslein-Volhard, C., and Wieschaus, E. (1980). Mutations affecting segment number and polarity in Drosophila. Nature *287*, 795–801.

Ohkawara, B., and Niehrs, C. (2010). An ATF2-based luciferase reporter to monitor non-canonical Wnt signaling in Xenopus embryos. Dev Dyn *240*, 188–194.

Ohkawara, B., Yamamoto, T.S., Tada, M., and Ueno, N. (2003). Role of glypican 4 in the regulation of convergent extension movements during gastrulation in Xenopus laevis. Development *130*, 2129–2138.

Okajima, T., Yoshida, K., Kondo, T., and Furukawa, K. (1999). Human homolog of Caenorhabditis elegans sqv-3 gene is galactosyltransferase I involved in the biosynthesis of the glycosaminoglycan-protein linkage region of proteoglycans. J Biol Chem *274*, 22915–22918.

Orford, K., Crockett, C., Jensen, J.P., Weissman, A.M., and Byers, S.W. (1997). Serine phosphorylation-regulated ubiquitination and degradation of beta-catenin. J. Biol. Chem. *272*, 24735–24738.

Ornitz, D.M. (2000). FGFs, heparan sulfate and FGFRs: complex interactions essential for development. Bioessays *22*, 108–112.

Orsulic, S., and Peifer, M. (1996). An in vivo structure-function study of armadillo, the beta-catenin homologue, reveals both separate and overlapping regions of the protein required for cell adhesion and for wingless signaling. J. Cell Biol. *134*, 1283–1300.

Orsulic, S., Huber, O., Aberle, H., Arnold, S., and Kemler, R. (1999). E-cadherin binding prevents beta-catenin nuclear localization and beta-catenin/LEF-1-mediated transactivation. J Cell Sci *112*, 1237–1245.

Ossipova, O., Dhawan, S., Sokol, S., and Green, J.B. (2005). Distinct PAR-1 proteins function in different branches of Wnt signaling during vertebrate development. Dev Cell *8*, 829–841.

Otsuki, S., Hanson, S.R., Miyaki, S., Grogan, S.P., Kinoshita, M., Asahara, H., Wong, C.-H., and Lotz, M.K. (2010). Extracellular sulfatases support cartilage homeostasis by regulating BMP and FGF signaling pathways. PNAS *107*, 10202–10207.

Ozawa, M., Baribault, H., and Kemler, R. (1989). The cytoplasmic domain of the cell adhesion molecule uvomorulin associates with three independent proteins structurally related in different species. EMBO J *8*, 1711–1717.

Pai, L.M., Orsulic, S., Bejsovec, A., and Peifer, M. (1997). Negative regulation of Armadillo, a Wingless effector in Drosophila. Development *124*, 2255–2266.

Paine-Saunders, S., Viviano, B.L., Economides, A.N., and Saunders, S. (2002). Heparan sulfate proteoglycans retain Noggin at the cell surface: a potential mechanism for shaping bone morphogenetic protein gradients. J. Biol. Chem. *277*, 2089–2096.

Panáková, D., Sprong, H., Marois, E., Thiele, C., and Eaton, S. (2005). Lipoprotein particles are required for Hedgehog and Wingless signalling. Nature *435*, 58–65.

Peifer, M., Rauskolb, C., Williams, M., Riggleman, B., and Wieschaus, E. (1991). The segment polarity gene armadillo interacts with the wingless signaling pathway in both embryonic and adult pattern formation. Development *111*, 1029–1043.

Peifer, M., Sweeton, D., Casey, M., and Wieschaus, E. (1994a). wingless signal and Zeste-white 3 kinase trigger opposing changes in the intracellular distribution of Armadillo. Development *120*, 369–380.

Peifer, M., Pai, L.-M., and Casey, M. (1994b). Phosphorylation of the Drosophila Adherens Junction Protein Armadillo: Roles for Wingless Signal and Zeste-white 3 Kinase. Developmental Biology *166*, 543–556.

Pellegrini, L., Burke, D.F., von Delft, F., Mulloy, B., and Blundell, T.L. (2000). Crystal structure of fibroblast growth factor receptor ectodomain bound to ligand and heparin. Nature *407*, 1029–1034.

Pepinsky, R.B., Zeng, C., Wen, D., Rayhorn, P., Baker, D.P., Williams, K.P., Bixler, S.A., Ambrose, C.M., Garber, E.A., Miatkowski, K., et al. (1998). Identification of a palmitic acid-modified form of human Sonic hedgehog. J. Biol. Chem. *273*, 14037–14045.

Perez-Vilar, J., and Hill, R.L. (1997). Norrie disease protein (norrin) forms disulfide-linked oligomers associated with the extracellular matrix. J. Biol. Chem. *272*, 33410–33415.

Perrimon, N., and Mahowald, A.P. (1987). Multiple functions of segment polarity genes in Drosophila. Developmental Biology *119*, 587–600.

Perrimon, N., and Smouse, D. (1989). Multiple functions of a Drosophila homeotic gene, zeste-white 3, during segmentation and neurogenesis. Developmental Biology *135*, 287–305.

Perrimon, N., Engstrom, L., and Mahowald, A.P. (1989). Zygotic lethals with specific maternal effect phenotypes in Drosophila melanogaster. I. Loci on the X chromosome. Genetics *121*, 333–352.

Peters, J.M., McKay, R.M., McKay, J.P., and Graff, J.M. (1999). Casein kinase I transduces Wnt signals. Nature *401*, 345–350.

Pettersson, I., Kusche, M., Unger, E., Wlad, H., Nylund, L., Lindahl, U., and Kjellén, L. (1991). Biosynthesis of heparin. Purification of a 110-kDa mouse mastocytoma protein required for both glucosaminyl N-deacetylation and N-sulfation. J. Biol. Chem. *266*, 8044–8049.

Phillips, R.G., and Whittle, J.R. (1993). wingless expression mediates determination of peripheral nervous system elements in late stages of Drosophila wing disc development. Development *118*, 427–438.

Piccolo, S., Sasai, Y., Lu, B., and De Robertis, E.M. (1996). Dorsoventral patterning in Xenopus: inhibition of ventral signals by direct binding of chordin to BMP-4. Cell *86*, 589–598.

Pilia, G., Hughes-Benzie, R.M., MacKenzie, A., Baybayan, P., Chen, E.Y., Huber, R., Neri, G., Cao, A., Forabosco, A., and Schlessinger, D. (1996). Mutations in GPC3, a glypican gene, cause the Simpson-Golabi-Behmel overgrowth syndrome. Nat. Genet. *12*, 241–247.

Pinson, K.I., Brennan, J., Monkley, S., Avery, B.J., and Skarnes, W.C. (2000). An LDL-receptor-related protein mediates Wnt signalling in mice. Nature *407*, 535–538.

Porter, J.A., Young, K.E., and Beachy, P.A. (1996). Cholesterol modification of hedgehog signaling proteins in animal development. Science *274*, 255–259.

Pyagay, P., Heroult, M., Wang, Q., Lehnert, W., Belden, J., Liaw, L., Friesel, R.E., and Lindner, V. (2005). Collagen triple helix repeat containing 1, a novel secreted protein in injured and diseased arteries, inhibits collagen expression and promotes cell migration. Circ. Res. *96*, 261–268.

Raftery, L.A., and Sutherland, D.J. (1999). TGF-β Family Signal Transduction in Drosophila Development: From Mad to Smads. Developmental Biology *210*, 251–268.

Rapraeger, A., Jalkanen, M., Endo, E., Koda, J., and Bernfield, M. (1985). The cell surface proteoglycan from mouse mammary epithelial cells bears chondroitin sulfate and heparan sulfate glycosaminoglycans. J. Biol. Chem. *260*, 11046–11052.

Ratzka, A., Kalus, I., Moser, M., Dierks, T., Mundlos, S., and Vortkamp, A. (2008). Redundant function of the heparan sulfate 6-O-endosulfatases Sulf1 and Sulf2 during skeletal development. Developmental Dynamics *237*, 339–353.

Ratzka, A., Mundlos, S., and Vortkamp, A. (2010). Expression patterns of sulfatase genes in the developing mouse embryo. Developmental Dynamics *239*, 1779–1788.

Reichsman, F., Smith, L., and Cumberledge, S. (1996). Glycosaminoglycans can modulate extracellular localization of the wingless protein and promote signal transduction. J. Cell Biol. *135*, 819–827.

Reversade, B., Kuroda, H., Lee, H., Mays, A., and De Robertis, E.M. (2005). Depletion of Bmp2, Bmp4, Bmp7 and Spemann organizer signals induces massive brain formation in Xenopus embryos. Development *132*, 3381–3392.

Riggleman, B., Schedl, P., and Wieschaus, E. (1990). Spatial expression of the Drosophila segment polarity gene armadillo is posttranscriptionally regulated by wingless. Cell *63*, 549–560.

Rijsewijk, F., Schuermann, M., Wagenaar, E., Parren, P., Weigel, D., and Nusse, R. (1987). The Drosophila homolog of the mouse mammary oncogene int-1 is identical to the segment polarity gene wingless. Cell *50*, 649–657.

Ringvall, M., Ledin, J., Holmborn, K., Kuppevelt, T. van, Ellin, F., Eriksson, I., Olofsson, A.-M., Kjellén, L., and Forsberg, E. (2000). Defective Heparan Sulfate Biosynthesis and Neonatal Lethality in Mice LackingN-Deacetylase/N-Sulfotransferase-1. J. Biol. Chem. *275*, 25926–25930.

Robbins, P.W., and Lipmann, F. (1956). Identification of enzymatically active sulfate as adenosine-3'-phosphate-5'-phosphosulfate. J. Am. Chem. Soc. *78*, 2652–2653.

De Robertis, E.M. (2009). Spemann's organizer and the self-regulation of embryonic fields. Mech. Dev. *126*, 925–941.

De Robertis, E.M., and Kuroda, H. (2004). Dorsal-ventral patterning and neural induction in Xenopus embryos. Annu Rev Cell Dev Biol *20*, 285–308.

Robertson, D.A., Freeman, C., Morris, C.P., and Hopwood, J.J. (1992). A cDNA clone for human glucosamine-6-sulphatase reveals differences between arylsulphatases and non-arylsulphatases. Biochem J *288*, 539–544.

Rogalski, T.M., Williams, B.D., Mullen, G.P., and Moerman, D.G. (1993). Products of the unc-52 gene in Caenorhabditis elegans are homologous to the core protein of the mammalian basement membrane heparan sulfate proteoglycan. Genes Dev. *7*, 1471–1484.

Rong, J., Habuchi, H., Kimata, K., Lindahl, U., and Kusche-Gullberg, K. (2000). Expression of heparan sulphate L-iduronyl 2-O-sulphotransferase in human kidney 293 cells results in increased D-glucuronyl 2-O-sulphation.

Rong, J., Habuchi, H., Kimata, K., Lindahl, U., and Kusche-Gullberg, M. (2001). Substrate Specificity of the Heparan Sulfate Hexuronic Acid 2-O-Sulfotransferase. Biochemistry *40*, 5548–5555.

Roose, J., Molenaar, M., Peterson, J., Hurenkamp, J., Brantjes, H., Moerer, P., van de Wetering, M., Destrée, O., and Clevers, H. (1998). The Xenopus Wnt effector XTcf-3 interacts with Groucho-related transcriptional repressors. Nature *395*, 608–612.

Rosin-Arbesfeld, R., Townsley, F., and Bienz, M. (2000). The APC tumour suppressor has a nuclear export function. Nature *406*, 1009–1012.

Rothbacher, U., Laurent, M.N., Deardorff, M.A., Klein, P.S., Cho, K.W., and Fraser, S.E. (2000). Dishevelled phosphorylation, subcellular localization and multimerization regulate its role in early embryogenesis. EMBO J *19*, 1010–1022.

Le Roy, C., and Wrana, J.L. (2005). Clathrin- and non-clathrin-mediated endocytic regulation of cell signalling. Nat Rev Mol Cell Biol *6*, 112–126.

Rubinfeld, B., Albert, I., Porfiri, E., Fiol, C., Munemitsu, S., and Polakis, P. (1996). Binding of GSK3beta to the APC-beta-catenin complex and regulation of complex assembly. Science *272*, 1023–1026.

Rubinfeld, B., Tice, B.A., and Polakis, P. (2001). Axin-dependent Phosphorylation of the Adenomatous Polyposis Coli Protein Mediated by Casein Kinase 1. J Biol Chem *276*, 39037–39045.

Rusnati, M., Coltrini, D., Caccia, P., Dell'Era, P., Zoppetti, G., Oreste, P., Valsasina, B., and Presta, M. (1994). Distinct role of 2-O-, N-, and 6-O-sulfate groups of heparin in the formation of the ternary complex with basic fibroblast growth factor and soluble FGF receptor-1. Biochem. Biophys. Res. Commun. *203*, 450–458.

Saha, K., and Schaffer, D.V. (2006). Signal dynamics in Sonic hedgehog tissue patterning. Development *133*, 889–900.

Saint-Jeannet, J.-P., He, X., Varmus, H.E., and Dawid, I.B. (1997). Regulation of dorsal fate in the neuraxis by Wnt-1 and Wnt-3a. PNAS *94*, 13713–13718.

Sakane, H., Yamamoto, H., Matsumoto, S., Sato, A., and Kikuchi, A. (2012). Localization of glypican-4 in different membrane microdomains is involved in the regulation of Wnt signaling. J Cell Sci *125*, 449–460.

Sarrazin, S., Lamanna, W.C., and Esko, J.D. (2011). Heparan sulfate proteoglycans. Cold Spring Harb Perspect Biol *3*.

Sasai, Y., Lu, B., Steinbeisser, H., Geissert, D., Gont, L.K., and De Robertis, E.M. (1994). Xenopus chordin: a novel dorsalizing factor activated by organizer-specific homeobox genes. Cell *79*, 779–790.

Sato, A., Yamamoto, H., Sakane, H., Koyama, H., and Kikuchi, A. (2009). Wnt5a regulates distinct signalling pathways by binding to Frizzled2. EMBO J *29*, 41–54.

Saulnier, D.M.E., Ghanbari, H., and Brändli, A.W. (2002). Essential function of Wnt-4 for tubulogenesis in the Xenopus pronephric kidney. Dev. Biol. *248*, 13–28.

Saunders, S., Jalkanen, M., O'Farrell, S., and Bernfield, M. (1989). Molecular cloning of syndecan, an integral membrane proteoglycan. J Cell Biol *108*, 1547–1556.

Schlessinger, J., Plotnikov, A.N., Ibrahimi, O.A., Eliseenkova, A.V., Yeh, B.K., Yayon, A., Linhardt, R.J., and Mohammadi, M. (2000). Crystal Structure of a Ternary FGF-FGFR-Heparin Complex Reveals a Dual Role for Heparin in FGFR Binding and Dimerization. Molecular Cell *6*, 743–750.

Schmidt, B., Selmer, T., Ingendoh, A., and von Figura, K. (1995). A novel amino acid modification in sulfatases that is defective in multiple sulfatase deficiency. Cell *82*, 271–278.

Schneider, S., Steinbeisser, H., Warga, R.M., and Hausen, P. (1996). β-catenin translocation into nuclei demarcates the dorsalizing centers in frog and fish embryos. Mechanisms of Development *57*, 191–198.

Schohl, A., and Fagotto, F. (2002). Beta-catenin, MAPK and Smad signaling during early Xenopus development. Development *129*, 37–52.

Schroeder, K.E., Condic, M.L., Eisenberg, L.M., and Yost, H.J. (1999). Spatially Regulated Translation in Embryos: Asymmetric Expression of Maternal Wnt-11 along the Dorsal–Ventral Axis in Xenopus. Developmental Biology *214*, 288–297.

Schwarz-Romond, T., Asbrand, C., Bakkers, J., Kühl, M., Schaeffer, H.-J., Huelsken, J., Behrens, J., Hammerschmidt, M., and Birchmeier, W. (2002). The ankyrin repeat protein Diversin recruits Casein kinase Iepsilon to the beta-catenin degradation complex and acts in both canonical Wnt and Wnt/JNK signaling. Genes Dev. *16*, 2073–2084.

Schwarz-Romond, T., Merrifield, C., Nichols, B.J., and Bienz, M. (2005). The Wnt signalling effector Dishevelled forms dynamic protein assemblies rather than stable associations with cytoplasmic vesicles. J. Cell. Sci. *118*, 5269–5277.

Schwarz-Romond, T., Fiedler, M., Shibata, N., Butler, P.J.G., Kikuchi, A., Higuchi, Y., and Bienz, M. (2007a). The DIX domain of Dishevelled confers Wnt signaling by dynamic polymerization. Nat. Struct. Mol. Biol. *14*, 484–492.

Schwarz-Romond, T., Metcalfe, C., and Bienz, M. (2007b). Dynamic recruitment of axin by Dishevelled protein assemblies. J. Cell. Sci. *120*, 2402–2412.

Selmer, T., Hallmann, A., Schmidt, B., Sumper, M., and von Figura, K. (1996). The evolutionary conservation of a novel protein modification, the conversion of cysteine to serinesemialdehyde in arylsulfatase from Volvox carteri. Eur J Biochem *238*, 341–345.

Selva, E.M., Hong, K., Baeg, G.H., Beverley, S.M., Turco, S.J., Perrimon, N., and Häcker, U. (2001). Dual role of the fringe connection gene in both heparan sulphate and fringe-dependent signalling events. Nat. Cell Biol. *3*, 809–815.

Semenov, M.V., Tamai, K., Brott, B.K., Kuhl, M., Sokol, S., and He, X. (2001). Head inducer Dickkopf-1 is a ligand for Wnt coreceptor LRP6. Curr Biol *11*, 951–961.

Senay, C., Lind, T., Muguruma, K., Tone, Y., Kitagawa, H., Sugahara, K., Lidholt, K., Lindahl, U., and Kusche-Gullberg, M. (2000). The EXT1/EXT2 tumor suppressors: catalytic activities and role in heparan sulfate biosynthesis. EMBO Rep *1*, 282–286.

Sepich, D.S., Myers, D.C., Short, R., Topczewski, J., Marlow, F., and Solnica-Krezel, L. (2000). Role of the zebrafish trilobite locus in gastrulation movements of convergence and extension. Genesis *27*, 159–173.

Seto, E.S., and Bellen, H.J. (2004). The ins and outs of Wingless signaling. Trends Cell Biol. *14*, 45–53.

Sharma, R.P. (1973). wingless a new mutant in D.melanogaster. Drosophila Information Service *50*, 135.

Sharma, R.P., and Chopra, V.L. (1976). Effect of the Wingless (wg1) mutation on wing and haltere development in Drosophila melanogaster. Dev. Biol. *48*, 461–465.

Sheldahl, L.C., Slusarski, D.C., Pandur, P., Miller, J.R., Kuhl, M., and Moon, R.T. (2003). Dishevelled activates Ca2+ flux, PKC, and CamKII in vertebrate embryos. J Cell Biol *161*, 769–777.

Shen, M.M. (2007). Nodal signaling: developmental roles and regulation. Development *134*, 1023–1034.

Shi, W., Peyrot, S.M., Munro, E., and Levine, M. (2009). FGF3 in the floor plate directs notochord convergent extension in the Ciona tadpole. Development *136*, 23–28.

Shih, J., and Keller, R. (1994). Gastrulation in Xenopus laevis: involution a current view. Seminars in Developmental Biology *5*, 85–90.

Shimizu, H., Julius, M.A., Giarre, M., Zheng, Z., Brown, A.M., and Kitajewski, J. (1997). Transformation by Wnt family proteins correlates with regulation of beta-catenin. Cell Growth Differ *8*, 1349–1358.

Shindo, A., Hara, Y., Yamamoto, T.S., Ohkura, M., Nakai, J., and Ueno, N. (2010). Tissue-tissue interaction-triggered calcium elevation is required for cell polarization during Xenopus gastrulation. PLoS ONE *5*, e8897.

Siegfried, E., Chou, T.-B., and Perrimon, N. (1992). wingless signaling acts through zeste-white 3, the drosophila homolog of glycogen synthase kinase-3, to regulate engrailed and establish cell fate. Cell *71*, 1167–1179.

Simmonds, A.J., dosSantos, G., Livne-Bar, I., and Krause, H.M. (2001). Apical Localization of wingless Transcripts Is Required for Wingless Signaling. Cell *105*, 197–207.

Sivak, J.M., Petersen, L.F., and Amaya, E. (2005). FGF signal interpretation is directed by Sprouty and Spred proteins during mesoderm formation. Dev Cell *8*, 689–701.

Slack, J.M., Darlington, B.G., Heath, J.K., and Godsave, S.F. (1987). Mesoderm induction in early Xenopus embryos by heparin-binding growth factors. Nature *326*, 197–200.

Slusarski, D.C., Yang-Snyder, J., Busa, W.B., and Moon, R.T. (1997a). Modulation of embryonic intracellular Ca2+ signaling by Wnt-5A. Dev. Biol. *182*, 114–120.

Slusarski, D.C., Corces, V.G., and Moon, R.T. (1997b). Interaction of Wnt and a Frizzled homologue triggers G-protein-linked phosphatidylinositol signalling. Nature *390*, 410–413.

Smith, J.C. (1987). A mesoderm-inducing factor is produced by Xenopus cell line. Development *99*, 3–14.

Smith, W.C., and Harland, R.M. (1992). Expression cloning of noggin, a new dorsalizing factor localized to the Spemann organizer in Xenopus embryos. Cell *70*, 829–840.

Smith, J.C., Price, B.M.J., Green, J.B.A., Weigel, D., and Herrmann, B.G. (1991). Expression of a xenopus homolog of Brachyury (T) is an immediate-early response to mesoderm induction. Cell *67*, 79–87.

Smith, W.C., McKendry, R., Ribisi, S., and Harland, R.M. (1995). A nodal-related gene defines a physical and functional domain within the Spemann organizer. Cell *82*, 37–46.

Sokol, S., Christian, J.L., Moon, R.T., and Melton, D.A. (1991). Injected Wnt RNA induces a complete body axis in Xenopus embryos. Cell *67*, 741–752.

Solis, G.P., Lüchtenborg, A.-M., and Katanaev, V.L. (2013). Wnt secretion and gradient formation. Int J Mol Sci *14*, 5130–5145.

Solnica-Krezel, L. (2005). Conserved patterns of cell movements during vertebrate gastrulation. Curr Biol *15*, R213–28.

Solomon, L. (1964). Hereditary multiple exostosis. American Journal of Human Genetics *16*, 351–363.

Soreq, H., and Huez, G. (1985). The Biosynthesis of Biologically Active Proteins in mRNA-Microinjected Xenopus Oocyte. Critical Reviews in Biochemistry and Molecular Biology *18*, 199–238.

Stark, K., Vainio, S., Vassileva, G., and McMahon, A.P. (1994). Epithelial transformation of metanephric mesenchyme in the developing kidney regulated by Wnt-4. Nature *372*, 679–683.

Stennard, F., Carnac, G., and Gurdon, J.B. (1996). The Xenopus T-box gene, Antipodean, encodes a vegetally localised maternal mRNA and can trigger mesoderm formation. Development *122*, 4179–4188.

Stickens, D., Clines, G., Burbee, D., Ramos, P., Thomas, S., Hogue, D., Hecht, J.T., Lovett, M., and Evans, G.A. (1996). The EXT2 multiple exostoses gene defines a family of putative tumour suppressor genes. Nat Genet *14*, 25–32.

Strigini, M., and Cohen, S.M. (1999). Formation of morphogen gradients in the Drosophila wing. Semin. Cell Dev. Biol. *10*, 335–344.

Strigini, M., and Cohen, S.M. (2000). Wingless gradient formation in the Drosophila wing. Curr. Biol. *10*, 293–300.

Strutt, D.I. (2001). Asymmetric localization of frizzled and the establishment of cell polarity in the Drosophila wing. Mol. Cell *7*, 367–375.

Stuermer, C.A.O., and Plattner, H. (2005). The “lipid raft” microdomain proteins reggie-1 and reggie-2 (flotillins) are scaffolds for protein interaction and signalling. Biochem. Soc. Symp. 109–118.

Stuermer, C.A.O., Lang, D.M., Kirsch, F., Wiechers, M., Deininger, S.-O., and Plattner, H. (2001). Glycosylphosphatidyl Inositol-anchored Proteins and fyn Kinase Assemble in Noncaveolar Plasma Membrane Microdomains Defined by Reggie-1 and -2. Mol. Biol. Cell *12*, 3031–3045.

Suzuki, A., Thies, R.S., Yamaji, N., Song, J.J., Wozney, J.M., Murakami, K., and Ueno, N. (1994). A truncated bone morphogenetic protein receptor affects dorsal-ventral patterning in the early Xenopus embryo. Proc Natl Acad Sci U S A *91*, 10255–10259.

Tada, M., and Smith, J.C. (2000). Xwnt11 is a target of Xenopus Brachyury: regulation of gastrulation movements via Dishevelled, but not through the canonical Wnt pathway. Development *127*, 2227–2238.

Tahinci, E., Thorne, C.A., Franklin, J.L., Salic, A., Christian, K.M., Lee, L.A., Coffey, R.J., and Lee, E. (2007). Lrp6 is required for convergent extension during Xenopus gastrulation. Development *134*, 4095–4106.

Takada, R., Satomi, Y., Kurata, T., Ueno, N., Norioka, S., Kondoh, H., Takao, T., and Takada, S. (2006). Monounsaturated fatty acid modification of Wnt protein: its role in Wnt secretion. Dev Cell *11*, 791–801.

Takahashi, S., Yokota, C., Takano, K., Tanegashima, K., Onuma, Y., Goto, J., and Asashima, M. (2000). Two novel nodal-related genes initiate early inductive events in Xenopus Nieuwkoop center. Development *127*, 5319–5329.

Takei, Y., Ozawa, Y., Sato, M., Watanabe, A., and Tabata, T. (2004). Three Drosophila EXT genes shape morphogen gradients through synthesis of heparan sulfate proteoglycans. Development *131*, 73–82.

Tamai, K., Semenov, M., Kato, Y., Spokony, R., Liu, C., Katsuyama, Y., Hess, F., Saint-Jeannet, J.P., and He, X. (2000). LDL-receptor-related proteins in Wnt signal transduction. Nature *407*, 530–535.

Tanegashima, K., Zhao, H., and Dawid, I.B. (2008). WGEF activates Rho in the Wnt-PCP pathway and controls convergent extension in Xenopus gastrulation. EMBO J. *27*, 606–617.

Tang, R., and Rosen, S.D. (2009). Functional consequences of the subdomain organization of the sulfs. J. Biol. Chem. *284*, 21505–21514.

Tao, Q., Yokota, C., Puck, H., Kofron, M., Birsoy, B., Yan, D., Asashima, M., Wylie, C.C., Lin, X., and Heasman, J. (2005). Maternal wnt11 activates the canonical wnt signaling pathway required for axis formation in Xenopus embryos. Cell *120*, 857–871.

Taylor, J., Abramova, N., Charlton, J., and Adler, P.N. (1998). Van Gogh: A New Drosophila Tissue Polarity Gene. Genetics *150*, 199–210.

The, I., Bellaiche, Y., and Perrimon, N. (1999). Hedgehog Movement Is Regulated through tout velu–Dependent Synthesis of a Heparan Sulfate Proteoglycan. Molecular Cell *4*, 633–639.

Theisen, H., Purcell, J., Bennett, M., Kansagara, D., Syed, A., and Marsh, J.L. (1994). dishevelled is required during wingless signaling to establish both cell polarity and cell identity. Development *120*, 347–360.

Theveneau, E., and Mayor, R. (2012). Neural crest delamination and migration: from epithelium-to-mesenchyme transition to collective cell migration. Dev. Biol. *366*, 34–54.

Theveneau, E., Marchant, L., Kuriyama, S., Gull, M., Moepps, B., Parsons, M., and Mayor, R. (2010). Collective chemotaxis requires contact-dependent cell polarity. Dev. Cell *19*, 39–53.

Thompson, B., Townsley, F., Rosin-Arbesfeld, R., Musisi, H., and Bienz, M. (2002). A new nuclear component of the Wnt signalling pathway. Nat. Cell Biol. *4*, 367–373.

Topczewski, J., Sepich, D.S., Myers, D.C., Walker, C., Amores, A., Lele, Z., Hammerschmidt, M., Postlethwait, J., and Solnica-Krezel, L. (2001). The zebrafish glypican knypek controls cell polarity during gastrulation movements of convergent extension. Dev. Cell *1*, 251–264.

Topol, L., Jiang, X., Choi, H., Garrett-Beal, L., Carolan, P.J., and Yang, Y. (2003). Wnt-5a inhibits the canonical Wnt pathway by promoting GSK-3-independent beta-catenin degradation. J Cell Biol *162*, 899–908.

Torres, M.A., Yang-Snyder, J.A., Purcell, S.M., DeMarais, A.A., McGrew, L.L., and Moon, R.T. (1996). Activities of the Wnt-1 class of secreted signaling factors are antagonized by the Wnt-5A class and by a dominant negative cadherin in early Xenopus development. J Cell Biol *133*, 1123–1137.

Townsley, F.M., Cliffe, A., and Bienz, M. (2004). Pygopus and Legless target Armadillo/β-catenin to the nucleus to enable its transcriptional co-activator function. Nat Cell Biol *6*, 626–633.

Tran, T.H., Shi, X., Zaia, J., and Ai, X. (2012). Heparan sulfate 6-O-endosulfatases (Sulfs) coordinate the Wnt signaling pathways to regulate myoblast fusion during skeletal muscle regeneration. J Biol Chem *287*, 32651–32664.

Tree, D.R.P., Shulman, J.M., Rousset, R., Scott, M.P., Gubb, D., and Axelrod, J.D. (2002). Prickle mediates feedback amplification to generate asymmetric planar cell polarity signaling. Cell *109*, 371–381.

Tsuda, M., Kamimura, K., Nakato, H., Archer, M., Staatz, W., Fox, B., Humphrey, M., Olson, S., Futch, T., Kaluza, V., et al. (1999). The cell-surface proteoglycan Dally regulates Wingless signalling in Drosophila. Nature *400*, 276–280.

Uren, A., Reichsman, F., Anest, V., Taylor, W.G., Muraiso, K., Bottaro, D.P., Cumberledge, S., and Rubin, J.S. (2000). Secreted frizzled-related protein-1 binds directly to Wingless and is a biphasic modulator of Wnt signaling. J. Biol. Chem. *275*, 4374–4382.

Usui, T., Shima, Y., Shimada, Y., Hirano, S., Burgess, R.W., Schwarz, T.L., Takeichi, M., and Uemura, T. (1999). Flamingo, a seven-pass transmembrane cadherin, regulates planar cell polarity under the control of Frizzled. Cell *98*, 585–595.

Vincent, J.-P., Oster, G.F., and Gerhart, J.C. (1986). Kinematics of gray crescent formation in Xenopus eggs: The displacement of subcortical cytoplasm relative to the egg surface. Developmental Biology *113*, 484–500.

Vinson, C.R., Conover, S., and Adler, P.N. (1989). A Drosophila tissue polarity locus encodes a protein containing seven potential transmembrane domains. Nature *338*, 263–264.

Viviano, B.L., Paine-Saunders, S., Gasiunas, N., Gallagher, J., and Saunders, S. (2004). Domain-specific modification of heparan sulfate by Qsulf1 modulates the binding of the bone morphogenetic protein antagonist Noggin. J. Biol. Chem. *279*, 5604–5611.

Vyas, N., Goswami, D., Manonmani, A., Sharma, P., Ranganath, H.A., VijayRaghavan, K., Shashidhara, L.S., Sowdhamini, R., and Mayor, S. (2008). Nanoscale organization of hedgehog is essential for long-range signaling. Cell *133*, 1214–1227.

Wallingford, J.B., and Habas, R. (2005). The developmental biology of Dishevelled: an enilgmatic protein governing cell fate and cell polarity. Development *132*, 4421–4436.

Wallingford, J.B., Rowning, B.A., Vogeli, K.M., Rothbacher, U., Fraser, S.E., and Harland, R.M. (2000). Dishevelled controls cell polarity during Xenopus gastrulation. Nature *405*, 81–85.

Wallingford, J.B., Ewald, A.J., Harland, R.M., and Fraser, S.E. (2001). Calcium signaling during convergent extension in Xenopus. Curr. Biol. *11*, 652–661.

Wang, S., Krinks, M., Lin, K., Luyten, F.P., and Moos, M. (1997a). Frzb, a Secreted Protein Expressed in the Spemann Organizer, Binds and Inhibits Wnt-8. Cell *88*, 757–766.

Wang, S., Krinks, M., Kleinwaks, L., and Moos, M., Jr (1997b). A novel Xenopus homologue of bone morphogenetic protein-7 (BMP-7). Genes Funct. *1*, 259–271.

Wang, S., Ai, X., Freeman, S.D., Pownall, M.E., Lu, Q., Kessler, D.S., and Emerson, C.P. (2004). QSulf1, a heparan sulfate 6-O-endosulfatase, inhibits fibroblast growth factor signaling in mesoderm induction and angiogenesis. Proc Natl Acad Sci U S A *101*, 4833–4838.

Weaver, C., Farr, G.H., 3rd, Pan, W., Rowning, B.A., Wang, J., Mao, J., Wu, D., Li, L., Larabell, C.A., and Kimelman, D. (2003). GBP binds kinesin light chain and translocates during cortical rotation in Xenopus eggs. Development *130*, 5425–5436.

Weeks, D.L., and Melton, D.A. (1987). A maternal mRNA localized to the vegetal hemisphere in Xenopus eggs codes for a growth factor related to TGF-beta. Cell *51*, 861–867.

Wehrli, M., Dougan, S.T., Caldwell, K., O'Keefe, L., Schwartz, S., Vaizel-Ohayon, D., Schejter, E., Tomlinson, A., and DiNardo, S. (2000). arrow encodes an LDL-receptor-related protein essential for Wingless signalling. Nature *407*, 527–530.

Wei, G., Bai, X., Sarkar, A.K., and Esko, J.D. (1999). Formation of HNK-1 determinants and the glycosaminoglycan tetrasaccharide linkage region by UDP-GlcUA:Galactose beta1, 3-glucuronosyltransferases. J Biol Chem *274*, 7857–7864.

Wessely, O., and Tran, U. (2011). Xenopus pronephros development--past, present, and future. Pediatr. Nephrol. *26*, 1545–1551.

Van de Wetering, M., Cavallo, R., Dooijes, D., van Beest, M., van Es, J., Loureiro, J., Ypma, A., Hursh, D., Jones, T., Bejsovec, A., et al. (1997). Armadillo Coactivates Transcription Driven by the Product of the Drosophila Segment Polarity Gene dTCF. Cell *88*, 789–799.

White, I.J., Souabni, A., and Hooper, N.M. (2000). Comparison of the glycosyl-phosphatidylinositol cleavage/attachment site between mammalian cells and parasitic protozoa. J. Cell. Sci. *113 (Pt 4)*, 721–727.

Wieschaus, E., Nusslein-Volhard, C., and Jurgens, G. (1984). Mutations affecting the pattern of the larval cuticle inDrosophila melanogaster. Wilhelm Roux's Archives of Developmental Biology *193*, 296–307.

Willert, K., Logan, C.Y., Arora, A., Fish, M., and Nusse, R. (1999). A Drosophila Axin homolog, Daxin, inhibits Wnt signaling. Development *126*, 4165–4173.

Willert, K., Brown, J.D., Danenberg, E., Duncan, A.W., Weissman, I.L., Reya, T., Yates, J.R., and Nusse, R. (2003). Wnt proteins are lipid-modified and can act as stem cell growth factors. Nature *423*, 448–452.

Williams, P.H., Hagemann, A., Gonzalez-Gaitan, M., and Smith, J.C. (2004). Visualizing long-range movement of the morphogen Xnr2 in the Xenopus embryo. Curr Biol *14*, 1916–1923.

Wilson, P., and Keller, R. (1991). Cell rearrangement during gastrulation of Xenopus: direct observation of cultured explants. Development *112*, 289–300.

Winklbauer, R., Medina, A., Swain, R.K., and Steinbeisser, H. (2001). Frizzled-7 signalling controls tissue separation during Xenopus gastrulation. Nature *413*, 856–860.

Wojcinski, A., Nakato, H., Soula, C., and Glise, B. (2011). DSulfatase-1 fine-tunes Hedgehog patterning activity through a novel regulatory feedback loop. Dev Biol *358*, 168–180.

Wolda, S.L., Moody, C.J., and Moon, R.T. (1993). Overlapping Expression of Xwnt-3A and Xwnt-1 in Neural Tissue of Xenopus laevis Embryos. Developmental Biology *155*, 46–57.

Wolff, T., and Rubin, G.M. (1998). Strabismus, a novel gene that regulates tissue polarity and cell fate decisions in Drosophila. Development *125*, 1149–1159.

Wolpert, L. (1969). Positional information and the spatial pattern of cellular differentiation. Journal of Theoretical Biology *25*, 1–47.

Xu, Q., Wang, Y., Dabdoub, A., Smallwood, P.M., Williams, J., Woods, C., Kelley, M.W., Jiang, L., Tasman, W., Zhang, K., et al. (2004). Vascular development in the retina and inner ear: control by Norrin and Frizzled-4, a high-affinity ligand-receptor pair. Cell *116*, 883–895.

Yamaguchi, T.P., Bradley, A., McMahon, A.P., and Jones, S. (1999). A Wnt5a pathway underlies outgrowth of multiple structures in the vertebrate embryo. Development *126*, 1211–1223.

Yamamoto, H., Kishida, S., Kishida, M., Ikeda, S., Takada, S., and Kikuchi, A. (1999). Phosphorylation of axin, a Wnt signal negative regulator, by glycogen synthase kinase-3beta regulates its stability. J. Biol. Chem. *274*, 10681–10684.

Yamamoto, H., Komekado, H., and Kikuchi, A. (2006). Caveolin is necessary for Wnt-3a-dependent internalization of LRP6 and accumulation of beta-catenin. Dev Cell *11*, 213–223.

Yamamoto, H., Sakane, H., Michiue, T., and Kikuchi, A. (2008a). Wnt3a and Dkk1 regulate distinct internalization pathways of LRP6 to tune the activation of beta-catenin signaling. Dev Cell *15*, 37–48.

Yamamoto, H., Awada, C., Hanaki, H., Sakane, H., Tsujimoto, I., Takahashi, Y., Takao, T., and Kikuchi, A. (2013). Apicobasal secretion of Wnt11 and Wnt3a in polarized epithelial cells is regulated by distinct mechanisms. J. Cell. Sci.

Yamamoto, S., Nishimura, O., Misaki, K., Nishita, M., Minami, Y., Yonemura, S., Tarui, H., and Sasaki, H. (2008b). Cthrc1 selectively activates the planar cell polarity pathway of Wnt signaling by stabilizing the Wnt-receptor complex. Dev Cell *15*, 23–36.

Yamanaka, H., and Nishida, E. (2007). Wnt11 stimulation induces polarized accumulation of Dishevelled at apical adherens junctions through Frizzled7. Genes Cells *12*, 961–967.

Yan, D., and Lin, X. (2009). Shaping morphogen gradients by proteoglycans. Cold Spring Harb Perspect Biol *1*, a002493.

Yan, D., Wu, Y., Feng, Y., Lin, S.C., and Lin, X. (2009). The core protein of glypican Dally-like determines its biphasic activity in wingless morphogen signaling. Dev Cell *17*, 470–481.

Yanagawa, S., van Leeuwen, F., Wodarz, A., Klingensmith, J., and Nusse, R. (1995). The dishevelled protein is modified by wingless signaling in Drosophila. Genes Dev. *9*, 1087–1097.

Yanagawa, S., Matsuda, Y., Lee, J.-S., Matsubayashi, H., Sese, S., Kadowaki, T., and Ishimoto, A. (2002). Casein kinase I phosphorylates the Armadillo protein and induces its degradation in Drosophila. EMBO J. *21*, 1733–1742.

Yanez-Mo, M., Barreiro, O., Gordon-Alonso, M., Sala-Valdes, M., and Sanchez-Madrid, F. (2009). Tetraspanin-enriched microdomains: a functional unit in cell plasma membranes. Trends Cell Biol *19*, 434–446.

Yang, J.D., Sun, Z., Hu, C., Lai, J., Dove, R., Nakamura, I., Lee, J.-S., Thorgeirsson, S.S., Kang, K.J., Chu, I.-S., et al. (2011). Sulfatase 1 and sulfatase 2 in hepatocellular carcinoma: associated signaling pathways, tumor phenotypes, and survival. Genes Chromosomes Cancer *50*, 122–135.

Yang, X., Dormann, D., Münsterberg, A.E., and Weijer, C.J. (2002). Cell movement patterns during gastrulation in the chick are controlled by positive and negative chemotaxis mediated by FGF4 and FGF8. Dev. Cell *3*, 425–437.

Yost, C., Farr, G.H., 3rd, Pierce, S.B., Ferkey, D.M., Chen, M.M., and Kimelman, D. (1998). GBP, an inhibitor of GSK-3, is implicated in Xenopus development and oncogenesis. Cell *93*, 1031–1041.

You, J., Belenkaya, T., and Lin, X. (2011). Sulfated is a negative feedback regulator of wingless in Drosophila. Dev Dyn *240*, 640–648.

Zecca, M., Basler, K., and Struhl, G. (1996). Direct and long-range action of a wingless morphogen gradient. Cell *87*, 833–844.

Zeng, X., Tamai, K., Doble, B., Li, S., Huang, H., Habas, R., Okamura, H., Woodgett, J., and He, X. (2005). A dual-kinase mechanism for Wnt co-receptor phosphorylation and activation. Nature *438*, 873–877.

Zhang, L., Lawrence, R., Schwartz, J.J., Bai, X., Wei, G., Esko, J.D., and Rosenberg, R.D. (2001). The Effect of Precursor Structures on the Action of Glucosaminyl 3-O-Sulfotransferase-1 and the Biosynthesis of Anticoagulant Heparan Sulfate. J. Biol. Chem. *276*, 28806–28813.

Zhang, L., Jia, J., Wang, B., Amanai, K., Wharton, K.A., Jr, and Jiang, J. (2006). Regulation of wingless signaling by the CKI family in Drosophila limb development. Dev. Biol. *299*, 221–237.

Zilian, O., Frei, E., Burke, R., Brentrup, D., Gutjahr, T., Bryant, P.J., and Noll, M. (1999). double-time is identical to discs overgrown, which is required for cell survival, proliferation and growth arrest in Drosophila imaginal discs. Development *126*, 5409–5420.

Zimmerman, L.B., De Jesús-Escobar, J.M., and Harland, R.M. (1996). The Spemann organizer signal noggin binds and inactivates bone morphogenetic protein 4. Cell *86*, 599–606.

Zorn, A.M., Butler, K., and Gurdon, J.B. (1999). Anterior endomesoderm specification in Xenopus by Wnt/beta-catenin and TGF-beta signalling pathways. Dev. Biol. *209*, 282–297.